QC
.P5812
v.56
no.10

THE PHYSICAL REVIEW

VOLUME 56 | *Second Series* | NUMBER 10

NOVEMBER 15, 1939

Published for the

AMERICAN PHYSICAL SOCIETY

by the

AMERICAN INSTITUTE OF PHYSICS

Incorporated

LANCASTER, PA., AND NEW YORK, N. Y.

UNIVERSITY OF MICHIGAN LIBRARIES

THE PHYSICAL REVIEW

A journal of experimental and theoretical physics established by E. L. Nichols in 1893

Published by the American Institute of Physics for the

American Physical Society

OFFICERS

President

JOHN T. TATE
University of Minnesota
Minneapolis, Minnesota

Vice President

JOHN ZELENY
Yale University
New Haven, Connecticut

Secretary

W. L. SEVERINGHAUS
Columbia University
New York, New York

Treasurer

G. B. PEGRAM
Columbia University
New York, New York

Local Secretary for the Pacific Coast

PAUL KIRKPATRICK
Stanford University
California

Editor

JOHN T. TATE
University of Minnesota
Minneapolis, Minnesota

BOARD OF EDITORS

JOHN T. TATE, *Editor* J. W. BUCHTA, *Assistant Editor*

Associate Editors

K. T. BAINBRIDGE	A. L. HUGHES	W. BLEAKNEY
H. P. ROBERTSON	T. H. JOHNSON	G. BREIT
H. B. WAHLIN	F. A. JENKINS	D. M. DENNISON

Manuscripts for publication should be submitted to John T. Tate, University of Minnesota, Minneapolis, Minnesota.

Proof and all correspondence concerning papers in the process of publication, should be addressed to the Publications Manager, American Institute of Physics, 175 Fifth Avenue, New York, New York.

Subscription Price

United States and Possessions and Canada[1]. $15.00
Foreign. $16.50

Back Numbers

Complete set: Series 2,[1] Vol. 1, 1913–Vol. 54, 1938—$390.00
Yearly rate: $16.50
Single copies: $1.50 each prior to July, 1929; $.75 each after July, 1929.

Subscriptions and orders for back numbers should be addressed to Prince and Lemon Streets, Lancaster, Pennsylvania, or to the American Institute of Physics, 175 Fifth Avenue, New York, New York.

Advertising is not accepted for the *Physical Review* but attention is called to the *Review of Scientific Instruments* and the *Journal of Applied Physics* companion publications of the Institute, and media through which the field of physics can be reached most effectively. Rates and other information will be furnished on request.

Changes of address in the case of members of the American Physical Society, should be addressed to the Treasurer; in the case of other subscribers, to the Publications Manager.

[1] For Series 1 inquire of Physics Department, Cornell University, Ithaca, N. Y.

The Physical Review is published semi-monthly at Prince and Lemon Streets, Lancaster, Pennsylvania.

Entered at the Post Office at Lancaster, Pennsylvania, as second class matter.

Acceptance for mailing at special rate of postage provided for in section 1103, Act of October 3, 1917, authorized September 6, 1926.

Physics
Physics-USA
Journal
[illegible]

THE
PHYSICAL REVIEW

A Journal of Experimental and Theoretical Physics Established by E. L. Nichols in 1893

VOL. 56, NO. 10 NOVEMBER 15, 1939 SECOND SERIES

Beta-Spectra of Iodine

G. F. TAPE*
University of Michigan, Ann Arbor, Michigan
(Received September 5, 1939)

Artificial activation of tellurium and iodine by deuterons and neutrons yields four radioactive isotopes of iodine. The momentum distributions of the beta-particles emitted by these isotopes were examined in a large hydrogen-filled cloud chamber placed in a uniform magnetic field. Applications of the Fermi theory of beta-decay and of the Konopinski-Uhlenbeck modification were made and the extrapolated end points were compared to the inspection end points. Gamma-radiation was found with each activity. An estimate of energies of the gamma-radiation associated with I^{130} and I^{131} was determined from the electrons ejected from a lead absorber placed in the cloud chamber. The following results were obtained:

		Energy of Radiations	
Half-life	Probable Isotope	Beta	Gamma
25 ±1 minutes	I^{128}	2.40 ±0.07 Mev	(Yes)
13.0±0.3 days	I^{126}	1.20 ±0.03	(Yes)
8.2±0.3 days	I^{131}	0.687±0.010	0.27 Mev
			0.46
12.5±0.5 hours	I^{130}	0.83 ±0.03	0.59

The original Fermi theory is in better agreement with the experimental data, the Kurie plots being linear over a considerable range to the end-point.

INTRODUCTION

THE original work of Fermi and his associates[1] showed that tellurium and iodine were made radioactive when irradiated with slow neutrons. An activity of 60 minutes half-life was identified in tellurium when it was irradiated with 17-Mev gamma-rays[2] and with lithium neutrons.[3] Pool, Cork and Thornton[4] found an additional activity produced by fast neutrons in tellurium of about 30 days. Chemical identification of these two activities with tellurium and the discovery of activities of 10 hours and 8 days half-lives produced by deuteron bombardment of tellurium were included in a report by Tape and Cork.[5] The formation of an activity of 13 days half-life produced by fast neutron bombardment of iodine was also reported. Additional work on the isotopes of iodine was done by Livingood and Seaborg[6] producing iodine activities having half-lives of 4.0 days, 13 hours, and 8 days in addition to the 25-minute and 13-

* Now at the Department of Physics, Cornell University.
[1] Amaldi, D'Agostino, Fermi, Pontecorvo, Rasetti, Segrè, Proc. Roy. Soc. **A149**, 522 (1935).
[2] W. Bothe and W. Gentner, Zeits. f. Physik **106**, 236 (1938).
[3] F. A. Heyn, Nature **139**, 842 (1937).
[4] Pool, Cork and Thornton, Phys. Rev. **52**, 239 (1937).
[5] G. F. Tape and J. M. Cork, Phys. Rev. **53**, 676 (1938).
[6] J. J. Livingood and G. T. Seaborg, Phys. Rev. **54**, 775 (1938).

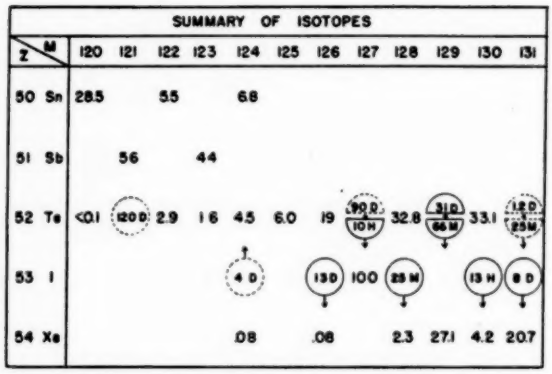

FIG. 1. Summary of stable and radioactive isotopes of iodine and tellurium.

day activities. Seaborg, Livingood and Kennedy[7] have shown that there are three pairs of radioactive tellurium isomers. The stable and radioactive isotopes of tellurium and iodine are shown in Fig. 1. Activities enclosed in solid lines have been verified in this laboratory.

The three tellurium activities of 66 minutes, 10.0 hours, and 31.5 days were produced by bombardment of tellurium with deuterons of energies up to 9 Mev and with fast neutrons. The 10-hour activity was also produced by fast neutron bombardment of iodine. The assignment of this activity to Te^{127} is made through $I^{127}(\eta, H^1)Te^{127}$. The assignment of the two other activities is made to Te^{129} since they are not formed by fast neutron bombardment of iodine but are formed by similar bombardment of tellurium or by irradiation with gamma-rays.[2] All radioactive isotopes of iodine and tellurium except Te^{121} and I^{124} have been definitely shown to emit negative beta-particles.

The beta-ray spectra of all iodine activities produced by deuteron and neutron activation of tellurium and iodine were measured. The momenta of the beta-particles emitted during decay of the iodine isotopes were measured in a twelve-inch cloud chamber placed in a magnetic field constant to 0.5 percent over the volume of the chamber. The control circuit of the vacuum tube type was designed by Richardson.[8] The chamber filled with hydrogen to a pressure slightly in excess of atmospheric was photographed by a single camera. The tracks thus photographed were reprojected to their original size and measured. Restrictions were placed on track selection to insure no scattering of the beta-particle, its origin in the radioactive sample, and a path perpendicular to the magnetic field and to insure against subjective weighting of certain energy groups.

All radioactive samples were prepared by deuteron or neutron bombardment in the University of Michigan cyclotron. After the samples were bombarded and the appropriate chemical separations had been performed, the activated material was finely divided and spread on filter paper. The sample was coated with a solution of paralodion dissolved in alcohol and ether and, after drying, was cut to a length of 3 cm and to a width determined by its activity, the width in all cases being less than 0.5 cm. The mounting frame inside the chamber was made from copper strip and cemented to the wall of the chamber. The frame was made in the shape of a C with the sample placed across the open end and the body of the C next to the chamber wall. By mounting the sample on the arms of the C-frame, there was only filter paper immediately behind the active material, and the glass wall of the chamber was at a minimum of 2 cm behind the paper. Back scattering was thus materially reduced. The filter paper mounting weighed 7.5 mg/cm^2.

IODINE^{128}

This well-known slow neutron period having a half-life of 25 ± 1 minutes was first observed by Fermi and his co-workers.[1] Since iodine has but a single stable isotope, I^{127}, this activity has been

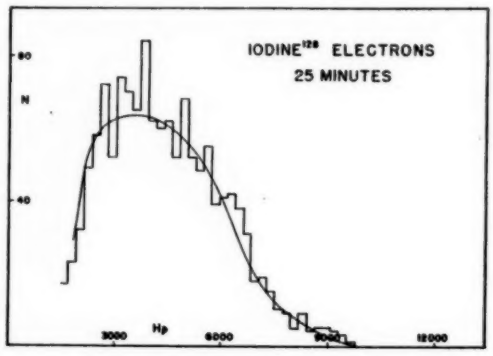

FIG. 2. Momentum distribution of electrons from I^{128}.

[7] Seaborg, Livingood and Kennedy, Phys. Rev. **55**, 794 (1939).
[8] J. R. Richardson, Rev. Sci. Inst. **9**, 152 (1938).

definitely assigned to I^{128} through neutron capture. Livingood and Seaborg[6] produced the same radioactive isotope by bombarding tellurium with 8-Mev deuterons. This reaction has been checked in this laboratory with 9-Mev deuterons.

Since Te^{127} is unstable, the transmutation must be $Te^{126}(H^2, \gamma)I^{128}$ or $Te^{128}(H^2, 2n)I^{128}$ with the latter reaction more likely. I^{128} decays to Xe^{128} with the emission of negative beta-particles and gamma-rays.

Absorption measurements in aluminum[6] indicated a maximum energy of 2.2 Mev. Using a magnetic spectrometer, Alichanian, Alichanow and Dzelepow[9] determined the upper end-point of the I^{128} spectrum to be at 2.1 Mev. Bacon, Grisewood and van der Merwe[10] using a cloud chamber found a complex spectrum. Their analysis of a K-U application showed end-points at 1.2 and 2.1 Mev.

For cloud-chamber work samples of C.P. lead iodide were bombarded for 10 microampere minutes with 7-Mev deuterons. These samples were mounted in the chamber without performing any chemistry. The decay of a fraction of the activated sample was followed at the same time that photographs were being taken. The decay curve showed a pure period of 25 minutes during the period of photography and no contamination due to the presence of the lead. Since the half-life of I^{128} is only 25 minutes, several samples had to be used to obtain a large number of tracks. Of all samples used to obtain the momentum distribution of the beta-particles, the maximum surface density used was 15 mg/cm². This does not include the paper mounting of 7.5 mg/cm².

The momentum distribution of the 1330 measured tracks is shown in Fig. 2. The magnetic field was maintained at 448 oersteds. The inspection end-point is at 9680 $H\rho$ or 2.44 Mev. Below 2500 $H\rho$ the spectrum has very little significance. That this is true comes from the criteria used in track selection. From the demand that a track be at least 10 cm long to minimize the error due to the use of a single camera, it is seen that for a field of 448 oersteds the lower end of the spectrum loses significance around 2500 $H\rho$.

Taking the expressions developed by Fermi and by Konopinski and Uhlenbeck for the probability of emission of a beta-particle having a momentum between η and $\eta+d\eta$, Kurie, Richardson and Paxton[11] have shown that the expression $(N/f)^{1/k}$ plotted against the kinetic energy of the beta-particle will give a straight line if the theory be valid. N is the number of particles in a given momentum interval, f is a function of Z and η, and k equals 2 for the Fermi theory and 4 for the

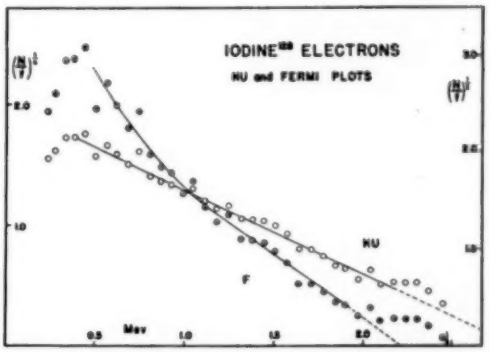

FIG. 3. Fermi and K-U treatments of I^{128} electrons.

Konopinski-Uhlenbeck modification. An approximation given by Bethe and Bacher[12] was used to evaluate f for iodine, where Z equals 53. This evaluation takes care of the Coulomb effect of the nucleus on the emitted particle.

The two plots showing the application of the Fermi and Konopinski-Uhlenbeck theories to the beta-spectrum of I^{128} are shown in Fig. 3. The points shown on K-U and Fermi diagrams are points determined from actual experimental data and not from the distribution curves, which are averages of the data. Thus the same statistical fluctuations appear in the K-U and Fermi curves as appear in the momentum histograms. It was hoped that the use of such a method would give an additional means of averaging the collected data and yield an independently determined end-point. If the uncertainty in each point is taken into account, one sees that for momentum intervals in which only one track is measured, the ordinate of the histogram would have a spread in value between 0 and 2 with a most probable

[9] Alichanian, Alichanow and Dzelepow, Physik. Zeits. Sowjetunion **10**, 78 (1936).
[10] Bacon, Grisewood and van der Merwe, Phys. Rev. **54**, 315 (1938).
[11] Kurie, Richardson and Paxton, Phys. Rev. **49**, 368 (1936).
[12] H. A. Bethe and R. F. Bacher, Rev. Mod. Phys. **8**, 194 (1936).

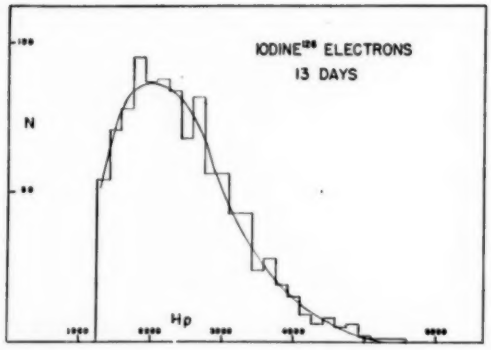

FIG. 4. Momentum distribution of electrons from I^{126}.

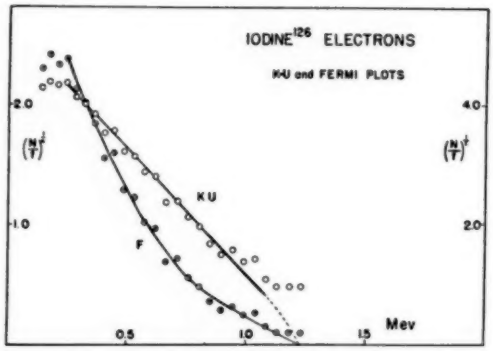

FIG. 5. Fermi and K-U treatments of I^{126} electrons.

value of 1. Similarly with the K-U and Fermi treatments, for $N=1$, the ordinate would have a spread of $2(1/f)^{1/k}$. It is thus seen that the uncertainty of each point near the upper end-point is extremely large.

The upper end-points determined by applications of the Fermi and K-U theories are at 2.20 and 2.94 Mev, respectively. The value of 2.94 Mev, determined by extrapolation, is definitely too high, in fact more than 20 percent higher than the maximum energy measured. The value of 2.20 Mev for the Fermi end-point was also determined by a short extrapolation. Since there were energies measured greater than 2.2 Mev, one must assume that either 2.2 Mev is too small and does not represent the true end-point of I^{128} or that it is all right and that the higher energy tracks are due to some contamination. The only contamination that might be present would be Al^{28} from the foil covering the PbI sample during bombardment. Its half-life is 2.3 minutes, and it emits negative betas with energies up to 3.3 Mev and gamma-rays having an energy of about 2.3 Mev. However, the decay curve did not show the presence of any short life activity. If radioactive aluminum were present, one would expect to measure energies up to 3.3 Mev. Since the upper limit of the spectrum as measured ends at 2.44 Mev, it would seem that the absence of higher energy particles shows the absence of Al^{28} contamination.

IODINE[126]

When iodine is bombarded with fast neutrons ($Li+H^2$), an iodine activity of 13.0 ± 0.3 days half-life is formed.[5] This activity chemically identified as iodine and checked by alpha-particle bombardment of antimony[6] is undoubtedly I^{126} formed by $I^{127}(n, 2n)I^{126}$. It is negative active and decays to stable Xe^{126}. The upper end-point of the beta-ray spectrum has been placed at 1.13 Mev by Livingood and Seaborg[6] who made absorption measurements in aluminum.

$NaIO_3$ was bombarded in the cyclotron with neutrons from the $Li+H^2$ reaction. The activated iodine was separated from the bulk of the $NaIO_3$ by the Amaldi modification[1] of the Szilard-Chalmers reaction. The concentrated sample prepared for cloud-chamber mounting as previously described had a surface density of 22 mg/cm². The sample was allowed to age for two days so that the entire activity would be of 13 days half-life.

The momentum distribution of the 1060 measured tracks is shown in Fig. 4. A field strength of 336 oersteds was used giving a maximum radius of curvature of 16 cm. By inspection the upper end-point of the I^{126} beta-ray spectrum is at 4300 ± 100 $H\rho$. This corresponds to a maximum energy of 1.20 ± 0.03 Mev. N, the number of tracks, is insignificant for values of $H\rho$ less than 1260. The shape of the spectrum is that of the general single beta-ray spectrum. Applications of the Fermi and K-U theories were made and the Kurie plots are shown in Fig. 5. The K-U end-point obtained by extrapolation from the region between 0.3 and 0.9 Mev is at 1.29 Mev, a difference of 7.5 percent as compared with the inspection upper limit of 1.20. The Fermi curve is concave upward over its major portion and from 0.9 Mev to the end-point it is best represented by a straight line. The Fermi end-point thus determined is at 1.22 Mev, 1.6 percent

higher than the end-point determined from the momentum histogram.

There are only two momentum intervals in which N differs markedly from the distribution curve (Fig. 4). These occur at 2520 and 2688 $H\rho$. Since these two variations are in opposite senses, it seems logical that a preference for one interval existed over the other. 2688 $H\rho$ corresponds to an energy of 0.44 Mev. If this point in the distribution corresponds to the conversion electrons from the K shell of Xe, the internally converted gamma-ray would have an energy of 0.48 Mev. This agrees with the value of 0.5 given by absorption in Pb.[6] However, such conclusions as to the identification of the electrons in the interval at 2688 $H\rho$ with conversion electrons seems impossible in the light of statistical fluctuations.

IODINE[131]

The 8-day activity produced when tellurium is bombarded with deuterons and originally associated with Te^{131} has since been assigned to I^{131}. This activity is produced directly by deuteron bombardment of tellurium and also by decay of Te^{131} to I^{131} with the emission of a negative beta-particle. That it is formed directly is verified by the intensity ratios of the initial iodine separation to subsequent separations from the active tellurium. The half-life has been measured at 8.2 ± 0.3 days. I^{131} decays with the emission of negative beta-particles to Xe^{131}. Gamma-rays have also been detected.

For cloud-chamber work, powdered tellurium metal prepared by pulverizing stick tellurium was bombarded in a vacuum with 10 microampere hours of 9-Mev deuterons. After bombardment the tellurium was placed in a distilling flask and a trace of KI added as a carrier for the active iodine formed during bombardment. The iodine was separated by oxidation and distilled off. The separated iodine was precipitated as AgI. The small amount of precipitate was evenly distributed over the surface of the filter paper. The solution containing the tellurium was neutralized with NH_4OH and the Te was precipitated by reduction to the free state with $SnCl_2$.

Two samples of AgI obtained from two bombardments of tellurium were used to determine the beta-spectrum of I^{131}. From the first sample weighing 10 mg/cm², over one thousand tracks were examined and an end-point of 0.692 ± 0.015 Mev was obtained. More recent work with a sample having a surface density of 2 mg/cm² showed no essential differences. Tyler and Lawson[13] found that the experimentally determined shape of a beta-ray spectrum was a function of the thickness of the source. The two independently obtained spectra were normalized to the same number of tracks and the shapes of the two were found to be the same within the limit of statistical fluctuations.

As a result of the comparison of the data from the two samples, the data were combined and the resulting spectrum of I^{131} is shown in Fig. 6. Over 2000 tracks are represented in the histogram. The inspection end-point for this resultant histogram is at 0.687 ± 0.010 Mev. The K-U and Fermi applications are shown in Fig. 7. The Fermi limit is within the range of the inspection end-point while the K-U extrapolation occurs at

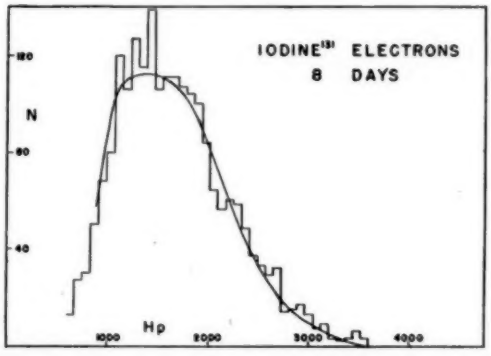

FIG. 6. Momentum distribution of electrons from I^{131}.

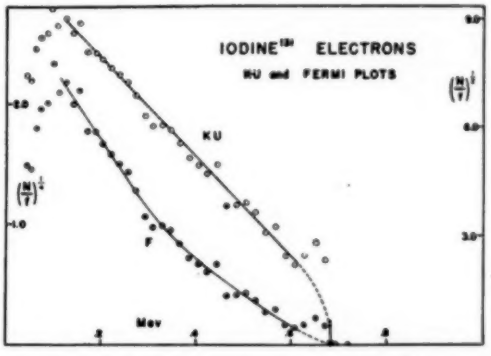

FIG. 7. Fermi and K-U treatments of I^{131} electrons.

[13] A. W. Tyler, Phys. Rev. **56**, 125 (1939); J. L. Lawson, Phys. Rev. **56**, 131 (1939).

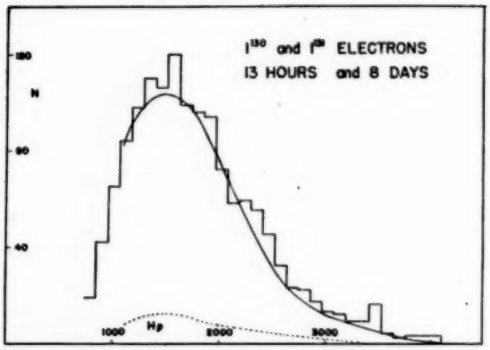

FIG. 8. Solid curve—momentum distribution of electrons from I^{130}. Broken curve—momentum distribution of electrons from I^{131}.

0.78 Mev, about 11.5 percent high. The curve shapes are the same as have been found for single spectra. With the curves as drawn, there are too many tracks in the vicinity of the end-point. It may be that there are too few tracks in the region of 0.6 Mev and thus the upper limit should be extended to slightly higher values, perhaps as high as 0.72 Mev. From examination of the rest of the curve this does not seem very likely. The value of 0.69 Mev does not compare favorably with 1.24 Mev found from absorption measurements.[6]

IODINE[130]

The formation of an iodine isotope of about 13 hours half-life from tellurium bombarded with deuterons was discovered by Livingood and Seaborg.[6] This activity has been checked and the half-life determined to be 12.5 ± 0.5 hours. Since this activity was not found in neutron activated samples of iodine or in subsequent iodine separations from tellurium bombarded with deuterons, it must be assigned to I^{130}. It decays with the emission of negative beta-particles to Xe^{130}.

I^{130} could not be obtained in pure form. It was always associated with I^{131} (half-life of 8 days). It was prepared in exactly the same way as was I^{131}. In fact, the beta-spectra of I^{130} and I^{131} were obtained from the same sample. The cloud-chamber sample had a surface density of 2 mg/cm² with the usual paper backing of 7.5 mg/cm². The decay of the remainder of the total sample was followed with an ionization chamber and electrometer. From the decay curves it was found that at the time the I^{130} spectrum was measured, the ratio of activities (I^{130} : I^{131}) was 10 to 1.

The beta-ray histogram of the combined spectra is shown in Fig. 8. From the histogram alone it would be difficult to tell that two activities are represented. The difference between this histogram and that of I^{131} (Fig. 6) is in the upper end-point. The maximum energy measured was 0.69 Mev for I^{131} and is here 0.83 for the combined spectra. These two values were obtained for the same sample of active iodine. A period of one week separated the measurement of the two spectra. Thus it must be assumed that the two spectra are almost identical with I^{130} having an upper end-point at 0.83 ± 0.03 Mev.

That the histogram in Fig. 8 is composite is shown by the K-U treatment (Fig. 9). It has been seen that K-U curves have been best represented by straight lines over their major portions. Here the K-U curve is definitely concave upward showing the presence of more than one component. The Fermi curve is also more concave than for a single spectrum. Two straight lines have been drawn through the high and low energy regions of the K-U curve to show its complexity. The extrapolations of these two lines do not

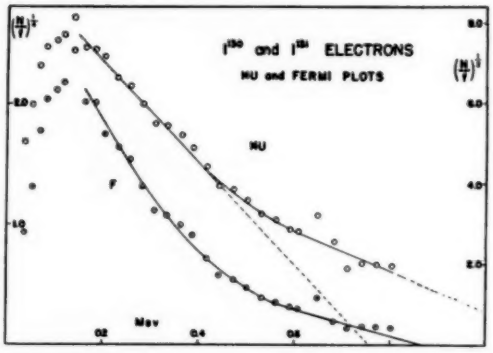

FIG. 9. Fermi and K-U treatments of I^{130} and I^{131} electrons.

indicate end-points. One concludes definitely that two spectra are present and from the histogram in Fig. 8 that the end-point of I^{130} is at 0.83 Mev. In Fig. 8, a contribution of about 0.1 of the total number of tracks (broken curve) was subtracted from the total to obtain the distribution for I^{130} (solid curve). Absorption measurements[6] showed an upper limit of 1.05 Mev for the I^{130} beta-ray spectrum. This is considerably larger than 0.83 Mev. Both methods of measurement indi-

cated that the upper limit of I^{130} and I^{131} are at about the same energy. However, the two methods differ in results in that they yield different values for the upper end-points and opposite signs for the energy difference between the two. The cloud-chamber work places I^{130} with a somewhat higher maximum energy.

Gamma-Rays

An attempt was made to measure the energies of the gamma-rays associated with each isotope. Two types of absorbers were used. A lead foil 0.0002 cm thick was placed along a diameter of the chamber. A lead collimator was used so that the source could see only the lead absorber. This arrangement was used to examine photoelectrons ejected by low energy gamma-rays. A second absorber used to study Compton recoils was essentially carbon. Paper 0.004 cm thick was smeared with carbon and dipped in paraffin. This was mounted in a manner similar to the lead. Recoil electrons in the forward direction only were examined.

Gamma-radiation was found associated with each of the iodine isotopes studied. Absorption measurements in lead have been carried out by Livingood and Seaborg.[6] Attempts to determine the energies of the gamma-rays associated with I^{126} and I^{128} were unsuccessful. With the strongest sources available and by using the largest solid angle possible, about one ejected electron was observed in fifty expansions.

Over 1000 photographs were taken of the electrons ejected from lead by the combined activities of I^{130} and I^{131}. With the strongest available sample, some 70 fair tracks were obtained. Indications of three lines were observed. The Compton recoils at 2580 $H\rho$ and the photoelectrons at 2900 $H\rho$ established quite definitely a gamma-ray having an energy of 0.59 Mev. Adding the energy of the scattered quantum to the recoil energy of 0.42 Mev corresponds to an energy of 0.58 Mev. Adding the K-electron binding energy of lead to the energy of the photoelectron yields 0.59 Mev. The second line occurred at about 1570 $H\rho$. From the relation of the Compton and photoelectric cross sections, it is seen that these electrons are probably entirely photoelectrons. Thus the energy of the gamma-ray is 0.27 Mev. A third line, rather uncertain, appeared at 0.46 Mev. This was identified by Compton recoils at 2100 $H\rho$ ($E=0.03$ Mev) and by photoelectrons at 2240 $H\rho$ ($E=0.36$ Mev). Applying the necessary corrections this indicates a gamma-ray energy of about 0.46 Mev.

At a later time additional pictures were taken when the I^{131} activity was present alone. Only a few tracks were obtained. However, these few tracks were grouped in two energy groups corresponding roughly to the 0.27- and 0.46-Mev lines. It was thus assumed that the line at 0.58 Mev was due to I^{130} and the other two lines due to I^{131}. The value of 0.58 Mev is in good agreement with the value of 0.6 Mev obtained by absorption measurements. The absorption value of 0.4 Mev for I^{131} means little for this case where there are two lines present.

The author is indebted to Professor J. M. Cork and other members of the nuclear physics group for their assistance. The chemical separations were performed by Mr. W. H. Sullivan. This work was made possible through a grant from the Horace H. Rackham Trust Fund.

The Diffraction of X-Rays by Small Crystalline Particles

A. L. PATTERSON
Department of Physics, Bryn Mawr College, Bryn Mawr, Pennsylvania
(Received July 24, 1939)

The problem of the diffraction of x-rays by small crystalline particles is discussed by the methods of Fourier analysis, and the calculation of the intensity of the x-ray scattering from a single particle is reduced to the evaluation of a simple Fourier transform. This approach leads immediately to the interference functions for the parallellepipedon and the octahedron as obtained by other authors. In addition, it makes possible the detailed discussion of the interference functions for the tetrahedron, the rhombic dodecahedron, the ellipsoid, and the elliptic cylinder. The method is shown to be applicable to any polyhedron. A simple method is also given for calculating the interference function and its integral breadth for specific directions of departure from the whole-numbered points. This is applied to obtain a partial discussion of the scattering from the tetrahexahedron and the trisoctahedron.

1. INTRODUCTION

THE phenomenon of line broadening in x-ray and electron diffraction offers a very valuable method for the determination of the size of crystalline particles whose linear dimensions are less than 1000A. The ultracentrifuge, the ultramicroscope, and osmotic pressure measurements have also been applied to particle size measurements in this range. These methods, however, possess two disadvantages in common. First, they do not distinguish clearly between single particles and aggregates of particles; and second, they give only indirect information as to the shape of the particles. The diffraction method measures the size of the individual grains regardless of their relation to one another, and in addition gives a direct indication of the shape of the particles.

In 1918 Scherrer published a simple formula connecting the breadth of the lines with the size of the particles of the substance producing the pattern. The first detailed treatment of the theory of a method for obtaining the size and shape of particles was given by v. Laue.[1] His paper has provided the basis for almost all subsequent work[2] in this field. However, recent work[3–5] has indicated that some of the simplifying assumptions made by v. Laue[1] are inadequate for an exact discussion of the phenomena observed. A more extensive treatment of the problem seems therefore desirable. Following v. Laue the problem can be treated in three stages: (i) The calculation of the scattering from an isolated crystalline particle which possesses a definite orientation with respect to an incident beam of parallel radiation. (ii) The calculation of the scattering of parallel radiation from a mass of particles oriented at random but of the same size and shape (Scherrer problem). The effect of a distribution of size can also be discussed at this stage. (iii) The detailed analysis of a given experimental arrangement, taking into account the configuration of the camera and the sample, the size of the slits or aperture, the divergence of the radiation, the absorption of the sample, etc.

This paper will present a treatment of the first stage outlined above, and a detailed discussion of the dependence of the diffraction pattern of a single particle on its size and shape will be given. In a second paper, these results will be applied to the analysis of the Scherrer problem. The general approach is similar to that of v. Laue[1, 4] but the details of the method are quite different. The particle is represented by a distribution of scattering power which is periodic within its boundaries and zero outside.[6] The methods of Fourier analysis can then be applied to the discussion of the diffraction problem.

[1] M. v. Laue, Zeits. f. Krist. **64**, 115 (1926).
[2] For bibliography see G. H. Cameron and A. L. Patterson, Symposium on Radiography and X-ray Diffraction Methods, Philadelphia 1937, Am. Soc. Testing Materials, pp. 324–338.
[3] C. C. Murdock, Phys. Rev. **35**, 8 (1930).
[4] M. v. Laue, Ann. d. Physik **26**, 55 (1936).
[5] A. L. Patterson, Phys. Rev. **49**, 884 (1936).
[6] Cf. A. L. Patterson, Zeits. f. Physik **44**, 596 (1927).

2. Diffraction from a Small Crystalline Particle of Arbitrary Shape

Let us consider a distribution of matter in space whose scattering power can be represented by a density function $\rho(x_i)$ electrons per unit volume. The coordinates (x_i) are the three components of the vector $\mathbf{r}$ from the origin to the point (x_i) expressed in terms of three non-coplanar vectors $\mathbf{a}_i$ by the relation

$$\mathbf{r}=\sum_1^3 x_i\mathbf{a}_i. \tag{1}$$

If a parallel beam of monochromatic radiation of wave-length λ and intensity I_0, falls on the distribution $\rho(x_i)$ in the direction of the unit vector $\mathbf{s}_0$, and we observe the scattered intensity I in the direction of the unit vector $\mathbf{s}$, it can be shown that

$$I=I_0C(\chi)\,|\,\varphi(A_i)\,|^2, \tag{2}$$

in which C is independent of $\rho(x_i)$ and is a known function of the angle between $\mathbf{s}$ and $\mathbf{s}_0$, of the state of polarization of the incident beam, and of certain universal constants. The function $\varphi(A_i)$ which may be called the interference function, is given by the Fourier transform[7]

$$\varphi(A_i)=v_0\int_{-\infty}^{\infty}\int\int\rho(x_i)e^{-i\Sigma A_ix_i}dx_1dx_2dx_3, \tag{3}$$

in which $v_0=(\mathbf{a}_1[\mathbf{a}_2\mathbf{a}_3])$ and the quantities A_i are coordinates in the reciprocal space, defined by the relations

$$k\mathbf{H}=\Sigma A_i\mathbf{b}_i, \quad (4a) \qquad k=2\pi/\lambda, \quad (4b)$$

$$\mathbf{H}=\mathbf{s}-\mathbf{s}_0, \quad (4c) \qquad |\mathbf{H}|=2\sin\chi/2. \quad (4d)$$

In (4a) the vectors $\mathbf{b}_i$ are the reciprocal lattice vectors associated with the vectors $\mathbf{a}_i$ by the relation

$$(\mathbf{a}_i\mathbf{b}_j)=\delta_{ij}, \tag{5}$$

in which δ_{ij} is the Kronecker delta.

We shall assume that the particle under discussion is a small perfect crystal. Within a definite boundary its electron density can be represented by the Fourier series

$$c(x_i)=\sum_{h_i=-\infty}^{\infty}\sum\sum F(h_i)e^{2\pi i\Sigma h_ix_i}, \tag{6}$$

in which $F(h_i)$ is the structure factor for the reflection of Miller indices (h_i). Outside the boundary, the density is zero. We can now define $\rho(x_i)$ for our particle by the relation

$$\rho(x_i)=c(x_i)s(x_i), \tag{7}$$

in which $c(x_i)$ is defined by (6) throughout space and

$$s(x_i)\begin{cases}=1 & \text{inside the particle boundary}\\ =0 & \text{outside the particle boundary.}\end{cases} \tag{8}$$

The integral (3) takes the form

$$\varphi(A_i)=v_0\int_{-\infty}^{\infty}\int\int c(x_i)s(x_i)e^{-i\Sigma A_ix_i}dx_1dx_2dx_3 \tag{9}$$

and is thus the Fourier transform of the product of two functions. It may consequently[8] be written

$$\varphi(A_i)=v_0\int_{-\infty}^{\infty}\int\int C(t_i)S^*(t_i-A_i)dt_1dt_2dt_3, \tag{10}$$

in which $C(t_i)$ and $S(t_i)$ are the Fourier transforms of $c(x_i)$ and $s(x_i)$, respectively, and S^* is the conjugate complex of S.

The Fourier transform of $c(x_i)$ is given by the integral

$$C(t_i)=(2\pi)^{-1}\int_{-\infty}^{\infty}\int\int\Sigma\Sigma\Sigma F(h_i)\times e^{i\Sigma(2\pi h_i-t_i)x_i}dx_1dx_2dx_3. \tag{11}$$

This integral may be evaluated by the use of an appropriate limiting process and can be shown to be a delta-function for the lattice of points $t_i=2\pi h_i$; the integral over the peak at $2\pi h_i$ having the value $(2\pi)^3F(h_i)$. With this information we can evaluate the integral (10) by inspection and write

$$\varphi(A_i)=(2\pi)^3v_0\sum_{h_i=-\infty}^{\infty}\sum\sum F(h_i)S^*(2\pi h_i-A_i). \tag{12}$$

[7] The double use of i as a subscript $i=1, 2, 3$ and $i=\sqrt{(-1)}$ should not lead to confusion.

[8] See for example: G. A. Campbell and R. M. Foster, *Fourier Integrals for Practical Applications* (Bell System Monograph B584, 1931), p. 39, pair 202; or Titchmarsh, *Theory of Fourier Integrals* (Oxford 1937), p. 50, §2.1.

Thus the interference function $\varphi(A_i)$ is built up of a number of similar functions having their respective origins at the whole-numbered points of the reciprocal lattice. It then remains to evaluate the transform*

$$S(t_i)=(2\pi)^{-3}\int_{-\infty}^{\infty}\int\int e^{-i\Sigma t_i x_i}dx_1dx_2dx_3 \quad (13)$$

for particles of various shapes, the integral being taken throughout the interior of the particle. This function $S(t_i)$ determines completely the effect of the size and shape of the particle on the diffraction pattern and is not directly dependent on the crystal lattice. For convenience we shall define a function $\Psi(t_i)$ by the relation

$$\Psi(t_i)=(2\pi)^{-3}v_0S^*(t_i)/V, \quad (14a) \qquad \Psi(0)=1, \quad (14b)$$

in which V is the volume of the particle. We shall call this function the shape function.

We note that in the present section, the only restriction on the vectors $\mathbf{a}_i$ is that they be three noncoplanar translations of the crystal lattice. We have not assumed that they are a primitive triplet, and they are not necessarily orthogonal. The results obtained are therefore quite general, and can be applied to particles of any shape and any crystal system. The only limitation is introduced by the practical problem of evaluating the integral (13) within the boundary surface of the particle.

3. Calculation of Shape Functions

The general problem of cataloging the surfaces inside of which the integral (13) can be evaluated is beyond the scope of this paper. Our main interest is in its evaluation for the various crystallographic polyhedra. Any polyhedron with plane faces can be built up from a number of irregular tetrahedra each having one vertex at an arbitrarily chosen origin within the boundary surface. Since the integral (13) is obviously additive for noninterpenetrating solids the shape function for a polyhedron will be the sum of the shape functions for its constituent tetrahedra. The shape function for a general tetrahedron with one vertex at the origin is evaluated below. It is therefore possible to evaluate such a function for any polyhedron. We also note that the ellipsoid and the skew elliptic cylinder can be transformed to the sphere and the right circular cylinder by appropriate linear transformations. The integral (13) for these latter shapes can be readily evaluated in polar and cylindrical coordinates, respectively.

Let us now consider the tetrahedron with vertices at the four noncoplanar points $x_i=0$ and $x_i=M_{ij}(i, j=1, 2, 3)$. We transform to a new coordinate system ξ_i in which the vertices are the origin and the three points (100), (010), (001). We then have*

$$x_i=M_{ki}\xi_k,$$

the Jacobian of the transformation being the determinant $J=|M_{ij}|$. If now we write

$$\tau_i=M_{ij}t_j,$$

the shape function for the general tetrahedron can readily be obtained in the form

$$\Psi(t_i)=(6i)\{(\tau_1\tau_2\tau_3)^{-1}+\sum_1^3[e^{i\tau_i}\tau_i(\tau_k-\tau_i)(\tau_i-\tau_j)]^{-1}, \quad (15a)$$

$$V=(1/6)Jv_0. \quad (16b)$$

We note that this function is complex, in common with the shape functions of all particles which do not possess a center of symmetry.

The particles for which shape functions have been calculated in the present paper all possess the following simple properties. They make intercepts $x_i=M_i$ on the axes. Thus when transformed to the coordinate system

$$\xi_i=x_i/M_i, \quad (16a) \qquad T_i=M_it_i, \quad (16b)$$

they make unit intercepts on the axes. In this system, the polyhedra become the symmetrical polyhedra of the cubic system, the ellipsoid becomes the unit sphere and the skew elliptic cylinder becomes the section of the unit right circular cylinder bounded by the planes $\xi_3=\pm1$.

The shape functions which have been calculated are given in Table I. The interference functions can then be derived from them by

* This integral is obviously similar to that obtained by v. Laue, reference 4, Eq. (7) by a different method. We shall here evaluate it directly instead of by a transformation to a surface integral.

* With summation over indices occurring in pairs.

TABLE I. *Shape functions:* $U_i = M_i(2\pi h_i - A_i)$.

SHAPE FUNCTIONS	$M_1M_2M_3W$	$N/(M_1M_2M_3)$
1. Parallelepipedon {100}		
$\Psi(U_i) = \prod_1^3 [\sin U_i/U_i]$	π^3	8
2. Octahedron {111}		
$\Psi(U_i) = 6\sum_1^3 [U_i \sin U_i (U_k^2 - U_i^2)^{-1}(U_i^2 - U_j^2)^{-1}]$	$6\pi^3$	4/3
3. Tetrahedron {111}		
$\Psi(U_i) = 3\sum_1^3 \frac{U_i(i \cos U_i \sin U_j \sin U_k - \sin U_i \cos U_j \cos U_k)}{(U_k^2 - U_i^2)(U_i^2 - U_j^2)}$	$3\pi^3$	8/3
4. Rhombic Dodecahedron {110}		
$\Psi(U_i) = \frac{16\sum\{U_i \sin \frac{1}{2}U_i[\cos \frac{1}{2}U_i - \cos \frac{1}{2}U_j \cos \frac{1}{2}U_k]\}}{(U_1+U_2+U_3)(-U_1+U_2+U_3)(U_1-U_2+U_3)(U_1+U_2-U_3)}$	$4\pi^3$	2
5. Ellipsoid		
$\Psi(U_i) = 3R^{-3}(\sin R - R \cos R)$; $R^2 = U_1^2 + U_2^2 + U_3^2$	$6\pi^2$	$4\pi/3$
6. Elliptic Cylinder		
$\Psi(U_i) = 2(\rho U_3)^{-1} J_1(\rho) \sin U_3$; $\rho^2 = U_1^2 + U_2^2$	$4\pi^2$	2π

means of the expression

$$\varphi(A_i) = V\sum\sum\sum F(h_i)\Psi(U_i), \qquad (17a)$$

$$U_i = M_i(2\pi h_i - A_i), \qquad (17b)$$

obtained by combining (12) and (14). We see that each whole-numbered point (h_i) in the reciprocal space is surrounded by a function

$$VF(h_i)\Psi(U_i), \qquad (17c)$$

whose form depends on the shape of the particle and whose extent depends on the scale factors M_i in (17b) and through them on the size of the particle. M. v. Laue[1] was the first to discuss the significance of functions of this type in the reciprocal space. From them we can calculate the intensity ratio I/I_0 (for given s and s_0) from (2) by making use of the relation (4).

Laue[1] has also introduced the concept of the integral breadth of an intensity function. This he defined as the ratio of the integral of $|\varphi(A_i)|^2$ over the neighborhood of a whole-numbered point to its maximum value. It is readily seen that the breadth W so defined is given by*

$$W = v_0^2(2\pi)^3 V^{-2} \int\int\int |S(t_i)|^2 dt_1 dt_2 dt_3 = (2\pi)^3 v_0 V^{-1}. \qquad (18)$$

If we write

$$V = Nv_0, \qquad (19)$$

in which N is the total number of unit cells in the particle, (18) takes the simple form

$$W = (2\pi)^3/N. \qquad (20)$$

The breadth W is thus inversely proportional to the number of unit cells N and is independent of the shape of the particle. However, in using this concept of breadth in setting up approximation functions for $|\varphi(A_i)|^2$ v. Laue was able to restore the dependence on the scale factors M_i. Values of $M_1M_2M_3W$ together with the corresponding values of $N/(M_1M_2M_3)$ are included in Table I.

It should be pointed out that the shape function obtained here for the parallelepipedon has already[9] been shown to be equivalent to the form obtained by M. v. Laue in his first paper on x-ray diffraction. The function obtained for the octahedron is identical with that given by Murdock[3] Eq. (8); while the result obtained by v. Laue and Riewe[10] can also be reduced to this form.

Obviously, it is possible by the present method to calculate shape functions for polyhedra other than those given above. The polyhedra of lower

* Since $S(t_i)$ is the Fourier transform of $s(x_i)$, the result (18) follows from the well-known identity (cf. Campbell and Foster, reference 8, p. 8, pair 202 footnote)

$$\int\int\int |s(x_i)|^2 dx_1 dx_2 dx_3 = \int\int\int |S(t_i)|^2 dt_1 dt_2 dt_3$$

and the special form of $s(x_i)$ given by (8). See also Titchmarsh, reference 8, formula (2.13), p. 50.

[9] A. L. Patterson, Zeits. f. Physik **44**, 596 (1927). This point has also been discussed more recently by K-H. Riewe, Zeits. f. Krist. **96**, 85 (1937).

[10] M. v. Laue and K-H. Riewe, Zeits. f. Krist. **95**, 414 (1936), Eq. (12).

symmetry which involve only 0 and 1 as Miller indices are very simple to calculate; while those which involve mixed indices (i.e., $\{hk0\}$, $\{hkk\}$, or $\{hkl\}$) are somewhat more complicated, but can readily be obtained if the necessity arises.

4. The Form of the Interference Function for Specific Directions

All the information which we may hope to obtain about the shape of the diffracting particle is contained in the function $|\varphi(A_i)|^2$. In particular, the simple derivation of the Scherrer equation given by W. L. Bragg[11] indicates that the breadth of an x-ray deflection depends to a large extent on the variation of the function $|\Psi(u_i)|^2$ along a line perpendicular to the plane producing the reflection. While this aspect of the problem will be dealt with in more detail in a later paper, we can obtain considerable information as to the effect of particle shape on x-ray diffraction by considering the variation of $|\Psi(u_i)|^2$ along the directions perpendicular to the principal planes of the crystal. The departure from spherical symmetry of this function will give us a direct measure of the possibility of the determination of the shape for a given case.

The shape of the particle depends on (i) the crystallographic form of its bounding faces, (ii) the scale factors M_i, and (iii) the shape of the elementary cell. We shall confine ourselves here to (i) and reserve the discussion of (ii) and (iii). For this reason, we shall assume that $M_1=M_2=M_3$ and that the lattice is cubic. Then, if u be the departure from the whole-numbered point measured in the direction of the normal to the plane in question, we can define a function $\psi(u)$ which will give the variation of $\Psi(U_1)$ along that normal. Functions $\psi(u)$ for the shapes of Table I are exhibited in Table II. They are obtained from the functions of Table I by the following substitutions

Plane	U_1	U_2	U_3
(100)	u	0	0
(110)	v	v	0
(111)	w	w	w

in which $v=u/\sqrt{2}$ and $w=u/\sqrt{3}$. Limiting values must be taken where necessary.

The function $\psi(u)$ can also be obtained directly from (13). It is given by the relation

$$\psi^*(u) = V^{-1}\int_{-\infty}^{\infty} A(x)e^{-iux}dx, \qquad (21)$$

in which $A(x)$ is the area of section of the particle by the plane of indices (h_i) whose perpendicular distance from the origin is x. We have used this approach to check the functions of Table II, and thus indirectly those of Table I.

We can now define an integral breadth B_I

[11] W. L. Bragg, *The Crystalline State* (London, 1933), Vol. I, p. 189.

Table II. *Shape functions $\psi(u)$ for specific directions.* (*For notation see text.*)

Shape	Direction	$\psi(u)$	B_I	$B_{\frac{1}{2}}$	β_I	$\beta_{\frac{1}{2}}$
1. Cube {100}	[100]	$\sin u/u$	3.142	2.783	3.142	2.783
	[110]	$\sin^2 v/v^2$	2.962	2.834	2.962	2.834
	[111]	$\sin^3 w/w^3$	2.993	2.851	2.993	2.851
2. Octahedron {111}	[100]	$6(u-\sin u)/u^3$	5.655	5.248	3.112	2.888
	[110]	$3(\sin v-v\cos v)/v^3$	5.332	5.133	2.934	2.825
	[111]	$3[(1+w^2)\sin w-w\cos w]/(4w^3)$	5.509	5.097	3.032	2.805
3. Tetrahedron {111}	[100]	$3(\sin u-u\cos u)/u^3$	3.770	3.630	2.614	2.517
	[110]	$3(2v-\sin 2v)/(4v^3)$	3.999	3.711	2.772	2.573
	[111]	$3e^{-iw}\{[4w-\sin 4w]+i[\cos 4w+8w^2-1]\}/(32w^3)$	4.897	3.754	3.396	2.603
4. Rhombic Dodecahedron {110}	[100]	$16\sin\frac{1}{2}u(1-\cos\frac{1}{2}u)/u^3$	4.817	4.626	3.035	2.914
	[110]	$\sin\frac{1}{2}v(v\cos\frac{1}{2}v+2\sin\frac{1}{2}v)/v^2$	4.813	4.590	3.032	2.892
	[111]	$8\sin w(1-\cos\frac{1}{2}w)/w^3$	4.807	4.577	3.028	2.883
5. Sphere	[hkl]	$3(\sin u-u\cos u)/u^3$	3.770	3.630	3.039	2.925
6. Circular Cylinder	[hk0]	$2J_1(u)/u$	3.395	3.233	3.133	2.983
	[001]	$\sin u/u$	3.142	2.783	2.899	2.568
	[hk1]	$2\sin vJ_1(v)/v^2$	3.162	3.031	2.918	2.797

TABLE III. *Integral breadths for complex polyhedra* ($h>k$).

SHAPES	FORM	α	$N/M_1M_2M_3$	DIRECTION	B_I	β_I
Tetrahexahedron	$\{hko\}$	$h/(h+k)$	$8\alpha^2$	[100]*	$\pi(8+7\alpha)/(15\alpha)$	$\alpha^{\frac{1}{3}}B_I$
				[110]	$\sqrt{2}\pi(1-9\alpha+45\alpha^2+3\alpha^3)/(60\alpha^3)$	$\alpha^{\frac{1}{3}}B_I$
	$\{210\}$	2/3	32/9	[100]	3.979	3.037
				[110]	3.971	3.030
Trisoctahedron	$\{hhk\}$	$h/(2h+k)$	4α	[100]	$\pi(3+20\alpha-6\alpha^2)/(15\alpha)$	$(\alpha/2)^{\frac{1}{3}}B_I$
	$\{221\}$	2/5	8/5	[100]	5.257	3.074

* The shape function for the tetrahexahedron $\{hk0\}$ in the [100] direction has also been obtained in the form

$$\psi(u)=2[(1-3\alpha+3\alpha^2)\sin\alpha u-\alpha u(1-\alpha)(1-2\alpha)\cos\alpha u-\alpha^2\sin u][\alpha^3u^3(1-\alpha)^2]^{-1}.$$

for the function $\psi(u)$ by the relation

$$B_I=\int_{-\infty}^{\infty}|\psi(u)|^2du, \tag{22}$$

which can be evaluated directly. From (21), however, we can obtain an expression for B_I which is strictly analogous to (18), i.e.,

$$B_I=2\pi V^{-2}\int_{-\infty}^{\infty}A^2(x)dx. \tag{23}$$

We can thus obtain B_I from the curve of areas without calculating $\psi(u)$. The values of B_I given in Table II have been checked by both methods. A few values of B_I for the twenty-four-fold forms of cubic holohedry obtained from (23) are given in Table III.

Another method of characterizing the breadth of a function of the type $\psi(u)$ is by means of the half-value breadth $B_{\frac{1}{2}}$ defined by the equation

$$|\psi(B_{\frac{1}{2}}/2)|^2=(1/2)|\psi(0)|^2. \tag{24}$$

Values of $B_{\frac{1}{2}}$ for the functions which have been computed are also given in Table II.

In order to be able to compare breadths for particles of different shape, it is necessary to establish some standard property which all particles must possess. Murdock has proposed a comparison on the basis of equal volumes. This is also suggested by the relation (20) and will be adopted here. We shall compute values of B_I and $B_{\frac{1}{2}}$ for particles having a volume $V=8M_1M_2M_3v_0$. Such values, which we shall denote by β_I and $\beta_{\frac{1}{2}}$, are also included in Tables II and III. They are connected with the corresponding B, for a given particle, by the relation

$$\beta=N^{\frac{1}{3}}(8M_1M_2M_3)^{-\frac{1}{3}}. \tag{25}$$

A comparison of the values of β for the various shapes suggests that it will be difficult to recognize complex forms from the measurements of breadth alone. In order to do this an accurate knowledge of the shape of the interference function is required, and this is difficult to obtain by means of x-rays from a random oriented powder sample. It may be that electron diffraction, following the suggestion of v. Laue,[4] may prove more fruitful for this purpose. Our results do, however, indicate that the approximate shape of a particle can be obtained from accurate x-ray measurements. It should certainly be possible to decide which of the simple shapes of Table II provides the closest approximation to the shape of a particle belonging to the cubic system. In investigating crystals of lower symmetry it will be necessary to calculate the interference functions for the simple forms of the system in question, and to prepare a table corresponding to Table II with which to compare the experimental results.

It is not profitable to discuss at this point the relative merits of the half-value breadth and the integral breadth as indices of particle size or shape. It should however be noted that for the functions calculated, the integral breadth is consistently higher than the half-value breadth by amounts varying from 4 to 30 percent.

The Scherrer Formula for X-Ray Particle Size Determination

A. L. PATTERSON
Department of Physics, Bryn Mawr College, Bryn Mawr, Pennsylvania
(Received July 24, 1939)

An exact derivation of the Scherrer equation is given for particles of spherical shape, values of the constant for half-value breadth and for integral breadth being obtained. Various approximation methods which have been used are compared with the exact calculation. The tangent plane approximation of v. Laue is shown to be quite satisfactory, but some doubt is cast on the use of approximation functions. It is suggested that the calculation for the ellipsoidal particle based on the tangent plane approximation will provide a satisfactory basis for future work.

1. INTRODUCTION

IN 1918, P. Scherrer[1] showed that, when parallel monochromatic radiation falls on a random oriented mass of crystals, the diffracted beam is broadened when the particle size is small. By an approximation method he obtained an expression for the half-value breadth B of the diffracted beam in the form

$$B=K\lambda/(L\cos\chi/2), \tag{1}$$

in which λ is the wave-length of the incident x-rays, L the linear dimension of particle, $\chi/2$ the Bragg angle and K a numerical constant for which he obtained the value $2(\ln 2/\pi)^{\frac{1}{2}}=0.93$. Since then, various workers[2-6] using different approximation methods and different definitions for the breadth B have obtained different values for the constant K. As a result, those interested in using the relation (1) for the determination of particle size have rightly been in doubt as to its correct value.

The results of the preceding paper in this issue[7] include as a special case the interference function for a spherical particle. For this particle, the calculation of the distribution in angle of the diffracted beam can be carried through exactly, and a value of the Scherrer constant can be obtained. The approximation methods of other authors are also applicable in this case, and consequently it is possible to obtain an estimate of their validity by comparison with the exact calculation.

2. EXACT CALCULATION OF $J(\chi)$

Following v. Laue[3] Eq. (28) and confining our attention to the contribution from one whole-numbered point ($A_i=2h_i\pi$) we may write, in the notation of I (Eq. (17c) etc.)

$$J(\chi)=\int\int\int\{|\Psi(U_i)|^2/(k^2|\mathbf{H}|^3v_0)\}\times dA_1dA_2dA_3, \tag{2a}$$

$$k|\mathbf{H}|=\sum A_i\mathbf{b}_i, \tag{2b}$$

$$U_i=M_i(2\pi h_i-A_i), \tag{2c}$$

in which the integration (2a) is taken between the spheres $k|\mathbf{H}|$ and $(k+\Delta k)|\mathbf{H}|$. $J(\chi)$ is then a quantity proportional[8] to the intensity of the x-rays scattered through an angle χ by a random oriented mass of crystal particles of uniform size, each of which has a shape function $\Psi(U_i)$.

We shall confine ourselves here to the simple case* in which the lattice is cubic of translation $a=1/b$ and $M_1=M_2=M_3=M$. We may then write

$$|\sum A_i\mathbf{b}_i|^2=b^2\sum A_i^2=\rho^2, \tag{3a}$$

$$|2\pi\sum h_i\mathbf{b}_i|^2=4\pi^2b^2\sum h_i^2=\rho_h^2, \tag{3b}$$

$$|2\pi\sum h_i\mathbf{b}_i-\sum A_i\mathbf{b}_i|^2=R_0^2/M^2a^2, \tag{3c}$$

$$R_0^2=M^2\sum(2\pi h_i-A_i)^2=\sum U_i^2. \tag{3d}$$

[1] P. Scherrer, *Göttinger Nachrichten* (1918); cf. also R. Zsigmondy, *Kolloidchemie* (3rd Ed. 1920), p. 394.
[2] N. Seljakow, Zeits. f. Physik **31**, 439; **33**, 648 (1925).
[3] M. v. Laue, Zeits. f. Krist. **64**, 115 (1926).
[4] C. C. Murdock, Phys. Rev. **35**, 8 (1930).
[5] W. L. Bragg, *The Crystalline State*, Vol. 1, p. 189.
[6] F. W. Jones, Proc. Roy. Soc. **A166**, 16 (1938).
[7] A. L. Patterson, p. 972, hereafter cited as I.

[8] F. W. Jones, reference 6, p. 40, has pointed out that the "constant" implicit in (2a) is constant only for small variations of χ, i.e., in the neighborhood of a whole-numbered point. It also contains factors which depend on the particle size, and cannot be used directly in a discussion of the distribution of particle size.

* These conditions are not necessary for the integration of (2a). More general conditions can be set up, but so far no practical use has been made of them.

Under such conditions, we may transform the integral (2a) to polar coordinates $(\rho, \vartheta, \varphi)$ with the vector **G** (cf. v. Laue,[3] Eq. (28a) and Eq. (8) below) as polar vector, when it takes the form

$$J(\chi)=\int_{k|\mathbf{H}|}^{(k+\Delta k)|\mathbf{H}|}\int_0^{\pi}\int_0^{2\pi}\{|\Psi(U_i)|^2/k^2|\mathbf{H}|^3\}\times\rho^2\sin\vartheta d\rho d\vartheta d\varphi.$$

The integration with respect to ρ can be carried immediately and we obtain

$$J(\chi)=\Delta k\int_0^{\pi}\int_0^{2\pi}|\Psi(U_i)|^2\sin\vartheta d\vartheta d\varphi, \quad (4)$$

subject to the condition

$$R_0^2/M^2a^2=k^2|\mathbf{H}|^2+\rho_h^2-2k|\mathbf{H}|\rho_h\cos\vartheta. \quad (5a)$$

To integrate this expression, we must be able to write the U_i in terms of the polar coordinates. If, as in the case of a spherical particle, $\Psi(U_i)$ is a function of R_0 alone and is independent of φ (cf. I Table I), we can integrate directly with respect to φ, and make the change of variable

$$M^2a^2k|\mathbf{H}|\rho_h\sin\vartheta d\vartheta=R_0dR_0. \quad (5b)$$

We then have (omitting a factor which is constant for a given whole-numbered point)

$$J(\chi)=\int_{\Delta}^{\Sigma}|\Psi(R_0)|^2R_0dR_0, \quad (6)$$

in which

$$\delta=\sin(\chi_h/2)-\sin(\chi/2), \quad (7a)$$

$$\sigma=\sin(\chi_h/2)+\sin(\chi/2), \quad (7b)$$

$$\Delta=2Mak\delta, \quad (7c)$$

$$\Sigma=2Mak\sigma. \quad (7d)$$

The exact evaluation of this integral for the spherical particle will be given below.

3. Calculation of $J(\chi)$ by Approximation Methods

Instead of attempting the evaluation of the integral (2a) between the spheres $k|\mathbf{H}|$ and $(k+\Delta k)|\mathbf{H}|$, v. Laue approximates it by an integral taken over the region between the tangent planes to these spheres at the points $k|\mathbf{H}|\mathbf{G}$ and $(k+\Delta k)|\mathbf{H}|\mathbf{G}$, in which **G** is a unit vector in the direction of the vector $\sum h_i\mathbf{b}_i$ i.e.,

$$\mathbf{G}=(\sum h_i\mathbf{b}_i)/|\sum h_i\mathbf{b}_i|. \quad (8)$$

Following v. Laue,[3] Eq. (32), we may then write[9]

$$J(\chi)=\int_{\delta/\eta}^{\infty}|\Psi(R)|^2RdR, \quad (9)$$

in which the assumption of cubic symmetry and the conditions (3) are no longer required. Instead we must, however, write

$$R^2=\sum M_i^2(2\pi h_i-A_i)^2=\sum U_i^2 \quad (10a)$$

and

$$\eta=(2k)^{-1}\{\sum[(\mathbf{b}_i\mathbf{G})/M_i]^2\}^{\frac{1}{2}}. \quad (10b)$$

We note that in the special case of cubic symmetry and under the conditions (3) the quantity δ/η takes the form $\delta/\eta=\Delta=2Mak\delta$.

W. L. Bragg[5] was led to make a further simplification of the discussion by considering only the intensity of the x-rays reflected while the vector **H** is in the same direction as the vector **G**. With this assumption we have simply

$$J(\chi)=|\Psi(\delta/\eta)|^2. \quad (11)$$

Although this approach is confessedly approximate, it has the advantage of being applicable to all possible forms of the function $\Psi(U_i)$.

Since the interference function $|\Psi(U_i)|^2$ is not in general a function of R alone, v. Laue[3] (Eqs. (26) and (27)) made use of approximation functions for the interference function in (9). These functions were of the type

$$f_1(A_i)=C_1\exp(-\omega_1^2R^2), \quad (12a)$$

$$f_2(A_i)=C_2(\omega_2^2R^2+1)^{-2}. \quad (12b)$$

In discussion with the author some years ago v. Laue has also suggested a third approximation function:

$$f_3(A_i)=\begin{cases}C_3(1-\omega_3^2R^2); & R^2<\omega_3^{-2}\\ 0; & R_2^2>\omega_3^{-2}.\end{cases} \quad (12c)$$

In each the constant ω is chosen so that the

[9] B. E. Warren, Zeits. f. Krist. **99**, 448 (1938) has given a simplified discussion of some of v. Laue's analysis.

integral breadth W defined by

$$W=[f(0)]^{-1}\int_{-\infty}^{\infty}\int\int f(A_i)dA_1dA_2dA_3 \quad (13)$$

(cf. I, Eq. (18)) has the same value for the approximation function and for the interference function to be approximated.

Jones[6] (Section V (2)) has also made use of the approximation functions (12a) and (12b), but he chooses values for ω such that the approximation function and the interference function give the same value for the integral breadth (in the scale of δ) for the function $J(\chi)$ for the axial planes.

4. Exact and Approximate Calculations for Spherical Particles

From the interference function for ellipsoidal particles (I, Table I, formula 5) under the special conditions (3) we obtain the interference function for a spherical particle of radius Ma. It has the form

$$|\Psi(R_0)|^2=(9/R_0^6)(\sin R_0-R_0\cos R_0)^2. \quad (14)$$

For this function the integrals (6) and (9) can be evaluated exactly, and we can therefore obtain an insight into the nature of the tangent plane approximation. We can also estimate the accuracy of the Bragg computation. Furthermore, we can set up approximation functions of the three types (12), using both the v. Laue and the Jones criteria for evaluating ω; and apply both the exact and the tangent plane calculations to them. It is thus possible to use the exact calculation as a test of the validity of the various approximation methods and to estimate their value in cases for which the exact calculation cannot be carried through.

We substitute (14) in (6) and after integration by parts we obtain exact form*

$$J(\chi)=\Delta^{-4}[(\sin\Delta-\Delta\cos\Delta)^2+\Delta^2\sin^2\Delta] -\Sigma^{-4}[(\sin\Sigma-\Sigma\cos\Sigma)^2+\Sigma^2\sin^2\Sigma]. \quad (15)$$

The integral (9) which follows from the tangent plane approximation then obviously takes the form

$$J(\chi)=(\eta/\delta)^4\{[\sin(\delta/\eta) -(\delta/\eta)\cos(\delta/\eta)]^2+(\delta/\eta)^2\sin^2(\delta/\eta)\}, \quad (16)$$

while the Bragg approximation leads to

$$J(\chi)=9(\eta/\delta)^6[\sin(\delta/\eta)-(\delta/\eta)\cos(\delta/\eta)]. \quad (17)$$

We are now in a position to compare the two approximation methods with the exact calculation for a spherical particle of a cubic crystal ($\delta/\eta=\Delta$). We note first that for all practical purposes, the expressions (15) and (16) become identical. The function $y^{-4}[(\sin y-y\cos y)^2+y^2\sin^2 y]$ has as its slope $-(4/y^5)(\sin y-y\cos y)^2$, and is therefore a monotonic decreasing function of y whose slope is small for large values of y. Since Σ will usually be large compared with Δ, the second term of (15) will merely result in a very small reduction in the background intensity due to the first term. In general its effect can be neglected, although in special cases (e.g., for χ small) it may have to be taken into account. It seems therefore possible to give strong support to v. Laue's use of the tangent plane approximation. There is nothing in the analysis to lead one to suppose that the case of the spherical particle is in any way peculiar as far as this assumption is concerned, and it is to be expected that the approximation will be just as good for particles of other shapes.

The integral breadths B_I and the half-value breadths $B_{1/2}$ (in the scale of δ) for the functions (16) and (17) are given in Table I together with the corresponding value of the Scherrer constant[10] K_I and $K_{1/2}$. It is seen that for the sphere, the Bragg approximation agrees with the exact calculation within 10 percent. This is unfortunately not close enough to enable us to place immediate trust in the results obtained by this approach for discussions of particle shape. It should be noted that values of the Scherrer

Table I. *Scherrer constants.*

	B_I/η	K_I	$B_{\frac{1}{2}}/\eta$	$K_{\frac{1}{2}}$
Exact (16)	4.189	1.333	3.477	1.107
Bragg (17)	3.770	1.200	3.630	1.155

* The scales have been chosen for (15), (16), and (17) so that they all have a maximum value unity.

[10] L in the Scherrer equation is then the diameter of the spherical particle. For particles of the same volume, the value obtained by Scherrer would correspond to 1.15 (cf. Murdock, reference 4, p. 20) and I, Eq. (25). Note also that B is redefined.

constant can be calculated by the Bragg method for all the functions given in the previous paper (I, Table II and Eq. (23)) and that the integral breadth B and the Scherrer constant K can be obtained to this approximation for any particle for which the curve of cross-sectional areas can be set up. A detailed examination of the nature of the Bragg approximation should therefore be of great value for discussions of particle shape.

It is hoped that in the future, tangent plane calculations can be carried out for some of the exact interference functions which have been obtained (I, Tables I and II).

We can now test the approximation functions (12a–c). We note that both the exact (6) and the tangent plane (9) integrals can be evaluated for functions of this type. We shall confine ourselves here to the tangent plane integral since it has been set up under more general conditions and has been shown to lead to almost the same results as the exact integral. We may use both the v. Laue and the Jones method for evaluating the constants ω. The values obtained and the corresponding values of the Scherrer constants K_I and $K_{1/2}$ are given in Table II.

These results show that the use of approximation functions in integrations of the type involved in deriving the Scherrer formula are by no means to be trusted. We see that the Laue approximation which has been made to give identical values for the integral breadth in the reciprocal space leads to very divergent values for the constant K_I, one measure of the integral breadth in the scale of χ; while the values for $K_{1/2}$ (another measure of that breadth) show relatively good agreement with one another. This latter result can only be described as fortuitous. The Jones approach forces the equality of the constant K_I for the various functions, but leads of course to quite different values for the integral breadth in the reciprocal space, and to quite discordant values for the constant $K_{1/2}$. The reason for this lies of course in the behavior of these functions at infinity.[11] The identity of the integral breadths is no guarantee for the identity of any other property of these curves. Furthermore, two curves which have been matched by any of the criteria discussed above, cannot be expected to agree after being subjected to an infinite integration of the nature of that involved in the derivation of the Scherrer formula.

[11] Cf. M. v. Laue, Ann. d. Physik **26**, 59 (1936).

TABLE II. *Scherrer constants from approximation functions.*

	ω		K_I		$K_{\frac{1}{2}}$	
	v. LAUE	JONES	v. LAUE	JONES	v. LAUE	JONES
Exact			1.333		1.107	
$f_1(A_i)$	0.455	0.423	1.241	1.333	1.166	1.252
$f_2(A_i)$	0.550	0.750	1.817	1.333	1.157	0.849
$f_3(A_i)$	0.305	0.255	1.115	1.333	1.133	1.353

In the discussion of the effect of the size and shape of the sample and of the nature of the radiation such as has been given by v. Laue[3] and Brill and Pelzer[12] it seems that the use of approximation functions is inevitable. The results of the present paper indicate that the conclusions drawn from such an analysis should be examined critically. It seems that the approximation functions must be chosen with much more care, particularly with respect to their behavior at infinity. Perhaps the more purely empirical approach suggested by Jones[6] will provide the best means for making allowance for the dimensions of the sample. It is, however, of great importance that the fundamental discussion given by v. Laue[3] be placed on a sound basis.

CONCLUSION

In the approximation methods of v. Laue[3] and Jones[6] the use of the expression (10b) is equivalent to the assumption of an ellipsoidal particle. They compare their approximation functions for such a particle with the exact interference function for a particle which is a parallelepipedon in shape, and obtain various values for ω which lead to the values for the Scherrer constant given in Table II. The results of the present paper seem to indicate that it would be safest to assume that the particle is ellipsoidal at the start and to use the values for the Scherrer constant obtained for the exact function for an ellipsoidal particle. Then, in a case in which the Scherrer formula is directly applicable, or after the application of an empirical analysis such as that given by Jones,[6] the values of L obtained from a given crystallographic form would be representative of the mean dimension of the particle in the direction

[12] R. Brill, Zeits. f. Krist. **68**, 387 (1928); R. Brill and H. Pelzer, *ibid.* **72**, 398 (1929); **74**, 147 (1930), etc.

normal to the faces of that form. If the assumption of an ellipsoidal particle is well-founded, the breadth should vary in the way suggested by (10b). If not, the departures from the ellipsoidal shape can be examined in the light of Table II of the preceding paper[7] and an indication of the actual particle shape can be obtained.

The work reported in this and the preceding paper was commenced at the Massachusetts Institute of Technology. It is a pleasure for the writer at this time to express his thanks to Professor J. C. Slater for the privilege of working in his laboratory, and to Professor B. E. Warren for many valuable discussions.

NOVEMBER 15, 1939 PHYSICAL REVIEW VOLUME 56

The Far Infra-Red Absorption Spectrum and the Rotational Structure of the Heavy Water Vapor Molecule

NELSON FUSON,* H. M. RANDALL, AND D. M. DENNISON
University of Michigan, Ann Arbor, Michigan

(Received September 7, 1939)

An investigation has been made of the spectrum of heavy water vapor (D_2O) in the region from 23μ to 135μ. The instrument used was a self-recording spectrograph of large aperture, using echelette gratings, vacuum thermopile, and a system of filters, shutters, and *reststrahlen* plates to remove higher order spectral impurity. The radiation path in the spectrograph could be evacuated. From this research the experimental positions and relative intensities of 210 pure rotation absorption frequencies were obtained. Absorption maxima were located with an accuracy of about 0.05 cm^{-1}. Lines 0.5 cm^{-1} apart were partially resolved, higher resolution and dispersion being of little advantage since the true width of these absorption lines was of this same order of magnitude. The energy levels of a zeroth-order approximation to the D_2O asymmetric rotator molecule were computed through quantum number $j=11$, and corrected for zero point vibration and centrifugal stretching in the ground state. A comparison of the positions and intensities of the experimental data with those of the transitions between these "key" levels showed a rather good agreement. These levels were therefore corrected to fit the data, and checked for consistancy by means of series regularities and combination relations. In all, 111 distinct energy levels based on the experimental data were computed. A graph of the experimental data contrasted with a similar graph of the transitions based on these corrected levels gives a clear picture of the success of the analysis.

I. INTRODUCTION

A LARGE amount of work has been done on the spectral analysis of ordinary water in its vapor state. Information concerning the molecule as a whole is largely limited to studies of the absorption frequencies occurring in the infra-red region of the electromagnetic spectrum. The vibration-rotation bands of H_2O have been examined a number of times.[1] Since the discovery[2] of the heavy hydrogen isotope, H^2 (often called deuterium, D), similar studies[3] have been made upon D_2O. In more recent years the extension of the spectrum of H_2O into the region of pure rotation frequencies has been made.[4] One of these latter studies[5] succeeded in establishing the rotational energy levels of the ground state with high accuracy. The present investigation was undertaken in the attempt to parallel this H_2O analysis with a similar study of D_2O.

The problem has been to map the far infra-red pure rotation absorption spectrum of heavy

* Now at Rutgers University.

[1] W. W. Sleator, Astrophys. J. **48**, 125 (1918); W. W. Sleator and E. R. Phelps, Astrophys. J. **62**, 28 (1925); R. Mecke, Zeits. f. Physik **81**, 313, 445, 456 (1933); L. G. Bonner, Phys. Rev. **46**, 458 (1935); E. Ganz, Ann. d. Physik **28**, 445 (1937).

[2] Urey, Brickwedde and Murphy, Phys. Rev. **40**, 1 (1932).

[3] J. W. Ellis and B. W. Sorge, J. Chem. Phys. **2**, 559 (1934); T. Shidei, Phys. and Math. Soc. of Japan Proc. **16**, 362 (1934); E. Bartholome and K. Clusius, Zeits. f. Elec. Chem. **40**, 529 (1934); E. F. Barker and W. W. Sleator, J. Chem. Phys. **3**, 660 (1935); L. Kellner, Proc. Roy. Soc. **159**, a410 (1937).

[4] H. Rubens, Berliner Ber. S: 8 (1931); H. Witt, Zeits. f. Physik **28**, 245 (1924); M. Czerny, Zeits. f. Physik **34**, 232 (1925); J. Kuhne, Zeits. f. Physik **84**, 722 (1933); N. Wright and H. M. Randall, Phys. Rev. **44**, 391 (1933); Barnes, Benedict and Lewis, Phys. Rev. **47**, 918 (1935).

[5] Randall, Dennison, Ginsberg and Weber, Phys. Rev. **52**, 160 (1937) (this paper will hereafter be referred to as RDGW).

water vapor and to analyze these data to obtain the rotational energy levels of the ground state of the D_2O molecule. The "far infra-red" is the term used generally for the region beyond about 20 μ. At this point the prisms of the prism spectrographs become opaque to the long wave-length radiation and recourse must be made entirely to grating spectrographs. For molecules with small moments of inertia, such as NH_3, HCl, and H_2O, the pure rotation frequencies are large enough to be located almost entirely on the short wave-length side of 100 μ. For heavy molecules, on the other hand, the rotational frequencies are so small that the detection of their positions depends on data from the wave-length region beyond 100 μ, a region which is as yet little explored under good dispersion since the energy concentrated in this region is so small.

The molecule of heavy water vapor is, as far as moments of inertia are concerned, a borderline molecule. It may be investigated while not completely, yet possibly with worthwhile results if the analysis is pushed to as long wave-lengths as it is possible to reach. This spectral examination must be at the same time of high enough resolution to separate the spectrum so that most of the lines may be clearly determined, experience with ordinary water vapor having shown that high resolution and dispersion are essential if the data obtained are to be used as the basis for a theoretical analysis.

II. Experimental

1. Experimental difficulties

The instrument used was a far infra-red grating spectrograph equipped with automatic recording mechanism and with an evacuable radiation path. This spectrograph and its predecessors have been rather completely described in the literature,[6] and for this reason no further reference will be made here to its general features. The experimental problems which came up during the research fell mainly under four divisions: lack of energy, overlap of spectral orders, irregularity of deflections, and contamination of the substance under investigation. A brief paragraph concerning each of these problems follows.

[6] H. M. Randall, Rev. Sci. Inst **3**, 196 (1932); H. M. Randall, Rev. Mod. Phys. **10**, 72 (1938); H. M. Randall and F. A. Firestone, Rev. Sci. Inst. **9**, 404 (1938).

a. Lack of energy.—The form of the Planck energy distribution curve for radiation from a blackbody is well known. It shows a tremendous tailing off on the long wave-length side. For this long wave-length region the Rayleigh-Jeans equation, $E_\lambda d\lambda = C\lambda^{-4}kTd\lambda$, is a good first approximation. A study of this equation shows, for example, that the energy given off from a blackbody source in the 50 μ region, though itself very small compared to the total radiation, is 16 times as great as that at 100 μ and 256 times that at 200 μ. Such an illustration gives a rough idea of the energy diminution with increase in wave-length, even though the source used, an electrically heated platinum strip coated with thorium oxide, had a more favorable energy distribution in this region than a blackbody would have.

Furthermore the problem was to examine this long wave-length region under high dispersion, that is with finely ruled gratings and narrow slits. (The "effective slit width" used in this research varied from 0.2 cm^{-1} to 0.5 cm^{-1} depending on the region.) This "spreading out" of the energy added materially to the smallness of the energy coming through the final slit to the thermopile. Indeed, beyond 150 μ the radiant energy was found to be almost negligibly small when the spectrum was examined at the dispersion required. To work at all in this borderline region of small energy between 100 μ and 150 μ it was necessary to keep the spectrograph in almost perfect adjustment to exclude energy deficiencies which were not intrinsic. In this connection mention of the over-all sensitivity of the spectrograph may be interesting. Calculations based on Cartwright's thermopile equations[7] indicated that 0.036 erg/sec. of radiant power delivered to the thermopile receivers would cause a deflection (at the recording camera drum) of 400 mm during one period (16 seconds) of the galvanometer. This deflection is 100 times that of the Brownian motion background and thus is measurable within an accuracy of one or two percent.

b. Overlapping spectral orders.—Six different agents contributed to the purification of the radiation, namely: the construction of the grating, and the materials out of which were made

[7] C. H. Cartwright, Zeits. f. Physik **92**, 153 (1934).

TABLE I. *Purification of radiation. Tests for presence of 2nd- or 3rd-order background radiation were made by introducing filters which cut out all 1st order in that region, but which pass the higher orders: in 20–30 μ region, use 2 mm* NaCl; *in the 27–60 μ region, use 2 mm* KBr; *and in 55–100 μ region, use 0.4 mm* KI.

SPECTRAL REGION	SHUTTER	*reststrahlen*	FILTERS PARAFFIN	FILTERS CRYSTALLINE QUARTZ
18– 23 μ	CaF_2	mirror	2 mm	
22– 36 μ	NaCl	CaF_2 or NaF	2 mm	
25– 40 μ	KCl or NaCl	NaF or CaF_2	4 mm	
40– 70 μ	KBr or KCl	mirror	4 mm	1 mm
65– 85 μ	KI	KBr	4 mm	1 mm
80–100 μ	KI	KI	4 mm	2 mm
100–125 μ	KI	TlBr	4 mm	3 mm
120–160 μ	KI	TlI	4 mm	3 mm

the source, the thermopile receivers, the shutter, the *reststrahlen* plate, and the filters. The first three factors mentioned were more or less fixed throughout the research. Echelette gratings were used. These may be so designed that the greater part of the first-order energy is concentrated in a narrow region of the first-order spectrum, called the "blaze." All higher orders are present, overlapping the desired radiation, this being especially true in the blaze. For this reason measurements were made in regions at some distance from the grating blaze. Certain apparently unpredictable differences in design gave some gratings a higher percentage of the total energy in the first-order spectrum than other gratings.

The thorium-oxide-coated source proved to be the most satisfactory emitter over the whole region. The thermopile receivers were made either of Aquadag (graphite) coated on tinfoil,[8] or of glass powder dusted over a thin glass receiver backed by an evaporated metal layer.[9] Both types of receivers appeared to work equally well in the long wave-length region, though only qualitative comparisons were made between them.

The latter three factors were varied with the different wave-length regions desired. Table I gives the different combinations found most satisfactory in obtaining pure radiation. Very pure spectra could be obtained with these combinations up to 100 μ. Beyond that wave-length good results were obtained with certain gratings and poor results with others. It should be mentioned that the window for the evacuated thermopile was made of paraffin and has been counted in as a filter in the table.

c. Irregularity of deflections.—A great deal of time was spent in tracking down causes for the occasional irregular periods of deflection which made measurements of absorption minima either very inaccurate or quite impossible in the region of disturbance, as well as spoiling the aesthetic appeal of the entire record! Aside from occasional mechanical vibration disturbances and direct electrical effects, the main trouble was eliminated finally by enclosing the primary galvanometer in an airtight steel case, and by putting a radiofrequency choke across the thermopile-to-galvanometer leads. The latter was installed to eliminate heating and rectifying effects in the thermopile due to pick-up of high frequency oscillations from the cyclotron power units in the neighborhood.

d. Contamination of the D_2O vapor.—The absorption cell available for work with this spectrograph was a cylindrical Pyrex cell, 20 inches long and 11 inches in diameter, containing a 10-inch focusing mirror (with gold mirror surface) which was supported at one end of the cell on a chromium plated adjustable mounting. The cell ends were heavy glass disks which were sealed to the cylinder with rubber cement and rubber splicing tape. The seals, source to cell, and cell to spectrograph case, were likewise made with this rubber tape. Crystalline quartz served as window material for the cell in the spectral region beyond 40 μ. From 20 μ to 40 μ quartz is opaque, so an organic plastic called "Metastyrene"* was used. This plastic was sufficiently transparent throughout this region (a broad absorption at 27 μ was too weak to be serious), but it warped, cracked, and melted under heat and pressure, so that windows had to be replaced frequently. It could not be used at all between the source and the cell, so for most of this work the glowing metal strip was in contact with the vapor in the absorption cell.

The cell had a radiation path of 90 cm. The usual procedure was to introduce enough D_2O

[8] N. Wright, Doctoral Thesis (U. of Mich., 1933); F. A. Firestone, Rev. Sci. Inst. **1**, 630 (1930).

[9] C. H. Cartwright and J. Strong, *Procedures in Experimental Physics* (Strong, Editor) (Prentice-Hall, 1938) pp. 321. G. B. B. M. Sutherland, *Infra Red and Raman Spectra* (Methuen, 1935), p. 7.

* Trade name for a commercial polystyrene

liquid into the cell so that it would, upon evaporation, fill the cell with saturated vapor (16 to 18 mm pressure on a mercury manometer) at room temperature. In some regions a longer absorption path would have been desirable if longer cells had been available. Calculations showed that 1 cc of D_2O liquid should be sufficient to saturate the cell volume. In actual practice 2 cc of D_2O were generally used in order to obtain the desired vapor pressure, for apparently a great deal of the D_2O was adsorbed on the cell walls.

Further evidence of this adsorption came from the observation that if the cell were well evacuated after having previously been full of air containing its usual amount of atmospheric H_2O vapor (the main spectrograph case is here assumed to be well evacuated at all times), the background energy records showed little if any trace of even the strongest H_2O absorption lines. Upon introducing a gram of D_2O (99.5 percent pure), immediately strong H_2O lines would appear in the spectrum as well as the expected D_2O lines, the former presumably being due mainly to the presence in the radiation path of H_2O molecules which had been dislodged from the cell walls upon impact from the freshly introduced D_2O molecules. Exchange phenomena, too, were undoubtedly present, resulting finally in an equilibrium mixture of H_2O, HDO, and D_2O molecules.

It was only after great pains were taken to dry the mirror, its mountings, and the interior walls of the absorption cell that a comparatively pure D_2O spectrum could be obtained upon introduction of the gram of D_2O. Ideally a cell is dried out by long baking at a temperature of 300 to 400 degrees centigrade. Such a procedure was impossible in this case since neither the cell walls, the windows, or the seals could stand such a high temperature. The method finally adopted for drying out this cell and introducing the D_2O vapor was about as follows: Gas from a cylinder tank of especially dried nitrogen, after being further dried by passing through three bubble bottles filled with fresh concentrated sulfuric acid and then through two large liquid-air traps, was introduced slowly into the previously evacuated cell until atmospheric pressure of nitrogen was obtained. A small stream of gas was then, for a six-hour period, allowed to pass through the cell, emerging from a second opening. The gas inlet then being closed, the cell was continuously evacuated by the Megavac pump for a second six-hour period. Throughout this 12-hour period the cell itself was heated to a temperature of 50 to 60°C to aid the drying out process by increasing the vapor pressure of the adsorbed vapor. This whole process of flushing with dried nitrogen followed by sustained evacuation under continuous gentle heating was repeated three or

TABLE II. *Frequencies attributed to* HDO. *Symbolism used in this table has the following significance:* × = *definitely* HDO (*no* H_2O *or* D_2O *lines fall in this region at all*); · = *very weak* H_2O *or* D_2O *lines overlap the* HDO *line*; ? = *possibly due to higher spectral order*; 2 = *probably 2nd-order absorption line.* (*A blank space indicates that there are* H_2O *or* D_2O *lines superposed on the* HDO *enough so that the assignment is somewhat questionable.*) (*The intensity symbols are explained in a later paragraph.*)

419.62×mS	232.38 mw	179.88×m	157.52 mS	136.70× m
397.56×mS	224.89×m	177.62 m	156.47× S	135.77× mS
393.38× S	218.08× w	176.07 · m	153.55 S	135.22× mS
368.88×m	216.05×mS	175.11 m	151.53 m	134.32 · S
360.46×m	215.04 mw	172.28 m	150.56 mw	131.90 m
356.19×m	213.67 · mS	171.63 m	150.10×m	129.88× m
345.10×m	212.50 m	170.35 mS	149.10 mS	125.80× m
340.74×mS	210.88×m	169.30 · S	148.65 m	124.67 mw
334.90×mS	209.75×m	167.19×m	147.65×m	122.82 m
331.30 · mS	206.40 m	166.46 · S	147.06 mS	119.58 · mS
330.31 mw	205.70 mw	165.25 m	145.90×mS	118.86 m
305.18 mw	197.10 m	164.10 mw	145.08 m	118.70× S
298.75 m	193.48 mw	163.50 m	144.53 · S	117.12× m
270.70×mS	190.42×mw	163.28 · S	142.10 m	116.61 m
259.18 S	189.86×m	162.42 m	141.50 mw	116.15 ?2m
250.15×mS	187.43×mw	161.68 mw	141.21 mw	115.40 S
246.95×mS	185.94×m	160.28 m	140.66 m	114.48×? S
246.42×mw	184.70 mS	159.64 m	139.80 mS	113.93×? S
237.82×mS	182.33×m	158.93 m	138.95 m	113.19×?2 S
	180.39×m	157.85 mS	137.16×mS	111.78×?2 S
				110.73×?2 S

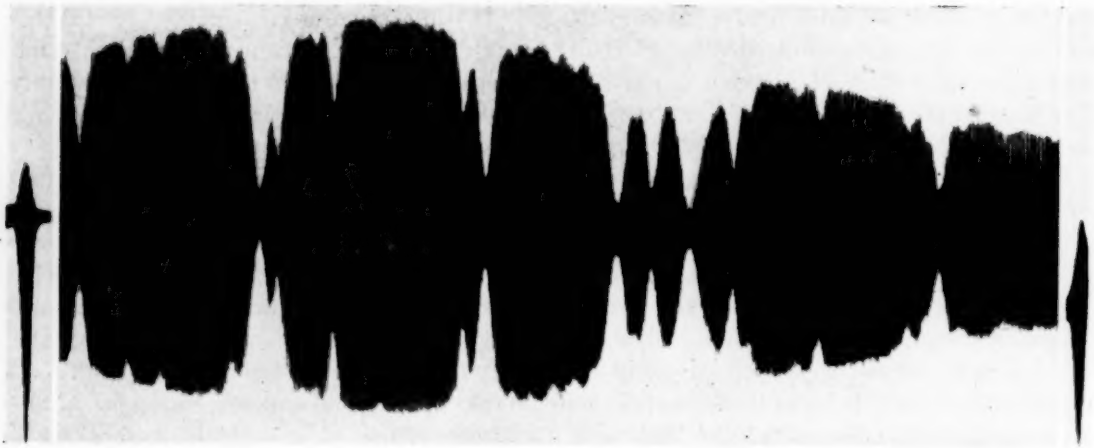

FIG. 1. H_2O vapor absorption in the region between 31 μ and 38 μ, using an echelette grating with 600 lines per inch (total number of lines is 12,000), low temperature source, amplification factor of $\times 200$, path length equivalent to 60 cm of saturated H_2O vapor at room temperature, effective slit width of 0.3 cm^{-1}. The dispersion is rather good in this record, as the "true width" of a strong absorption line is roughly four times the effective slit width. (Lines 0.5 cm^{-1} apart were separated but two strong doublets of 0.25 cm^{-1} separation distance look single.) The resolution is excellent. Optical path consists of thorium-oxide-coated source, Aquadag-coated thermopile receivers, NaF *reststrahlen* plate, NaCl shutter, 1 mm Metastyrene and 4 mm paraffin wax as filters. This arrangement gave excellent purity as is evidenced by the almost complete absorption of the stronger lines.

four times. Several one gram samples of D_2O liquid were then introduced into the cell, the heating and evacuation process being applied between each sample to further eliminate any remaining H_2O and to replace it by D_2O.

The final heavy water sample introduced was usually two grams. The D_2O reservoir flask was subjected to the same drying procedure. The liquid was introduced into it while dried nitrogen was being steadily passed through it. The reservoir was then attached to one of the cell inlets, and the D_2O vapor forced into the cell by gently heating the flask to quicken the evaporation process into the evacuated cell.

A rather complete transition from pure H_2O spectrum through a mixed H_2O, HDO, and D_2O spectrum to a pure D_2O spectrum was observed by making records of consecutive samples of supposedly pure D_2O introduced during different stages of the drying process. Indeed, the data on the HDO spectrum, which are given in Table II, were obtained from a critical comparison of such a series of transition spectra, and observation of which absorption lines disappeared at both ends of the spectral purity sequence.

2. Samples of records made

A large number of records of all kinds were made during the course of the work. While the majority of them were made with D_2O in the absorption cell, a complete set of background records were made, as well as a set of H_2O records. All regions of the D_2O spectrum from 23 μ to 135 μ were covered at least twice and sometimes as many as six or eight times. Records made with different gratings were taken so as to overlap as much as possible to check the mutual consistency of the gratings. The grating ruled with 900 lines-per-inch was used over the region from 22 μ to 40 μ, the 600-line-per-inch grating from 26 μ to 60 μ, the 360-line grating from 45 μ to 100 μ, the 133-line grating from 65 μ to 135 μ, and the 87.8-line grating from 80 μ to 200 μ. Three other gratings were also used for supplementary work.

Two records are reproduced here with a linear reduction factor of $\frac{1}{6}$ (see Figs. 1 and 2) and details in connection with them will be found under the figures. They do not give a complete picture of the types of records which may be taken on the spectrograph used, and for other illustrations of records reference may be made to previously published articles.[10]

3. Results of the experimental work

The 210 experimentally determined D_2O fre-

[10] Other records of D_2O and H_2O which were made during the course of this investigation may be found already published as follows: Randall and Firestone, reference 6, Figs. 5a, b, c, e, f, g.

FIG. 2. D_2O vapor absorption in the same region and under identical conditions used for the H_2O record shown in Fig. 1. A comparison of the two records reveals that the D_2O lines are much weaker and much more numerous. The weakness is due partly to the fact that the D_2O transitions here recorded are between energy levels having higher quantum numbers than those for the H_2O record, and partly to the intrinsically greater strength of the H_2O absorptions. The greater number is a result of the greater mass of the molecular components of D_2O which cause a crowding together of all the energy levels.

quencies obtained from the absorption records, together with their respective estimated intensities have been tabulated in Table III. These frequencies, and the HDO frequencies in Table II, are vacuum frequencies since the radiation path was well evacuated at all times. The relative intensity symbols have the followingsignificance: vvw (exceedingly weak) corresponds to from 0 percent to 5 percent absorption; vw (very weak) corresponds to from 5 percent to 10 percent; w (weak), 10 percent to 15 percent; mw (medium weak), 15 percent to 25 percent; m (medium), 25 percent to 40 percent; mS (medium strong), 40 percent to 55 percent; S (strong), 55 percent to 75 percent; and VS (very strong), 75 percent to 100 percent.

This research formed the first complete test of the recording spectrograph. For this reason it is interesting to notice the accuracy obtained for the frequency and intensity determinations. The latter are rough at best, as the instrument is not adapted for making simultaneous determinations of the energy background profile and the desired absorption curve. So many different optical path arrangements were used that such changes often changed the total energy background and the shape of this background. It will, however, be possible to install calibrated energy standards which will enable one to get rather high accuracy for the relative and absolute intensities without the need for simultaneous background determinations.

The accuracy of the frequency determinations was uniformly excellent over the whole range. In the regions of high accuracy and good dispersion for each grating the frequencies could be determined within an average uncertainty of 0.05 cm^{-1}. The gratings available were of sufficient number and of proper line spacing and blaze angle characteristics to give such accuracy over the entire range from 20 μ to 180 μ, assuming spectral purity in the first order. A great many retakes of different regions in the D_2O spectrum gave ample opportunity to check this stated accuracy. Absorption lines 0.5 cm^{-1} apart were partially resolved with ease, and under ideal conditions lines 0.3 cm^{-1} apart were detected as separate.

An interesting further check on the accuracy of the instrument was to compare the results obtained for H_2O with results previously obtained in this laboratory on a nonrecording spectrograph. One specific case will be cited. The vacuum values of measured frequencies of the twelve strongest single lines from the H_2O record reproduced in Fig. 1 were compared with the averaged data obtained on this hand operated

instrument.* (The weaker lines in the Fig. 1 record were not picked up in the earlier work.) The frequencies of Fig. 1 average 0.03 cm^{-1} higher than the RDGW values, a difference which is easily accounted for by the 0.05 cm^{-1} average uncertainty in the frequency determinations.

* This data is given in reference 5. The frequencies as tabulated in that paper, however, must be reduced to vacuum frequencies before they can be compared to those obtained from Fig. 1. Such a reduction diminishes each RDGW frequency by 0.03 percent (about 0.08 cm^{-1} on the average).

III. Theoretical

The problem now remains to identify the experimental absorption lines and from this identification to determine the rotational energy levels of the D_2O molecule.

1. Calculation of the "key" rotational energy levels

a. The energy level equations.—No attempt shall be made here to give a quantum theoretical derivation for the rotational energy levels, selection rules, and transition intensities of the asym-

TABLE III. *The rotation frequencies of heavy water vapor.*

*Legend: $x = \nu/c_{calc}$ uncertain (no comparison key). $xx = \nu/c_{calc}$ very uncertain. ? = I_{calc} is uncertain. * = ν/c_{obs} is uncertain; may be spurious. $a = \nu/c_{calc}$ is uncertain because of the overlapping of strong lines.*

ν/c_{OBS}	I_{OBS}	ν/c_{CALC}	I_{CALC}	$j'\tau'\leftarrow j''\tau''$ (ASSIGNED TRANSITION)
386.63	w			
383.70	w			
378.72	vw			
372.67	mw			
361.20	w			
358.36	m			
354.40	mw			
351.30	mw			
348.36	w	348.61 ?	2.0	$11_0 - 10_{-4}$
346.10	w			
343.50*	mw	343.67 ?	1.0	$10_1 - 9_{-3}$
339.50	m			
337.70	mw			
333.88	w			
331.30	w			
330.21	vvw			
328.90	w			
326.25	mw			
324.88	vw	324.9 xx	.8	$12_{12} - 11_{10}$
				$12_{11} - 11_{11}$
322.73	vvw			
321.45	vw			
320.95	vw			
319.95	vw			
316.95	mS			
315.10	m			
313.89	mS			
310.98	m			
309.40	w			
308.65	mw			
307.75	w			
305.18	mw			
302.02	S	301.80	2.5	$11_{11} - 10_9$
				$11_{10} - 10_{10}$
300.74	mw	300.75	.8	$11_{-6} - 10_{-10}$
299.85	mS	299.8 xx	2.0	$14_2 - 13_0$
				$14_1 - 13_1$
298.78	mS	298.38 ?	1.0	$11_{-2} - 10_{-6}$
297.38	vw			
296.52	w			
295.38	m	295.42	.5	$11_{-7} - 10_{-9}$
293.25	m			
292.37	mw			
291.53	m			
		289.6 xx	4	$12_6 - 11_4$
				$12_5 - 11_5$
289.59	mS	289.59	5	$11_9 - 10_7$
				$11_8 - 10_8$
288.56	m	288.5 xx	3	$13_1 - 12_1$
				$13_2 - 12_2$
		287.40 a	1.4	$11_{-4} - 10_{-8}$
287.26	S	287.3 xx	.8	$12_{-6} - 11_{-8}$
		287.06 ?a	1	$10_{-1} - 9_{-5}$
285.13	mw			
284.22	m			
281.57	m			
280.85	m			
277.90	m	277.99 ?	2	$9_0 - 8_{-4}$
		277.30	8	$10_{10} - 9_8$
				$10_9 - 9_9$
277.11	S	277.11	8	$11_7 - 10_5$
				$11_6 - 10_6$
275.38	mS	275.4 xx	8	$12_4 - 11_2$
				$12_3 - 11_3$
274.44	mS			
273.48	mS	273.62	.6	$10_{-5} - 9_{-9}$
272.65	mS			
272.12	S			
271.52	m	271.5 xx	4	$13_1 - 12_{-1}$
				$13_0 - 12_0$
269.94	w			
269.51	m	269.50 ?	2	$8_1 - 7_{-3}$
268.18	w			
265.54	m	265.50 ?	1	$10_{-2} - 9_{-7}$
264.56	m	264.56	15	$10_8 - 9_6$
				$10_7 - 9_7$
263.75	mw	263.80	1.5	$10_{-6} - 9_{-8}$
		263.65 ?	4	$7_2 - 6_{-2}$
263.11	mS	263.11	13	$11_5 - 10_3$
				$11_4 - 10_4$
262.18	w			
260.19	S	260.2 x	8	$12_2 - 11_0$
				$12_1 - 11_1$
259.18	mS			
258.23	mw	258.28	.6	$11_{-5} - 10_{-7}$
257.37	m			
256.95	mS			
255.00	m	254.93 ?		$6_3 - 5_{-1}$
254.00	mw	254 xx?	1.8	$12_{-4} - 11_{-6}$
252.09	m	252.09	21	$9_9 - 8_7$
				$9_8 - 8_8$
250.80	m	250.80	22	$10_6 - 9_4$
				$10_5 - 9_5$
250.15	mw			
249.55	w			
248.77	w			
		248.10 a	6	$11_3 - 10_1$
248.07	m	248.03	12	$11_2 - 10_2$
		245.5 xx	7	$12_0 - 11_{-2}$
245.10	mS	245.39 ?	2	$9_{-2} - 8_{-6}$
		244.96	2	$9_{-4} - 8_{-8}$
244.17	mS			
241.35	mw	241.3 xx	3	$12_{-1} - 11_{-1}$
238.38	mS	238.38	30	$9_7 - 8_5$
				$9_6 - 8_6$
237.47	m			
235.96	m	235.97	20	$10_4 - 9_2$
		235.95	10	$10_3 - 9_3$
232.52	m	232.50 ?	1	$9_{-5} - 8_{-7}$
		232.42	8	$11_1 - 10_{-1}$
231.50	w	231.5 xx	10	$12_{-2} - 11_{-4}$
230.93	w	230.98	15	$11_0 - 10_0$
228.90	mS	228.90 ?	4	$10_{-4} - 9_{-6}$
		227.18 ?	2	$8_{-1} - 7_{-5}$
225.94	m	225.94	45	$8_8 - 7_6$
				$8_7 - 7_7$
		225.94 ?	2	$11_{-3} - 10_{-5}$
223.71	mS	223.71	16	$9_5 - 8_3$
		223.70	32	$9_4 - 8_4$
221.41	w			
		220.50 a	1.3	$8_{-3} - 7_{-7}$
220.30	S	220.26	8	$11_{-1} - 10_{-3}$
		220.26	26	$10_2 - 9_0$
219.52	m	219.47	13	$10_1 - 9_1$
216.05	m			
213.80	m			
212.42	w	212.55 ?	3	$7_0 - 6_{-4}$
		211.4 xx	4.5	$12_{-3} - 11_{-5}$
211.35	mS	211.35	68	$8_6 - 7_4$
				$8_5 - 7_5$
		208.00	20	$9_3 - 8_1$
207.88	mS	207.88	38	$9_2 - 8_2$
206.55	mw	206.55	17	$11_{-2} - 10_{-2}$
205.59	m	205.62	29	$10_9 - 9_{-2}$
203.90	m			
202.80	mw	202.80 ?	6	$10_{-2} - 9_{-4}$
201.60	vw			
200.44	m			
		199.50 a?		$6_1 - 5_{-3}$
199.45	m	199.40 a	2.5	$8_{-4} - 7_{-6}$
198.78	mS	198.78	96	$7_7 - 6_5$
				$7_6 - 6_6$
		198.75 a	8	$9_{-3} - 8_{-5}$
		198.56 a	13	$10_{-1} - 9_{-1}$
197.18	m			
195.64	S	195.65	54	$8_4 - 7_2$
		195.61	27	$8_3 - 7_3$
194.74	m	194.72	3.5	$7_{-2} - 6_{-6}$
194.28	mw			
192.15	mS	192.10	22	$9_1 - 8_{-1}$
		189.42 ?		$5_2 - 4_{-2}$
189.28	mS	189.26	43	$9_0 - 8_0$
188.28	mw			
186.22	w			
184.69	S			
		183.43	36	$7_5 - 6_3$
183.42	VS	183.42	72	$7_4 - 6_4$
		183.20 a	20	$9_{-1} - 8_{-3}$
181.55	m			
179.37	S	179.37	60	$8_2 - 7_0$
178.32	S	178.32	30	$8_1 - 7_1$
177.72	mw			
176.93	w			
176.19	m	176.2 xx	5.5	$12_{-5} - 11_{-3}$
175.15	w			
173.58	mS			
		172.65 a	2	$6_{-1} - 5_{-5}$
172.37	mS	172.37 ?	20	$8_{-2} - 7_{-4}$
171.66	m			
170.81	VS	170.81	142	$6_6 - 5_4$
				$6_5 - 5_5$
169.88	vw			
		169.40 a?	2	$7_{-3} - 6_{-5}$
169.32	mS	169.30	17	$11_{-4} - 10_{-4}$
168.40	m			
		166.88	38	$7_3 - 6_1$
		166.76	50	$8_0 - 7_{-2}$
166.67	VS	166.75 a	14	$10_{-3} - 9_{-3}$
		166.60	77	$7_2 - 6_2$
165.25	vw			
164.15	w			

metric rotator, D_2O. Such derivations have been worked out completely in the literature.[11] It was found convenient to use the Nielsen[12]-Wang[13] equations as corrected and extended by Dennison.[5] These equations are

$$W/hc=j(j+1)\tfrac{1}{2}(C+B)+p[A-\tfrac{1}{2}(C+B)]$$
$$p=p(j,b);\quad b=\tfrac{1}{2}(C-B)[A-\tfrac{1}{2}(C+B)]^{-1}.$$

In these equations W/hc is the energy constant in cm^{-1}; j is the rotational quantum number; A, B, and C are quantities proportional to the reciprocals of the moments of inertia of the D_2O molecule, for example

$$A=(h^2/8\pi^2c)(1/I_A).$$

The choice of these "reciprocal moments" was finally made as follows: $A=15.38$ cm^{-1}, $B=7.25$ cm^{-1}, and $C=4.830006$ cm^{-1}. With this choice the asymmetry parameter, b, takes on the exact value -0.12955, making computations convenient. The general D_2O energy level expression then becomes:

$$W/hc=6.04j(j+1)+9.34p.$$

The $p(j, b)$ are roots of polynomial equations in

[11] For example, see D. M. Dennison, Rev. Mod. Phys. **3**, 280 (1931).
[12] H. H. Nielsen, Phys. Rev. **38**, 1432 (1931).
[13] S. C. Wang, Phys. Rev. **34**, 243 (1929).

TABLE III.—(*Continued*)

ν/c_{OBS}	I_{OBS}	ν/c_{CALC}	I_{CALC}	$j'\tau'\leftarrow j''\tau''$ (ASSIGNED TRANSITION)
163.57	mS			
163.25	vw			
162.50	w			
161.85	mS	161.88	40	$9_{-2}-8_{-2}$
160.95	w			
159.56	mS	159.6 *xx*	4	$15_{-13}-14_{-11}$
				$15_{-12}-14_{-12}$
159.10	S			
158.55	vw			
157.50	m			
155.15	mS	155.15	29	$8_{-1}-7_{-1}$
154.54	VS	154.57	100	6_1-5_2
		154.51	50	6_2-5_3
153.65	vvw			
		153.11 *a*	.2	11_9-11_7
				11_8-11_6
		152.97 *a*	.2	$10_{10}-10_8$
				10_9-10_7
152.72	mS	152.70 ?	6	5_0-4_{-4}
		152.7 *x*?	3	$13_{-8}-12_{-8}$
151.65	S	151.65	38	7_1-6_{-1}
150.63	w			
		149.8 *xx*	10	$14_{-12}-13_{-1}$
				$14_{-11}-13_{-11}$
149.67	S	149.6 *xx*	10	$15_{-15}-14_{-13}$
				$15_{-14}-14_{-14}$
148.60	vvw			
147.95	mS	147.95 ?	10	$7_{-1}-6_{-3}$
146.80	S	146.80	70	7_0-6_0
145.25	vvw	145.2 *xx*	6	$12_{-7}-11_{-7}$
144.42	vw			
		142.15	57	5_2-4_2
142.14	S	142.14	113	5_4-4_4
141.10	vw	141.04	.4	11_7-11_5
				11_6-11_4
		140.63 *a*	.6	10_8-10_6
				10_7-10_5
140.21	S	140.3 *x*	17	$13_{-11}-12_{-9}$
				$13_{-10}-12_{-10}$
		140.23 *a*	.6	9_8-9_7
				9_8-9_6
		140.1 *x*	19	$14_{-14}-13_{-12}$
				$14_{-12}-13_{-13}$
		138.73 *a*?	25	$6_{-2}-5_{-4}$
		138.61 *a*	20	$11_{-6}-10_{-6}$
138.40	VS	138.33	90	6_2-5_0
136.95	mw	136.9 *x*	12	$12_{-8}-11_{-6}$
136.15	mS	136.15	45	6_1-5_1
		135.52 ?	3	4_1-3_{-3}
134.43	m			
133.12	mS	133.12	13	$10_{-5}-9_{-5}$
131.25	m	131.2 *x*	9	$12_{-9}-11_{-9}$
		130.6 *x*	18	$12_{-10}-11_{-8}$
130.52	m	130.4 *x*	28	$13_{-13}-12_{-11}$
				$13_{-12}-12_{-12}$
127.96	S	127.96 ?	60	6_0-5_{-2}
		127.96	40	$9_{-4}-8_{-4}$
		127.61 *a*	.6	11_4-11_2
		127.59 *a*	.3	11_3-11_3
		127.04 *a*	1.3	10_6-10_4

ν/c_{OBS}	I_{OBS}	ν/c_{CALC}	I_{CALC}	$j'\tau'\leftarrow j''\tau''$ (ASSIGNED TRANSITION)
				10_5-10_3
126.88	S	126.87 *a*	1.7	9_7-9_5
				9_6-9_4
		126.52 *a*	2	8_8-8_6
				8_7-8_5
125.40	w			
		125.13	50	5_2-4_1
124.90	mS	124.70	100	5_2-4_2
123.60	mS	123.60	25	$8_{-3}-7_{-3}$
		123.52 *a*	8	$11_{-7}-10_{-5}$
122.28	w			
121.95	mS			
121.41	S	121.41	25	$11_{-5}-10_{-3}$
120.81	VS	120.8 *x*	42	$12_{-12}-11_{-1}$
				$12_{-11}-11_{-11}$
		120.68 ?		3_2-2_{-2}
		120.64	13	$11_{-9}-10_{-7}$
119.61	m			
118.76	mw			
117.95	VS	117.95	60	$7_{-2}-6_{-2}$
116.55	mw			
114.86	w			
		113.10 *a*?	3	$5_{-1}-4_{-3}$
		112.87	18	$10_{-7}-9_{-7}$
112.60	VS	112.61	104	4_4-3_2
		112.58 *a*	1.5	10_3-10_1
		112.57	57	4_3-3_3
		112.53 *a*	1	10_4-10_2
		112.21 *a*	2.5	9_4-9_2
		112.20 *a*	1	8_5-8_3
		112.19 *a*	1	9_5-9_3
		112.19 *a*	3	8_6-8_4
		111.93 *a*	3	7_7-7_5
				7_6-7_4
		111.32 *a*	1	11_2-11_0
		111.19 *a*	.5	11_3-11_1
		111.06	39	$11_{-10}-10_{-10}$
		111.05	18	$11_{-11}-10_{-9}$
111.05	VS	111.05	40	5_1-4_{-1}
		111.05	34	$6_{-1}-5_{-1}$
		110.97	20	$10_{-6}-9_{-4}$
		110.80	34	$10_{-8}-9_{-6}$
110.01	mw			
109.40	m			
108.78	mw			
108.12	mS			
106.49	mS			
105.65	m	105.65	1.5	$11_{-5}-10_{-3}$
104.48	S	104.48	45	$9_{-6}-8_{-6}$
103.38	S	103.38	66	5_0-4_0
		101.76 *a*	1.6	$11_{-3}-11_{-1}$
		101.72	24	$10_{-9}-9_{-9}$
101.70	S	101.66	48	$10_{-10}-9_{-8}$
101.28	m	101.39 *a*	.9	$11_{-9}-11_{-11}$
100.95	mw			
100.54	m			
100.00	m	100.00	20	$9_{-7}-8_{-5}$
99.49	w			
98.92	m			
98.24*	mS			

ν/c_{OBS}	I_{OBS}	ν/c_{CALC}	I_{CALC}	$j'\tau'\leftarrow j''\tau''$ (ASSIGNED TRANSITION)
		97.60	1.2	11_0-11_{-2}
		96.82 *a*	3.5	9_2-9_0
		96.58 *a*	2	6_5-6_3
		96.57 *a*	4	6_6-6_4
		96.49 *a*	6	7_4-7_2
		96.48 *a*	2	8_3-8_1
		96.46 *a*	3	7_5-7_3
		96.39 *a*	5	8_4-8_2
		96.33	27	$8_{-5}-7_{-5}$
96.33	mS	96.33	70	4_2-3_0
		96.10 *a*	2	9_3-9_1
		95.51 *a*	1.1	10_1-10_{-1}
94.70	mw	94.70	10	$9_{-5}-8_{-3}$
		94.27 *a*	2.2	10_2-10_0
93.74	mw	93.74	35	4_1-3_1
		93.57 *a*	.6	11_1-11_{-1}
92.05	S	92.13	56	$9_{-3}-8_{-3}$
		92.00	28	$9_{-9}-8_{-7}$
		91.80 *a*	1.2	$10_{-7}-10_{-9}$
91.31	vw	91.41	2.5	$10_{-8}-10_{-10}$
		89.45 ?	30	4_0-3_{-2}
89.10	mS	89.10	57	$7_{-4}-6_{-4}$
		88.86	45	$8_{-6}-7_{-4}$
88.00	vw	87.99 ?	4	$10_{-4}-9_{-2}$
		87.93 *a*	1.5	$11_{-6}-11_{-8}$
86.35	mS			
84.50	vw			
		82.98 *a*	.7	$11_{-7}-11_{-9}$
		82.90	32	3_3-2_1
		82.70	33	$8_{-7}-7_{-7}$
82.52	S	82.40	66	$8_{-8}-7_{-6}$
		82.40	65	3_3-2_3
		82.27 *a*	3.5	$9_{-6}-9_{-8}$
		82.21	30	$6_{-8}-5_{-8}$
		81.71 *a*	1.5	$11_{-2}-11_{-4}$
		81.41 *a*	1.4	$10_{-1}-10_{-3}$
		80.65 *a*	1.5	$9_{-7}-9_{-9}$
		80.34 *a*	6	5_4-5_2
		80.29 *a*	4	5_5-5_3
		80.20 *a*	3	8_1-8_{-1}
80.00	mS	80.11 *a*	8	7_2-7_0
		80.10 *a*	1.1	$10_{-5}-10_{-7}$
		79.91 *a*	5	6_3-6_1
		79.67 *a*	9	6_4-6_2
		79.63 *a*	4	9_0-9_{-2}
		79.19 *a*	4	7_3-7_1
		78.20	6	8_2-8_0
78.10	vw	78.08 ?	16	$8_{-4}-7_{-2}$
		78.06 *a*	1.8	$11_{-4}-11_{-6}$
76.00	S	76.05	50	$5_{-2}-4_{-2}$
		75.92	23	$7_{-5}-6_{-3}$
		74.60	2	9_1-9_{-1}
73.50	m	73.40	62	$7_{-6}-6_{-6}$
		73.17 *a*	2	10_0-10_{-2}
		72.65 *a*	2.1	$8_{-5}-8_{-7}$
		72.53 *a*	1.3	$10_{-3}-10_{-5}$
		72.50	30	$7_{-7}-6_{-5}$
72.05	w			

TABLE IV. *Ground state rotational energy levels of the heavy water vapor molecule.*

$W-W_k$	SYM	j_τ	W	$W-W_k$	SYM	j_τ	W	$W-W_k$	SYM	j_τ	W	$W-W_k$	SYM	j_τ	W
0.0	++	0_0	0.00	.24	++	6_{-2}	308.69	2.74	−+	9_{-1}	708.80	1.89	−+	11_{-7}	876.94
				.97	−+	6_{-3}	288.20	2.32	++	9_{-2}	703.03	1.48	++	11_{-8}	794.33
.0	+−	1_1	22.63	.88	−−	6_{-4}	279.68	1.89	+−	9_{-3}	659.20	1.46	+−	11_{-9}	793.96
.0	−−	1_0	20.20	.18	+−	6_{-5}	232.60	1.15	−−	9_{-4}	632.68	1.39	−−	11_{-10}	692.57
.0	−+	1_{-1}	12.08	.06	++	6_{-6}	231.92	2.32	−+	9_{-5}	620.30	1.39	−+	11_{-11}	692.57
								1.25	++	9_{-6}	562.12				
.0	++	2_2	74.03	.33	+−	7_7	780.76	1.07	+−	9_{-7}	560.45		++	12_{12}	2162.8
.02	−+	2_1	73.56	.33	−−	7_6	780.76	1.03	−−	9_{-8}	479.85		−+	12_{11}	2162.8
.0	−−	2_0	49.20	.91	−+	7_5	668.83	1.02	−+	9_{-9}	479.80		−−	12_6	1668.15
.0	+−	2_{-1}	41.94	.91	++	7_4	668.83						+−	12_5	1668.15
.0	++	2_{-2}	35.75	1.26	+−	7_3	572.37	−2.02	++	10_{10}	1536.09		++	12_4	1526.35
				1.26	−−	7_2	572.34	−2.02	−+	10_9	1536.09		−+	12_3	1526.35
.03	+−	3_3	156.46	1.36	−+	7_1	493.18	.17	−−	10_8	1383.12		−−	12_2	1400.0
.04	−−	3_2	156.43	1.26	++	7_0	492.23	.17	+−	10_7	1383.12		+−	12_1	1400.0
.0	−+	3_1	112.02	1.21	+−	7_{-1}	436.15	1.64	++	10_6	1242.49		++	12_0	1287.55
.0	++	3_0	109.81	.52	−−	7_{-2}	426.64	1.64	−+	10_5	1242.49		−+	12_{-1}	1287.5
.0	+−	3_{-1}	88.76	1.82	−+	7_{-3}	402.00	2.46	−−	10_4	1115.45		−−	12_{-2}	1191.8
.30	−−	3_{-2}	74.58	.51	++	7_{-4}	368.78	2.46	+−	10_3	1115.45		+−	12_{-3}	1190.75
.0	−+	3_{-3}	70.24	.95	+−	7_{-5}	364.12	2.37	++	10_2	1002.92		++	12_{-4}	1136.25
				.44	−−	7_{-6}	305.32	2.38	−+	10_1	1002.87		−+	12_{-5}	1107.8
.04	++	4_4	269.04	.47	−+	7_{-7}	305.10	2.86	−−	10_0	908.65		−−	12_{-6}	1081.65
.04	−+	4_3	269.03					2.86	+−	10_{-1}	907.36		+−	12_{-7}	1022.15
.21	−−	4_2	206.14	.16	++	8_8	1006.70	2.13	++	10_{-2}	835.48		++	12_{-8}	1019.15
.25	+−	4_1	205.76	.16	−+	8_7	1006.70	2.19	−+	10_{-3}	825.95		−+	12_{-9}	925.15
.25	++	4_0	164.03	1.05	−−	8_6	880.18	2.75	−−	10_{-4}	791.02		−−	12_{-10}	924.95
.52	−+	4_{-1}	158.29	1.05	+−	8_5	880.18	2.84	+−	10_{-5}	753.42		+−	12_{-11}	813.35
.77	−−	4_{-2}	141.42	1.60	++	8_4	767.99	1.67	++	10_{-6}	743.65		++	12_{-12}	813.35
.41	+−	4_{-3}	117.37	1.60	−+	8_3	767.98	1.31	−+	10_{-7}	673.32				
.08	++	4_{-4}	114.71	1.70	−−	8_2	671.60	1.64	−−	10_{-8}	672.92		−+	13_3	1688.5
				1.75	+−	8_1	671.50	1.29	+−	10_{-9}	581.52		++	13_2	1688.3
.21	+−	5_5	411.18	1.34	++	8_0	593.40	1.30	++	10_{-10}	581.51		+−	13_1	1559.0
.22	−−	5_4	411.18	1.48	−+	8_{-1}	591.30						−−	13_0	1559.0
.33	−+	5_3	330.89	1.09	−−	8_{-2}	541.15	−4.45	+−	11_{11}	1837.89		−−	13_{-8}	1171.85
.32	++	5_2	330.84	2.34	+−	8_{-3}	525.60	−4.45	−−	11_{10}	1837.89		++	13_{-10}	1065.25
.88	+−	5_1	269.34	1.00	++	8_{-4}	504.72	−1.68	−+	11_9	1672.71		+−	13_{-11}	1065.45
.45	−−	5_0	267.41	.87	−+	8_{-5}	460.45	−1.68	++	11_8	1672.71		−−	13_{-12}	943.75
1.05	−+	5_{-1}	230.47	.93	−−	8_{-6}	457.64	1.14	+−	11_7	1519.60		−+	13_{-13}	943.75
.46	++	5_{-2}	217.47	.75	+−	8_{-7}	387.80	1.14	−−	11_6	1519.60				
1.57	+−	5_{-3}	205.99	.78	++	8_{-8}	387.72	2.45	−+	11_5	1378.56		++	14_2	1858.8
.24	−−	5_{-4}	169.96					2.45	++	11_4	1378.56		−+	14_1	1858.8
.34	−+	5_{-5}	168.88	−0.55	+−	9_9	1258.79	2.72	+−	11_3	1250.97		−+	14_{-11}	1215.2
				−0.55	−−	9_8	1258.79	2.70	−−	11_2	1250.95		−−	14_{-12}	1215.0
.32	++	6_6	581.98	.87	−+	9_7	1118.56	3.56	−+	11_1	1139.78		+−	14_{-13}	1083.8
.32	−+	6_5	581.98	.87	++	9_6	1118.56	3.49	++	11_0	1139.63		++	14_{-14}	1083.8
.56	−−	6_4	485.41	1.75	+−	9_5	991.69	2.96	+−	11_{-1}	1046.21				
.57	+−	6_3	485.40	1.75	−−	9_4	991.69	2.39	−−	11_{-2}	1042.03		++	15_{-12}	1374.7
.96	++	6_2	405.74	2.15	−+	9_3	879.50	3.15	−+	11_{-3}	979.36		+−	15_{-13}	1374.8
.98	−+	6_1	405.49	2.15	++	9_2	879.48	2.84	++	11_{-4}	960.32		−−	15_{-14}	1233.4
0.79	−−	6_0	345.43	2.09	+−	9_1	783.40	1.21	+−	11_{-5}	931.60		−+	15_{-15}	1233.4
.89	+−	6_{-1}	341.53	1.77	−−	9_0	782.66	2.43	−−	11_{-6}	882.26				

b, there being four such equations for each value of j, and a total of $2j+1$ roots for each value of j. The energy levels for each j are arbitrarily arranged by order of magnitude and labeled with an index, τ, which runs from $+j$ to $-j$.

Energy levels through $j=11$ were calculated by means of these equations. They were then corrected for rotational stretching by a method to be described later. These corrected energy levels, hereafter called the key energy levels, are not listed in this paper explicitly, but may be obtained from Table IV by subtracting from each member in column 4 the corresponding member of column 1. It remains to explain the basis for the choice of the moments of inertia, and the method of correcting for the rotational stretching effects. These two subjects will be considered in order.

b. Calculation of "reciprocal moments" of inertia.—The three principal moments of inertia of any rigid molecule may be computed by the equations of classical mechanics if the atomic

masses and interatomic distances are known. The masses in this case are well known, and the other atomic constants have been computed by Mecke[14] for H_2O from experimental data. Assuming that the potential constants, which govern the interatomic distances, are independent of mass changes in the molecule, these H_2O values will also hold for D_2O. With Mecke's value for the atomic constants, r, and φ (see Fig. 3), the reciprocal moments for D_2O become; $A=15.15$ cm^{-1}, $B=7.21$ cm^{-1}, and $C=4.89$ cm^{-1}. (Note that these do not differ greatly from the values finally used.)

The D_2O molecule is, however, not a rigid rotator. It has vibrational modes and in the ground vibrational state, even for the case of no rotation, it has a certain amount of energy due to the everpresent vibrational half-quantum numbers. Since there is a vibration-rotation interaction, this gentle vibration of the molecule causes the moments of inertia for the ground state to differ from the "true" moments determined above.

The choice of the moments of inertia upon which to base the preliminary energy levels was crucial; they had to be very nearly correct if the identification was to be straightforward. The "true" moments were of the right order of magnitude, but it was decided to attempt to find a better set which would depend somewhat on this vibration effect. Mecke[14] has evaluated the "effective" moments of inertia of H_2O for the ground state as well as for a number of the excited vibrational states from measurements of the vibration-rotation bands in the near infra-red. If the "isotope effect" upon the moments is known, the corresponding effective moments for D_2O may be found. The evaluation of this mass dependence for an asymmetric or even for a symmetric molecule would involve a great deal of analysis and computation. The process is known, however, for the simpler case of the diatomic molecule.[15] If mass variations are assumed to affect the moments of inertia in the same way for various types of molecules, then an analogy will prove helpful.

The procedure followed was to find the zeroth-order and the 2nd-order solutions of the diatomic molecule, then to determine what changes in the moments of inertia of the zeroth-order solution would give the results gotten straightforwardly by means of the more exact solution. Such computation gave the following expression

$$(h^2/8\pi^2)(1/I_{eff})=K_1+K_2(n+\tfrac{1}{2})+K_3j(j+1)$$

where the K's are constants dependent on the true moment of inertia of the molecule (diatomic molecule has only one nonzero moment) and upon the normal frequency of vibration. The mass dependency only gives

$$1/I_{eff}=k\mu^{-1}+k'\mu^{-\frac{3}{2}}(n+\tfrac{1}{2})+k''\mu^{-2}j(j+1),$$

where the k's are constants which are independent of mass. (Dependence on vibrational state only is considered here. Rotational perturbation effects will be considered separately later. For this reason the last term on the right will be ignored.) Application of the analogy between the diatomic molecule and the asymmetric rotator molecule suggests that the effective reciprocal moments of the water vapor type molecule be written in the following form

$$A=a_0+\sum_{i=1}^{3}a_i(n_i+\tfrac{1}{2})$$

where $a_0=k_0\mu^{-1}$, and $a_i=k_i\mu^{-\frac{3}{2}}$, with similar equations for B and C.

The 12 constants in the three H_2O equations of this type were so chosen that they gave a minimum deviation between the moments of inertia calculated by means of them and the moments

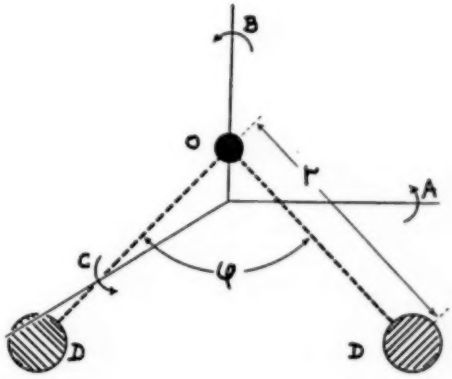

FIG. 3. Diagram of the D_2O vapor molecule, showing the dimensional quantities, r, and φ, and the axes of inertia, A, B, and C.

[14] R. Mecke, *et al.*, Zeits. f. Physik **81**, 313, 445, 465 (1933).
[15] W. F. Colby, Phys. Rev. **34**, 53 (1929); E. Fues, Ann. d. Physik **80**, 367 (1926).

determined by Mecke from the experimental data of his 17 most accurately located vibration bands. Since the constants for D_2O are related to those for H_2O as follows,

$$a_{0_D}=\left(\frac{\mu_H}{\mu_D}\right)_A a_{0_H}; \quad a_{i_D}=\left(\frac{\mu_H}{\mu_D}\right)_A^{\frac{1}{2}} a_{i_H}, \quad i=1, 2, 3$$

the effective reciprocal moments for D_2O may be determined by means of the following combined relation

$$A=\left(\frac{\mu_H}{\mu_D}\right)_A a_{0_H}+\left(\frac{\mu_H}{\mu_D}\right)_A^{-\frac{1}{2}} \sum_{i=1}^{3} a_{i_H}(n_i+\tfrac{1}{2})$$

(with similar expressions for B and C) if the value of the reduced mass ratios is known. This problem of choosing reduced masses for the asymmetric molecules presents an additional problem. Strictly speaking, the term "reduced mass" applies only to a two-body system. However if the analogy be drawn upon again, it is possible to make a choice of reduced masses associated with the moments of inertia about the two principal axes lying in the plane (A and B; see Fig. 3) which are quite unambiguous. For the reduced mass associated with the reciprocal moment, C, about the axis perpendicular to the molecular plane, different values could be obtained when calculated from different but perhaps equally valid points of view. It was finally decided to evaluate C for any particular vibration state by means of the classical relationship: $I_C=I_A+I_B$. This relation holds for any rigid plane figure but can only be an approximation for a vibrating plane molecule.

Table V gives the values of the inertial constants for H_2O and D_2O. They are of value for the calculation of reciprocal moments for vibration states other than the ground state. It was by means of these constants that the reciprocal moments finally used were evaluated.

c. The rotational stretching correction.—The perturbing action of rotation on the moments of inertia was not evaluated through the use of the diatomic molecule analogy as was done for the vibration-rotation interaction. An additional rotational quantum number is present, there being no parallel to τ or k in the diatomic case. Thus any computation of rotational correction based on this simpler molecule would be too incomplete to be valuable. This rotational perturbation upon the moments of inertia of the asymmetric rotator was a problem which had not been solved at the time this analysis was made. Yet it is a very important correction, having especially large influence upon light molecules. Qualitatively it differs for each value of j and τ, increasing rapidly for higher quantum numbers.

TABLE V. *Inertial constants.*

	H_2O	D_2O		H_2O	D_2O		H_2O	D_2O
a_0	27.41	15.22	b_0	14.56	7.28	c_0	9.53	4.92
a_1	−0.70	−0.29	b_1	−0.24	−0.09	c_1	−0.17	−0.06
a_2	2.70	1.12	b_2	0.22	0.08	c_2	−0.17	−0.06
a_3	−1.20	−0.50	b_3	−0.10	−0.04	c_3	−0.15	−0.06

It was found more feasible to correct the energy levels themselves for rotation, rather than to attempt some correction directly to the reciprocal moments. Order of magnitude rotational corrections for the highest and the lowest energy levels of any particular j value might have been computed in the same manner that was done[5] for H_2O. However since a complete list of the rotational corrections had been found[5] for H_2O, it was more convenient to find how these correction factors depended on mass changes, and to apply this mass dependence ratio to get the D_2O factors from the H_2O factors. This dependency may easily be found from Dennison's zeroth-order rotational energy level correction development. He gives

$$\delta W_0/hc=\alpha j^4/\beta$$

where

$$\alpha=h/8\pi^2\mu y_0^2; \quad \beta=(ab-d^2)y_0^2/2b.$$

Therefore

$$\delta W_0\sim\mu^{-2}; \quad \delta W_{0_D}=(\mu_H/\mu_D)^2\delta W_{0_H}.$$

This discussion, for any given j value, applies (1) to rotation about the least axis of inertia (the 2 largest τ values) in which the mass factor is approximately 0.308; and (2), to a lesser approximation, to rotation about the greatest axis (the 2 smallest τ values) for which the mass ratio factor is about 0.268. Corrections for the energy levels between the highest and the lowest τ value pairs, for a given j, fitted in only roughly with this discussion of mass dependence. The conversion factor for them was assumed to lie some-

where between the two values given above. Thus for many of the corrections terms there was an uncertainty of 10 percent to 20 percent, assuming that the H_2O values to which the mass factors were applied were essentially correct. Rigorous analysis of the effect of rotation upon rotation must be made before this uncertainty is eliminated.

2. Intensities of the rotation lines

a. Relation between the τ and k index.—(This preliminary discussion of the relation between symmetric rotators and asymmetric rotators will prove valuable for reference later when line intensities are considered.) There is no direct relation between the index, τ, of the asymmetric rotator and the quantum number, k, of the symmetric rotator. However Dennison[16] has shown that if for any particular value of j, the $2j+1$ values of W/hc are plotted for varying degrees of asymmetry (letting $I_A<I_B<I_C$, and letting I_B vary in value from I_A to I_C), in both limiting cases where the asymmetry disappears, single τ values or pairs of τ values may be associated with each of the k's for the resulting symmetric rotator. Also each energy level retains its original τ index throughout as the ordering by magnitude does not change.

Further Dennison shows that an asymmetrical rotator, when in one of its closely paired energy states corresponding to its larger τ values, it is very similar to a symmetric rotator whose least moment of inertia lies along the unique axis (axis of rotation). The asymmetric rotator in these states, may, therefore, be qualitatively considered as rotating around its axis of least inertia. By the same reasoning an asymmetric rotator, when in energy states of lowest (large negative) τ values, can be best pictured as rotating around its greatest inertial axis. Levels corresponding to the intermediate values of the index, τ, are badly paired, and fit in poorly with either of the symmetric rotator cases considered. Therefore these levels are associated roughly with rotations about the intermediate moment of inertia axis, a case having no counterpart in the symmetric rotator.

b. Symmetry classes and selection rules.—Each wave function, $\psi_{j\tau}$, belongs to one of four symmetry classes, $(++)$, $(--)$, $(+-)$, and $(-+)$. The first sign in the bracket is determined by the symmetric rotator k number to which the τ index is associated when the asymmetric rotator is pictured as spinning about its axis of greatest inertia, being positive for even values of this k, and negative for odd values. The second sign is similarly positive or negative depending on the "even"ness or "odd"ness of the k value associated with the wave function's τ value for assumed rotation about the least moment of inertia axis. The reasons for this scheme of assignment are given in Dennison's paper[16] together with a derivation of the following selection rules: (1) for j, $\Delta j=\pm 1, 0$; (2) for τ, if the electric moment lies along the middle moment of inertia axis (this being true of D_2O and H_2O in the ground state) transitions may occur only between $(++)$ and $(--)$, or between $(+-)$ and $(-+)$.

c. Transition probabilities and intensities.—Tolman[17] gives a derivation of the expression for the intensity of an absorption transition in the general molecular case. Applying this to the special case of the D_2O molecule asymmetric rotator, the intensity of a transition from state $\psi_{j''\tau''}$ up to state $\psi_{j'\tau'}$ is given by

$$I_{j''\tau''}^{j'\tau'} \cong I_{j''k''}^{j'k'} = CF(\nu/c)BDA_{j''k''}^{j'k'}.$$

C is a constant for any given molecule. It has the value

$$C=4\pi^3NM^2/3h\sum_a g_a e^{-W_a/kT}$$

where M is the constant factor in the symmetric rotator electric moment matrix, N is the total number of molecules per cc, g_a is the statistical weight of the state with energy W_a.

F is the factor accounting for alternation of intensities due to nuclear spin contributions. For D_2O it takes on the values

$F=\frac{2}{3}$ for even τ valued transitions
$F=\frac{1}{3}$ for odd τ valued transitions

ν/c is the transition frequency expressed in cm^{-1}.

B is the Boltzmann factor accounting for the statistical distribution as a function of energy.

[16] D. M. Dennison, Rev. Mod. Phys. **3**, 280 (1931). In this regard see especially Fig. 15 on page 322 of this reference.

[17] R. C. Tolman, *Statistical Mechanics with Applications to Physics and Chemistry* (New York, 1927), p. 268.

As usual it is written $\exp[-W_{j''\tau''}/kT]$; for room temperature it has the value, when written in more convenient form,

$$B=\exp[-0.0049W_{j''\tau''}/hc].$$

D, the factor accounting for differences between induced absorption and induced coherent emission, has the value

$$D=1-e^{-h\nu/kT}.$$

The $A^{j'k'}_{j''k''}$ are factors in the symmetric rotator electric moment matrix which are dependent on the quantum numbers j and k. (They are also made to include the statistical weight factor, $2j+1$, introduced because of the energy expression being degenerate in the third quantum number, m.) Specifically, as calculated by Dennison,[16]

$$A^{j\ k}_{j-1\ k\mp1}=\frac{(j\pm k)(j\pm k-1)}{j},$$

$$A^{j\ k}_{j\ k\mp1}=\frac{(2j+1)(j\pm k)(j\mp k+1)}{j(j+1)}.$$

There are a number of important remarks still to be made in connection with this intensity expression. First of all a justification for the use of symmetric rotator elements in the intensity expression for an asymmetric rotator must be given. $A^{j'\tau'}_{\tau j''\tau''}$ is the matrix element of the electric moment corresponding to the transition whose intensity is sought. It is to be calculated from the minors of the secular determinant constructed from the energy matrix of the asymmetric rotator. Dennison[5] has calculated these matrix elements through $j=3$, and has shown that an easier method of getting the approximate intensities of the more important transitions is through the use of symmetric rotator elements. This can be shown qualitatively by recalling that wave functions of large τ index can be associated with rotation of the asymmetric rotator about its least inertial axis, and that corresponding energy levels may be approximated by energy levels of a symmetric rotator spinning about a comparable "least" axis. These approximations also hold good for the matrix elements of transitions between members within this class of wave functions. Thus the intensities of this class of transitions may be well approximated by the intensities of the corresponding symmetric rotator transitions.

A like discussion shows that intensities of transition between levels of low τ index are fairly well approximated by intensities calculated for corresponding transitions of a symmetric rotator when spinning about its comparable axis of greatest inertia. The levels with intermediate τ indices being poorly approximated, a transition into this region or across this region must be computed from both "points of view," and some sort of weighted average taken which will give a rough idea of the line intensity. A large number of transitions allowed for the asymmetric rotator cannot be calculated in this approximate way as the selection rules forbid them in the case of the symmetric rotator. These lines will be ignored as they will be assumed to be too weak to be of importance in the identification of experimentally observed absorption lines.

Furthermore the evaluation of the constant, C, demands some notice. To compute absolute intensities the "*zustande summa*" for the D_2O molecule would have to be computed. This is impossible without previous knowledge of all the important energy levels. Relative intensities were accordingly used in this analysis. It was helpful to adjust the constant so that the D_2O intensities are on the same relative scale as the H_2O intensities of the RDGW study. The latter molecule's transition intensities have been tabulated[5] assuming the C for H_2O to be unity. The constants C_H, and C_D, differ only because of different masses. If the assumption is made that the effect of mass changes upon this constant is somewhat the same for different types of molecules, then it can be evaluated easily through the solution of the problem for the diatomic molecule. In this case,

$$W=\frac{j(j+1)h^2}{8\pi^2I},\quad g_j=2j+1$$

and the *zustande summa*

$$\sum_{j=0}^{\infty}(2j+1)\exp[-\{j(j+1)h^2/8\pi^2IkT\}].$$

Let $s=h^2/8\pi^2IkT$, and approximate the summation by an integral over j.

$$\int_0^\infty (2j+1)e^{-j(j+1)S}dj = \frac{1}{S}\int_0^\infty e^{-j(j+1)S}d(j(j+1)S) = \frac{1}{S} \sim \mu.$$

The *zustande summa* varies directly, and therefore the constant C, varies inversely with the reduced mass.

$$C_D\mu_D = C_H\mu_H; \quad C_D = (\mu_H/\mu_D)C_H; \quad C_H \equiv 1.$$

These mass ratios may be shown to take on values of 0.5, 0.555, and 0.543 depending upon which axis is chosen in computing the reduced masses. Since both the analogy and the calculation itself are only approximate, the value $C_D = 0.5$ has been used throughout the analysis.

Finally a word about the nuclear spin factor, F. The D_2O molecule contains two identical nuclei, deuterons, which obey Einstein-Bose statistics. Each has a nuclear spin of $h/2\pi$. Alternating intensities are observed in the rotation spectra of such homonuclear molecules. The intensity of transition between symmetric levels divided by that between antisymmetric levels[18] is for this case: $(S_n+1)/S_n = 2/1$. The $(++)$ and $(--)$ levels (even τ values) are symmetric, while the $(+-)$ and $(-+)$ levels (odd τ) are antisymmetric. For this analysis, then, we let $F = \frac{2}{3}$ for even-τ transitions, and $F = \frac{1}{3}$ for the odd.

3. The analysis

The records, as experimentally made, were photographic plots of intensity as the ordinate against *wave-length* as the approximately linear abscissa. Different records had widely different coordinate scale factors and were thus often difficult to compare with each other. For the purpose of study and analysis it was convenient to plot the average of these data on a linear *frequency* scale. This plot appears as the connected curve in Fig. 4.

The method of analysis was essentially to identify the lines of the experimental data by means of a comparison with the "key" transitions, and then to construct a "true" or "adjusted" set of energy levels which were consistent with the data. Details of this process follow.

[18] R. de L. Koenig, *Band Spectra and Molecular Structure* (Macmillan, 1930), p. 96.

a. The key.—The key frequencies for allowed transitions were determined from the key energy levels together with the selection rules. Approximate intensities were calculated for as many transitions as possible. In Fig. 4 these key frequencies are plotted as similar isosceles triangles below the experimental data, the same frequency scale being used for both. The areas of the triangles have been chosen to be proportional to the intensities of the corresponding key transitions. (An unsuccessful attempt was made to plot theoretical intensities in terms of an experimentally determined absorption coefficient.)

b. The first assignment.—A study of the correlations between the experimental lines and the key transitions led to the observation that strong lines in the data occurred in general a few tenths of a wave number above intense lines in the key. Accordingly the first tentative assignment was made by the simple procedure of associating each key transition with the closest absorption line in the data which appeared to have a reasonably similar intensity. Further examinations of the two sets of lines were made to see if any other over-all assignment would be found upon shifting the key frequencies up or down by a few wave numbers together with proportional increase or decrease in line separations. No such alternative assignment gave nearly as satisfactory an account of the lines as did this first and most obvious one. It appeared reasonable, then, to assume that the preliminary choice of moments of inertia, together with the approximate corrections applied, had produced an energy level key which was rather close to the true level scheme sought.

c. Series regularities.—After making this first assignment a study of series regularities and combination relations brought about some adjustment, and occasionally a reassignment of transition frequencies, leading to the final values which are to be found plotted in the top lines of Fig. 4. More should be said about these aids in the analysis. It has been pointed out[5] that there are analytic series regularities associated with the pairs of transitions which have a common value of $(j-k)$ when considered as symmetric rotator transitions. An example of one such series is given in Table VI, in which the regularity of the 2nd differences of the transitions based on

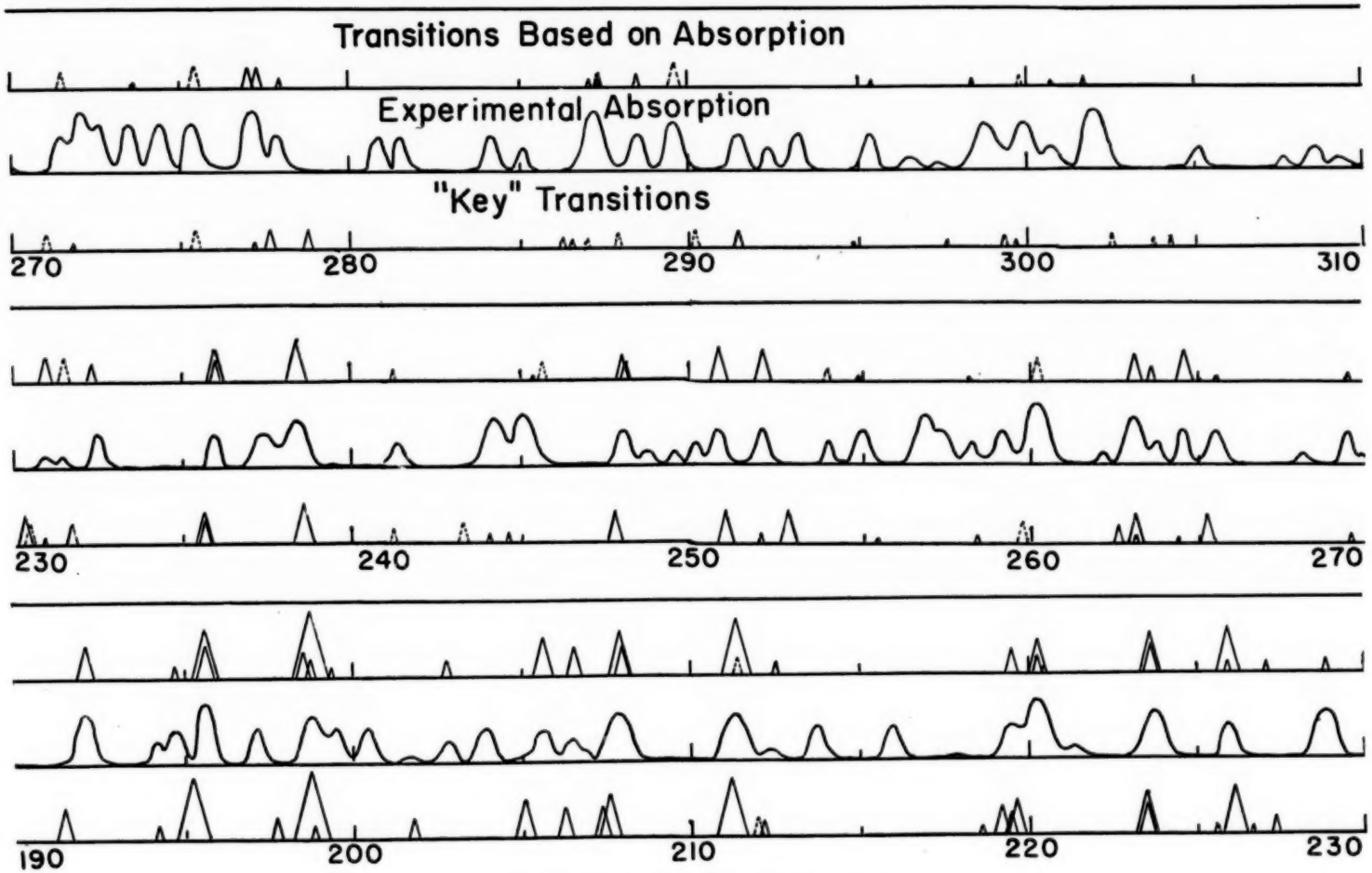

(This figure is continued on opposite page.)

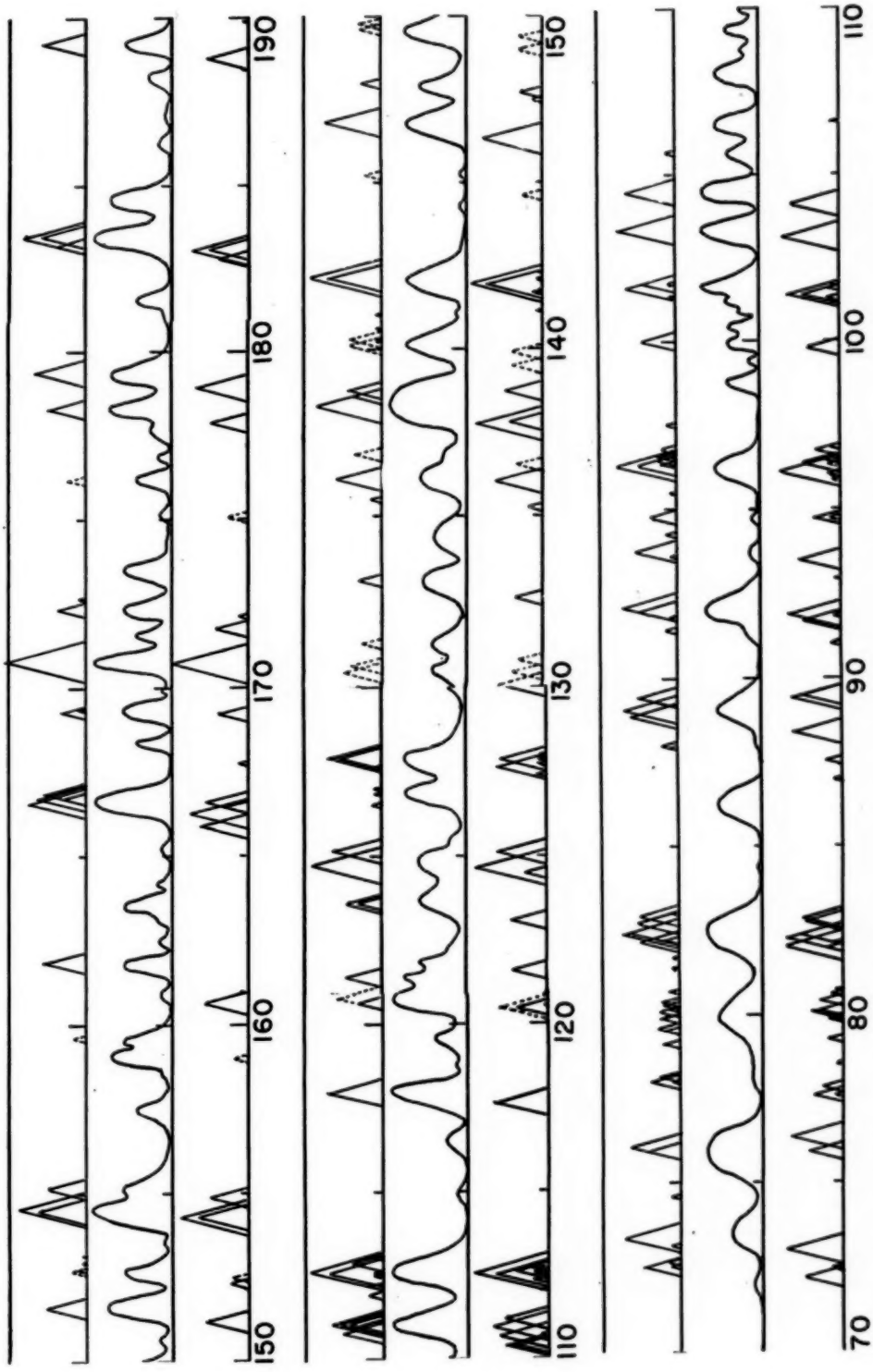

FIG. 4. Plot of D_2O frequencies in waves per centimeter. The bottom row of triangles is a graph of transitions between the key energy levels. The middle curve is a graph of the experimentally measured absorption spectrum of D_2O. The upper triangles represent the transition frequencies as assigned on the basis of the experimental data.

data is shown to compare favorably with those of the key transitions. Other groups of analytic series were found useful, though it will not be necessary to discuss the types in detail. In all, a dozen series were found which included five or more energy level transitions. A study of these series showed that the 2nd differences for the adjusted frequencies averaged 0.1 to 0.2 cm^{-1} greater than the corresponding 2nd differences in the key transition series.

Series with fewer than five terms were not useful for checking assignments. Also a number of series were composed of transition pairs of very low intensity and so did not aid much in the adjustment of frequencies. In some cases different series of the same type were nearly superposed upon each other, especially for the higher values of j. This superposition made assignments in these cases quite ambiguous. It also made it difficult if not impossible to correlate experimentally observed line intensities with calculated intensities of single or superposed transitions.

Extrapolation of the best series gave tentative assignments, consistent with the data, for transitions between some of the levels above $j=11$. The lowest series (low τ indices) could be extended up to $j=15$ with some degree of assurance. These extrapolated frequencies are plotted in Fig. 4 as broken-line triangles to differentiate them from those based more directly on comparisons with the computed key transitions.

d. Combination relations.—In order to further adjust values of transitions and to make the correct assignments two skeleton diagrams were drawn, one to show the allowed transitions between symmetric levels, and the other, between antisymmetric levels. (The numerical values of the energy levels themselves were not included until toward the end of the analysis.) This framework proved convenient in the process of visualizing and computing combination relations. Such relations were computed around as many closed circuits as possible. They were especially important in connecting the upper part of each diagram with the lower part, and in working out the consistency of the lower parts themselves, for series regularities gave little help in these regions.

Transitions of the vertical type (e.g., 6_6-6_4), and those so-called "inverted" transitions in which $\Delta\tau=4$ (e.g., 5_0-4_{-4}), were essential members in each combination relation loop. Unfortunately these lines usually were of very small intensity. They were also in a great many cases almost exactly superposed both upon each other and upon other more intense transitions. This superposition (see Fig. 4) was so marked in the low frequency region that sometimes as many as eight transitions were assigned to an experimental absorption line which itself appeared single. Accordingly the frequencies of most of these vertical and inverse transitions could not be fixed more accurately than within a range of several tenths of a frequency unit. For convenience in the analysis these frequencies were so assigned within their allowed uncertainty range that combination relations gave zero sums around closed loops. Such circuit relations are, then, not to be considered more than rough checks on the consistency of the assignment. In Table III a suffix, a, distinguishes these arbitrarily adjusted frequencies from those whose values were sharply fixed by the experimental data. It should be mentioned that in the few cases where these weak transitions fell in isolated regions, their value was fixed by the experimental data, and such assignments could be used as criteria for judging the correctness of other lines.

e. Energy level assignment.—The transitions having been assigned in as satisfactory a manner as possible, the energy levels were obtained by assuming the correctness of the following key levels; 2_2, 2_1, 3_1, and 3_0. The rest of the energy levels were determined by means of transitions from these starting point levels. Eight low levels, 1_1, 1_0, 1_{-1}, 2_0, 2_{-1}, 2_{-2}, 3_{-1}, 3_{-3}, were not reached by the assigned transitions. Key level values

TABLE VI. *Highest series* ($j-k=0$).

	KEY SERIES				EXPERIMENTAL SERIES		
j	FREQ.	1ST DIFF.	2ND DIFF.	j	FREQ.	1ST DIFF.	2ND DIFF.
2	52.37						
3	82.62	30.25		3	82.65		
4	112.59	29.97	0.28	4	112.59	29.94	
5	141.96	29.37	.60	5	142.15	29.56	0.38
6	170.70	28.74	.63	6	170.81	28.77	.79
7	198.77	28.07	.67	7	198.78	27.97	.80
8	226.11	27.34	.63	8	225.94	27.16	.81
9	252.80	26.69	.65	9	252.09	26.15	1.01
10	278.77	25.97	.72	10	277.30	25.21	.94
11	304.23	25.46	.51	11	301.80	24.50	.71

TABLE VII. *Difference between experimental levels and key levels.*

$(j-k)$	$j=2$	3	4	5	6	7	8	9	10	11
0	0.00	0.03	0.04	0.21	0.32	0.33*	0.16	−0.55	−2.02	−4.45
1		.00	.23	.32	.55	.89	1.05*	.87	.17	−1.68
2			.38	.70	.97	1.25	1.60	1.75*	1.65	1.14
3				.60	.88	1.28	1.72	2.15	2.46*	2.45
4						1.00	1.39	1.93	2.38	2.70*

were assigned to these also, no other method of assignment being possible. (2_{-2} and 3_{-3} were deducible each through a single weak inverse transition but key level values were adopted as giving the more reliable value.)

The levels of even τ value could be computed quite separately from those of odd τ value by means of the skeleton transition diagrams to which reference has been made. The consistency of the energy levels could, then, be checked at many points by the requirement that the even and odd τ indexed level pairs had to have identical values or small separation values given approximately by the key level separations.

These levels based on data are tabulated in Table IV. Column 1 shows the deviation of these experimental levels from the key levels. If the deviations are regrouped by series, as shown in Table VII for the five most important series, the amount of this deviation and the rate of increase of deviation with quantum number changes may be seen to show a reasonable regularity. It is also to be noted that in each series the deviations increase to a maximum then decrease, this maximum point (indicated by * in the body of Table VII) shifting to higher values of j as one goes from the highest toward the lower series.

IV. SUMMARY AND DISCUSSION

The experimental D_2O absorption frequencies together with their assignments as transitions between energy levels of the rotating D_2O molecule have been placed in Table III. Experimental and calculated intensities are also included in this tabulation. In Fig. 4 the top row is a plot of the experimentally assigned transition frequencies, the center row is an averaged plot of the experimental data, and the bottom row is a plot of the key frequencies which were computed quite independently of the experimental data here shown. A comparison of these three frequency diagrams gives a graphic picture of the results of the analysis and shows how closely the key diagram fitted the actual data. From this analysis 184 rotational energy levels for the ground state of D_2O vapor have been evaluated. These have been recorded in Table IV.

210 absorption lines were observed experimentally. 192 key transitions were used in the analysis (this number included all transitions up through $j=11$ which had measurable intensities and which fell within the 75 cm^{-1} to 350 cm^{-1} range.) 111 distinct energy levels (single or fused doublets) resulted from the analysis. 24 levels above $j=11$ were tentatively assigned by means of 24 transitions consistent with the data. The maximum intensity of a fused pair of transitions was 170 units; for a single transition, 110 units. There were, in round numbers, 100 transitions with intensities less than 5 units, 50 with intensities between 5 and 20 units, 50 with intensities between 20 and 60 units, and 15 with intensities over 60 units.

The theoretical transition frequencies are well accounted for by the experimental absorption lines. The only transitions to which no satisfactory assignment could be made were (4_1-3_{-3}), $(8_{-1}-7_{-5})$, and $(11_{-2}-10_{-6})$ which were weak inverse transitions, and $(7_{-7}-6_{-5})$, a medium strong line which fell at the extreme long wavelength limit of the region covered by this experimental research, a region where the absorptions were very uncertain at best. This latter line was arbitrarily assigned to satisfy combination relations with lines, which were in more reliable regions from the experimental point of view, even if they were less intense. Incidently this arbitrary assignment gave the desired amount of splitting of the two transitions making up a term in the lowest series, the other transition being independently assigned.

There were a large number of experimentally determined absorption lines for which no theoretical assignment could be made. Most of these were found in the high frequency region, where it was legitimate to assume that transitions between higher energy levels might be found to account for them if the analysis were to be extended to higher energy levels. There are, however, a number of lines in the low wave number range which could not be accounted for in this way, notably a medium strong line at 86.35

cm^{-1}, several medium lines lying between 98 cm^{-1} and 101.3 cm^{-1}, another group between 105 cm^{-1} and 110 cm^{-1}, as well as the following scattered strong and medium lines in the medium wave number range: 157.50 cm^{-1}, 159.10 cm^{-1}, 163.57 cm^{-1}, 173.58 cm^{-1}, and 184.69 cm^{-1}.

Neither were these lines to be explained as being due to H_2O impurities or to 2nd-order spectral impurities, as they did not coincide with the strongest H_2O lines or 2nd-order lines in the region. It was also quite improbable that they were spurious lines as they were found time and time again on different gratings and with different optical paths.

It is possible that the HDO impurities were not completely eliminated and thus were responsible for these absorptions. If so, it should be possible to eliminate them by a more complete drying out of the absorption cell. Another possibility is that certain of the allowed transitions whose intensities could not be calculated by means of the symmetric rotator matrix elements do, nevertheless, have measureable intensities and should be considered. Finally, there is the possibility that the whole assignment of theoretical transitions has been incorrect. If this be true, then it means that the effective moments of inertia calculated in the analysis are greatly in error. The assignment would have to be completely reconsidered in order to account for these lines at all. As has been previously stated, several attempts were made during the analysis to find alternative assignments which would account for the experimental data, and none were found to be nearly as satisfactory as the one developed here.

Assuming the general correctness of the analysis however, the next problem is to develop rigorous methods of computing the rotational distortion of the asymmetric rotator so that the effective moments of inertia may be recomputed with precision from the energy levels obtained from this research. The dimensions of the molecule may then be well established.

One of the authors (N. F.) would like to acknowledge support from a Rackham Predoctoral Fellowship during 1937–38, the year in which the experimental part of this work was done.

NOVEMBER 15, 1939 PHYSICAL REVIEW VOLUME 56

Van der Waals Potential in Helium

H. MARGENAU
Yale University, New Haven, Connecticut

(Received September 22, 1939)

Part I is an investigation of the fundamental question concerning the additivity of first-order exchange and second-order van der Waals potentials. The method employed is a variational one which allows both first- and second-order exchange effects to be calculated simultaneously with the second-order attractive terms. It is shown that the assumption of additivity is entirely false for atomic hydrogen, but that it is almost legitimate for He. By extrapolation one might conclude it to be quite safe for heavier structures. Part II is a redetermination of the numerical values occurring in the attractive part of the potential, based on the use of oscillator strengths (f values) which are adjusted to give the best value for the atomic polarizability of He. It appears that the value of the dipole-dipole coefficient in the Slater-Kirkwood formula has been too high. The final result for the van der Waals potential (Eq. (20)) seems on the whole to be consistent with independent determinations of this quantity from empirical data.

NUMEROUS questions arising in the study of the behavior of helium at low temperatures require for their treatment a fairly accurate knowledge of the van der Waals potential between helium atoms.

Considerable attention has therefore been devoted[1–4] to attaining an empirical answer to the

[1] J. Lennard-Jones, Proc. Roy. Soc. **106**, 463 (1924).
[2] J. de Boer and A. Michels, Physica **5**, 945 (1938); **6**, 409 (1939).
[3] J. O. Hirschfelder, R. B. Ewell and J. R. Roebuck, J. Chem. Phys. **6**, 205 (1938).
[4] H. S. W. Massey and R. A. Buckingham, Proc. Roy. Soc. **168**, 378 (1938); **169**, 205 (1938).

problem at hand; i.e., curves for the van der Waals potential in He have been derived from thermodynamic data. The present paper is the converse to these attempts in as much as it endeavors to deduce the potential in a more *a priori* manner from the atomic structure of He.

Previous work on this problem[5, 6] stands in need of improvement principally in two respects. The first concerns the common procedure of adding exchange forces calculated by one method to the asymptotic van der Waals forces calculated by quite a different method. This, if it is legitimate at all, requires analytic justification. Secondly, the accuracy of former calculations of the coefficients of the attractive terms in the potential should be improved. In accordance with these considerations, the present paper will consist of two parts dealing with these two points.

It is perhaps unfortunate that the most interesting part of the potential in question, the minimum, arises from an interplay of two types of forces—exchange and dispersion forces—and its determination, therefore, requires about equal accuracy in our knowledge of both. This means that the calculation may not be restricted to the $1/R^6$ term in the dispersion part, and that the repulsive forces must be studied with considerable care. It is usually assumed that the potential energy in question may be written in the form

$$\Delta E = Ae^{-\mu R} - \frac{c_1}{R^6} - \frac{c_2}{R^8}; \qquad (1)$$

the higher terms of the series have been shown to be negligible for He.[6]

I. Second-Order Exchange Forces

The simple form of Eq. (1) is the result of the following procedure. One adds the *second*-order perturbation $(-c_1/R^6 - c_2/R^8)$ calculated with atomic functions *not* satisfying the Pauli principle to the *first*-order perturbation $(Ae^{-\mu R})$ calculated with functions *satisfying* the Pauli principle. This is clearly inconsistent; for if it is necessary to go to the second perturbation in connection with the attractive terms this should also be done with the others. Eisenschitz and London[7] have calculated the complete second-order perturbation for atomic hydrogen. Their method, however, is not easily applied to the Helium problem, nor does it yield results which allow a ready comparison with the terms of (1). We shall use for the same purpose a more direct variational method, the results of which are equivalent to those of Eisenschitz and London for hydrogen. The procedure will first be described in detail for hydrogen, and afterwards the complications appearing in the helium problem will be dealt with.

Hydrogen

The variation function which yields the attractive part of the van der Waals potential may be written[8]

$$\psi = (1+\lambda D)\psi_0,$$

where D is the operator $H-E_0$ (H being the total Hamiltonian of the system consisting of two atoms, one at a, the other at b, and E_0 twice the energy of one isolated atom), ψ_0 is the function $\varphi_a(1)\varphi_b(2)$ (φ being the atomic function for the normal state), and λ is a variation parameter. With the use of ψ we find

$$\int \psi H \psi d\tau = \int \psi (D+E_0)\psi d\tau = D_{00} + 2\lambda (D^2)_{00} + \lambda^2 (D^3)_{00} + E_0 \int \psi^2 d\tau, \qquad (2)$$

if we note the Hermitean character of D. The subscripts 0 indicate, of course, matrix elements computed with ψ_0. The order of magnitude of the different terms in (2) is important. If we denote by V the perturbation function $H-H_0$, we have $D_{00}=V_{00}$, a quantity which is of appreciable size only at distances of separation $R=|\mathbf{a}-\mathbf{b}|$ considerably smaller than that at which the van der Waals minimum occurs. Indeed when V is expanded in powers of $1/R$, as is customary, V_{00} vanishes exactly. Furthermore it may be shown that $(D^2)_{00}=(V^2)_{00}$, but we are not permitted to replace $(D^3)_{00}$ by $(V^3)_{00}$

[5] J. C. Slater and J. G. Kirkwood, Phys. Rev. **37**, 682 (1931).
[6] H. Margenau, Phys. Rev. **38**, 747 (1931).
[7] R. Eisenschitz and F. London, Zeits. f. Physik **60**, 491 (1930).
[8] The present development is essentially an application of the Hassé method, first applied to this problem in reference 5.

because of the noncommutability of the operators H_0 and V. In fact

$$(D^3)_{00}=\int D\psi_0 D^2\psi_0 d\tau=\int V\psi_0 DV\psi_0 d\tau$$

$$=(V^3)_{00}+\int V\psi_0(H_0-E_0)V\psi_0 d\tau,$$

and the last integral may be transformed by partial integrations[9] into

$$\frac{\hbar^2}{2m}\sum_i\left[\left(\frac{\partial V}{\partial x_i}\right)^2\right]_{00}.$$

But this quantity may be written as $-(1/2m)\Sigma_i \times[(P_iV)^2]_{00}$ where P_i is the momentum operator, which indicates at once that the order of magnitude of the term is not the same as that of $(V^3)_{00}$, but of $E_0(V^2)_{00}$. We see, therefore, that even if λ is small (it will be seen to be $\approx 1/E_0$), the term $\lambda^2(D^3)_{00}$ in (2) must be retained as comparable in size with $\lambda(D^2)_{00}$.

On the other hand, the integral

$$\int\psi^2 d\tau=1+2\lambda D_{00}+\lambda^2(D^2)_{00}$$

contains terms of descending orders of magnitude and may safely be approximated by 1 because $D_{00}=0$. Hence we find

$$\int\psi H\psi d\tau\Big/\int\psi^2 d\tau=2\lambda(D^2)_{00}+\lambda^2(D^3)_{00}+E_0 \quad (3)$$

and this becomes

$$\lambda'(D^2)_{00}+E_0=\lambda'(V^2)_{00}+E_0,$$

when it is minimized with respect to λ. The value of λ at the minimum, here denoted by λ' and given by $-(D^2)_{00}/(D^3)_{00}$, may be found from other considerations. The attractive part of the van der Waals potential, which will henceforth be denoted by E_2, is seen to be

$$E_2=\lambda'(D^2)_{00}. \quad (4)$$

The approximation thus obtained is equivalent to that of second-order perturbation theory.

Let us now turn to the repulsive exchange energy. In the Heitler-London method, which was used by Slater[10] in calculating the term $Ae^{-\mu R}$ for He, it is given simply by

$$E_1=\int\psi D\psi d\tau\Big/\int\psi^2 d\tau, \quad (5)$$

when ψ is taken to be $(1-P)\psi_0$, ψ_0 being defined as before. P is understood to be the operator which permutes electrons 1 and 2. In expanded form, Eq. (5) reads

$$E_1=\frac{D_{00}-(DP)_{00}}{1-P_{00}}. \quad (6)$$

On comparing the two variation functions which yield, respectively, E_1 and E_2, it is clear that the two separate procedures may be combined and a better approximation to the van der Waals forces obtained by using the variation function

$$\Psi=(1+\lambda D)(1-P)\psi_0. \quad (7)$$

It leads to the following integrals:

$$\int\Psi^2 d\tau=2\{1-P_{00}+2\lambda[D_{00}-(DP)_{00}]$$

$$+\lambda^2[(D^2)_{00}-(D^2P)_{00}]\}.$$

Here again, terms in different powers of λ form a rapidly descending sequence, and restriction to the terms linear in λ is proper.

$$\int\Psi D\Psi d\tau=2\{D_{00}-(DP)_{00}$$

$$+2\lambda[(D^2)_{00}-(D^2P)_{00}]+\lambda^2(\ )\}. \quad (8)$$

The term in λ^2 is comparable in size with the one preceding it. In minimizing $\int\Psi D\Psi d\tau/\int\Psi^2 d\tau$ with respect to λ, which is the next step to be taken, one can easily convince himself that the term proportional to λ in the denominator has very little effect upon the value of the minimum. Beyond this we shall assume in order to simplify the analysis, that the value of λ which minimizes (8) is nearly the same as the one which minimizes (3). As before, we get for this value of λ an expression identical with (8), but with the term in λ^2 missing and the numerical coefficient of the preceding one reduced to unity. Con-

[9] Cf. for instance H. Margenau, Rev. Mod. Phys. **11**, 1, 25 (1939).

[10] J. C. Slater, Phys. Rev. **32**, 349 (1928).

sequently

$$\int \Psi D\Psi d\tau \Big/ \int \Psi^2 d\tau = \frac{D_{00}-(DP)_{00}+\lambda'[(D^2)_{00}-(D^2P)_{00}]}{1-P_{00}+2\lambda'[D_{00}-(DP)_{00}]}.$$

This expression represents the van der Waals energy we are seeking. When it is compared with (6) and (4) it is at once seen to reduce to

$$\Delta E = \frac{E_1+(1-P_{00})^{-1}[E_2-\lambda'(D^2P)_{00}]}{1+2\lambda'E_1}. \quad (9)$$

Of course our result shows clearly that one may not, in general, add E_1 and E_2 and expect to get a good approximation to the van der Waals energy. Let us look at the magnitude of the various quantities in (9). For atomic hydrogen the minimum comes at $R\approx 7a_0$, a_0 being the first Bohr radius. (Cf. Eisenschitz and London or reference 9.) At this distance, E_1 and $-E_2$ are about 2 millivolts. $\lambda'\approx 1/E_0$ (cf. below). Therefore the quantity $2\lambda'E_1$ is less than 0.001 and may be neglected against 1 for our purposes. A further simplification arises on decomposing P_{00}. We have

$$P_{00}=\int \psi_0 P\psi_0 d\tau = \int \varphi_a(1)\varphi_b(2)\varphi_a(2)\varphi_b(1)d\tau = \delta^2,$$

where

$$\delta = \int \varphi_a\varphi_b d\tau_1 = e^{-\rho}(1+\rho+\rho^2/3)$$

and

$$\rho \equiv R/a_0.$$

At $\rho=7$, $\delta=0.022$ so that $1-P_{00}$ may be safely replaced by 1. At larger distances the error is even smaller, and smaller distances are not of interest in connection with the present problem. We may say, therefore, that as long as the overlap integral δ^2 is small compared to unity, the van der Waals energy is composed additively of 3 terms:

$$\Delta E = E_1+E_2-\lambda'(D^2P)_{00}, \quad (10)$$

the last of which will now be calculated.

As to notation, we specify that r_{12} shall be the distance between electrons 1 and 2, and that a_2, for instance, shall be the distance between nucleus a and electron 2. On writing down the Hamiltonian operator H and also recalling that ψ_0 and $P\psi_0$ satisfy the equations

$$[E_{\text{kin}}-e^2(a_1^{-1}+b_2^{-1})\psi_0 = E_0\psi_0,$$
$$[E_{\text{kin}}-e^2(b_1^{-1}+a_2^{-1})P\psi_0 = E_0P\psi_0,$$

one sees immediately that

$$D\psi_0 = e^2(r_{12}^{-1}+R^{-1}-b_1^{-1}-a_2^{-1})\psi_0$$

and

$$DP\psi_0 = e^2(r_{12}^{-1}+R^{-1}-a_1^{-1}-b_2^{-1})P\psi_0.$$

Consequently

$$(D^2P)_{00}=\int D\psi_0 DP\psi_0 d\tau = e^4\int (r_{12}^{-1}+R^{-1}-b_1^{-1}-a_2^{-1})(r_{12}^{-1}+R^{-1}-a_1^{-1}-b_2^{-1})\psi_0 P\psi_0 d\tau.$$

The integrals here encountered are all listed in the appendix to the paper by Eisenschitz and London.[11] When the results are collected, the expression reads

$$\begin{aligned}(D^2P)_{00}=\frac{e^4}{a^2}\Big\{ & e^{-2\rho}\Big(\frac{5}{4\rho}-\frac{13}{10}+\frac{24}{5}\rho+\frac{53}{15}\rho^2+\frac{2}{3}\rho^3-\frac{4}{81}\rho^4-\frac{4}{27}\rho^5\Big)\\ & +2e^{-\rho}\delta\Big[\Big(1-\frac{1}{\rho}\Big)(1-C-\log\rho)\Big]\\ & +\frac{\delta^2}{\rho^2}\Big[1+\frac{12}{5}(C+\log\rho)\Big]\\ & +\frac{4}{3}e^{-\rho}Ei(-\rho)\Big(\rho^2+\rho^3+\frac{2}{9}\rho^4-\frac{1}{9}\rho^5-\frac{1}{27}\rho^6\Big)\\ & -Ei(-2\rho)\Big(\frac{24\delta\delta'}{5\rho^2}-\frac{4}{\rho}+\frac{8}{3}\rho+\frac{4}{3}\rho^2-\frac{20}{27}\rho^4+\frac{16}{81}\rho^6\Big)\\ & +Ei(-4\rho)\Big[\frac{12\delta'^2}{5\rho^2}+e^{\rho}\delta'\Big(2-\frac{2}{\rho}\Big)\Big]\Big\};\end{aligned} \quad (11)$$

$$\delta' = e^{\rho}(1-\rho+\rho^2/3); \quad C=0.577.$$

It now becomes necessary to evaluate λ. It is well known from the work of London that

$$E_2 = -(V^2)_{00}/p|E_0|$$

where p is a number, usually not far from unity,

[11] The last integral in their list contains an error (presumably typographical). It should read: $2e^{-\rho}\sqrt{S}$. Their S is our δ^2.

which depends on the position of the "centroid" of excited energy states. For hydrogen, $p=0.92$. But according to Eq. (4),

$$E_2=\lambda'(D^2)_{00}=\lambda'(V^2)_{00}.$$

Hence

$$\lambda'=-1/p|E_0|.$$

To illustrate the significance of the correction term we assemble the constituents of ϵ for $\rho=7$, i.e., near the v.d.W.-minimum in hydrogen:

E_1	E_2	$-\lambda(D^2P)_{00}$	ΔE
2.2	−1.95	−0.98	−0.73 millivolts

E_2 here includes, as it should, the dipole-quadrupole and quadrupole-quadrupole contributions. The result agrees with that of reference 7, which was obtained by second-order perturbation theory. The second-order exchange term is indeed larger than the depth of the minimum itself, and its omission would falsify the total result completely.

For purposes of rough calculations it is convenient to have a simpler function by means of which $(D^2P)_{00}$ can be approximated. It was found that

$$(D^2P)_{00}\doteq-(e^4/a_0^2)4.20e^{-1.675\rho} \qquad (12)$$

within an accuracy of 5 percent for values of ρ between 6 and 10.

Helium

The energy E_1 has been calculated by Slater[10] with the use of a nonanalytic wave function which describes the atomic properties of He very well, a function which is undoubtedly superior by far to the one we shall employ in the calculation of the second-order exchange effect. To carry through the integrations conveniently hydrogenic wave functions with suitable screening constants will be chosen in this work. This has the further advantage that the calculations yield expressions similar to those which have already been evaluated for hydrogen.

Let φ_a stand for the wave function of a single electron. Screening may be taken account of by a change in the "equivalent Bohr radius" a: the exponent in the wave function is $(Z-s)(r/a_0)=r/a$; this makes $a=a_0/1.688$ for He. Thus all integrals will be the same as for H except for this change in a. The usual v.d.W.-energy E_2 corresponds to the function

$$\psi=(1+\lambda D)\psi_0$$

with

$$\psi_0=\varphi_a(1)\varphi_a(2)\varphi_b(3)\varphi_b(4).$$

On the other hand, E_1 corresponds to

$$\psi=(1+P_{13}P_{24}-P_{24}-P_{13})\psi_0,$$

where P_{ij} is the operator interchanging the arguments of the ith and jth electrons in the function on which it acts. Explicitly,

$E_2=\lambda'(D^2)_{00}$ as before, and

$$E_1=(1-\delta^2)^{-2}[D_{00}-(DP_{13})_{00}-(DP_{24})_{00}+(DP_{13}P_{24})_{00}].$$

We propose to use the function

$$\Psi=(1+\lambda D)(1+P_{13}P_{24}-P_{24}-P_{13})\psi_0,$$

assuming again that the minimizing value of λ for this function is not affected by the addition of the exchange operators. The minimum value of the expression $\int\Psi D\Psi d\tau/\int\Psi^2 d\tau$ with this function is

$$\Delta E=\frac{(1-\delta^2)^{-2}\{[D_{00}-(DP_{13})_{00}-(DP_{24})_{00}+(DP_{13}P_{24})_{00}]+\lambda'[(D^2)_{00}-(D^2P_{13})_{00}-(D^2P_{24})_{00}+(D^2P_{13}P_{24})_{00}]\}}{1+2\lambda'(1-\delta^2)^{-2}[D_{00}-(DP_{13})_{00}-(DP_{24})_{00}+(DP_{13}P_{24})_{00}]}$$

$$\doteq E_1+E_2-\lambda'[(D^2P_{13})_{00}+(D^2P_{24})_{00}-(D^2P_{13}P_{24})_{00}].$$

In the last step we have again neglected δ^2 and $2\lambda'E_1$ against unity, an approximation which is entirely safe in the neighborhood of the v.d.W.-minimum and beyond. It is now necessary to compute three correction terms.

We have

$$H=E_{\text{kin}}+e^2(-2a_1^{-1}-2a_2^{-1}+r_{12}^{-1}-2b_3^{-1}-2b_4^{-1}+r_{34}^{-1}-2b_1^{-1}-2b_2^{-1}-2a_3^{-1}-2a_4^{-1}+r_{13}^{-1}+r_{14}^{-1}+r_{23}^{-1}+r_{24}^{-1}+4R^{-1}),$$

whereas ψ_0 satisfies the equation

$$[E_{\text{kin}}+e^2(-2a_1^{-1}-2a_2^{-1}+r_{12}^{-1}-2b_3^{-1}-2b_4^{-1}+r_{34}^{-1})]\psi_0=E_0\psi_0.$$

Therefore $D\psi_0=(H-E_0)\psi_0=U\psi_0$

where

$$U=e^2(-2b_1^{-1}-2b_2^{-1}-2a_3^{-1}-2a_4^{-1}+r_{13}^{-1}+r_{14}^{-1}+r_{23}^{-1}+r_{24}^{-1}+4R^{-1}).$$

(U is not symmetrical with respect to an interchange of electrons, as is D.) The integral

$$(D^2P_{13})_{00}=\int D\psi_0 DP_{13}\psi_0 d\tau=\int U\psi_0 P_{13}(U\psi_0)d\tau$$

$$=\int (UP_{13}U)(\psi_0 P_{13}\psi_0)d\tau.$$

The next integral is equal to this; for ψ_0 is symmetrical with respect to the transpositions (1, 2) and (3, 4), so that

$$(D^2P_{24})_{00}=\int \psi_0 D^2P_{24}\psi_0 d\tau$$

$$=\int P_{12}P_{24}\{\psi_0 D^2P_{24}\psi_0\}d\tau=\int \psi_0 D^2P_{13}\psi_0 d\tau.$$

Finally, in the approximation in which δ^2 is neglected against unity, the integral $(D^2P_{13}P_{24})_{00}$ may be disregarded. This can be seen roughly as follows.

The factor $(\psi_0 P_{13}P_{24}\psi_0)$ appearing in the integrand would, if integrated alone, yield δ^4, while the (00)-element of the single permutation P_{13} is δ^2. Though this does not prove the smallness of all integrals appearing in $(D^2P_{13}P_{24})_{00}$, it is a hint which is verified on calculating this quantity in detail.

We may say, then, that

$$\Delta E \doteq E_1+E_2-2\lambda'(D^2P_{13})_{00} \qquad (13)$$

and we shall now show that the integral of the correction term is reasonably well approximated by the quantity $(D^2P)_{00}$ already computed for hydrogen.

This can be seen on physical grounds. When the helium atom is in its normal state, the chance that both of its electrons be far away from the nucleus is very much smaller than that one shall be far away and one near it. Thus, when two helium atoms interact, at distances several times the atomic diameter, exchange will effectively take place only between two electrons at one time. The other two will be near their nuclei, so that the interaction is essentially hydrogenic. When one is interested in the forces at smaller distances of separation, this argument may not be used.

Mathematically, the result comes about in this way. When

$$(D^2P_{13})_{00}=\int U(P_{13}U)\varphi_a(1)\varphi_b(1)\varphi_a^2(2)\times\varphi_a(3)\varphi_b(3)\varphi_b^2(4)d\tau$$

is expanded, it contains, besides the integrals occurring in the foregoing section, a considerable number which do not represent pure exchange but involve direct parts as well. Examples are:

$$\int \frac{\varphi_a^2(1)\varphi_a(2)\varphi_b(2)}{b_1 r_{12}}d\tau$$

and

$$\int \frac{\varphi_a^2(1)\varphi_a(2)\varphi_b(2)\varphi_a(3)\varphi_a(3)}{r_{13}r_{23}}d\tau.$$

The leading term in these integrals is obtained by treating φ_a^2 as strongly concentrated about the nucleus a (δ-function). In the complete integral this term is multiplied by an expression of the form $[1+e^{-\rho}$ (polynomial)$]$. This will here be taken as 1; the error thus introduced is hardly greater than 5 percent at values of ρ in which we are interested here ($e^{-\rho}\approx 10^{-4}$). If this procedure is adopted, these two integrals reduce to

$$\frac{1}{R}\int \frac{\varphi_a(1)\varphi_b(1)}{b_1}d\tau_1$$

and

$$\int \frac{\varphi_a(1)\varphi_b(1)\varphi_a(2)\varphi_a(2)}{a_2 r_{12}}d\tau.$$

When similar approximations are carried out on all integrals of this type, $(D^2P_{13})_{00}$ for helium collapses to $(D^2P)_{00}$ for hydrogen (though D^2 contains many more and quite different terms in the former case than in the latter).

λ' will be determined as before; p is very nearly 1, so that $\lambda'=-1/2E_i$, where E_i is the

first ionizing potential of He. For $(D^2P)_{00}$ we may take the approximate expression (12). Now the minimum of the v.d.W. potential in helium occurs at about $R=5.5a_0=9.3a$, that is, the equivalent $\rho(=R/a)$ for He is much greater than that for $H(=R/a_0)$, although the minimum actually occurs at a smaller distance of separation in He.

On inserting these values, we have

$$-2\lambda'(D^2P)_{00} \doteq -(e^4/E_i a^2)\cdot 4.20e^{-1.675\rho}$$
$$= -350e^{-1.675\rho} \text{ volts},$$

which, for $\rho=9.3$, has the value -5.9×10^{-5} ev. Again we list the constituent parts of ΔE at the minimum ($R=2.9$A). The conclusion is that the

E_1	E_2	$-2\lambda(D^2P)_{00}$	ΔE
0.72	−1.75	−0.06	−1.09 e. millivolts

second-order exchange effect for He is almost negligible, a fact which is perhaps surprising in view of the large rôle it plays in H. It explains why the simpler theories have had some measure of success in connection with the helium problem.

It is probably safe to add a remark about the magnitude of this effect in the heavier rare gases without further calculation. A detailed investigation would be complicated by the fact that the electrons involved are no longer 1*s*-electrons. Nevertheless, if the exponential part of the wave function is the decisive feature, the effect is determined by the magnitude of $(D^2P)_{00}$ for the equivalent value of ρ at the v.d.W. minimum, and this equivalent value of ρ depends on the screening constant for the outer electrons through a. If we take Slater's screening constants and identify the distance of the v.d.W. minimum with the kinetic theory diameter, the values of ρ turn out quite large; for Ne and Ar, e.g., they are about 18. At these distances the exponential (12) is entirely insignificant even after multiplication by the factor 8, the number of electrons in the outer shell. We conclude, therefore, that for heavier atoms the second-order exchange effect is negligible.

Slater's expression for the first-order exchange potential in He is not likely to be much in error; at any rate it would be very difficult to improve it. Hence we turn our attention now to the attractive terms in Eq. (1).

II. Attractive Forces

Several calculations of these terms, using widely different methods, have been made;[12] the results are not as consistent, however, as might be desired. The most important quantity is c_1, the coefficient of the dipole term; the main part of the subsequent considerations will deal with its evaluation.

Survey of previous results for the coefficient c_1

There are two general methods for calculating c_1. The first is based upon the use of London's formula

$$c_1=\frac{3}{2}\left(\frac{e^2\hbar^2}{m}\right)^2 \times\sum_{ij}\frac{f_{0i}f_{0j}}{(E_0-E_i)(E_0-E_j)(2E_0-E_i-E_j)}, \quad (14)$$

wherein the f_{0i} are the spectroscopic oscillator strengths pertaining to transitions to the ground state. They may be taken from empirical dispersion formulas. Now it happens that the refractive index of He is given with very good approximation by a formula in which only one f appears,[13] at least in the relatively small range to which observations are confined. In that case (2) is equivalent to

$$c_1=-\tfrac{3}{4}\Delta\cdot\alpha^2, \quad (15)$$

where Δ is the energy difference between ground state and mean excited state, and α the static polarizability.[9] Using Cuthbertson's Δ, Eq. (3) gives

$$c_1=1.20\times10^{-60} \text{ erg cm}^6. \quad \text{(a)}$$

Herzfeld and Wolf[14] suggest a slightly different one-term dispersion formula, and also one containing two f's. Both, if used in calculating (2), lead to

$$c_1=1.28\times10^{-60} \text{ erg cm}^6. \quad \text{(b)}$$

The inaccuracy of results (a) and (b) arises

[12] See references 5, 6, 9; prior to these F. London's well-known papers; more recently R. A. Buckingham, Proc. Roy. Soc. **160**, 94 (1937); C. H. Page, Phys. Rev. **53**, 426 (1938).

[13] C. and M. Cuthbertson, Proc. Roy. Soc. **84**, 13 (1910).

[14] K. F. Herzfeld and K. L. Wolf, Ann. d. Physik [4] **76**, 567 (1925).

principally from the circumstance that the mean f value to be inserted in the dispersion formula is not identical with the proper mean for Eq. (14). These results can only be improved by taking detailed account of the variation of f with frequency, both in the discrete and in the continuous spectrum.

The second method for determining c_1 is the variational one, in which ψ_0 is approximated in a suitable manner and the perturbing van der Waals energy is computed. In the hands of Slater and Kirkwood[5] it has yielded

$$c_1=1.49\times10^{-60}\text{ erg cm}^6, \qquad \text{(c)}$$

whereas Buckingham[12] computes

$$c_1=1.62\times10^{-60}\text{ erg cm}^6. \qquad \text{(d)}$$

The error in these results is difficult to estimate; but it is to be noted that they may not be interpreted as upper limits to the true value of c_1. This simply follows from the fact that the perturbation energy is calculated as the difference between the perturbed energy E and E_{00}, the latter being only approximate because ψ_0 is not exact. A survey of cases other than helium indicates that the variational method generally gives values of c_1 considerably greater than would be obtained from any empirical dispersion formula. One is therefore inclined to believe that its tendency is to overshoot the mark.

Recalculation of c_1

It is possible to make a calculation which is based upon Eq. (14), taking adequate account of the variation of the f values with frequency. The method to be employed has already been used for this purpose,[15] but with a rather uncertain choice of f's. (It yielded $c_1=1.44\times10^{-60}$.) Meanwhile, f values for He have been calculated by Wheeler.[16] They will here be used as basis for computation, later to be corrected for empirical reasons.

We denote the f values relating to the discrete spectrum by f_{0i}; for the continuous spectrum they are available as df_{0E}/dE. In accordance with this division of the frequency range Eq. (14) may be written

$$c_1=A\left\{\sum_{ij}\frac{f_{0i}f_{0j}}{v_iv_j(v_i+v_j)}+2\sum_i\int_0^\infty\frac{f_{0i}(df_{0\epsilon}/d\epsilon)d\epsilon}{v_i(1+\epsilon)(1+v_i+\epsilon)}+\int\int_0^\infty\frac{(df_1/d\epsilon_1)(df_2/d\epsilon_2)d\epsilon_1d\epsilon_2}{(1+\epsilon_1)(1+\epsilon_2)(2+\epsilon_1+\epsilon_2)}\right\}, \qquad (16)$$

use being made of the following abbreviations:

$$A=-\frac{3}{2}\left(\frac{e^2\hbar^2}{m}\right)^2\frac{1}{|E_0|^3},\quad v_i=1-\frac{E_i}{E_0},\quad \epsilon=\frac{E}{-E_0}.$$

E without subscript refers to the continuous spectrum. In evaluating (16) it is convenient to introduce the auxiliary function

$$G(\alpha)\equiv\int_0^\infty\frac{(df/d\epsilon)d\epsilon}{(1+\epsilon)(\alpha+\epsilon)}, \qquad (17)$$

which can be computed for a sufficient range of α's by numerical integrations. In terms of it, we now have

$$c_1=A\left\{\sum_{ij}\frac{f_{0i}f_{0j}}{v_iv_j(v_i+v_j)}+2\sum_i\frac{f_{0i}G(1+v_i)}{v_i}+\int_0^\infty\frac{(df/d\epsilon)G(2+\epsilon)d\epsilon}{1+\epsilon}\right\}.$$

In calculating the first sum, only the v's corresponding to the first four lines of the principal series need be considered; the remainder may be treated as a single transition near the series limit ($v_5=0.99$). The integration has been carried out numerically, since it seems difficult to approximate G by simple functions. The three terms in brackets yield, respectively, 0.126, 0.358, and 0.271. The coefficient A has the value -1.97×10^{-60}; hence

$$c_1=1.49\times10^{-60}\text{ erg cm}^6$$

in exact agreement with the result of Slater and Kirkwood (Eq. (c)).

The present method is of course exact as far as the coefficient c_1 is concerned; errors are due only to the use of inaccurate f values, and these may be estimated and corrected. We subject the f's to two requirements: they shall satisfy the sum rule

$$\sum_i f_{0i}=2, \qquad (18)$$

[15] H. Margenau, Phys. Rev. **37**, 1425 (1931).
[16] J. E. Wheeler, Phys. Rev. **43**, 258 (1933).

and they shall yield the correct polarizability

$$\alpha=\frac{e^2\hbar^2}{m}\sum_i\frac{f_{0i}}{(E_0-E_i)^2}.$$

In terms of our present convention, and with the use of the function (17), this reads

$$\alpha=\frac{e^2\hbar^2}{m}\left\{\sum_i\frac{f_{0i}}{v_i^2}+G(1)\right\}. \tag{19}$$

Wheeler's f values already satisfy Eq. (18). They give for the bracketed expression in (19) the value $\{0.532+0.621\}$, and thus for α: 2.11×10^{-25} cm³. Experimentally, α may be obtained from measurements of the dielectric constant of He at radiofrequencies[17] and from extrapolation on the refractive index.[18] The former lead to the value 2.1×10^{-25} cm³. However, the experimental difficulties attending these measurements are such as to make this value less certain than that deduced from Cuthbertson's observations on the refraction of visible light. From these, Born and Heisenberg[18] have found $\alpha=2.02\times10^{-25}$ cm³.

Assuming this to be correct, we conclude that Wheeler's f values are slightly in error. In correcting them, we assume the trend of $df/d\epsilon$ to be unaltered, but redistribute the relative weights of the discrete and the continuous spectrum in such a way that both Eq. (18) and Eq. (19) are satisfied for $\alpha=2.02\times10^{-25}$ cm³. Thus if f' denotes the corrected oscillator strength, we put

$$f_{0i}'=(1-a)f_{0i} \quad \text{and} \quad df'/d\epsilon=(1+b)(df/d\epsilon).$$

It is found that $a=0.134$, $b=0.036$. This correction seems quite compatible with the accuracy of Wheeler's calculation. If now we use the corrected f's in Eq. (14), the result is

$$c_1=1.39\times10^{-60} \text{ erg cm}^6.$$

A change in the value of α produces about twice as great a relative change in c_1 in the same direction.

[17] H. E. Watson, G. Gundo Rao and K. L. Ramaswamy, Proc. Roy. Soc. **A132**, 569 (1931).
[18] M. Born and W. Heisenberg, Zeits. f. Physik **23**, 388 (1924).

Conclusion

As to the coefficient c_2 of Eq. (1), there are several detailed calculations which agree quite well. In particular, they lead to almost the same ratio c_2/c_1, and this turns out to be 2.2×10^{16} cm². Thus we take c_2 to be 3.0×10^{-76} erg cm⁶.

Summarizing the present results we obtain:

$$\Delta E=\left\{770e^{-4.60R}-560e^{-5.33R}-\frac{1.39}{R^6}-\frac{3.0}{R^8}\right\}10^{-12} \text{ erg} \tag{20}$$

as the formula which appears best in the face of present evidence. Here R is measured in A.U. The repulsive term is taken from Slater without recalculation. As already pointed out, the second term is a small correction; its form is valid in the region of the minimum and down to about 2A. For purposes of using the formula in calculations it may well be taken care of by increasing the dipole-quadrupole coefficient from 3.0 to 3.7. The minimum of ΔE comes at $R\approx2.8$A and has a value of -18×10^{-16} erg.

The formula most frequently used in applications is Slater and Kirkwood's, which neglects the quadrupole term but has -1.49 for the coefficient of the dipole term. It seems that the reason for its approximate validity lies in the compensating effect of these two features. Recent calculations of Gropper[19] on the second virial coefficient of He indicate that the correct potential must lie between the Slater-Kirkwood potential and that obtained by the present author on adding the quadrupole term to the latter. The same result is reached by de Boer and Michels[2] who actually deduce a potential which best fits experimental data. The potential given here (Eq. (20)) does have the property of being intermediate between the two. Dr. de Boer has kindly pointed out,[20] however, that this expression does not give quite as good a fit with the experimental data of Keesom and Kraak[21] as the one derived by him from an analysis of thermodynamic data.

[19] L. Gropper, Phys. Rev. **55**, 1095 (1939).
[20] Private communication, for which the author wishes to express his gratitude.
[21] W. H. Keesom and H. H. Kraak, Physica **2**, 37 (1935).

The Coefficient of Thermal Diffusion of Methane

ALFRED O. NIER
Department of Physics, University of Minnesota, Minneapolis, Minnesota
(Received September 20, 1939)

According to the theories of Enskog and Chapman, if a mixture of two gases is confined in a vessel in which there exists a temperature gradient a concentration gradient of the gases should also exist. The effect is confirmed for the isotopic gases $C^{12}H_4$ and $C^{13}H_4$ and the coefficient of thermal separation for methane has been determined. As the value found for this coefficient is somewhat less than that arbitrarily assumed by Furry, Jones and Onsager in their theory on carbon isotope separation by thermal diffusion, the attainable separation factor for a given length column would be materially lower than that computed.

ENSKOG[1] in 1911 and Chapman[2] in 1917 showed from theoretical considerations that if a mixture of two gases was confined in a vessel in which there existed a temperature gradient one should also expect to find a gradient in the relative concentrations of the two constituents. The theory predicted that, in general, the heavier molecules would tend to move toward the cooler part of the vessel and vice versa. The concentration gradient increases until such a value is reached that the effect of thermal diffusion is just matched by the opposing effect of ordinary diffusion. The theory predicts that the coefficient of thermal diffusion vanishes for molecules interacting with a force varying with the inverse fifth power of the separation and is a maximum for rigid elastic spheres.

Experimental confirmation of the phenomenon was made by Chapman and Dootson[3] who obtained partial separations of mixtures of hydrogen and carbon dioxide in a vessel consisting of two bulbs maintained at different temperatures and joined by a connecting tube. Further experiments[4] demonstrated the existence of the effect in other gases as well.

The recent experiments of Clusius and Dickel[5] and other investigators[6] indicate that by using a tall column consisting of concentric cylinders at different temperatures and confining a gas in the annular space between the cylinders, the combination of the convection currents and thermal diffusion effect give rise to an appreciable isotopic separation in the gas. Furry, Jones and Onsager[7] and Waldmann[8] have discussed the theory of the operation of such a column and the former group have worked out an example in which they considered the possibility of separating the carbon isotopes by using methane gas. As no numerical value for the coefficient of thermal diffusion for methane was available, Furry, Jones and Onsager tentatively assumed a value and made their computations.

The purpose of the present investigation was to make a direct experimental determination of this coefficient. As was pointed out by Furry, Jones and Onsager, a determination of the thermal diffusion coefficient is not only of practical value in designing columns for the separation of isotopes, but also a knowledge of its value for isotopic gases should yield valuable information about the nature of the intermolecular forces in the gas in question, without the complications that arise if one studies mixtures of dissimilar gases.

APPARATUS AND PROCEDURE

The apparatus used in the present experiments consisted of two 100-cc bulbs joined by a connecting tube 7 cm long and 8.5 mm inside diameter. A three-way stopcock which had a hole 2 mm in diameter and 1.5 cm long was part of

[1] D. Enskog, Physik. Zeits. **12**, 56, 533 (1911).
[2] S. Chapman, Phil. Trans. **A217**, 115 (1917).
[3] S. Chapman and F. W. Dootson, Phil. Mag. **33**, 248 (1917).
[4] For a complete list of these, up to 1937, see T. L. Ibbs, Physica **4**, 1133 (1937). For recent work on rare gas mixtures, Atkins, Bastick and Ibbs, Proc. Roy. Soc. **A172**, 142 (1939).
[5] K. Clusius and G. Dickel, Naturwiss. **26**, 546 (1938); **27**, 148 (1939).
[6] See review paper, H. S. Taylor, Nature **144**, 8 (1939).
[7] W. H. Furry, R. Clark Jones and L. Onsager, Phys. Rev. **55**, 1083 (1939).
[8] Waldmann, Naturwiss. **27**, 230 (1939).

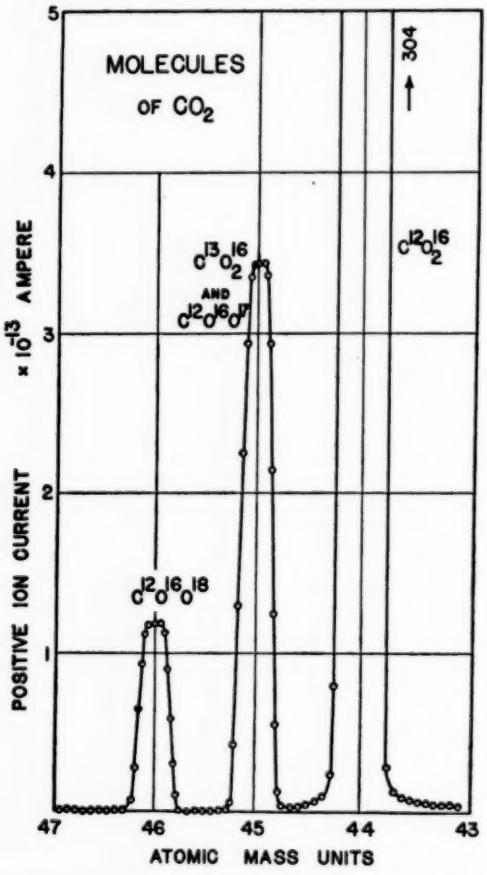

FIG. 1. Mass spectrum showing the most abundant molecular ions of CO_2 formed from carbon and oxygen isotopes. The experimental points are obtained by plotting positive ion current passing through the exit slit of the analyzer of the mass spectrometer as a function of the energy of ions while the magnetic field is held constant. As there is a definite relation between the energy and the mass of the ions collected, namely, energy x mass = a constant, the voltage scale can be readily changed to a mass scale as was done in the figure. The width of the peaks is, of course, caused by the finite width of slits used and imperfections in focusing.

the connecting tube. The system was evacuated and filled with methane to a pressure of approximately 60 cm. One bulb was placed in a water bath and the other in a furnace. After waiting a period of time at least three times the relaxation time of the system, the stopcock was turned and the hot bulb was evacuated. The stopcock was again turned, this time to allow the contents of the cold bulb to expand into the evacuated hot bulb. This process was repeated twelve times, so that in the end the change in concentration in the cold bulb was twelve times what it would have been for a single process. Of course the pressure decreased for succeeding runs, but as the effect measured should be practically independent of pressure, errors due to this score should be negligible compared to others in the experiment. The final gas remaining in the cold bulb was then analyzed with a mass spectrometer and the relative abundance of the carbon isotopes determined. The ratio obtained was compared with that for some of the original gas.

A calculation indicated that for methane at atmospheric pressure the relaxation time of the system was approximately one hour. As the coefficient of ordinary diffusion of methane varies inversely with the pressure, this time amounted to only a few minutes for the last few runs in the series of twelve. However, in all cases, at least one-half hour was allowed for a separation.

The mass spectrometer used for analyzing the gas samples consisted of a tube containing a 180° magnetic analyzer. Positive ions were formed by electron impact of the gas at low pressure. The analyzed ion currents were measured with an electrometer tube amplifier. The spectrometer tube was similar to one already described.[9] It differed mainly in that the slits S_1, S_2, and S_3 in Fig. 1 of reference 9 were 0.25, 0.23, and 0.90 mm wide, respectively. In order to insure freedom of difficulties with water vapor ($O^{16}H^+$ has the same mass as $C^{13}H_4^+$) the methane was burned to CO_2 in an excess of O_2. Heated $KClO_3$ was used as a source of O_2 and a platinum filament heated to approximately 1000°C caused the burning. The CO_2 was purified by condensation in a liquid-air trap while excess O_2 or unburned CH_4 were pumped off. Water vapor was later removed by placing dry ice on the trap which was originally immersed in liquid air. Fig. 1 shows a typical mass spectrum obtained for CO_2. The C^{13}/C^{12}

TABLE I. *Ratio of galvanometer deflections corresponding to ratio of mass* 45 *to mass* 44 *ion currents for three individual samples of* CH_4 *burned to* CO_2.

SAMPLE	12A	11A	10A	12A–11A	12A–10A
Aug. 20	0.9087	0.9043	0.9080	0.0044	0.0007
	.9017	.8974	.8997	.0043	.0020
Aug. 21	.9041	.9017	.9010	.0024	.0031
	.9019	.8977	.9029	.0042	.0010
	.9036	.9059	.9039	−.0023	−.0003
Average	0.9040	0.9014	0.9031	0.0026	0.0009
Grand average		0.9028			

[9] A. O. Nier, Phys. Rev. **52**, 933 (1937).

ratio was determined by comparing the relative heights of the peaks corresponding to masses 45 and 44.

Results

As a test to see whether or not the burning of the methane had any effect upon the C^{13}/C^{12} ratio, a preliminary experiment was performed. Three samples of methane gas, called 12A, 11A, 10A, were removed from the supply bulb and burned separately. The C^{13}/C^{12} ratio was measured for each of these. The results obtained are tabulated in Table I. Each of the numbers there given is the average of ten determinations and represents the *ratio of galvanometer deflections* corresponding to the 45 and 44 peaks. As the mass 45 ion current is only about one percent that for mass 44, different resistances in the grid circuit of the electrometer tube were used for the two ions and also the Ayrton shunt in the galvanometer circuit had different settings. Thus, to obtain the absolute C^{13}/C^{12} abundance ratio one would have to multiply the ratios recorded by a suitable factor, the numerical value of which is not important to us here, as we are interested only in fractional changes of the C^{13}/C^{12} ratio. In addition one would have to make a correction for the fact that the ion $C^{12}O^{17}O^{16}$ made a contribution of about seven percent to the 45 peak. Also a small correction (about one percent) for the background under the 45 peak would have to be made (See Fig. 1). As one is only interested in changes in relative abundance in these experiments, these background corrections are not important, provided they are constant. Every effort was made to study each sample under as nearly as possible the same conditions and thus insure constancy of background and other discriminatory effects. The same source of oxygen was used to burn each of the samples so that the correction due to $C^{12}O^{17}O^{16}$ would be the same in each case.

The procedure in obtaining the readings was to make ten determinations of the ratio, then to introduce the next sample and make ten determinations for this, etc. Thus the samples were introduced in the order 12A, 11A, 10A, 12A, etc., until all the readings given were obtained. As may be seen, the ratio varied somewhat from day to day, but as it is differences that one is interested in, this slight variation is not important.

As is evident in the consistent differences in columns 12A–11A, and 12A–10A, slight discriminations are introduced in burning and manipulating the separate samples. However, as we note by comparing the averages, the individual sample averages agree to better than 0.2 percent with the grand average. These data also indicate to what extent it is possible to reproduce readings with a mass spectrometer of the sort employed.

The procedure employed in analyzing the samples which had been through the thermal diffusion process was similar to that described above. In Table II are recorded the data obtained when the hot and cold bulb temperatures were 455°C and 23°C, respectively. Three separate runs were made. The samples are designated as 6A, 8A, and 9A. Sample 12A (ordinary meth-

TABLE II. *Comparison of galvanometer deflection ratios for sample 12A of Table I and three samples which had been through the thermal diffusion process. Temperature: hot bulb* 455°C, *cold bulb* 23°C.

Sample	12A	6A	8A	9A	6A–Ave 12A	8A–Ave 12A	9A–Ave 12A
Aug. 22	0.8992	0.9217	0.9194	0.9172	0.0190	0.0167	0.0145
	.9047	.9253	.9289	.9175	.0226	.0262	.0148
	.9041						
Average	.9027						
Aug. 24	.9057	.9291	.9392	.9238	.0201	.0302	.0148
	.9116	.9309	.9300	.9241	.0219	.0210	.0151
	.9098						
Average	.9090						
Aug. 25	.9092	.9283	.9290	.9246	.0193	.0200	.0156
	.9088						
Average	.9090						
Average of differences					0.0206	0.0228	0.0150
Grand average of differences = 0.0195							

TABLE III. *Comparison of galvanometer deflection ratios for sample 12A of Table I and three samples which had been through the thermal diffusion process. Temperature: Hot bulb* 300°C, *cold bulb* 23°C.

Sample	12A	15A	14A	16A	15A–Ave 12A	14A–Ave 12A	16A–Ave 12A
Aug. 27	0.9145	0.9292	0.9303	0.9233	0.0164	0.0175	0.0105
	.9111						
Average	.9128						
Aug. 27	.8996	.9117	.9127	.9168	.0175	.0185	.0126
	.9043	.9161	.9187	.9176	.0119	.0145	.0144
	.9075	.9198	.9197	.9240	.0156	.0155	.0198
	.9047	.9184	.9229	.9442*	.0142	.0187	—
	.9050						
Average	.9042						
Average of differences					0.0151	0.0169	0.0143
Grand average of differences = 0.0154							

* Value believed unreliable and hence discarded in final computations.

ane from Table I) was used as a standard for comparison. For the data in Table III the hot and cold bulb temperatures were 300°C and 23°C, respectively. Three samples, 15A, 14A, and 16A were obtained under these conditions, and 12A was again used as a standard.

The results clearly indicate that as a result of the existence of the phenomenon of thermal diffusion a slight, but definite, change in relative abundance of the carbon isotopes takes place.

Computation of Coefficient of Thermal Separation

For the equilibrium condition in the present experiment we may write

$$D \text{ grad } C_2 = -\frac{D_T}{T} \text{ grad } T, \tag{1}$$

where D is the coefficient of self-diffusion of methane, D_T the coefficient of thermal diffusion, T, the absolute temperature and C_2 the concentration of the molecule $C^{13}H_4$ in the gas. C_1 is the concentration of $C^{12}H_4$ and $C_1+C_2=1$. Upon integrating (1) we arrive at the result:

$$C_2^0 - C_2^1 = \frac{D_T}{D} \log \frac{T_1}{T_0}, \tag{2}$$

where C_2^0 and C_2^1 represent the concentrations C_2 in the bulbs (0) and (1) and T_0 and T_1 the respective temperatures of the two bulbs. According to Enskog's[7] treatment of the problem of thermal diffusion, D_T/D in the case of isotopes reduces to the simple, approximate form:

$$D_T/D = k_T = \alpha C_1 C_2, \tag{3}$$

where α is a constant; k_T is called the coefficient of thermal separation.

If m_0 and m_1 represent the respective masses of gas in the two bulbs, then

$$m_0 T_0 = m_1 T_1. \tag{4}$$

Also, to express the fact that there is conservation of $C^{13}H_4$ during the diffusion process we may write

$$m_0 C_2^0 + m_1 C_2^1 = (m_0+m_1) C_2. \tag{5}$$

Then, by suitable algebraic manipulations between Eqs. (3), (4) and (5), we arrive at the result:

$$\alpha = \frac{(C_2^0 - C_2)}{C_2} \cdot \frac{1}{C_1} \cdot \frac{T_1/T_0+1}{\log T_1/T_0}. \tag{6}$$

For $T_1=455+273°K$, $T_0=23+273°K$ (data Table II)

$$\frac{C_2^0 - C_2}{C_2} = \frac{0.0195+0.0012}{0.9\times 0.92\times 12} = 0.0021. \tag{7}$$

The factor 12 arises from the fact that in the experiment the process was repeated twelve times in order to enlarge the effect. The factor of 0.92 arises because only ninety-two percent of the 45 peak is associated with C^{13}. The remaining eight percent is due to $C^{12}O^{17}O^{16}$ and background. As the sample 12A was 0.0012 higher than the average of the three samples in Table I, we have corrected for this by adding 0.0012 to the 0.0195. As $(C_2^0-C_2)/C_2$ represents the fractional change in the relative abundance of the carbon isotopes, we may use the data in Table II directly inasmuch as the numbers there recorded are proportional to the relative heights of the 45 and 44 peaks in the mass spectrometer. For normal carbon $C_2 \cong 0.011$[10] and $C_1 \cong 1$. Thus, substituting in (6), we arrive at the result:

$$\alpha = 0.0080. \tag{8}$$

Likewise, from the data in Table III we obtain the value:

$$\alpha = 0.0074. \tag{9}$$

As a first approximation for elastic spheres Enskog's[7] results give

$$\alpha = (105/118)(M_2-M_1)(M_2+M_1)$$

where the M's are the relative masses of the two types of molecules. In the case of methane this gives

$$\alpha = 0.027. \tag{10}$$

The writer's results are thus in rough accord with the results of experiments with dissimilar molecules where, except for the rare gases, the experimental values of α are less than half the theoretical values.

The consistency of the data leads one to believe

[10] A. O. Nier and E. A. Gulbransen, J. Am. Chem. Soc. **61**, 697 (1939).

that the values in (8) and (9) are each accurate within perhaps ten percent. Although one would expect α to increase slightly with temperature, it is doubtful whether the apparent variation observed here is significant.

For want of any experimental data on the value of α for methane, Furry, Jones and Onsager aribtrarily assumed a value of 0.0106 for this quantity. In view of the present results it appears that a separation factor of only about one-third as great as computed would be obtained for the particular carbon isotope separating column proposed by these authors.

The writer is indebted to Professor John Bardeen for numerous interesting and helpful conversations. The methane was supplied by Dr. T. I. Taylor and Professor G. Glockler of the Chemistry Department.

NOVEMBER 15, 1939 PHYSICAL REVIEW VOLUME 56

Fluctuations, Thermodynamic Equilibrium and Entropy

EDWIN C. KEMBLE
Harvard University, Cambridge, Massachusetts

(Received January 3, 1939)

To eliminate exceptions to the second law due to fluctuation phenomena, etc., the following changes are necessary. First we must state the laws of thermodynamics in terms of Gibbsian ensembles rather than of individual systems. Second we must sharpen our conception of the experimental procedure required for producing states of thermodynamic equilibrium. It will not suffice to isolate the system and wait. We must have the positive stirring action of thermal contact with a thermostat. Using the new definition of thermal equilibrium we can place statistical mechanics on a more satisfactory footing by showing that the thermostat experimental procedure leads to the canonical ensemble and maximizes v. Neumann's microscopic entropy. (Details of this proof appear in succeeding paper.) Difficulties with his macroscopic definition of entropy are avoided by showing that his original microscopic definition is satisfactory when used in conjunction with a proper operational definition of thermodynamic equilibrium. In conclusion the second law of thermodynamics is derived from quantum statistics on the basis of the microscopic definition of entropy.

IT IS customary to regard fluctuation phenomena as minor violations of the second law of thermodynamics marking the limits of validity of the law.[1] It is also customary to regard thermodynamics as a branch of physics applicable only to matter in bulk. Thus the concept of temperature is usually considered to be meaningless when applied to a single molecule. These two limitations on the scope of thermodynamics are, of course, really one, since it is the very large fluctuations in the behavior of microscopic systems that have led to the exclusion of such systems from the domain of this branch of physics. Statistical mechanics affords a point of view from which the dogma of the second law for macroscopic systems and the existence of fluctuations are both intelligible. It is well recognized, however, that the phenomenological point of view of classical thermodynamics has its own advantages. Hence a restatement of the laws of thermodynamics—especially the second—in such form as to eliminate the apparent exceptions is *prima facie* desirable. Such a restatement has been proposed by G. N. Lewis.[2] In this paper I offer an alternative procedure for reaching the same goal which has the advantage that it closely preserves the form of the original statement of the second law.

Although this procedure is from an experimental point of view extremely plausible, the

[1] See, for example, P. S. Epstein's *Textbook of Thermodynamics* (New York, 1937), pp. 385–6 and accompanying references.

[2] G. N. Lewis, J. Am. Chem. Soc. **53**, 2578 (1931). A general idea of Lewis's proposal will be gleaned from the following statement of his cardinal postulate. "When a given content is partitioned between two systems, the ratio of the specific probabilities of any two partitions of this content depends solely upon the nature of the two systems and upon the respective contents."

reader will naturally ask for something more than good conjectural support for a proposal to modify or extend an empirical law as sacrosanct as the second law of thermodynamics. Direct experiments of a type needed to fully verify the suggested alterations are lacking and would be difficult to perform, although the study of the thermodynamic behavior of gases at low pressures affords an approximation to them. Fortunately, however, the study of statistical mechanics, which has always given the only rational interpretation of thermodynamics, furnishes the support required to put the new proposals on a solid basis. In fact these modifications in the usual formulation of thermodynamic theory originated in a study of the foundations of quantum statistical mechanics. The primary purpose of this paper and a mathematical one to follow is to report on a contribution to the fundamental problem of the latter subject. It is convenient, however, to approach this contribution from the thermodynamic angle, since in this way the conclusions can be made available to readers who have not time to go through the details of the mathematical argument.

The Gibbsian Ensemble in Thermodynamics

Although statistical mechanics provides a rational explanation of the laws of thermodynamics it is a striking fact that whereas the empirical laws of the latter subject, as usually stated, refer to individual systems, the object of interest in statistical mechanics is an ensemble of structurally identical independent systems. Gibbs found analogies between the properties of such ensembles and the properties ascribed to individual systems in thermodynamics. He saw that the fluctuations in the more readily observable properties of a mechanical system when calculated for an ensemble of canonical form tend to become negligible as the number of degrees of freedom becomes very large. Thus he was led to the observation that "A very little study of the statistical properties of conservative systems of a finite number of degrees of freedom is sufficient to make it appear, more or less distinctly, that the general laws of thermodynamics are the limit toward which the exact laws of such (ensembles of) systems approximate when their number of degrees of freedom is indefinitely increased."[3] Similarly, R. C. Tolman in his recent work on statistical mechanics[4] says of the statistical explanation of thermodynamics that the fundamental idea "lies in regarding the thermodynamic behavior of a single system of interest as equivalent to the mechanical behavior which would be exhibited by a suitably chosen ensemble of systems of similar structure."

To my mind this distinction between statistical mechanics and thermodynamics, which compares the ensemble in the former picture with the individual system in the latter, is quite irrational. The fundamental difference between the two disciplines is that thermodynamics is based on direct observation and is free from hypotheses regarding either the microscopic structure of matter, or the rules of mechanics, whereas statistical mechanics makes use of assumptions of both kinds. This difference has nothing directly to do with the choice of the individual system or the ensemble as the object of interest. We can make observations of the properties of microscopic systems and of the properties of microscopic parts of macroscopic systems. A completely satisfactory formulation of thermodynamics would cover such observations when used for the study of the thermal behavior of matter. The first step towards such a formulation is to bring the concept of the Gibbsian ensemble of independent systems into thermodynamics as well as statistical mechanics. I therefore suggest that we *replace all the statements which thermodynamics makes about individual systems by corresponding statements regarding ensembles of identically constructed independent systems similarly prepared, or subject to the same experiment.*[5]

Consider, for example, the eventual application of the theorems regarding the Carnot engine to a

[3] J. Willard Gibbs, *Elementary Principles in Statistical Mechanics* (New Haven, reprint of 1914), p. 166.

[4] R. C. Tolman, *The Principles of Statistical Mechanics* (Oxford, 1938), p. 560.

[5] It is important to stress the complete independence of the members of the Gibbsian ensemble. All thermodynamic systems are assumed to be enclosed and we can think of each member as enclosed in a separate box. In my book, *Fundamental Principles of Quantum Mechanics*, I have translated the French word "ensemble" into the English "assemblage," having unfortunately overlooked the distinction drawn by Fowler, who uses "ensemble" in the same sense as Gibbs and introduces the word "assembly" for a single thermodynamic system consisting of many identical molecules.

"working fluid" consisting of a single gas molecule. If we carry through the appropriate operations we can in principle carry this fluid through the conventional Carnot cycle, taking heat Q_1 from a hot reservoir at temperature T_1, imparting heat Q_2 to a cold reservoir at T_2, and converting the difference into mechanical work. In the case of such a fluid, however, the heats Q_1 and Q_2 will be subject to violent fluctuations in successive cycles and the efficiency of the single cycle will fluctuate on both sides of the value $(T_1-T_2)/T_1$ indicated by the second law. If the efficiencies were consistently high we should have a worrisome violation of the thermodynamic rule. We can be sure, however, that the over-all efficiency of 10^{10} cycles will be to all intents and purposes exactly the same as for a macroscopic working fluid and so equal to the value prescribed by the second law. The same argument applies if we take 10^{10} independent identical microscopic systems, each carried through a Carnot cycle between the temperatures T_1 and T_2. We revise the usual rule by saying that if $\bar{Q}_1$ and $\bar{Q}_2$ denote the average values of Q_1 and Q_2 for such an ensemble of systems, whether microscopic or macroscopic, each carried through the same cycle of operations, $(\bar{Q}_1-\bar{Q}_2)/\bar{Q}_1$ is always equal to $(T_1-T_2)/T_1$.

The new statement applied to macroscopic systems is less definite than the old. We can supplement it, however, by the observation—whether based on empirical or theoretical grounds—that the fluctuations in any property characteristic of a complete system rather than a small part of it[6] approach zero for an ensemble of such systems in thermal equilibrium as the mass of the system becomes infinite while its temperature and chemical composition remain constant. The two statements together then tell the whole story in a most logical and comprehensive manner.

Personally I am inclined to go still farther and say that the primary object of inquiry in physics ought *always* to be identified with a Gibbsian ensemble of systems similarly prepared and subject to the same operations. This point of view is forced upon us in quantum mechanics unless we are willing to use the probability concept without assigning to it any definite operational significance.[7] It is admitted in a way by the old deterministic definition of a physical law as a description of "what always happens in a given physical situation." This definition is imperfect in its suggestion that in a fully specified physical situation "the same thing" does always happen. It is correct in emphasizing the need of many repetitions of each experiment before the results can be elevated to the rank of a portion of scientific law. Astronomy and geology are semi-historical sciences that acquire most of their meaning from the background of physical and chemical law against which we read their observations, but for physics and chemistry truly isolated events and observations are of little scientific significance. Everyone will recognize, for example, that the simple statement to the effect that a measurement shows my desk to be five feet long takes most of its meaning from the vast quantity of experience which testifies to the fact that repeated length measurements on such an object as a desk give results whose variations are insignificant for most purposes. Hence the preceding statement implies that a statistical measurement of a Gibbsian ensemble of similar desks would give a distribution function with a maximum near five feet and with a spread which can be neglected.

Before proceeding farther with the general argument it seems advisable to clear up any possible ambiguity in the reader's mind regarding the meaning of the phrase "similarly prepared" in connection with an ensemble of independent systems. This phrase is intended to indicate that all our information regarding any member of the ensemble applies equally to every other member. Hence our knowledge of the state of each system is identical with our knowledge of the state of the ensemble as a whole.

It may happen that our knowledge of the state of a system as defined by a laboratory record, or otherwise, is sufficient so that the problem of constructing an ensemble of independent systems in the same state has a unique solution. In that case any two ensembles constructed in accordance with the formula defined by our

[6] I am not quite sure what is the best way to characterize mathematically these "normal" properties of an ensemble of macroscopic systems. Obviously they are properties involving some sort of average over a large number of molecules.

[7] See, for example, my book on quantum mechanics, pp. 53–55.

information must be experimentally indistinguishable and we shall say that the system is known to have a definite state.[8] On the other hand, our information may be insufficient for the above purpose so that a variety of ensembles can be constructed all of them in harmony with our (incomplete) formula. In this case the only predictions that can be made regarding systems "in the same state" as the given system are those which apply to *every* ensemble allowed by the formula.

Thermodynamic Equilibrium

A second fundamental change of procedure required by our program consists in a sharpening of the concept of thermodynamic, or thermal, equilibrium. So long as we are dealing solely with gross, or macroscopic, systems we get along very well treating the energy as a definite function of the temperature. We then say that two systems are in thermal equilibrium if no net energy is transmitted from one to the other when they are placed in thermal contact with one another. An individual system can be considered to be in thermal equilibrium if no net energy transfers are taking place between its parts. To attain thermal equilibrium it then suffices to isolate the system and allow its parts to transfer energy until a balance is reached. We designate this procedure by the symbol α. An alternative procedure β for securing thermal equilibrium is to place the given system A for a long time in thermal contact with a heat reservoir B of very large heat capacity relative to A, whose temperature as observed by a thermometer is known to be uniform and constant. We shall refer to such a reservoir as a thermostat. The only assumption which we need to make regarding the initial state of A is that its energy is negligible in comparison with that of the thermostat. The combined system $A+B$ is to be isolated during the period of thermal contact.

Although these procedures are apparently equivalent when applied to macroscopic systems, they are definitely not equivalent when applied to ensembles of microscopic systems. Thus the energy of a single gas molecule confined to a chamber with walls at a temperature T will fluctuate wildly. Hence a Gibbsian ensemble of single gas molecules will develop an energy *distribution* with a relatively large standard deviation if subjected to procedure β. This will be true even if the ensemble is started off in a unique energy state. On the other hand, procedure α has no power to alter whatever energy distribution exists initially in the ensemble. If there is such a thing as a definite state of thermal equilibrium for a Gibbsian ensemble of identical independent systems there must be a definite corresponding energy distribution. This state certainly cannot be attained by applying the procedure α. It is plausible, however, to suppose that procedure β will create a definite energy distribution and definite state. At any rate we can say with confidence that if a definite state of thermal equilibrium exists the procedure β is designed to produce it.

At this point the reader is likely to object that we are arguing in a circle, since procedure β requires that in order to put a Gibbsian ensemble into a state of thermal equilibrium we must first prepare an ensemble of thermostats with equal temperatures. This requirement of equal temperatures is necessary since without it there can be no possibility of a unique final energy distribution. It does not really create a circular definition, however, because it is applied to an ensemble of macroscopic systems for which the thermometer reading can be interpreted as an approximate energy measurement. It is not required that the ensemble of thermostats, which we conveniently suppose to be of identical structure, shall be in complete thermal equilibrium but merely that they shall be in a state of quasi-thermal equilibrium, with a very small standard deviation in energy. We can safely postulate that such a state can be attained by the use of thermometer readings.

We should like to believe that the procedure β is sufficient to define a definite state of thermal equilibrium appropriate to the chosen temperature. In other words, we should like to believe that any two ensembles constructed in accordance with procedure β must necessarily be indistinguishable by any conceivable experiment. Before dealing with this question, however, some additional remarks about the multiple-valued

[8] By a definite state we do *not* mean a pure state in the quantum-mechanical sense, but a definite quantum-mechanical mixed state. See next section.

word "state" are in order (cf. end of preceding section).

In conventional thermodynamics the state of a system can be identified with a collection of measured values of macroscopically observable quantities, whether externally variable or not, deemed sufficient to characterize the macroscopic thermodynamic behavior of the system. The number of parameters required to specify the thermodynamic state of a macroscopic system is, of course, greatly reduced when the system has been subjected to either of the operations α, β. In such cases it suffices to specify the temperature and the externally variable parameters, such as the volume.

In elementary wave mechanics the fundamental assumption is often made that the microscopic dynamical state of a system is to be defined or described by means of a suitable wave function ψ. This wave function varies in time for a system which is isolated—and hence free from the disturbance of any observation—in accordance with the Schrödinger equation. It is postulated that ψ describes the statistical behavior of a large ensemble of independent systems all prepared so as to be in the same "state." An ensemble with a unique ψ-function, and every member of it, is said to be in a *pure state*. However, the actual preparation of such an ensemble is a practical impossibility except in a few extremely simple cases. Hence it is necessary to postulate that any actual ensemble behaves like a mixture of pure state subensembles. Such a general ensemble is said to have a definite *mixed state*. The most general ensemble containing some very large number[9] of systems, N, will have the properties of a mixture of a certain number of systems, say $N_1=w_1N$, in the pure state ψ_1, of a number $N_2=w_2N$ in the pure state ψ_2, etc. The complete ensemble can be described by an Hermitian statistical matrix ρ whose rows and columns refer to the members of a complete orthonormal system of standard wave functions $\varphi_1, \varphi_2, \varphi_3, \cdots$. Specifically

$$\rho(n, m)=\sum_s w_s(\psi_s, \varphi_n)(\varphi_m, \psi_s). \qquad (1)$$

Here (ψ_s, φ_n) is the Hermitian scalar product of ψ_s and φ_n. The matrix has the important property that the average value, or expectation value, of any observable α for the ensemble is given by the spur of the matrix product $\alpha\rho$. The matrix ρ obeys a deterministic law of evolution in time so long as the members of the ensemble are isolated. It describes the statistical behavior of the general ensemble in quantum-mechanical language and so specifies its *quantum-mechanical state.*

The thermodynamic state of a system is determined by crude macroscopic measurements, whereas the exact specification of the statistical matrix from empirical data would imply the determination of a large number of exact microscopic wave functions. Thus the quantum-mechanical state is defined by far more exact measurements than the thermodynamic state. This means that in principle many different ensembles could be built up which are indistinguishable by means of the measurements used in defining the thermodynamic state, but involving different quantum-mechanical states.

Let us now return to the question of the uniqueness of the state of an ensemble of systems which has been subjected to the experimental procedure designed to secure thermodynamic equilibrium. We here interpret the phrase "unique state" in the quantum-mechanical sense as meaning a specific matrix ρ. If the operation β has the desired property, it means that we can take an ensemble of identical independent systems with an arbitrary initial ρ and by subjecting it to the process β convert it into an ensemble with a specific statistical matrix, say σ. Symbolically

$$\beta\rho=\sigma, \qquad (2)$$

where ρ is arbitrary except for the trivial energy qualification mentioned at the beginning of this section, and σ is independent of ρ. Of course σ will depend on the choice of temperature required in the definition of β and on the values of the externally variable parameters which enter into the Hamiltonian function of the system.

Stated in the foregoing bald form the proposition is not quite true. On the other hand, it is possible to give a reasonably satisfactory proof of a theorem in quantum statistical mechanics which is for practical purposes equivalent to Eq. (2). The precise statement of this theorem

[9] Throughout this paper the number of systems N in an ensemble is taken to be so large that we can attribute to the finite ensemble properties which are strictly speaking true only in the limit when N becomes infinite.

and its proof will be given in a later mathematical paper. An approximate statement will suffice for our present purpose.

When a system A is brought into thermal contact with another, B, the Hamiltonian of the combined system becomes

$$H=H_A+H_B+H',$$

where H_A, H_B are the initial Hamiltonians of the separate systems and H' is a mutual term involving the coordinates of both systems. The effect of the interaction on the statistical matrix ϱ_A is determined by the matrix $\mathbf{U}$ of the canonical transformation from a scheme which makes H_A+H_B diagonal to one which makes H_A+H_B+H' diagonal. The matrix $\mathbf{U}$ will depend on the nature of the systems A and B and on the interaction energy H' characteristic of the thermal contact. $\mathbf{U}$ will, of course, vary from one specific problem to another. In any case when B is a thermostat we know nothing useful about $\mathbf{U}$ except such conclusions as can be drawn from the fact that the interaction energy is always so small that for most purposes it can be neglected. Under these circumstances it is appropriate to adopt a procedure previously used by von Neumann[10] and compute a mean value of $\beta\varrho_A$ by averaging each component over all forms of $\mathbf{U}$ consistent with the assumption that H' is small compared with H_A and H_B and also over all values of the time t in which A and B are in thermal contact. Group integration affords a unique procedure for making the $\mathbf{U}$-average without favoring any one permitted form of the matrix over the others. I have carried out the double averaging process with the following result. In a matrix scheme which diagonalizes H_A, the average matrix $\beta\varrho_A$ is also diagonal and has the form

$$\overline{(\beta\varrho_A)(n,n')}=\delta_{nn'}e^{-\gamma E_{An}}/\sum_n e^{-\gamma E_{Am}}. \qquad (3)$$

Here γ is a function of the measured temperature of B which can be identified with the reciprocal of the product of the absolute thermodynamic temperature T and the gas constant k. Thus (3) describes a Gibbs canonical ensemble in quantum-mechanical language.

It is also possible to compute by the same averaging process the standard deviation of $(\beta\varrho_A)(n,n')$ from the mean value given in (3). This can be made as small as desired if B is given a sufficiently large heat capacity and the energy H' is made sufficiently small. Hence appreciable discrepancies between $\beta\varrho_A$ and its average value can be regarded as of negligible probability. We may accordingly assume that if σ in Eq. (2) is the matrix of the appropriate canonical ensemble the deviations from this equation will be of negligible importance.

This conclusion makes it possible to avoid the use of the extremum postulate of Elsasser[11] and the closely related postulate of "equal *a priori* probabilities and random phases of the quantum-mechanical states of a system" introduced by Tolman.[12] These hypotheses are used to provide us with definite statistical matrices for systems whose states are too ill-defined by our measurements to permit setting up unique statistical matrices on the basis of quantum-mechanical principles alone. They afford a simple and attractive way of getting answers to questions in statistical mechanics which agree with experience, but in my opinion leave something to be desired from a logical standpoint.

To assume with Tolman that a set of alternative possibilities are "equally probable" just because we have no basis for assigning unequal probabilities is to use the probability concept in a weak form to be sharply distinguished from the frequency-distribution form, i.e., the standard operational form specified in a previous reference.[7] The latter and stronger form of the concept can be based on induction from statistical observations, while the weak form has no such background. Hence we must guard against drawing conclusions from the weak form of the concept which are actually appropriate only to the stronger form. It seems to me that Tolman and Elsasser have made just this mistake.

A simple example will make the distinction clear.[13] Consider the probability that a given automobile approaching a fork in a road will choose the right branch. Observer A, with no information relative to the amount of travel

[10] J. v. Neumann, Zeits. f. Physik **57**, 30 (1929).

[11] W. M. Elsasser, Phys. Rev. **52**, 987–999 (1937), Section 3.

[12] R. C. Tolman, *The Principles of Statistical Mechanics* (Oxford, 1938), p. 350.

[13] The writer is indebted to Professor P. W. Bridgman for instructive discussion of the two forms of the probability concept.

over the two branches, may be expected to say that for him the probability of the right branch must be adjudged equal to that of the left branch, namely 50 percent. In making this statement he uses the weak form of the probability concept thus giving a deceptive form to the assertion that he has no basis for anticipating the choice. Observer B has just completed a traffic survey at the junction and has observed that for some time about 60 percent of the automobiles approaching the fork have taken the right branch. He can accordingly take this rule to be a statistical law[14] and will then say that the chance that the given automobile will take the right branch is 60 percent. This use of the strong form of the probability concept means that in general 60 percent of automobiles approaching the fork go to the right, while 40 percent go to the left. Obviously no such frequency-distribution is predicated by A's use of the word "probability." But to assume with Tolman and Elsasser that, in the absence of all information relative to a choice between a multitude of quantum-mechanical pure states consistent with our observations, we are permitted to make statistical predictions from a matrix in which these states are equally represented is to draw "strong" inferences from "weak" premises.

In my opinion the apparent success of the postulates of Elsasser and Tolman is due to the fact that we normally have available an item of information of great value which they do not take into consideration. This is that the thermodynamic systems under investigation have been taken directly from an initial thermal environment in which they have been subjected to the external stirring characteristic of the process β. It is the history destroying character of this process which has made the postulate of equal *a priori* probabilities useful. On the other hand, this postulate would fail dismally if we tried to apply it to a case in which the systems under investigation were not drawn from a natural thermal environment, but were received from a skillful and mischievous friend who wished to spoil our calculations.

The reader may object that in averaging over different forms of the transformation matrix $\mathbf{U}$ we have tacitly introduced an hypothesis of equal *a priori* probabilities as objectionable as that of Tolman. It is true that we have used the weak form of the probability concept, but I think we have not misused it. To take an average value of $\beta\varrho_A$ and demonstrate that the standard deviations if its elements from their means are very small is, in effect, to demonstrate that the average value is a good approximation to the exact value for the vast majority of a set of possible matrices $\mathbf{U}$ concerning which we have no basis for choice. To use the average value instead of the unattainable exact value is a matter of practical necessity rather than of logic. It is a procedure by which all of us must act every day and cannot be reduced to an absurdity by the argument about the mischievous friend. Moreover, it seems to me to represent the inescapable minimum use of the weak *a priori* probability concept similar to that employed in the "proofs" of the quasi-ergodic theorem in quantum mechanics and in classical mechanics by v. Neumann[15] and by Birkhoff.[16]

Entropy, Disorder and Ignorance

The foregoing theorem completes the justification of the operation β as the standard procedure for securing thermal equilibrium. At the same time it gives us a precise quantum-mechanical description of the state of thermal equilibrium.

An essential feature of the sharpened definition of thermal equilibrium is the new light which it throws on the statistical definition of entropy. We owe to the profound researches of v. Neumann two definitions of entropy appropriate to the quantum-mechanical form of statistical mechanics.[17] The first, or *microscopic*, definition is based on the second law of thermodynamics itself and seems to be forced upon us by thermodynamic argument if we treat all conceivable quantum-mechanical measurements as proper bases for mental experiments. This definition, however, leads to difficulty when one uses opera-

[14] In such a fundamentally human problem the question whether the statistical law of the past is also to be the statistical law of the future would be more pressing than in purely physical problems.

[15] J. v. Neumann, reference 10, also Proc. Nat. Acad. Sci. **18**, 70 (1932).

[16] G. D. Birkhoff, Proc. Nat. Acad. Sci. **17**, 656 (1931).

[17] J. v. Neumann, *Math. Grundlagen d. Quantenmechanik* (Berlin, 1932), Kap. V, 2, 3; Zeits. f. Physik **57**, 30 (1929).

tion α to define thermal equilibrium. Hence v. Neumann was led to introduce a *macroscopic* definition similar to that previously used by Pauli[18] and appropriate to an observer who can make only crude macroscopic measurements. He identifies the macroscopic entropy with the entropy of phenomenological thermodynamics and uses it in setting up a quantum-mechanical derivation of the second law. This entropy definition is not applicable to microscopic systems, however, and does not make satisfactory connections with the Boltzmann interpretation of entropy as a measure of disorder, or with the Nernst heat theorem. Fortunately it turns out that our improved definition of thermal equilibrium permits us to circumvent the difficulties connected with microscopic entropy and so to abandon macroscopic entropy as anything other than a secondary concept.

Before introducing either statistical definition of entropy we need briefly to recall a few simple properties of the statistical matrix ρ. It is well known that ρ can always be given diagonal form by referring it to a properly chosen orthonormal system of wave functions φ_1', φ_2', $\cdots\varphi_j'$, $\cdots$. Each diagonal element $r_j=\rho(j,j)$ is then correlated with a corresponding wave function φ_j'. The ensemble in the state ρ is indistinguishable from one constructed by mixing N_1 systems in the state φ_1', N_2 in the state φ_2', etc., where

$$N_j=r_jN;\quad N=\sum_j N_j.$$

This means incidentally that in the case of a pure state ensemble the diagonal form of ρ contains but a single nonvanishing element. Its value is unity.

The first step in setting up the microscopic statistical definition of entropy is to show by thermodynamic argument that the entropy of all pure states of an ensemble must be the same. This permits us to fix the absolute value by arbitrarily setting the entropy of every pure state equal to zero. The second step is to show by thermodynamic argument involving a reversible mixing of orthogonal pure state ensembles that the entropy of a mixture of such states can be calculated as we calculate the entropy of mixing perfect gases. This leads to the formula

$$S(N)=-kN\sum_j\frac{N_j}{N}\ln\left(\frac{N_j}{N}\right)=-kN\sum_j r_j\ln r_j. \quad (4)$$

The second sum is the (invariant) spur of the matrix $\rho\ln\rho$. Dividing by N to get the entropy of a single system in the state ρ we obtain

$$S=-k\,\text{Spur}\,\rho\ln\rho. \quad (5)$$

For maximum entropy consistent with a given average energy ρ can be proved to have the form of Eq. (3). Thus the state of thermal equilibrium as defined by the process β is the state of maximum microscopic entropy for the given mean energy. Since each state of thermodynamic equilibrium in phenomenological thermodynamics is the state of maximum entropy consistent with its energy, this conclusion lends strong support to the idea that the entropy of phenomenological thermodynamics should be identified with the microscopic statistical entropy of Eq. (5).

Now for the question of disorder. Let us imagine ourselves in the process of creating a mixed ensemble out of a collection of pure state subensembles with orthogonal wave functions φ_1', φ_2', $\cdots\varphi_j'\cdots$. Before mixing the subensembles are laid out before us in separate space compartments. We know the exact microscopic state (ψ-function) of each system in the whole collection. Our information is a maximum and the order of the super-ensemble, like that of a brigade of regiments on parade, is perfect. The entropy is zero. Mixing these subensembles involves discarding our knowledge of the individual systems with the individual pure states. It replaces order by disorder and creates the entropy of Eq. (4). We take as our measure of the disorder the number of ways in which the N systems can be distributed among the various substates without altering the ρ of the complete mixed ensemble. This number is

$$W=\frac{N!}{N_1!N_2!\cdots}.$$

Let us now allow N to become infinite while the r_j's approach definite asymptotic limits.[19]

[18] W. Pauli, Jr., in the *Sommerfeld Festschrift*, "Probleme der Modernen Physik," (Leipzig, 1928), p. 31.

[19] Each $r_j=N_j/N$ can be kept approximately constant after N_j has become a large number.

Stirling's formula can be applied to each $N_j!$ when it becomes large so that

$$\lim_{N\to\infty} (1/N) \ln W = -\sum_j r_j \ln r_j. \qquad (6)$$

Thus in the case of a very large mixed assembly we can write

$$S = (k/N) \ln W. \qquad (7)$$

The mathematics used in establishing this relation between entropy and disorder is the same as that used by Boltzmann and Planck, but the arrangements counted are arrangements of completely independent systems in different pure states and not rearrangements of molecules belonging to one system in cells of phase space. The usual objection to the use of Stirling's formula is avoided.

The quantity W can be regarded as a measure of the information discarded in forming the mixture. This correlation of entropy with lack of information is fundamental in view of the quasi-subjective character of all wave functions and statistical matrices.[20] The existence of such a correlation has been noted by v. Neumann.[21]

The Principle of Entropy Increase

The microscopic entropy has the peculiar property that it is constant in time for an isolated system. This is not surprising since the laws of quantum theory permit us to compute in principle from any initial ψ a unique corresponding final ψ at any later time t, provided only that the system is isolated and moves under the influence of a known Hamiltonian function. Thus our knowledge would not be altered by the passage of time if we were sufficiently expert mathematicians. Nevertheless, this property of microscopic entropy is disconcerting in view of the fundamental place which the principle of the increase of entropy for isolated systems occupies in thermodynamic theory. It was the discrepancy which this property brought to light which induced v. Neumann to develop the less simple concept of macroscopic statistical entropy.

From our present point of view, however, the situation is not unsatisfactory. The notion that the entropy approaches its maximum by the mere passage of time in the case of an isolated system is a corollary on the use of the operation α as the procedure for securing thermodynamic equilibrium in phenomenological thermodynamics. We have abandoned the premise and must expect to abandon the corollary. Actually the operation of producing perfect isolation is an ideal one which we can only approximate in practice. So far as I can see the only customary use of the principle we are giving up is to prove that the state of maximum entropy for a given energy is a state of thermodynamic equilibrium. From the point of view of statistical mechanics the latter principle is already established and we do not need to base it on the postulate we are discarding.

Moreover, it is possible to work out a substitute for the usual formulation of the principle of increase of entropy. I have been able to prove, for example, that if we establish thermal contact between two or more systems with independent initial states and isolate the united system, the sum of the entropies of the component systems[22] at an arbitrary later time will practically always be greater than at the beginning. It can never exceed its initial value. Furthermore, if we subject any system A to the operation β and choose the temperature of the thermostat so that the energy expectation value of $\bar{E}$ of A is unchanged by the contact—no net heat imparted by the thermostat—the system A will approach thermodynamic equilibrium with its initial $\bar{E}$. Hence the entropy must increase.

Other useful theorems connected with the increase of entropy may be revealed by further study.

The Reversible Path

In classical thermodynamics a reversible path is often defined as a succession of states of thermodynamic equilibrium (equilibrium path). When we carry this definition over into the new theory we must note that slow adiabatic compression of a gas in an ideal cylinder whose walls are completely impervious to heat will not insure an equilibrium path. As a matter of fact, it is not

[20] Cf. E. C. Kemble *Fundamental Principles of Quantum Mechanics* (New York, 1937), Sections 41 d, e.

[21] J. v. Neumann, *Math. Grundlagen d. Quantenmechanik*, p. 212.

[22] The microscopic entropy of a system is equal to the sum of the entropies of two or more component parts when the system is in thermodynamic equilibrium and the mutual energies of the parts are negligible. In all other cases the entropy of the complete system is not necessarily equal to the sum of the entropies of the parts.

a new observation that such a compression does not necessarily carry a canonical ensemble over into a canonical ensemble. To obtain a true adiabatic equilibrium path we must accordingly carry the compression out infinitely slowly in an adiabatic calorimeter that will "stir" the system under investigation without imparting heat to it. This type of adiabatic path should be used in the ideal Carnot cycle. Otherwise there will be an irreversible change when the system is brought into contact with a heat reservoir at the end of each adiabatic line. If the compression (or expansion) is carried just far enough so that contact with the reservoir at constant volume produces no change in $\bar{E}$, the pressure can still be altered and with it the efficiency of the cycle. The effect is a negligible one in the case of the ordinary macroscopic "working fluid."

To see how this works out let us consider first the case of a working fluid consisting of a single monatomic gas molecule. Let the molecule be confined to a rectangular parallelepiped with edges of length a, b, c. Let the compression be produced by variation in a only. Let σ_x, σ_y, σ_z denote the wave number components and let i, j, k be integers. The energy of a normal mode of vibration is

$$E_{ijk}=\frac{h^2}{2m}(\sigma_x^2+\sigma_y^2+\sigma_z^2)=\frac{h^2}{8m}\left(\frac{i^2}{a^2}+\frac{j^2}{b^2}+\frac{k^2}{c^2}\right).$$

Corresponding to each such mode of vibration we have a constant diagonal element r_{ijk} of the statistical matrix ϱ, provided that the system belongs to an ensemble in statistical equilibrium. We assume that this condition is satisfied. The average pressure for the ensemble is then

$$\bar{p}=-\frac{1}{bc}\sum_{i,j,k} r_{ijk}\frac{\partial E_{ijk}}{\partial a}=\frac{1}{a^3bc}\frac{h^2}{4m}\sum_{i,j,k} r_{ijk}i^2.$$

If the system is compressed in a box with ideal perfectly reflecting walls, the quantum-mechanical form of Ehrenfest's adiabatic theorem[23] tells that the population numbers r_{ijk} will be constant. Hence the expression $\sum_{i,j,k} r_{ijk}i^2$ will be constant. The volume V is abc and we have

$$\bar{p}V^3=\frac{b^2c^2h^2}{4m}\sum_{i,j,k} r_{ijk}i^2=\text{Const.}$$

[23] M. Born and V. Fock, Zeits. f. Physik **51**, 165 (1928).

On the other hand, if the compression takes place in an adiabatic calorimeter the r_{ijk}'s are not constant, but functions of the energy and the temperature. It is easy to see that in this case $\bar{p}V$ is equal to $\frac{2}{3}$ of the expectation value of the total energy and that $\bar{p}V^{5/3}$ is constant. The excess pressure in the former case is due to the fact that most of the work of compression is pumped into those modes of vibration which exert the greatest pressure against the piston. In the case of a macroscopic sample of gas consisting of interacting molecules the energy eigenfunctions become very complex and each one exerts sensibly equal pressures on all of the walls of the chamber. In this case the pressure must remain uniform on all walls no matter which type of compression we use and so it makes no practical difference whether we use the adiabatic calorimeter, or not.

The Statistical Derivation of the Second Law

At this stage of the argument it is easy to show that for an element of an equilibrium path the increment in microscopic entropy is equal to the average heat absorbed multiplied by an integrating factor γ which we identify with $1/kT$. Combining Eqs. (3) and (5) we have

$$\begin{aligned} S_{\text{equil}} &= -k\sum_j r_j \ln r_j, \\ &= k\sum_j r_j\{\gamma E_j+\ln \textstyle\sum_i e^{-\gamma E_i}\}. \\ &= k\gamma\bar{E}+k\ln \textstyle\sum_i e^{-\gamma E_i}. \end{aligned} \tag{8}$$

Differentiation gives

$$\begin{aligned} (dS)_{\text{equil}} &= k\left\{\gamma d\bar{E}+\bar{E}d\gamma \right. \\ &\qquad \left. -\frac{[\sum_i e^{-\gamma E_i}(\gamma dE_i+E_i d\gamma)]}{\sum_i e^{-\gamma E_i}}\right\} \\ &= k\gamma\left\{d\bar{E}-\frac{\sum_i dE_i e^{-\gamma E_i}}{\sum_i e^{-\gamma E_i}}\right\}. \end{aligned} \tag{9}$$

The second term in brackets is easily recognized as the average external work due to the variation in the externally controllable parameters. Hence the whole quantity in brackets is the statistical average of the heat absorbed in the path element.

We can now define the absolute thermodynamic temperature by the equation

$$\gamma = 1/kT$$

and verify without difficulty that it has the usual properties of thermodynamic temperature. This justifies the statement following Eq. (3).

As a final point in the argument one can derive the second law of thermodynamics from the statistical theory in the following manner. Let us assume that we have a self-acting cyclic mechanism which can pump heat out of a cold reservoir and supply it to a hot reservoir. We can then suppose that we have an ensemble of cold reservoirs in thermodynamic equilibrium at temperature T_2 and a similar ensemble of hot reservoirs in thermodynamic equilibrium at temperature T_1. Let the mechanism be used to pump heat from each cold reservoir to the corresponding hot reservoir, the combination being isolated. Then entropy decrease of the cold reservoirs would exceed the entropy increase of the hot reservoirs. As the mechanism and working fluid return cyclically to the same condition they contribute no entropy change. Thus the sum of the entropies of the parts of the combination system increases in time contrary to the principle of increase of entropy for such cases as stated at the end of the preceding section. Hence the supposed mechanism is contrary to our statistical theory and we have derived the second law of thermodynamics.

NOVEMBER 15, 1939 PHYSICAL REVIEW VOLUME 56

A Precision Determination of the Viscosity of Air

J. A. BEARDEN
Department of Physics, Johns Hopkins University, Baltimore, Maryland

(Received August 8, 1939)

The rotating cylinder method has been used for making a precise determination of the viscosity of air. The inner cylinder was rotated, which made possible a higher degree of accuracy in the construction of the apparatus and in its adjustment than was possible if the outer cylinder had been rotated. Two rotating cylinders were used, and the error introduced into the viscosity by inaccuracies in machining and measurements was for the best cylinders 2.01×10^{-3} percent. Torsion wires were studied in detail and a method of treatment used which removed the defects of zero drift and variability of torsion constant for static and dynamic conditions. A precision telescope and calibrated comparator were used in measuring the angular deflection of the deflecting cylinder. The timing and driving mechanism consisted of a tuning fork controlled d.c. motor whose speed was constant within one part in 10^6, as checked by N.A.A. time signals. The viscosity of air at 20.00°C is $(1819.20 \pm 0.06)\ 10^{-7}$ c.g.s. unit.

INTRODUCTION

REDETERMINATIONS[1-5] of the viscosity of air during the past two years have shown that the major part of the discrepancy between Millikan's oil-drop value of the electronic charge and that obtained by x-rays[6] was primarily due to an error in the viscosity measurements. Not only are the oil-drop and x-ray methods intrinsically the most accurate available from the standpoint of experimental difficulties, but neither, fortunately, requires a knowledge of Planck's constant h. Since the electronic charge is one of the most important constants in physics, it is essential that its evaluation be made by both methods with the highest precision attainable with modern experimental technique.

The experimental value of the viscosity of the gas surrounding the oil drop enters the final calculation of e to the three-halves power. This is the most important and most difficult measure-

[1] W. N. Bond, Proc. Phys. Soc. **49**, 205 (1937).
[2] G. Kellström, Phil. Mag. **23**, 313 (1937).
[3] W. V. Houston, Phys. Rev. **52**, 751 (1937).
[4] G. B. Banerjea and B. Plattanaik, Zeits. f. Physik **110**, 676 (1938).
[5] P. J. Rigden, Phil. Mag. **25**, 962 (1938).
[6] J. A. Bearden, Phys. Rev. **47**, 883 (1935). Jesse W. M. DuMond, Phys. Rev. **56**, 153 (1939), reference 17.

ment that has to be made in the evaluation of e by this method. This measurement has been undertaken first, and the present report is entirely on this phase of the problem.

Experimental Method

The only methods available for making accurate measurements of the viscosity of a gas are: the rotating cylinder method and the flow through a capillary tube. The latter method is experimentally much simpler than the rotating cylinder method, but the numerous corrections which must be made make the results unreliable for precision measurements. There are also theoretical questions concerning the velocity gradients near the ends of the capillary which have not been completely solved. The rotating cylinder method possesses the distinct advantages of precision in the mechanical construction and freedom from theoretical objections. This method has therefore been chosen for the present experiments.

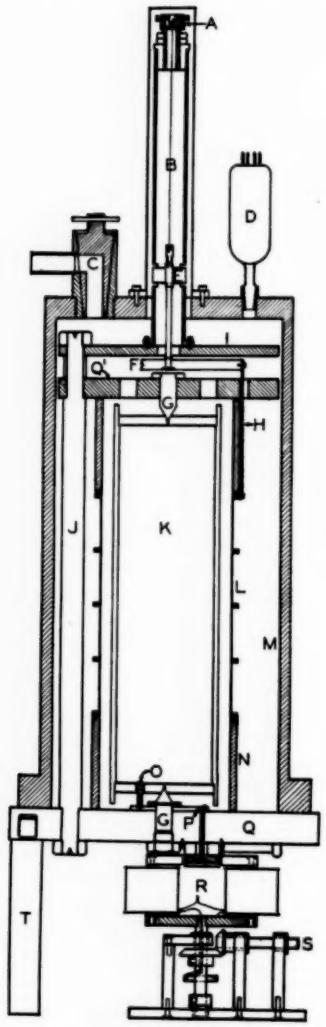

FIG. 1. Cross section of apparatus. A, adjustable torsion wire support; B, torsion wire; K, inner cylinder rotating on centers G; L, suspended cylinder; N, guard cylinders; M, bell jar; R, magnetic drive.

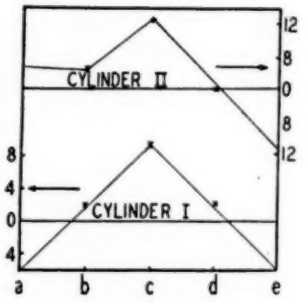

FIG. 2. Diameters of cylinders plotted as a function of their length. The ordinates are in cm$\times 10^6$.

The design finally adopted for the apparatus differs mainly in one respect from that used by previous experimenters. In this work the constantly rotating cylinder was made the inner cylinder and the deflecting cylinder was on the outside. This method has four important advantages: first, it is possible to machine the external diameter of a long cylinder with much greater precision than can be accomplished on the internal diameter of a cylinder of the same length. The deflection cylinder is short, permitting its internal diameter to be accurately machined without difficulty. Second, the measurements of the diameters and lengths can be made with high precision. Third, the assembly and adjustments can be made easily and accurately. Fourth, the rotating cylinder can be rotated on centers.

It is obvious that the theoretical expression for the viscosity is exactly the same for the present

TABLE I. *Diameters of rotating cylinders.*

Position	Cylinder I Diameter	Cylinder II Diameter
a	12.44218	13.57041
b	12.44226	13.57040
c	12.44233	13.57048
d	12.44226	13.57035
e	12.44218	13.57011
Average	12.44224	13.57035

TABLE II. *Measured diameter of suspended cylinder.*

Position *A*	14.95296 cm
Position *B*	14.95302
Position *C*	14.95295
Average	14.95298±0.00050 cm

arrangement as for the previous one. This expression may be written

$$\eta=\frac{F}{8\pi^2}\frac{b^2-a^2}{La^2b^2}\varphi t,$$

$$\eta=KF\varphi t/8\pi^2 \quad \text{where} \quad K=(b^2-a^2)/La^2b^2, \quad (1)$$

where b is the radius of the outer suspended cylinder, a is the radius of the inner cylinder, L is the effective length of the suspended cylinder, ϕ is the angular deflection of the suspended cylinder, F is the torsion constant of the suspension, t is the time of revolution of the inner cylinder. K may be considered a constant of the apparatus unless the spacings between the guard rings and suspended cylinder are altered. The effective L for the present apparatus is equal to the length of the suspended cylinder plus one-half the sum of the spacings between the guard rings and cylinder.

CONSTRUCTION AND DIMENSIONS OF VISCOSITY APPARATUS

A low density, strong, machinable, nonmagnetic metal was essential for the rotating and suspended cylinders and for the guard rings. It was also necessary that the material could be easily freed of strains so it retained its shape after machining and grinding. It was found that a magnesium alloy, Dow metal *J*, fulfilled the requirements better than any other available material.

Previous interferometer experience with high precision spectrometer bearings and spectrometer shafts mounted on centers showed that the method of centers for the mounting of the constantly rotating cylinder is much superior to the usual precision cone bearing. The cylindrical surface could be given its final finishing while rotating on the centers later used in the measurements. Failure of the cylindrical surface to rotate about its true center is doubtless an appreciable source of error in former work. The design of the apparatus used in the present work is shown schematically in Fig. 1.

Two inner rotating cylinders K were constructed of different diameters. In each case the inside of a Dow metal tube was machined to a uniform diameter except at the ends where it was enlarged to receive a metal disk. The wall thickness was about 1.1 cm. The finished disks contained the centers, two holes each for air to pass freely in and out, and a hole 0, Fig. 1, for the driving pin. These disks were pressed in and secured by Dow metal pins. The outside surface was rough machined (within 0.001 inch) and then the entire cylinder was annealed to remove all strains. Afterwards the outside surface was finished on a cylindrical grinding machine in which the cylinder rotated on dead centers and water was flowed over the cylinder to maintain it at constant temperature.

The diameter of each cylinder was measured at five positions along its length and around its circumference by the National Bureau of Standards. Measurements were made with different pressures on the contact surfaces and the final result obtained by extrapolating to zero pressure. All measurements were made at 20.00°C and this same temperature has been maintained in all the experimental work, thus avoiding any correction for expansion or contraction. The results of the measurements on the two cylinders are given in Table I. Positions *a* and *e* are at points corresponding to the ends of the suspended cylinder *L* Fig. 1; *b*, *c*, and *d* are equally spaced between *a* and *e*. The result for each point is an average of the diameters along different directions. These diameters differed by only one part in 10^6.

In Fig. 2 the diameters of the cylinders are plotted as a function of their lengths. The diameters are greatest at the center of the cylinders and taper to a smaller diameter at each end.

TABLE III. *Diameter of suspended cylinder by volumetric method.*

Trial 1	4573.831 cm³
2	0.807
3	.843
4	.783
5	.779
6	.807
Average	4573.808±0.006
Diameter = 14.95289±0.00005 cm	

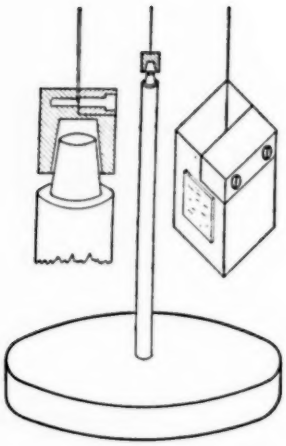

FIG. 3. Lower clamp for the suspension wire and the ground joint for attaching it to the rod which holds the inertia disk. Inertia disk and supporting rod.

Cylinder I is better than II and for this reason has been used in most of the measurements. The value of a which should be used in Eq. (1) is $(n^{-1}\Sigma a^2)^{\frac{1}{2}}$, but the variations are so small this is exactly the same as the average value which is given in Table I. The probable error can be estimated from the irregularities of the curves in Fig. 2 plus the errors in the gauges used in measuring the diameters. For cylinder I this amounts to ± 0.00002 cm, and for cylinder II ± 0.00004 cm.

The suspended cylinder L was designed with five sustaining ribs, as shown in Fig. 1. This gave the cylinder sufficient strength to retain its accurate dimensions and was also light enough to be supported by a small torsional wire. The end ribs were made larger than the remaining three in order that they could be used for supporting the cylinder on a precision face plate for final finishing.

The cylinder was machined from a well-annealed Dow metal tube. It was then annealed again and its diameter changed in different places by as much as 0.007 cm. The cylinder was remachined, removing only sufficient material to make it true. Again the annealing distorted the cylinder. The process of machining and annealing was repeated with a higher annealing temperature. Successive attempts finally located the best annealing temperature and thence the cylinder retained its dimensions accurately. The final machining removed less than 0.002 cm of material from both outside and inside after the last annealing.

The length and diameter of this cylinder were measured by the National Bureau of Standards. The length is

$$L = 26.04583 \pm 0.00008 \text{ cm}.$$

The only method available for measuring the inside diameter must make use of spherical contact points. The contact pressure for precise measurements is such that with the present metal slight indentations were undoubtedly made. The pressure was prevented from warping the cylinder by applying an equal pressure on the outside directly in line with the internal pressure. The average results for the three positions are given in Table II. These results are very consistent, but inside diameter measurements are difficult, and correction for the contact indentation cannot be made accurately. The $\pm$ error given in Table II is a limiting error of the measurement and not a probable error.

The length of the cylinder was accurately known, so a determination of the volume of the cylinder was used as a more precise method of determining the above diameter. The cylinder was clamped to a flat (ground) Dow metal plate. A fine ground flat glass plate was used as a top for the cylinder. The cylinder with ends was weighed on a large balance in a constant temperature room at 20.00°C. The cylinder was then filled with distilled water at the same temperature and reweighed. Buoyancy corrections for air were made and the weights were calibrated by the National Bureau of Standards. The density of water at 20.00°C was taken as

$$\rho = 0.998232,$$

which is given in the *International Critical Tables*. Landolt and Börnstein give 0.998230 which differs by only two parts in 10^6 from the above value. The resulting values for seven independent determinations are given in Table III. These measurements give a diameter in good agreement with that of Table II. A weighted average of the two results has been used for calculating b^2 and the probable error has been taken as that of Table III.

$$2b = 14.95290 \pm 0.00005 \text{ cm}.$$

The guard cylinders N were made with an inside diameter the same as the finished diameter of the suspended cylinder. The outside diameters were 0.0005 cm larger than the outside diameter of the ribs on the suspended cylinder. The inside and outside cylindrical surfaces were concentric with the centers which supported the rotating cylinder. The inside edges of the guard cylinders and suspended cylinder were cut with sharp right angle edges.

In constructing the guard cylinders, the steel base Q and the secondary base Q' were first rough machined and all holes drilled and tapped, including those (not shown) for attaching the guard cylinders. The top and bottom surfaces were then finished plane and parallel. The two plates were then bolted together and the holes for the centers G and three supporting rods J were carefully bored perpendicular to the surfaces with a boring mill. Only a small amount of metal was removed in this finishing process in order to reduce warping to a minimum. The lower guard cylinder whose end had previously been finished was fastened permanently to the base Q with eight machine screws. The base was then bolted to the lathe face plate which had just previously had a finishing cut taken over its surface making it accurately perpendicular to the axis of the lathe spindle. A tight fitting ground rod was inserted in the center hole G and was used to accurately center the base Q on the lathe axis. The center G was inserted and its cone, together with the inside and outside diameters of the guard cylinders, were finished without disturbing the position of the work on the face plate. The final 0.0025-cm cuts were taken without letting the lathe spindle stop, in order to avoid changes in oil films on the bearings. The top guard cylinder was machined in exactly the same manner as the bottom one.

The secondary steel base Q' was supported by three posts J. These were made of steel and were 28 mm in diameter except at the ends, where they were 20 mm. The rods were carefully machined on centers, and particular care was taken to make the small diameters so the rods could just be pushed into the holes in the bases. A special device was arranged to make the length between the shoulders of all three rods exactly the same. This distance determines the separation and parallelism of the guard cylinders.

A shelf I was necessary for supporting the torsion head assembly. A steel disk with parallel sides was supported above Q' by three cylinders of equal length slipped over the rods J.

The spider F which supported the suspended cylinder was milled from a finished Dow metal disk containing a central hole bored perpendicular to the surfaces. This hole was used as a guide in milling away the material to leave three arms 120° apart and the center of gravity exactly in the center of the hole. Similar Dow metal strips H and screws were used for connecting the spider to the suspended cylinder L.

The diameter of the rod where the mirror E was mounted was enlarged and one-half of the rod milled away, so that the reflecting surface of the mirror was on the axis of rotation. The lower end fitted snugly into the spider and the top end was tapered to fit the torsion wire clamp as shown in Fig. 3. The size of rod and mirror were adjusted to keep the center of gravity as near the axis of the rod as possible.

The torsion wire clamps were found to affect the characteristics of the torsion wire B considerably. If the wire was not clamped correctly, its damping constant was increased, the zero position was not stable, and the period of oscillation was not constant. These effects introduced errors of the order of one part in 10^4, which were entirely too great for the present work.

The final design of the lower clamp is shown

TABLE IV. *Separation of guard rings.*

POSITION	SEPARATION
1	26.0760 cm
2	26.0763
3	26.0761
4	26.0765
5	26.0766
6	26.0764
7	26.0764
8	26.0762
9	26.0763
10	26.0760
11	26.0764
12	26.0767
13	26.0765
14	26.0762
15	26.0763
16	26.0765
Average	26.07634 ±0.00020

in Fig. 3. An ideal clamp would be a cylindrical hole of exactly the size of the wire such that the wire is held rigidly up to the point where it leaves the holder. This was approximated by cutting two 90-degree grooves in the flat clamping surfaces to such a depth that when clamped together with the wire between them, the surfaces were separated by about 0.001 cm. The grooves were accurately machined so that the wire was concentric with the mirror rod. The tapered joint made it possible to remove the wire and clamp from the mirror rod, permitting the torsional constant of the wire to be measured in a separate apparatus.

The upper torsional wire clamp A was made similar to the lower except that no tapered joint was necessary. This support was made so that it could be moved horizontally in any direction, rotated about its vertical axis or adjusted as to height. When it was necessary to remove the torsion wire for calibration, the tapered lower joint was loosened from the mirror rod and then the wire with the entire upper assembly was raised out of the supporting brass tube.

A magnetic drive R rotated the inner cylinder. This allowed the cylinder to be rotated in vacuum if desired and also made it possible to evacuate the apparatus and fill it with the desired gas without disturbing any of the driving mechanism.

A soft iron rod $1.0\times1.0\times4$ cm was attached perpendicularly to the shaft which rotated the spur gear P, Fig. 1. This drive was enclosed in a vacuum-tight brass housing U. The soft iron bar was driven by the electromagnet R. The weight of the coils was balanced so in rotating they caused no perceptible vibration of the apparatus. The 0.1-ampere exciting current was carried through a small armature on the lower part of the rotating shaft. The driving was through S and the two-to-one reduction bevel gears.

An 1800-r.p.m. d.c. motor was connected to S Fig. 1 through a reduction and ratio changing gear system. A 100-to-one worm gear reduced the motor speed to 18 r.p.m. Spur gears were used to change the 18-r.p.m. shaft speed in 12 steps from 3 r.p.m. to 108 r.p.m. An arrangement of four spur gears was used which allowed the shaft S Fig. 1 to be rotated in either direction. The inner rotating cylinder could be rotated in either direction at 12 speeds, ranging from one revolution in 6.67 seconds to one revolution in 240 seconds.

A test of the possible effect of the rotating magnetic drive on the suspended cylinder was made. A Celluloid cylinder was placed between the inner cylinder K Fig. 1 and the suspended cylinder L such that it did not touch either. The inner cylinder was rotated at various speeds with the magnetic drive, but no deflection of the suspended cylinder was observed. The current through the magnetic coils was increased to 1.0 ampere and no deflection was observed. A deflection could have been observed which would have caused an error in the final viscosity measurements of one part in 5×10^4.

The bell jar M was made of cast Dow metal and painted on the outside with Glyptol. A mercury metal diffusion pump with a speed of 10 liters per second was used for evacuating the apparatus through the large metal stopcock C Fig. 1. An ionization gauge D and a Piranni gauge (not shown) were used for measuring the low pressure, and a mercury-in-glass manometer for pressures up to one atmosphere. Apiezon Q was used for sealing all joints. Gases were admitted through a needle valve (not shown) screwed into the base Q Fig. 1. The vacuum usually attainable was about 10^{-5} mm, and when the stopcock C was closed the pressure did not increase to more than 10^{-4} mm in 12 hours.

A heavy steel subbase $2.5\times50\times61$ cm mounted about 15 cm from the floor was used as a base upon which to mount the viscosity apparatus. The base was supported on four steel rods 32 mm in diameter and 60 cm long. These rods were rigidly secured to the concrete floor of the room with nuts and washers above and below the floor. The steel base was also fastened by nuts which allowed it to be leveled.

Temperature Control

The measurements of the important dimensions were all made at a temperature of 20.00°C. In order to avoid expansion corrections, this temperature was chosen for the room temperature in which all measurements have been made.

The normal temperature of the room used is about 21 to 22°C. In the winter months the necessary cooling was obtained by admitting air from the top of the building through a small shaft that

could be connected to the room. A blower type fan operated by a thermostat admitted cold air as needed. The speed of the blower and electrical heating were adjusted to give the optimum heating and cooling cycle. A recording clock was used to keep the heating and cooling cycle adjusted.

In the summer months an ammonia cooling system was used to maintain a 300-gallon tank of water at about 10°C. The tank and ammonia plant were in a room underneath the constant temperature room. The cold water was circulated through an auto radiator and a blower, controlled by the thermostat, circulated air through the radiator as needed.

A thermostat was needed which would respond very quickly to small changes in air temperature. This was attained by making a thermostat whose expanding liquid was xylol in a copper tube 6 mm in diameter and 13 meters long, coiled into a helix of 24 turns. On one end of the copper tube a small sylphon bellows was attached which permitted accurate adjustment of the thermostat. A glass capillary U-tube with electrical contacts was sealed to the other end. Mercury was used for closing the contacts. A 0.1°C change in air temperature opened or closed the contacts in about 20 seconds. A current of 6 ma at 6 volts operated a low wattage relay which in turn operated a mercury relay in the blower circuit. Four fans were used to circulate the air at a sufficient rate to maintain the same temperature in all parts of the room.

The heating and cooling cycle gave rapid changes in temperature of about 0.1°C. The temperature as read on a Beckman thermometer inside the thick-walled bell jar of the apparatus varied less than 0.01°C in 24 hours. Since practically all pieces of apparatus used were massive, their average temperature variations were less than 0.01°C.

TABLE V. *Mirror to wire distance.*

DATE	DISTANCE
November 22, 1937	2784.37 mm
March 26, 1938	2784.38
October 11, 1938	2784.37
January 3, 1939	2784.38
February 7, 1939	2784.39
Average	2784.38 mm
Window correction	2.94
Effective mirror-to-wire distance	2781.44 mm

ASSEMBLY AND ADJUSTMENT OF APPARATUS

In order for the suspended cylinder to be accurately concentric with the guard rings and rotating cylinder, it was necessary to make the base Q accurately horizontal. This was accomplished by assembling the lower part of the apparatus and firmly fastening it to the subbase (not shown) and then leveling with a high precision level by raising or lowering the clamping nuts which held the subbase to the concrete floor. A few hours were allowed for the temperature of these parts to return to normal and the leveling was further adjusted. This process was repeated until the base Q and the top of the guard cylinder were level within three seconds of arc. The leveling has been rechecked several times, and at no time has the base been out of level by more than six seconds of arc.

The distance between the guard cylinders was measured several times at 16 equally spaced positions with a calibrated bar and inside micrometer. This was accomplished by disconnecting the spider arms H and sliding the deflecting cylinder in against the inner cylinder at the point of measurement. The results obtained for each position are recorded in Table IV, from which the parallelism can be judged. The probable error takes into account the uncertainty of the calibrated gauges. The error calculated from the table (consistency) is about one-seventh that used. The difference between this separation and the length of the suspended cylinder is 0.03051 cm, which gave a gap of 0.0153 cm at the top and bottom when the suspended cylinder was adjusted. This gap distance was also measured with the suspended cylinder in place but resting centrally on the lower guard ring. This measurement gave 0.031 cm, which is in good agreement with the above measurements.

The horizontal position of the upper guard cylinder was checked by resting the suspended cylinder on the lower guard cylinder. The outside diameter of the guard cylinders was made 0.001 cm larger than the outside diameter of the suspended cylinder ribs. A sharp angle straightedge held against the outside diameter of the lower guard cylinder with a light opposite from the observer made it very easy to locate the suspended cylinder centrally with respect to the

lower guard cylinder. An examination of the top guard cylinder and suspended cylinder with the light and straight edge showed them to be concentric within 0.0005 cm.

A selected torsion wire of the correct length was inserted in the wire clamps and placed in the torsion head assembly. A small twisting force was sufficient to attach the taper joints of the mirror rod and wire clamp. The vertical and horizontal head motions were then adjusted until the suspended cylinder was centrally located between the guard cylinders and concentric with them. The vertical adjustment is relatively unimportant, but the concentric adjustment is very important. The latter adjustment was checked with the straight edge and light, as used above on both guard cylinders. It was possible to make the suspended cylinder concentric within 0.0005 cm, and in all adjustments the discrepancy never exceeded 0.001 cm. The vertical adjustment located the suspended cylinder within 0.01 mm of the central position. The angular position of the suspended cylinder was adjusted so that the mirror was normal to center of the optical scale (comparator). The bell jar was put in place and rotated until the plane parallel window was almost parallel to the mirror.

Optical System

The optical system, consisting of a telescope and comparator, was mounted on a steel table firmly bolted to the concrete floor.

The telescope objective was a very high quality corrected lens 7.5 cm in diameter and 100 cm focal length. The micrometer eyepiece was the same as used by the Societe Genevoise in the microscopes on the high precision x-ray spectrometers. The parallel cross hairs are moved by a precision screw which was calibrated for both periodic error and error of run. The size of the light source was selected so that the width of its image formed by the telescope objective in the plane of the cross hairs was just less than the separation of the parallel cross hairs. This method permits a minimum error of setting for this type of measurement.

The graduated scale usually used was replaced in the present method by a high precision comparator calibrated to within 0.001 mm for both periodic error and error of run.

The light source, which was mounted on the comparator, consisted of a vertical wire with a neon lamp placed directly behind it. Thus the image in the telescope was a dark line on a uniformly lighted background.

In order for the angles to be easily computed from the comparator measurements, it is necessary to set the ways of the comparator parallel to the reflecting mirror at its zero position. A 30-mm objective telescope equipped with a Gauss eyepiece was set perpendicular to the mirror in its zero position and about nine meters away. A plane front silvered mirror 18×8 cm was placed about 10 cm from the comparator and adjusted normal to the telescope axis, which made it parallel to the suspended mirror within five seconds of arc. A sensitive indicator was attached to the comparator slide and touching the large silvered mirror. The base of the comparator was then adjusted until the indicator showed no variation as the carriage was moved through the entire length of the mirror (18 cm).

The distance from the vertical wire to the mirror was measured with the aid of a steel alloy measuring bar having parallel ends. This bar, which was calibrated by the National Bureau of Standards, was mounted horizontally in appropriate supports between the mirror and vertical wire. The remaining short distances, about 6 cm, were measured with calibrated inside micrometers. Instead of measuring the distance between the measuring bar and mirror directly, the distance between bar and mirror rod was measured, and to this was added one-half the diameter of the rod. This eliminated the difficulty caused by the oscillation of the suspended mirror. The distance was measured five times during the course of the experiments, and the results of these measurements are given in Table V.

The probable error in this distance is about 0.01 mm and certainly does not exceed 0.02 mm, which has been accepted as the probable error in calculations.

The measured distance given in Table V must be corrected for the glass window. The thickness of the window was 8.585 mm and the index of refraction was $\mu=1.5216$. The equation for the shortening of the optical path is

$$X=(\mu-1)d/\mu$$

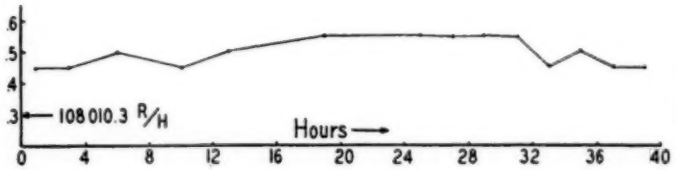

FIG. 4. A 40-hour test on the speed of the tuning fork controlled motor. The maximum variation in the motor speed is 0.1 revolution per hour or one part in 10^6.

where d is the thickness and μ the index of refraction of the glass plate. This gives 2.94 mm which must be subtracted from the result in Table V, and gives 2781.44 mm as the corrected mirror-to-wire distance.

After the above measurements were made, the torsion head of the suspension was rotated until the image of the vertical wire was visible in the field of the telescope. This established the zero point on the scale. Rotation of the inner cylinder then produced a deflection θ on either side of the zero depending upon the direction of rotation. If d represents the total deflection on the comparator, then

$$2 \tan 2\theta = d/2781.44.$$

Two methods of observation were used. In the first, the suspended cylinder was brought to rest either in its zero position or in the deflected position. The micrometer was set at its zero position and the comparator carriage moved until the vertical illuminated wire appeared midway between the cross hairs. This method required that the suspended cylinder be brought exactly to rest or that a large number of settings be made. Both of these required so much time that this method was used only as a check on the second procedure.

In the second method, the suspended cylinder was purposely oscillated at its natural period sufficiently to give a displacement of the telescope image of about ± 0.05 mm. The comparator carriage was then set approximately in position. The extreme positions of several oscillations were determined with the micrometer. The mean of these indicated the correction that had to be added to the comparator setting. The correction usually did not exceed 0.020 mm. Since different amplitudes were used and each setting of the micrometer head was made in a darkened room, it is obvious that this method reduces the human error which falsifies so many precision measurements.

DRIVING AND TIMING APPARATUS

The drive for the rotating cylinder has to maintain a very constant and known speed for long periods of time. In the torsional measurements a high precision printing clock is essential. A single powerful clock has been constructed which serves for both purposes. The clock is accurate to better than one part in 10^6 for both long and short intervals, and because of its possible use in other experimental work, it will be described in some detail.

The essential feature of the present apparatus is the synchronizing of a high quality 0.5-horsepower ball-bearing d.c. motor with a precision electrically driven tuning fork by a Thyratron circuit.[7] The maximum possible variation in synchronism from the mean position is 0.25 revolution of the motor, and this can occur only for large changes in the supply voltage (20 volts) or similar changes in load. In the present work a 240-volt battery supplied the voltage and the small load changed very little at any time. The variation in synchronism under these conditions was less than 0.02 of a revolution of the motor.

The time between any two events could be determined by recording the number of revolutions of the motor by the usual method of reduction gears and divided dials. The positions of the dials were recorded photographically by a Sept movie camera with positive film. The illumination was obtained from an evacuated mercury discharge tube, similar to those previously described.[8] A 10-mf condenser at 2500 volts was discharged through the tube, which gave ample light to photograph all dials. The duration of the flash was less than 10^{-5} second, making it possible to photograph the divisions of the most rapidly moving dial without blurring. Two methods were provided for setting off the discharge tube: a hand key which could be used for timing oscilla-

[7] J. A. Bearden and C. H. Shaw, Rev. Sci. Inst. **5**, 292 (1934).

[8] H. E. Edgerton and K. J. Germeshausen, Rev. Sci. Inst. **3**, 535 (1932).

tion periods, etc., and a connection to a time signal receiver which allowed the time signals from N.A.A. to set off the discharge automatically. This made it possible to record the time signals with an error not exceeding 0.001 second. If the tuning fork vibrated at exactly 60 cycles, then the motor should revolve 108,000.0 revolutions between two hourly time signals. The error in the time signals is about 0.01 second, so for precision checks one must obtain the correction sheets which show how much each hourly time signal was in error.

The constancy of the tuning fork frequency is the determining factor in how accurately the motor speed can be maintained. The first fork used was an Invar fork maintained at constant temperature ($\pm 0.01°C$) driven by the usual vacuum tube method, in which a sine wave current is applied to the magnetic driving coils. This method not only drives by magnetic coupling to the tines of the fork, but also uses a magnetic pick-up for the input to the grid of the first vacuum tube. It is practically impossible to avoid undesirable coupling between these coils. It was proved that this method usually drives the fork at a frequency other than its natural frequency. It may drive the fork either too fast or too slow, depending on the phase relations of the electrical couplings in the amplifier and pick-up system.

Two fundamental changes were made in the method of driving. The first was to use a condenser pick-up for the input to the first vacuum tube. The second was to arrange a Thyratron circuit such that a very short driving impulse could be applied to the tines of the fork as they passed through their normal position at maximum velocity. Small phase errors then have practically no effect on the frequency of the fork, and the fork is driven at exactly its natural frequency.

The new vacuum tube drive made it possible to maintain the frequency of the fork under good conditions to about one part in 10^5 for a few hours at a time. The frequency of the fork was very sensitive to amplitude changes and even though the amplitude was maintained consant, the fork occasionally drifted to a new frequency as if internal damping and stresses had been altered. If the fork stopped for a few hours, it took 12 to 36 hours to attain a constant frequency after restarting. When Elenvar became available for making large forks, one was obtained and this has proved very satisfactory. The tines of the fork were carefully balanced and length adjusted to give a natural frequency of 216,020 vibrations per hour. This fork has none of the bad characteristics of the Invar fork and its frequency has remained constant for 18 months. Fig. 4 shows a typical 48-hour run in which the number of revolutions of the motor per hour is plotted against time. This shows a deviation of less than one part in 10^6, which is more than adequate for the present experiments. Improvements in the circuit and voltage supply should improve the operation so that variations of less than one part in 10^7 should be attainable.

Determination of the Torsional Constant

The method used was the measurement of the period of oscillation of suspended objects of calculable moment of inertia. This is the dynamic method of determining the torsional constant, and in the viscosity measurements the torsion wire is used statically. It is possible that the two torsion constants are not the same, but if not, one would expect the torsional constant to be a function of the period of oscillation. Six inertia objects of different moment of inertia were used to test this point. The period of oscillation was varied from 11 to 67.5 seconds and in some wires a small difference was detected. The wire finally selected showed no difference, as is shown later in Table VII. The expression connecting the period of oscillation T, the moment of inertia I and the torsional constant F is

$$T=\frac{2\pi}{(F/I-K^2/4I^2)^{\frac{1}{2}}},$$

where K is determined from the logarithmic decrement λ by

$$\lambda=(K/2I)\cdot(T/2).$$

It is to be expected that the torsion constant of a given wire will depend on the mass it supports. The exact magnitude of this effect cannot be calculated, for the reduction in cross section of the wire which should lower the torsion constant, may be more than compensated for by

the hardening of the wire due to stretching. Tests were made on several wires and in general the torsion constant increased with load. A steel wire of the type used by Harrington was tested with loads similar to those used in his experiments and it was found that the error made by neglecting this effect might easily account for his low results. In the present experiments the inertia objects were designed to have the same mass as that of the suspended cylinder, together with that of the spider, mirror E, and rod and supports H. The difference in mass did not exceed 0.1 gram in any case.

The torsion measurements were made in a separate bell-jar vacuum system designed for this purpose. The base was a steel plate 2.5×50×60 cm to which was attached a yoke platform for supporting the torsion head assembly as used in the viscosity apparatus. The height of the platform was such that the vertical adjusting nuts would permit lowering the tapered joint until connection could be made to the tapered joints of the inertia objects which were resting on the base. The nuts were used to raise or lower the inertia objects, which avoided any sudden tension being applied to the wire. A high speed oil diffusion pump, connected through the base, was used in conjunction with a Megavac pump for evacuating the system to about 10^{-4} mm. A flexible connection was made through the base which permitted the amplitude of vibration to be adjusted without disturbing the vacuum. The steel bell jar contained an observation window and the jar was raised and lowered by a pulley and counterbalance arrangement.

A small thin mirror (0.5×1.×2. mm) was attached to the tapered joint wire clamp Fig. 3. The oscillations of the inertia object were then observed by the usual telescope and scale method. The time was photographically recorded for 10 initial oscillations of the torsion pendulum and then repeated at eight to fifteen times as the amplitude slowly decreased. Recording 10 initial vibrations and 10 more one hour later, permitted a determination of the period for that amplitude within 1 part in 10^5. The amplitude dropped to one-half in times ranging from 3 hours to 18 hours, depending on the moment of inertia of the object. The effect of damping on the period of oscillation was neglected, since in the worst

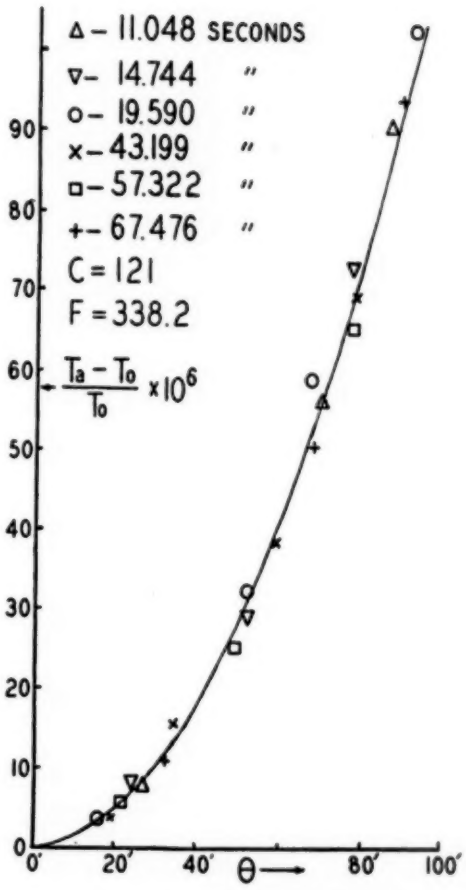

FIG. 5. The variation in the period of oscillation as a function of the amplitude.

case it caused an error in the torsion constant of less than one part in 10^6.

The period of oscillation was found to be a function of the amplitude of vibration. For a one-degree amplitude the period was about one part in 25,000 greater than for zero amplitude. This means a deviation from Hooke's law and the oscillatory motion is anharmonic. Since the deviation from Hooke's law and the amplitude of oscillation are small, one needs to retain in the differential equation of motion only terms of the first and third power of the displacement. The solution of this equation gives

$$T_a = T_0\left(1 - \frac{3c}{8F_0}\theta^2 \cdots\right), \qquad (2)$$

where T_a is the period of oscillation for an amplitude θ, T_0 the period for $\theta = 0$, F_0 the usual torsion constant as calculated from T_0 and the moment

of inertia, c is a constant of the torsion wire and is independent of the period of oscillation. Several values of c were determined for different values of $T_a - T_0$ and for different periods. The average value of c was

$$c = +121.$$

A graph of $(T_a - T_0)/T_0$ as a function of θ is shown by the solid line in Fig. 5. The points plotted are representative of all those taken for the different inertia objects. It was found that c was a sensitive function of the temperature and had to be determined for the same temperature as was used in the viscosity apparatus.

The period of oscillation increased with θ which made c positive. This means that the torsion constant decreases with increasing deflection and since the torsion wire is used statically in the viscosity measurement, a correction must be subtracted from the torsion constant as determined from T_0 for each angle of deflection used. It is easily seen that the effective value of the torsion constant for an angle of deflection θ is

$$F_\theta = F_0 - c\theta^2, \qquad (3)$$

where F_0, c and θ have their usual meanings. The maximum correction applied to any measurement was less than one part in 7000.

Six inertia objects were used whose mass and dimensions could be accurately measured, making it possible to calculate their moment of inertia with high precision. The smallest moment of inertia was obtained with a Dow metal rod 3.6 cm diameter and 35.3 cm long, and the largest with a Dow metal ring whose outside and inside diameters were 18.7 and 16.7 cm. A steel sphere and three Dow metal disks were also used. Fig. 3 shows how the disks and rods were constructed. The steel sphere was a high precision ball 5.4 cm in diameter, used in ball bearings, and uniformly hardened throughout. The construction of the other objects was carried out with the same high degree of accuracy as was used in machining the rotating cylinders and other precision parts of the apparatus. The dimensions and masses were determined by the National Bureau of Standards. Table VI contains these measurements of the diameters together with a calculation of the moment of inertia for each object.

TABLE VI. *Inertia measurements.*

OBJECT	DIAMETER	MOMENT OF INERTIA C.G.S. UNITS
Rod	3.61392 cm	1,045.61
Sphere	5.39612	1,862.17
Cylinder 1	6.39820	3,287.89
Cylinder 2	14.26903	15,986.31
Cylinder 3	18.95308	28,148.03
Ring	18.67921 16.67943	39,002.91

The most important characteristics of a torsion wire are that it have no zero drift in either its normal or deflected position and that the static and dynamic torsion constant be exactly the same. It should also have a high tensile strength in order that a small diameter wire can be used which will give measurable deflections for the small viscous force available. Several wires were tested and it soon became evident that tungsten wires were of much higher quality than any other type. The failure to maintain a constant zero and a difference between the torsion constant as measured by short and long periods were the most common faults. Tungsten wires were not perfect, but it was thought that suitable heat treatments might improve them sufficiently to make them usable. Dr. Irving Langmuir of the General Electric Company had some tungsten wires of the appropriate diameter and length selected and treated at high temperatures in very dry hydrogen. These wires gave decidedly better results than untreated wires and in particular those treated at 1200°C gave the best results. The late Dr. Archer Hoyt of the Gulf Research Laboratories found that in constructing a precision gravity meter, the roundness of the wire was important and it should not be coiled during the drawing process and should be kept under tension at all times.

Through the cooperation of Dr. W. E. Forsyth of the General Electric Laboratories in Cleveland, some tungsten wires were obtained which were drawn through selected round diamond dies and not coiled in the drawing process. Two of these were treated at 1200°C for five minutes in pure dry hydrogen. The wires were under slight tension during the process. The results on these wires were superior to any previous ones and the one which had had the greatest tension during the processing was the better of the two. This suggested the use of greater tension. It was found that a tension of about one-half that required for

rupture at 1200°C gave the best results. The time of heating was varied and about 10 minutes seemed the best.

The wire selected for the present measurements gave excellent results on all tests except when the tension was removed. When a change was made in the apparatus which required removing the tension on the wire for several hours, it was found that when reassembled the zero drifted in one direction for a period of 12 to 30 hours. The total amount of the drift never exceeded 0.1 mm on the comparator scale, which was 2781.44 mm from the mirror, or a total angular shift of the suspended cylinder of less than 3 seconds. After this readjustment took place, tests for a shift of zero were made when the cylinder was also deflected, and none could be detected. This was done by two methods. In the first the deflected position was recorded as soon as possible after starting the rotation of the inner cylinder. The position was rechecked by the eyepiece micrometer several times over a period of an hour or more. The rotating cylinder was then stopped, which allowed the suspended cylinder to swing almost an equal angle from the normal zero in the opposite direction. Just prior to the suspended cylinder's attaining its maximum deflection, the inner cylinder was started rotating in the opposite direction. The deflection in this opposite direction was recorded and rechecked as before for an hour or more. Failure to detect any drift of greater than one part in 30,000 of the total deflection was conceded satisfactory. The second method of checking the zero was to take the average of the comparator readings for the deflections to each side of the normal zero. This average always agreed with the normal zero position within the error of observation.

The wire used has retained the same torsion constant for over a year. The results of all measurements made on this wire are shown in Table VII.

The average and probable errors were calculated in the usual manner assuming each determination to be an independent one and of equal weight. To assume the resulting values of the torsion constant to be independent is not quite correct, because the same dimensional measurements are used in calculating all values of F for each object. However, the error in determining the period is about the same as that in the dimensions of the suspended bodies, and to this extent constitutes an independent determination. The precision of these measurements is such that the probable error calculated by any method is so small as to be negligible.

TABLE VII. *Constant of torsion wire.*

DATE	OBJECT	PERIOD SEC.	TORSION CONSTANT
2/3/38	Cylinder (3.6)	11.0477	338.209
4/9/38	Cylinder (3.6)	11.0475	338.221
3/18/38	Sphere (5.4)	14.7438	338.189
11/24/38	Sphere (5.4)	14.7434	338.208
10/13/38	Cylinder (6.4)	19.5910	338.191
11/22/38	Cylinder (6.4)	19.5906	338.206
11/30/38	Cylinder (6.4)	19.5907	338.203
12/6/38	Cylinder (6.4)	19.5909	338.196
11/21/38	Cylinder (14.3)	43.1995	338.192
12/5/38	Cylinder (14.3)	43.1999	338.185
1/7/39	Cylinder (14.3)	43.1986	338.207
1/10/39	Cylinder (14.3)	43.1989	338.201
10/10/38	Cylinder (19.)	57.3228	338.184
11/20/38	Cylinder (19.)	57.3211	338.204
12/4/38	Cylinder (19.)	57.3225	338.187
1/5/39	Cylinder (19.)	57.3209	338.206
3/16/38	Ring (18.7–16.7)	67.4766	338.182
10/9/38	Ring (18.7–16.7)	67.4763	338.185
		Average	338.198 ±0.002

FURTHER TEST ON APPARATUS

If the cylinders had not been perfectly cylindrical the suspended cylinder should have possessed forced vibrations of the frequency of the speed of rotation of the inner cylinder. As noted earlier, no such effect was observed for the speeds then used. The amplitude of the forced vibrations should be a maximum at an inner cylinder speed corresponding to the natural period of the suspended cylinder, which was 61.620_1 seconds. The closest speed to this that could be obtained with the gears was one revolution in 53.3 seconds. No detectable vibration was observable and similar tests were made at speeds ranging from one rotation in 6.67 seconds to 240 seconds.

If the cylinders are not coaxial then the velocity gradient will not be the same in all angular directions in a plane perpendicular to the axis of the cylinders. Couette[9] made a theoretical estimate of the error introduced by the failure of the cylinders to be coaxial. In this he assumed a

[9] M. Couette, Ann. Chim. Phys. **21**, 433 (1890).

uniform velocity distribution in every angular element and integrated the usual expression for the torque on the deflecting cylinder under this condition. This theory was tested experimentally by Kellström, who found that theory and experiment disagreed not only in magnitude but also in the sign of the correction. Inglis[10] has derived an expression for the torque on the deflecting cylinder which includes the pressure gradient term neglected by Couette and also did not assume the spacing between the cylinders to be small compared to the radii of the cylinders. His expression for the torque $F\phi$ on the deflecting cylinder is

$$F\phi=\frac{2\pi\eta U(a+g)}{g}\left[1-\frac{g}{2a}-c^2+\frac{9gc^2}{4a}\cdots\right], \quad (4)$$

where U is the linear velocity of the rotating surface, $g=b-a$, c is the ratio of the separation of the axes of the cylinders to the spacing g, and the remaining quantities are the same as in Eq. (1). It is seen that Eq. (4) reduces to Eq. (1) if only the first two terms of the bracket are retained. The last two terms are negative, giving a reduced torque as observed by Kellström.[2] The calculated reduction is greater than the observed, which is probably due to the large value of c (theory assumed c small) used, and also to the end effects introduced when the deflecting cylinder was not concentric with the guard cylinders. In the present experiment the eccentricity of the cylinders was about 0.0005 cm, which gives a negative correction for the viscosity less than one part in 10^6 and has been neglected.

In the present method where the inner cylinder rotates, it is not permissible to use as large angular velocities as in the case where the outer cylinder rotates. Taylor[11] has shown theoretically and experimentally that when the space between concentric cylinders is filled with water, laminar flow ceases at angular velocities of the inner cylinder greater than ω where ω is defined by the relation

$$\omega^2=\frac{\pi^4\eta^2(a+b)}{2\rho^2(a-b)^3b^2P},$$

$$P=0.0571\left[1-\frac{0.652(a-b)}{b}\right] \quad (5)$$

$$-0.00056\left[1-\frac{0.652(a-b)}{b}\right]^{-1}.$$

ρ is the density of the liquid and the remaining symbols are the same as used in Eq. (1). The same relation should be valid for gases, and if the constants of the present apparatus are substituted in the above equation, one finds $\omega=1.89$ radians per second, which is about twice the maximum velocity attainable with the present gear system. An examination of Tables XI and XII shows that there was no consistent change of the results as the speed of the rotating cylinder was varied which proves that no turbulence existed at any of the speeds used in the present experiments.

Theoretically[3] it should be expected that for the present construction the effective length of the suspended cylinder should be the average of the actual length of the cylinder and the distance between the guard cylinders. Since no test of this theory exists, three sets of measurements were made in which the distance between the guard cylinders was varied. This was accomplished by placing parallel spacers between the top base and the shoulders on the posts J. A constant value of viscosity was assumed and the effective length of the suspended cylinder calculated. The calculated lengths and the directly measured lengths assuming the correctness of the theory are compared in Table VIII. The differences are within the experimental errors. The errors are larger than those of the final measurements because the adjustments were not made with the highest accuracy. These results are in complete accord with theory and justify the use of the effective length of the suspended cylinder as the average of the distance between the guard cylinders and the length of the suspended cylinder. From Table IV the distance between the guard cylin-

TABLE VIII. *Effective length of suspended cylinder.*

CALCULATED LENGTH	MEASURED LENGTH
26.0610 cm	26.0610 cm
26.0755	26.0749
26.0902	26.0891

[10] D. R. Inglis, following paper.
[11] G. I. Taylor, Trans. Roy. Soc. London **A223**, 289 (1923).

TABLE IX. *Sample viscosity determination. Initial zero* = 243.480 *cm. Final zero* = 243.483 *cm.* $t = 10.90803$ *seconds. Pressure* = 76.2 *cm.**

TEMPERATURE	LEFT, MM	RIGHT, MM	DIFFERENCE	$\eta \times 10^7$	$\eta \times 10^7$† 20.00°C
20.032	314.530	172.440	142.090	1819.49	1819.35
20.034	314.535	172.440	142.095	1819.55	1819.40
20.032	314.535	172.435	142.100	1819.62	1819.48
20.036	314.530	172.435	142.095	1819.55	1819.39
20.036	314.530	172.445	142.085	1819.43	1819.27
20.036	314.525	172.445	142.080	1819.36	1819.20
20.040	314.525	172.430	142.095	1819.55	1819.37
20.038	314.530	172.430	142.100	1819.62	1819.45
20.040	314.530	172.440	142.090	1819.49	1819.31
20.042	314.540	172.440	142.100	1819.62	1819.43
20.042	314.540	172.435	142.105	1819.68	1819.49
			Average		1819.38
			Correction for $F_\theta = F_0 - c\theta^2$		0.11
					1819.27

* Viscosity measurements have been made at pressures of 38 cm, 7.6 cm and 0.8 cm, and when corrected for slip, these pressures indicate an increase in viscosity with pressure. From 7.6 cm to 76 cm, the increase is about one part in 2000. All measurements recorded have been made with a pressure of 74.5±0.5 cm.

† The slip correction of 1.26 parts in 10^4 has been applied to the results in this column. See below.

ders is 26.07634±0.00020 cm. The length of the suspended cylinder is 26.04583±0.00008 cm. The average of these gives for the effective length of the suspended cylinder

$$L = 26.0611 \pm 0.0002 \text{ cm.}$$

and the largest of the two errors has been retained as the probable error of the average.

APPARATUS CONSTANT AND PROBABLE ERROR OF MEASUREMENTS

The apparatus constant K in Eq. (1) is

$$K = (b^2 - a^2)/La^2b^2.$$

The error ΔK can be obtained by taking partial derivatives. ΔK is then

$$\Delta K = [(\partial K/\partial b)^2(\Delta b)^2 + (\partial K/\partial a)^2(\Delta a)^2 + (\partial K/\partial L)^2(\Delta L)^2]^{\frac{1}{2}}. \quad (6)$$

From Tables II and III $b = 7.47654 \pm 0.000025$ cm. The effective length of the suspended cylinder is $L = 26.0611 \pm 0.0002$ cm. Two inner cylinders a were used, and from Table I

$$a_I = 6.22112 \pm 0.00001 \text{ cm}$$
$$a_{II} = 6.78517 \pm 0.00002 \text{ cm.}$$

From these values one obtains

$$K_I = 3.04988 \times 10^{-4} \text{ and } [\Delta K/K]_I = 2.01 \times 10^{-3} \text{ percent,} \quad (7)$$

$$K_{II} = 1.46999 \times 10^{-4} \text{ and } [\Delta K/K]_{II} = 4.5 \times 10^{-3} \text{ percent.} \quad (8)$$

The torsion constant and speed of rotation enter to the first power in the numerator of the viscosity equation. From Table VII the torsion constant $F_0 = 338.198 \pm 0.002$ or the error is 0.59×10^{-3} percent. The error in the speed of the driving motor is about one in 10^6 or 0.1×10^{-3} percent. Combining these errors with those of Eqs. (7) and (8), the factor $KF_0/8\pi^2$ becomes for the two rotating cylinders I and II

$$(KF_0/8\pi^2)_I = 13.06363 \pm 2.10 \times 10^{-3} \text{ percent,} \quad (9)$$

$$(KF_0/8\pi^2)_{II} = 6.29645 \pm 4.56 \times 10^{-3} \text{ percent.} \quad (10)$$

The only other instrumental error is that due to θ which involves the ratio of the comparator scale measurements and the effective distance of the mirror from the vertical wire on the comparator carriage. The error in the comparator measurements does not exceed 0.002 mm for any measurement and no angles giving less than 10 cm comparator distance have been used. The error due to the comparator then does not exceed 2.10^{-3} percent. This does not include the random error of setting the image of the vertical wire between the parallel cross hairs, which is taken into account by the deviations of the independent measurements. The effective mirror to wire distance as given in Table V is 2781.44±0.02 mm $\pm 0.72 \times 10^{-3}$ percent. The combination of these gives for the instrumental error in θ 2.13×10^{-3} percent. The viscosity equations may then be

TABLE X. *Temperature coefficient.*

AUTHOR	DATE	RESULT
Millikan[12]	1913	$4.93 \times 10^{-7}/c^\circ$
Rigden[5]	1938	$4.93 \times 10^{-7}/c^\circ$
Banerjea and Plattanaik[4]	1938	$4.95 \times 10^{-7}/c^\circ$
	Average	$4.94 \times 10^{-7}/c^\circ$

[12] R. A. Millikan, Ann. d. Physik **41**, 759 (1913).

TABLE XI. *Final results rotating cylinder I. Rotating cylinder radius = 6.2211 cm.*

t(SECONDS)	$\eta \times 10^7$
6.67	1819.18
6.67	1819.23
10.91	1819.14
10.91	1819.21
10.91	1819.24
10.91	1819.12
10.91	1819.19
10.91	1819.27
16.00	1819.31
16.00	1819.24
16.00	1819.09
16.00	1819.16
16.00	1819.20
16.00	1819.28
40.00	1819.35
40.00	1819.29
146.65	1819.17
146.65	1819.00
239.98	1819.11
239.98	1819.39
Average	1819.21 ±0.02

written

$$\eta_I = 13.06363\theta t \pm 3.0\times10^{-3} \text{ percent}, \quad (11)$$

$$\eta_{II} = 6.29645\theta t \pm 5.0\times10^{-3} \text{ percent}, \quad (12)$$

where the errors include all instrumental errors.

A Typical Viscosity Determination

The system was evacuated to 10^{-4} mm and tested for leaks by closing the stopcock C. Air from outside the building was admitted through a cylindrical brass trap 3×20 cm filled with copper shavings which was immersed in a mixture of dry ice and alcohol. The rate of flow of air through the trap was about 500 cm³ per minute, which allowed adequate time for removal of the water vapor. The apparatus was usually filled to about 74.5 cm pressure. Several hours were allowed for temperature equilibrium to be established. The measurements then consisted in recording the zero position, a deflection with the rotating cylinder turning in one direction and then an equal but opposite deflection with the direction of rotation of the rotating cylinder reversed. The temperature was recorded by a calibrated Beckman thermometer whose bulb was very close to the suspended cylinder inside the bell jar. This process of taking readings was repeated about 10 times for each run. The total time taken for such a run was from 45 to 60 minutes. Table IX gives the result of a typical run. The correction of the viscosity to 20.00°C was made by taking an average of the results in Table X on the temperature coefficient. It makes practically no difference which value of the coefficient one uses because measurements were made slightly above and below 20°C, so that any small error in the correction term is canceled. This average value of the temperature coefficient has been used with the present results to calculate a value of the viscosity at 23°C which can be compared with previous results.

A small correction has to be applied to the above values of the viscosity which is due to the influence of slip. This has been studied in detail by Millikan,[13] Stacy,[14] States,[15] and Blankenstein[16] with apparatus very similar to that used in the present experiments. The expression for the true viscosity including the slip correction may be written in the form

$$\eta = \frac{F}{8\pi^2}\frac{b^2-a^2}{La^2b^2}\varphi t\left[1+2\rho\frac{a^3+b^3}{ab(b^2-a^2)}\right], \quad (13)$$

where ρ is the slip coefficient and the other symbols represent the same quantities as in Eq. (1). The value of ρ for the present surfaces should not be greater than that for brass which is 75.4×10^{-7}. Substituting this in the bracket term of Eq. (13) together with the values of a and b, one finds the true value of the viscosity is greater than the normally calculated value by only 1.26 parts in 10^5 for the smallest rotating cylinder and 2.19 in 10^5 for the largest.

TABLE XII. *Final results rotating cylinder II. Rotating cylinder radius = 6.7817.*

t(SECONDS)	$\eta \times 10^7$
10.91	1819.13
10.91	1819.25
16.00	1819.16
16.00	1819.16
16.00	1819.11
16.00	1819.09
146.65	1819.31
146.65	1819.10
Average	1819.16 ±0.02

[13] R. A. Millikan, Phys. Rev. **21**, 217 (1923).
[14] L. J. Stacy, Phys. Rev. **21**, 239 (1923).
[15] M. N. States, Phys. Rev. **21**, 662 (1923).
[16] E. Blankenstein, Phys. Rev. **22**, 582 (1923).

The average of the results in Table IX must be corrected for the change in torsion constant with angle of deflection. This correction can be easily made by the use of Eq. (3), which for the deflections of Table IX amounts to about one part in 17,000. This correction has been applied to the average of the 11 determinations as indicated at the end of the table.

Results

The results obtained in 28 independent runs of the type recorded in Table IX are given in Tables XI and XII. Six different angular velocities of the rotating cylinders have been used and in each table the results have been grouped according to the velocity used. The maximum velocity of one revolution in 6.67 seconds was used primarily to test for possible turbulence. The agreement of the first two results in Table XI with the results for lower velocities indicates a complete absence of turbulence at all velocities used. The best results were obtained with velocities corresponding to one revolution in 10.91 and 16 seconds. The statistical fluctuation of the results in this group is least in both Tables XI and XII, but the average of this group is practically the same as that for the remaining results. In the final average all values were given equal weight.

The results of Tables XI and XII were taken over a period of about 14 months and during this time the rotating cylinders were changed three times, which necessitated a complete realignment of the apparatus. The torsion wire was removed for calibration on six other occasions and when replaced in the apparatus, the suspended cylinder was readjusted for height and axial centering. The deviations in the results of Tables XI and XII are due then not only to statistical errors of observation but also to possible errors in adjustment which may not have been sufficiently allowed for in the estimation of errors. The probable errors of Tables XI and XII calculated in the usual manner are not sufficiently large to permit an overlapping of the two averages. This can be explained by the fact that two rotating cylinders were used, and the errors involved in the measurement of their diameters easily accounts for the difference between the average results of the two tables.

Table XIII. *Comparison of recent viscosity measurements.*

Observer		$\eta \times 10^{-7}$ c.g.s. unit at 23°C
Kellström[2]		1834.9±2.7*
Houston[3]		1829.2±4.5
Banerjea and Plattanaik[4]		1833.3±2.2
Bond[1]	1834.8	
Rigden[5]	1830.3+	1832.6±2.3
Weighted average		1833.1±1.3

* Kellström makes no mention of applying a correction for the gap between the deflecting cylinder and guard rings. If this was not done then his value should be reduced to 1832.9×10^{-7} c.g.s. unit.

The final probable error of the results in Table XI can be obtained by combining the probable error indicated with that of Eq. (11). This gives for the smallest rotating cylinder

$$\eta_{20.00°C} = (1819.21 \pm 0.06)10^7 \text{ c.g.s. units.}$$

Likewise for Table XII and Eq. (12) the largest rotating cylinder gives

$$\eta_{20.00°C} = (1819.16 \pm 0.10)10^7 \text{ c.g.s. units.}$$

The larger probable error for the latter result is due to the smaller value of $(b-a)$ in Eq. (1) and to the greater inaccuracy of cylinder 11 as shown in Fig. 2. If the two values are weighted inversely proportional to square of the probable errors, then

$$\eta_{20.00°C} = (1819.20 \pm 0.06)10^7 \text{ c.g.s. units.}$$

Since the results are dependent except for the rotating cylinder, the probable error of the average cannot be calculated by the usual method, which would yield a value of ±0.02. The probable error obtained for the results with the smallest rotating cylinder has been adopted as the probable error of the final weighted average. Assuming the temperature factor of Table X, the viscosity of air at 23.00°C is $(1834.12 \pm 0.06) \times 10^7$ c.g.s. units.

Recent Determinations of the Viscosity of Air

All previous viscosity measurements which have been made in an effort to solve the problem of the discrepancy between the x-ray and oil-drop evaluations of e are recorded in Table XIII. The only notable discrepancy in the results is that of the capillary tube method of Bond and Rigden. Rigden used Bond's apparatus in which some

improvements were made and obtained a much lower value of the viscosity than Bond. The probable error given by Bond is ± 0.8 and by Rigden is ± 0.7, or statistically there is only one chance in 2×10^4 of Rigden's value being as high as Bond's. From a study of the two reports, it seems unlikely that the improvements introduced by Rigden should have lowered Bond's results by one part in 400. In view of this discrepancy, which is not discussed, an average of the results is given in Table XIII and a probable error has been assigned which includes both values. The weighted average was obtained by the usual method of assigning weights inversely proportional to the square of the probable errors. The probable error from external consistency is 0.6 and from the internal is 1.3. In accordance with usual practice, the probable error of the average has been taken as ± 1.3. This probable error is more than 20 times that of the present experiment. A weighted average of the result from Table XIII and the author's value thus gives a final average identical with the present experimental value.

Final Value of the Viscosity of Air

In view of the above discussion the final value of the viscosity of air at 20.00°C is adopted as

$$\eta = (1819.20 \pm 0.06) \times 10^{-7} \text{ c.g.s. unit.}$$

The Electronic Charge

If Millikan's[17] oil-drop data are used with the above value of the viscosity of air, one finds $e = 4.815 \times 10^{-10}$ e.s.u. Correspondingly for Backlin and Flemberg's[18] data $e = 4.797 \times 10^{-10}$ e.s.u. and from Ishida, Fukushima and Suetsugu's[19] data $e = 4.852 \times 10^{-10}$ e.s.u. The latter results differ by more than one percent and the first two by almost 0.4 percent. The x-ray value of e as recalculated by Dunnington[20] is $(4.8025 \pm 0.0004) \times 10^{-10}$ e.s.u. and lies within the spread of the above values obtained by the oil-drop method. New oil-drop measurements are in progress in this laboratory from which it is hoped that a value of e can be obtained which is comparable in accuracy with the present viscosity results. In this work pure argon is being used instead of air, and the viscosity of the argon has been determined with an accuracy at least as great as the above results on air.

The writer is greatly indebted to Drs. Lyman J. Briggs and H. L. Dryden of the National Bureau of Standards for their cooperation in securing the highest precision in the measurements of the important dimensions and weights, and for theoretical discussions on turbulence; to Drs. Irving Langmuir and W. E. Forsyth of the General Electric Company and the late Dr. Archer Hoyt of the Gulf Research Laboratories for the specially treated tungsten suspensions and information on methods of treating suspension wires; and to the General Electric Company for supplying the large quantity of pure argon needed for the viscosity measurements and in the oil-drop measurements. The assistance and interest of Professors A. H. Compton and James Franck of the University of Chicago is greatly appreciated. The writer is greatly indebted to Professor A. H. Pfund for discussions of the optical system and the precise measurement of the index of refraction of the apparatus window; to Drs. D. R. Inglis and R. H. Lyddane* for many theoretical discussions; and to Dr. C. H. Shaw for assistance in designing, constructing, and operating the apparatus. It is a pleasure to acknowledge the financial assistance of the National Research Council which made this work possible.

[17] R. A. Millikan, *Electrons, Protons, Photons, Neutrons and Cosmic Rays* (University of Chicago Press, 1935).
[18] E. Backlin and H. Flemberg, Nature **137**, 655 (1936).
[19] Y. Ishida, I. Fukushima and T. Suetsugu, Sci. Papers of the Inst. of Phys. and Chem. Research **32**, 57 (1937).
[20] F. G. Dunnington, Rev. Mod. Phys. **11**, 65 (1939).
* Now at the University of North Carolina.

Viscous Force Between Almost-Coaxial Cylinders

D. R. INGLIS
Rowland Physical Laboratory, The Johns Hopkins University, Baltimore, Maryland
(Received August 8, 1939)

For the sake of an estimate of the errors which might enter the measurements of the preceding paper by accidental misalignment, the problem of the viscous flow between almost-coaxial cylinders, one of which is rotating, is treated theoretically. The torque exerted on the stationary cylinder is calculated by means of a series expansion which treats both the curvature and the eccentric displacement as small. It is shown incidentally that a calculation in the theory of lubrication in the previous literature, which neglects the curvature altogether, is not correct in all its steps although it happens to lead to a correct result for the torque.

THE method of measuring the torque transmitted by the intervening fluid from a rotating cylinder to a coaxially suspended stationary cylinder is of importance in the precision determination of coefficients of viscosity.[1] The question arises concerning the magnitude of the error which might be introduced by a small accidental eccentricity of the mounting. The problem then resembles the problem of the lubrication of a journal bearing, but in the latter the eccentric displacement is not apt to be small compared to the gap between the cylinders and the gap is small compared to the radius of curvature.

The viscosity-measurement problem was discussed by Couette[2] in a very rough approximation which resulted in a theoretical increase in viscous drag with eccentricity. On the basis of this treatment, Kellström[3] was perplexed to find experimentally a decrease. Harrison[4] has developed (from earlier work by Reynolds and Sommerfeld[5]) a theory of the lubrication of a journal bearing, in which it appears that the moment acting on the stationary outer cylinder should decrease with eccentricity, while that on the rotating inner cylinder should increase. It does not seem to have been pointed out that this result, which is based on a much more thorough treatment than that of Couette, is in nice accord with the sign of the experimental result of Kellström. It is true that his experiment did involve a revolving outer cylinder and a stationary inner cylinder, but it is rather obvious that it is not a question of which cylinder is outside, but of which cylinder is moving, in applying Harrison's formulas, since the formulas were developed from an approximation which neglects the curvature.

In the present paper we first present a further simplification of Harrison's treatment of the problem, by means of the approximation that the eccentric displacement is small compared to the width of the gap. The results are reached by use of the most elementary integrations. The approximation is valid only for the viscosity-measurements problem, but the simplified treatment should have some value for a student of lubrication as well, the simple derivation of a qualitatively correct result making it easy to understand which physical effects are the most important.

In particular, it will appear that the change in drag with the introduction of eccentricity may be explained qualitatively as follows: the fact that the eccentricity makes the channel wider in one portion and narrower in the other results in a net decrease in the transport of fluid, as is intuitively plausible. This means that the average velocity at the center of the channel is decreased, and thus that the average velocity gradient (transverse gradient of parallel velocity) is decreased near the stationary boundary and increased near the moving boundary. Being proportional to this gradient, the viscous drag on the stationary boundary is decreased and that on the moving boundary is increased.

Since the gap is not really very small in com-

[1] See preceding paper by J. A. Bearden.
[2] M. Couette, Ann. Chim. Phys. **21**, 433 (1890).
[3] G. Kellström, Phil. Mag. **23**, 313 (1937), especially p. 337.
[4] W. J. Harrison, Trans. Camb. Phil. Soc. **22**, 39 (1913). Further discussed by Bateman in "Hydrodynamics" (Dryden, Murnaghan, and Bateman), Bull. Nat. Research Council **84**, 236 (1932).
[5] A. Sommerfeld, Zeits. f. Math. und Physik **50**, 97 (1904).

parison with the radius of curvature in viscosity measurements, the second section of the paper takes the curvature into account as far as the first new term in a series expansion. The qualitative results just mentioned are not altered thereby.

I. Negligible Curvature and Small Eccentricity

In order to describe the motion at a point in the fluid by means of the familiar right-handed Cartesian coordinates at the point, and still have $dy=dr$ and $dx=rd\theta$, we take θ to be measured in the clockwise sense, contrary to the usual convention, as indicated in Fig. 1. The velocity components are $u=\dot{x}$ and $v=\dot{y}\approx 0$. The inner cylinder has the radius a about the center 0, the outer cylinder has the radius $a+g$ about the center $0'$. As long as the distance $00'=cg$ is small compared to a, we have for the distance between the two cylinders

$$h=g(1+c\cos\theta) \tag{1}$$

valid up to terms in c^2g^2/a. By considering the forces per unit volume exerted in the x direction on an infinitesimal prism[6] of the fluid by the pressure on its ends and by the viscous force on its sides, we have

$$\frac{\partial p}{\partial x}=\eta\frac{\partial^2 u}{\partial y^2}-\rho u\frac{\partial u}{\partial x}. \tag{2}$$

The last term arises from inertia, and we shall neglect it, following Harrison, on the basis of the assumption that $\partial u/\partial x \ll \partial u/\partial y$.

In discussion of this point, it might be remarked that, for ordinary air, ρ is numerically about ten times η in *cgsu*, and u must change by about cu in a displacement a in the x direction and $\partial u/\partial y$ by about cu/h in a displacement h in the y direction (since the flow uh is the same at the constriction as at the enlargement of the channel), so $\partial u/\partial x \approx (h^2/a)\partial^2 u/\partial y^2$. Neglect of the last term of (2) then implies that $Uh \ll (a/10h)$ cm^2/sec.

In a similar approximation we may consider $\partial p/\partial y=0$ so $\partial p/\partial x$ may be considered constant in integrating (2) over y. Thus we have

$$\eta u=\tfrac{1}{2}y^2\partial p/\partial x+c_1y+c_2 = U(1-y/h)+\tfrac{1}{2}y(y-h)\partial p/\partial x, \tag{3}$$

[6] Although this step, used in the work of Harrison (and in part of the work of Sommerfeld) is an over-simplification, it is of interest for purposes of orientation, and the moments derived from it are correct. See footnote 9.

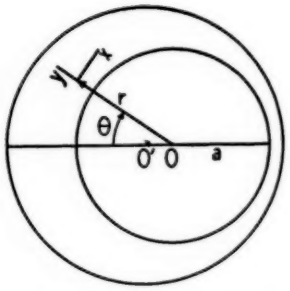

Fig. 1. Cross section and coordinates.

if the constants are adjusted to satisfy the boundary conditions $u=U$ where $y=0$, $u=0$ where $y=h$ (inside cylinder rotating). Because of the constant density distribution, the flow across all cross sections of the channel is the same,[7]

$$\eta\int_0^h u\,dy=\tfrac{1}{2}\eta h U-\frac{1}{12}h^3\partial p/\partial x\equiv\tfrac{1}{2}\eta h_1 U, \tag{4}$$

where $h_1=g(1+c\cos\theta_1)$ is a constant. Then

$$\partial p/\partial x=6\eta U(h-h_1)/h^3=(6\eta Uc/g^2) \times(\cos\theta-\cos\theta_1)(1+c\cos\theta)^{-3}\approx(6\eta Uc/g^2) (\cos\theta-\cos\theta_1)(1-3c\cos\theta+\cdots). \tag{5}$$

This is $(1/a)\ \partial p/\partial\theta$, and its average value must be zero as θ increases by 2π if $p(\theta)=p(\theta+2\pi)$. Since $\langle\cos\theta\rangle_{Av}=0$ and $\langle\cos^2\theta\rangle_{Av}=\frac{1}{2}$,

$$\cos\theta_1=-(\tfrac{3}{2})c+\cdots, \tag{6}$$

θ_1 is the angle at which the average velocity is the same as it would be with $c=0$. The fact that θ_1 is slightly greater than $\pi/2$, and h_1 slightly less than g, indicates that the total flow is less than it would be if c were zero.

We can now calculate the total lateral force R (per unit height) on the inner cylinder due to the difference of pressure on the opposite sides:

$$R=\int_0^{2\pi}p(\theta)\sin\theta\,d\theta\approx(6\eta Uc/g^2)\int_0^{2\pi}a\sin\theta \cdot\sin\theta\,d\theta=6\pi\eta Uca/g^2,$$

neglecting higher powers of c. Using (3), we can

[7] We neglect the compressibility of the gas, as is justified by the very small relative change of pressure. From (5) we see that the total change of pressure Δp is about $6\eta Uac/g^2$. With the data of Bearden's measurements, and his maximum U, this gives $\Delta p/p\approx 10^{-7}c$. With much larger velocities and eccentricities, this may become appreciable, as is illustrated by the numerical integrations of Harrison (reference 4, Figs. 4, 5 and 6).

calculate the viscous torque (per unit height) on the inner cylinder:

$$M=\eta a^2\int_0^{2\pi}\left(\frac{\partial u}{\partial y}\right)_{y=0}d\theta=\eta a^2(-F-G)$$

and on the outer cylinder:

$$M'=-\eta(a+g)^2\int_0^{2\pi}\left(\frac{\partial u}{\partial y}\right)_{y=h}d\theta$$
$$=\eta(a+g)^2(F-G),$$

where

$$F=\int_0^{2\pi}(\eta U/h)d\theta=(2\pi\eta U/g)(1+c^2/2+\cdots),$$

$$G=\tfrac{1}{2}\int_0^{2\pi}h(\partial\rho/\partial x)d\theta$$
$$=(3\eta Uc/g)\int_0^{2\pi}(\cos\theta+3c/2-\cdots)\times(1-2c\cos\theta+\cdots)d\theta$$
$$=(3\pi\eta U/g)c^2+\cdots.$$

Thus

$$M=-(2\pi\eta Ua^2/g)(1+2c^2-\cdots)$$

and

$$M'=(2\pi\eta U/g)(a+g)^2(1-c^2+\cdots)$$
$$\approx(2\pi\eta Ua^2/g)(1-c^2).$$

The negative sign in the last equation descends from the negative sign in (6) and gives rise to the decreased torque observed by Kellström on the stationary outer cylinder. R acts downward on the inner cylinder as it is drawn in Fig. 1, corresponding to an increased pressure before the constriction, and exerts a positive torque Rcg about 0′ on the inner cylinder. We observe that the total torque on the inner cylinder about 0′ is equal and opposite to that on the outer cylinder

$$M+Rcg=-M',$$

making the reaction torque on the fluid vanish, as is necessary for a constant flow.

II. Appreciable Curvature and Small Eccentricity

We shall now take the curvature into account and extend the derivation of M' to include the case wherein g is still considered small, but not negligibly small, compared to a, and $c\ll 1$. In laminar flow describable as the rotational slipping of thin cylindrical shells, the viscous force transmitted across a unit area of a cylindrical surface in the fluid is $\eta(\partial u/\partial r-u/r)$. The second term allows the force to reduce to zero for the case of rigid rotation of the whole fluid. By requiring that the moment of force about the center acting on a segment of a thin cylindrical shell must vanish for steady flow, we have

$$\partial p/\partial\theta=(\eta/r)(\partial/\partial r)r^2(\partial u/\partial r-u/r)\qquad(2')$$

in the approximation in which we neglect inertial effects, as before. Again considering $\partial p/\partial r=0$ and integrating[8] along r, we have

$$u=(Pr/a)\ln r/d+C/r$$
$$=P(1+z)[(z-z^2/2+z^3/3-\cdots)+\ln a/d]+(1-z+z^2-z^3+\cdots)C/a.$$

Here we have put $a(\partial p/\partial\theta)/2\eta=P$, and $r=a(1+z)$ so that $z=y/a$. We further put $k=h/a$ and $\gamma=g/a$, making $k=\gamma(1+c\cos\theta)$. Determining the constants of integration C and d by the boundary conditions $u=U$ where $z=0$, $u=0$ where $z=k$, we have[9]

$$u=[1+z-(1/k+\tfrac{3}{2})(z-z^2/2)+\cdots]U+[z+z^2/2-z^3/6-(1+k-k^2/6)\times(z-z^2/2+z^3/2)+\cdots]P.\qquad(3')$$

From the condition

$$\int_0^k u\,dz=(k/2-k^2/12)U$$
$$-P(1-k/2)k^3/6=k_1U/2,\qquad(4')$$

---

[8] The second integration follows division by r, so as to use $(du/dr-u/r)/r=(d/dr)u/r$.

[9] The term in P may be reduced to $[z^2-zk+\cdots]P$, twice the corresponding term in (3). Eq. (3) does not agree with (3′) because the differential equation used in the derivation of (3), following Harrison, is inadequate. In approximating a sector of cylindrical shell by a prism, one neglects the fact that the viscous force acts over a larger area on one side than on the other, while taking a small difference between the viscous forces on the two sides. (3) may be erroneously derived from (2′) by approximating u by

$$u\approx Pa(1+z)(z-z^2/2-\ln ad)+(1-z)C/a$$

before fitting the boundary conditions. The fact that the false factor of P gives the correct result is due to the use of the periodicity of P to determine P from (3) before it is substituted back into (3).

we have

$$P=\{3c(\cos\theta-\cos\theta_1)[(1-3c\cos\theta+6c^2\cos\theta-\cdots)+(1-2c\cos\theta+\cdots)\gamma/2]-(1-c\cos\theta+c^2\cos^2\theta-\cdots)\gamma/2)\}U/\gamma^2$$
$$=\{(3c\cos\theta+9c^2/2+\gamma/2-2\gamma c^2\cdots)\times[(1+c\cos\theta)^{-3}+(1+c\cos\theta)^{-2}\gamma/2]-(1+c\cos\theta)^{-1}\gamma/2\}U/\gamma^2, \quad (5')$$

$\cos\theta_1$ having been determined by the condition $\langle P\rangle_{Av}=0$. After substituting this in $(\partial u/\partial z)_{z=k}=(\frac{1}{2}-1/k)U+Pk(1-5k/6)$ from (3'), and again using $\langle\cos^2\theta\rangle_{Av}=\frac{1}{2}$, we obtain for the viscous torque on the stationary outer cylinder about its center,

$$M'=-2\pi\eta(a+g)^2\langle(\partial u/\partial z)_{z=k}\rangle_{Av}/a=[2\pi\eta U(a+g)^2/g]\times[1-g/2a-c^2+9gc^2/4a+\cdots].$$

With $c=0$ and $g=b-a$ this reduces to Eq. (1) of the preceding paper.[1] The error to be expected because of a nonvanishing c is thus slightly decreased by taking the curvature into account.

NOVEMBER 15, 1939 PHYSICAL REVIEW VOLUME 56

Magnetic Studies of Solid Solutions

I. Methods of Observations and Preliminary Results on the Precipitation of Iron from Copper

F. BITTER AND A. R. KAUFMANN
Massachusetts Institute of Technology, Cambridge, Massachusetts

(Received September 13, 1939)

This paper represents the first step in an extended program whose aim is the investigation of solid solutions with special reference to the structures that may be formed by heat treatment and plastic deformation. It is hoped to include eventually observations in high fields (100,000 gauss) and at low temperatures. The present work deals with observations up to 40,000 gauss and temperatures ranging from 20 to 1000°C. The manner of observation and reliability of the results is described in some detail. A series of observations on alloys of copper containing up to 0.7 percent iron are reported. Up to about 4 percent of iron can be put into solution in copper at high temperatures, but the solubility decreases to an exceedingly small value at room temperature. Our observations indicate that iron atoms in solution in copper retain a permanent magnetic moment of approximately 3.5 Bohr magnetons, and obey a Curie-Weiss law at high temperatures, the Curie temperature of an alloy containing 0.7 percent iron by weight being 150°K. The solution seems to be sluggish and can be greatly supercooled. The manner of precipitation from solution appears to be fairly complex, and the results are being tentatively interpreted as follows: First there is a rearrangement of the atoms in the solution followed by the precipitation of a nonmagnetic phase which can be converted into a ferromagnetic phase by cold work. This ferromagnetic phase can be made to grow thermally, but apparently does not form readily of its own accord.

IN a paper appearing concurrently in the *Review of Scientific Instruments* a newly equipped magnetic laboratory at The Massachusetts Institute of Technology is described in some detail. One of the projects for which this installation was designed is the investigation of the structures of alloys. Relatively little is known of the magnetic properties of matter except in the form of pure elements and compounds, or in solutions in thermodynamic equilibrium. Under certain circumstances magnetic properties may be exceedingly sensitive indicators of structure because they depend to a great extent on the interactions of neighboring atoms, and may be used to detect very small amounts of a particular phase. There is also a very attractive field in low temperature research that has hardly been touched, and what observations have been made indicate that, especially in the high fields which we can produce, effects exist which may help us to understand some of the complexities of alloy structures. For these reasons we have decided to start a magnetic investigation of alloys, especially in the conditions of metastable equilibrium in which they manifest their most valuable properties.

The work of Tammann and his collaborators[1] indicated an interesting starting point. They used

[1] G. Tammann and W. Oelsen, Zeits. f. anorg. Chemie V, **186**, 267 (1930).

magnetic methods with great success to determine the solubility limits of ferromagnetic metals in a series of solutions. More recently Gordon and Cohen[2] have investigated the aging of copper-iron and copper-cobalt alloys. They did not have available a sufficiently strong magnet to make a clear distinction between strong paramagnetism and weak ferromagnetism possible, but their results indicated so many interesting possibilities that we determined to follow it up with our more adequate equipment.

Methods of Measurement

The data which it is desired to obtain consist of a magnetization curve in which the intensity of magnetization of a sample is plotted as a function of magnetic field in fields ranging from zero to as large values as can be obtained. These curves should moreover be obtainable at any temperature. Magnetization curves for typical diamagnetic or paramagnetic substances are straight lines whose slope is called the susceptibility. Very few actual metals however, behave in this way, but show saturation effects which are commonly attributed to ferromagnetic impurities. In order to correct for these it is necessary to apply sufficiently strong fields to saturate any ferromagnetic components that are present, and to measure the slope of the magnetization curve in even stronger fields. The magnetization curve of a piece of ferromagnetic material depends, among other things, on its shape, and unless the ferromagnetic inclusions in a para- or diamagnetic sample are in the form of long needles pointing in the direction of magnetization, fields at least of the order of 10–20,000 gauss will be required to magnetize them to within a few percent of their saturation value. Strong magnetic fields should therefore be used, especially for samples containing appreciable amounts of ferromagnetism.

The magnet available for this work is described as magnet No. 1 in the above-mentioned publication appearing in the *Review of Scientific Instruments*. This is more or less of a legacy from our preliminary experiments on magnet design, and is not very greatly superior to a large iron core magnet. Its chief advantage lies in the fact that one can produce fields of any intensity up to 40,000 gauss without hysteresis effects, in that one can produce these fields in an adequate space, and especially in that the lateral stability of even a strongly magnetic sample is satisfactory. We have had little difficulty due to samples sticking to the inner walls of the solenoid.

The most satisfactory and most used method of measuring magnetization, especially in weakly magnetic materials, is to hang a sample near a magnet and measure the force exerted on it. This magnetic pull may best be interpreted in terms of magnetizations in two special cases. In the first the sample is in the form of a long cylinder with its lower end in the most intense part of the field and its upper end out of the field. This is called the Gouy method. The force on the sample in dynes is given by the expression

$$F=A\int_0^{H_m} IdH, \tag{1}$$

where A is the cross-sectional area of the sample in sq. cm, I is the intensity of magnetization per unit volume, and H_m is the field strength at the center of the magnet. From Eq. (1) it is possible to calculate the intensity of magnetization at any field strength by differentiation.

$$I=\frac{1}{A}\frac{\partial F}{\partial H_m}. \tag{2}$$

The process of differentiation, however, magnifies the observational errors and introduces new ones. It is therefore desirable to interpret the observations in the following way if one is concerned only with the saturation value of a ferromagnetic component and the susceptibility of a para- or diamagnetic component. In this case the intensity of magnetization has the form

$$I=I_s+kH \tag{3}$$

for values of H greater than H_c, the critical field necessary to saturate the ferromagnetic component. I_s is this saturation intensity measured per unit volume of the alloy, and k is the volume susceptibility. Substituting this expression into Eq. (1) one gets

$$F=A\int_0^{H_c} IdH+AI_s(H-H_c)+\tfrac{1}{2}Ak(H^2-H_c^2). \tag{4}$$

[2] This work is to be presented in the Trans. American Society for Metals, Age-Hardening Symposium.

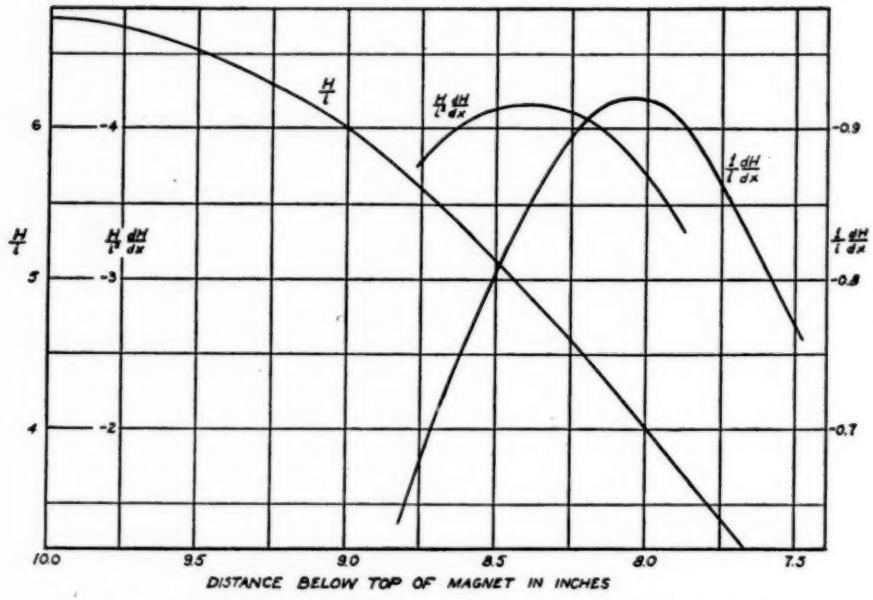

FIG. 1. Distribution of field along the axis of the magnetizing coil.

The behavior of the material in low fields may be completely eliminated by the following device.* Let H_0 be any particular value of the field greater than H_c, and let F_0 be the corresponding value of the magnetic force. We may then write

$$\frac{F-F_0}{H-H_0}=AI_s+Ak\frac{H+H_0}{2}. \tag{5}$$

The expression on the left plotted as a function of H is then a straight line from whose slope and position one may calculate I_s and k, provided only that H is greater than H_c. The advantage of the Gouy method lies in the fact that the position of the specimen in the magnet need not be accurately known if the field at the center of the magnet is homogeneous. The disadvantage lies in the fact that the specimen must be homogeneous, and must of course be at a uniform temperature. Both of these items are difficult to achieve if the specimen is as long as it must be in our magnet; namely, one foot.

The second method is called the Curie method, and consists of hanging a small sample of any shape at a point near the magnet where both the field and its gradient are known. The force acting on the sample is then given by the expression

$$F=m\sigma\partial H/\partial x, \tag{6}$$

from which one can calculate the magnetization at any field strength directly. Here m is the mass of the sample and σ is the intensity of magnetization per unit mass. The great advantage of this method lies in the fact that one can make measurements on almost any kind of sample. The disadvantage is that one must know the position of the sample in the magnet accurately and that one cannot use the full field strength of the magnet. In our magnet these points turned out not to be serious. The magnetization of any sample may be expressed by a formula of the form

$$\sigma=a+bH \tag{7}$$

in a sufficiently small range of fields, a and b being constants. The force exerted on the sample will therefore be given by

$$F=ma\partial H/\partial x+mbH\partial H/\partial x. \tag{8}$$

The force therefore depends only on the quantities $\partial H/\partial x$ and $H\partial H/\partial x$ at the point where the sample is hung, and it is not necessary to know H itself accurately for the interpretation of the observation as the quantities a and b define the magnetization curve in the vicinity of the field strength used, and may be determined by observation at two field strengths near enough together so that a and b may be treated as constants. If in sufficiently large fields the magnetization curve becomes a straight line, as in

* This is more satisfactory than the usual procedure of plotting F/H^2 as a function of $1/H$ and extrapolating the resulting curve to infinite H to find k.

Eq. (3) for instance, the quantities a and b are truly constants, being the saturation intensity per unit mass σ_s, and the mass susceptibility χ, respectively.

The distribution of field in our magnet is shown in Fig. 1. The quantities plotted are independent of the magnet current i. By choosing a point $8\frac{1}{4}''$ below the top of the magnet to hang the specimens to be measured, conditions are such that an error of $\pm\frac{1}{32}''$ in locating the specimen will not result in an error of more than one percent in either $\partial H/\partial x$ or $H\partial H/\partial x$. Actually it is possible to locate the sample much more precisely than this, but this accuracy is ample for the present investigation. The values adopted for the constants of the magnet at this point are

$$\begin{aligned} H &= 4.58\, i \\ \partial H/\partial x &= -0.895\, i \\ H\partial H/\partial x &= -4.10\, i^2. \end{aligned} \qquad (9)$$

The absolute value of these constants has been determined only to within about 5 percent since we are chiefly interested in relative values. Both methods have been used in the following investigation, and the Curie method found the more satisfactory except for the measurement of pure elements at room temperature.

The forces exerted on the specimens were measured with a chemical balance. This was found very convenient as it was necessary to vary the sensitivity in the course of the measurements because the balance tends to become unstable when the magnetic force is large, and this could easily be done by adding weights to the pointer. The magnet is provided with a platinum wound quartz furnace which can heat the sample to be measured to 1000°C. The design of the furnace is shown in Fig. 2. The sample S hangs in the hot zone, and its position can be located by means of a quartz stop A. Any desired atmosphere can be maintained by first flushing the furnace and then preventing air from diffusing in by passing a small amount of the desired gas in at the side arm B and out through the small opening in the glass plate C. Samples are held in a sling of molybdenum foil 0.001″ thick hanging by means of a fine wire from one arm of the balance. A slight correction has always to be made for the force exerted on the sample-holder and balance.

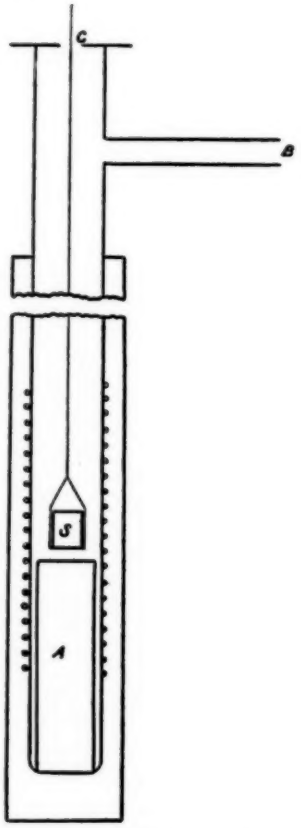

FIG. 2. Diagram of magnet furnace.

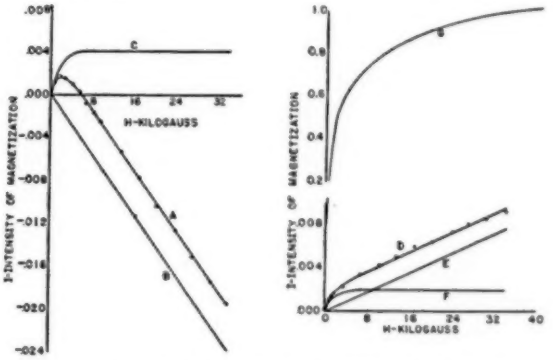

FIG. 3. Typical magnetization curves obtained on Cu-Fe alloys.

Typical magnetization curves are shown in Fig. 3. Curve A was obtained on a sample of commercial copper. It may be interpreted as the sum of two curves B and C. B is the curve of a typically diamagnetic substance with a volume susceptibility of -0.714×10^{-6}. C is very similar to the magnetization curve to be expected of a small amount of ferromagnetic material in the form of more or less spherical particles. If this

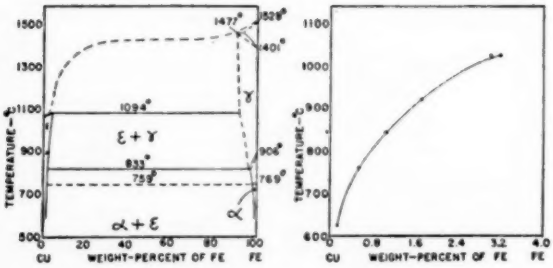

FIG. 4. The copper-iron phase diagram.

material were iron, whose saturation intensity is about 1700, it would represent only 0.0002 percent of the sample. We shall here confine ourselves to the observation of the saturation intensity of the ferromagnetic component, and leave to some future date the interpretation of the initial portion of the magnetization curve of these ferromagnetic inclusions. Curve *D* was obtained on a sample of copper containing 0.1 percent of iron by weight. It may be interpreted as the sum of two curves *E* and *F* resulting from a paramagnetic and a ferromagnetic component in the alloy. Evidently some of the iron in this sample is in solution, thus making the diamagnetic copper paramagnetic, and a part of the iron is in its usual ferromagnetic form. Curve *G* was obtained on a sample of copper containing 0.7 percent of iron. This sample contains so much ferromagnetic material in a form difficult to magnetize that even in a field of 40,000 gauss we are not near enough to saturation to separate the paramagnetism from the last part of the approach to ferromagnetic saturation. Even larger fields would be required to do this, and we must remain content with a rough estimate of the amount of ferromagnetism in such samples.

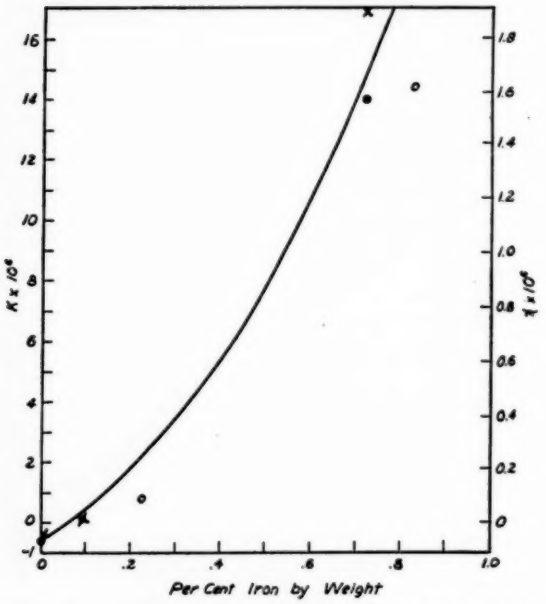

FIG. 5. Volume and mass susceptibility of Cu-Fe alloys after annealing at 950°C for 16 hr. in H_2 and quenching in water.

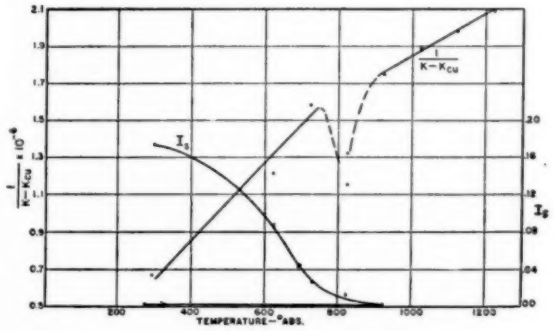

FIG. 6. Magnetic susceptibility and saturation intensity per unit volume of a powder compact containing 0.22 percent Fe during cooling.

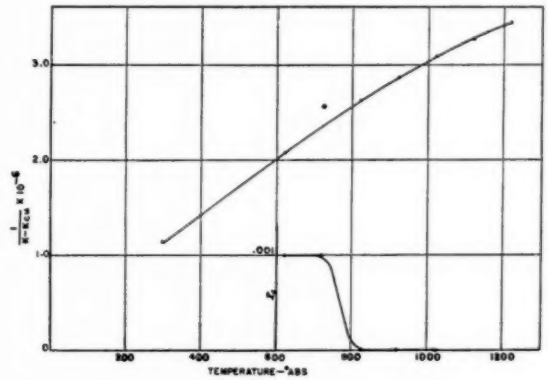

FIG. 7. Magnetic susceptibility and saturation intensity per unit volume of a cast specimen containing 0.09 percent Fe in solution during cooling.

OBSERVATIONS

The phase diagram for copper-iron alloys as given by Hansen[3] is shown in Fig. 4. According to this, copper rich alloys should exist in the form of solid solutions at elevated temperatures, and should precipitate out ferromagnetic iron at low temperatures. Our first concern was to determine whether it was satisfactory to prepare samples by the simple methods of powder metallurgy, or whether it was desirable to cast them in con-

[3] M. Hansen, *Der Aufbau der Zweistofflegierungen* (Springer, Berlin, 1936).

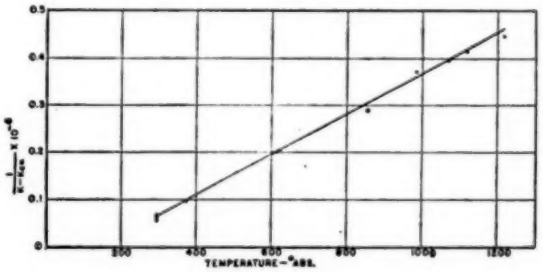

FIG. 8. Magnetic susceptibility per unit volume of a cast specimen containing 0.7 percent iron in solution.

trolled atmospheres. Alloys having compositions in the range 0–1 percent iron were prepared by both methods. The powder compacts were kindly supplied by John Wulff. Magnetic measurements on the latter after compression without the application of heat showed an amount of ferromagnetic material present in satisfactory agreement with the known composition. Samples of both types were then annealed at about 950°C in hydrogen for 16 hours and quenched in water. After this treatment all but a slight trace of ferromagnetism had disappeared, and the samples had the susceptibilities shown in Fig. 5. The points indicated by dots were obtained on Gouy specimens, those indicated by crosses were obtained on Curie specimens, and those indicated by circles were obtained on the powder compacts as Curie specimens. The latter showed consistently low values, indicating incomplete solution. A cast sample and a powder compact were then taken to a high temperature and measurements made during slow cooling. The results are shown in Figs. 6 and 7.

I_s is the saturation intensity per unit volume of the alloy, k is the volume susceptibility of the alloy, and K_{Cu} is the volume susceptibility of the copper used in making it. Our measurements indicate that this varies from -0.73×10^{-6} at room temperature to -0.61×10^{-6} at 1000°C.[4] If the iron in solution obeys a modified Curie law one might expect the total susceptibility of the quenched alloys to have the form

$$K=K_{Cu}+\frac{C}{T-\theta},$$

so that $(K-K_{Cu})^{-1}$ should be a linear function of the temperature if the above law is obeyed.

[4] This result is in close agreement with the measurements of K. Honda, Ann. d. Physik **32**, 1056 (1910).

The reappearance of a marked amount of ferromagnetism in the powder compact confirms the assumption of incomplete solution after the original heat treatment. Probably the copper penetrated the iron particles during the 16-hour heating at 950°C sufficiently to destroy their ferromagnetism, and diffused out of these particles again to a certain extent during the subsequent slow cooling. In the cast specimen, however, in which there was supposedly complete mixing during the solution treatment, no appreciable changes occurred during the subsequent slow cooling. The sluggishness of these alloys led us to give up the use of powder compacts, and to make our observations on cast specimens only. The above results indicate, however, that magnetic measurements may be of some value in powder metallurgy, and that powder compacts may be particularly adapted to producing special types of structures in alloys.

The next point on the program was to determine the behavior of the alloys in the form of solid solutions. From Fig. 5 it would appear that the susceptibility at room temperature is not directly proportional to the concentration. The behavior at high temperatures of the alloy containing 0.7 percent of iron is shown in Fig. 8. A Curie-Weiss law is at least approximately obeyed, with a Curie temperature in the neighborhood of 150°K. The number of Bohr magnetons per atom was calculated from the data in Figs. 7 and 8, and the values found are 3.4 and 3.6, respectively. This indicates the magnetic moment of the iron atoms in this range of compositions is independent of concentration, and that the departure from linearity in the susceptibility

TABLE I. *Mass susceptibility* χ *and saturation intensity per unit mass of alloy measured at room temperature, in samples containing* 0.7 *percent* Fe *by weight.*

SAMPLE	$\chi\times10^6$	σ_s
A2E Quenched	1.82	0.0005
Cold Worked 12%	1.84	0.0002
A2F Quenched	1.78	0.0005
Annealed at 525°C for 20 min.	~0.9	
Cold Worked 12%	0.94	0.0001
A2G Quenched	1.96	0.0005
Annealed at 525°C for 2 hr.	0.609	0.001
Annealed from 685–440°C for 6 hr.	0.237	0.006
Cold Worked 12%	0.3	0.38

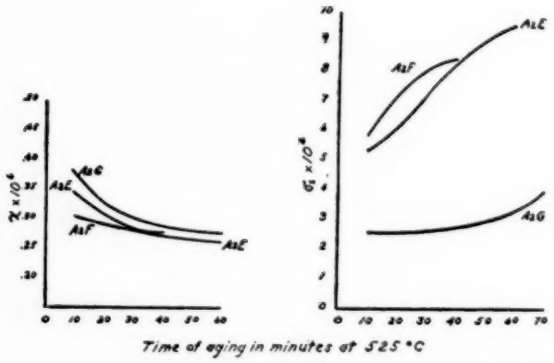

FIG. 9. Susceptibility and saturation intensity per unit mass of various samples during aging.

vs. temperature curves in Fig. 5 is due to interactions giving rise to a Curie temperature. The magneton number found above is rather lower than that found in salts (5 to 6 Bohr magnetons) or for iron in solution in gold (about 4.5 Bohr magnetons).[5]

A series of experiments was next undertaken to study the manner of precipitation from solution in a set of alloys containing approximately 0.7 percent of iron. The solubility limit for this composition is 800°C according to Fig. 4. The results of these experiments are summarized in Table I.

In the quenched samples the iron is retained in solution. Aging these supersaturated solutions below the solubility limit decreases the susceptibility, but does not cause ferromagnetism to appear. Cold working the alloy in the quenched or partly aged condition does not affect the magnetic properties, but cold working a more fully aged sample produces ferromagnetic inclusions.

An experiment was also performed to see whether recrystallization during aging altered the manner of precipitation. Samples A2E and A2F were measured at 525°C after the cold working operation, as was sample A2G immediately after the quench. The results are shown in Fig. 9. No observations during the first ten minutes are recorded as the samples were not completely up to temperature until after that time. A slightly greater amount of ferromagnetism appears in the cold worked samples A2E and *F* which are assumed to be recrystallizing but outside of this all the samples aged in a very similar manner. The aging of sample A2G was continued for two hours, during which time the susceptibility decreased to 0.25×10^{-6}, but the amount of ferromagnetism showed no appreciable further change. There is apparently little tendency for the iron which presumably is precipitating out of this solution to appear in its ferromagnetic form. If, however, appreciable amounts of ferromagnetic iron are present in a partly aged sample, further aging will make this amount of ferromagnetism increase. A partly aged and cold worked sample having a saturation intensity per unit mass at room temperature of 0.23 was aged for 27½ hours at 520°C. After this treatment the above quantity had increased to 0.45.

An attempt was made to find the temperatures at which precipitation first occurs, and at which the ferromagnetic and nonmagnetic precipitates dissolve. These experiments could not be carried through because it was found that the alloys could be supercooled about 100°C, and because the nearness of the Curie point to the solubility limit of the alloy we were working with made the interpretation of the results doubtful. Further attempts to make these measurements on alloys of different compositions are now under way.

CONCLUSIONS

The chief conclusion to be drawn from the above report is that the equipment now available and functioning is adequate for making measurements of considerable interest to both physicists and metallurgists. The preliminary observations made in the course of testing the equipment and establishing the methods of measurement indicate that the process of precipitation from solid solution in the copper-iron alloys investigated is a complex one in which equilibrium can be reached apparently only by the use of both cold work and aging at high temperatures. The results indicate that there may be at least two intermediate stages in the process. During the first, the solution is somehow disturbed, possibly by the appearance of fluctuations in concentration. In this stage the paramagnetic susceptibility is greatly reduced, but plastic deformation does not affect the structure. Further aging does not greatly affect the magnetic properties, but a feebly magnetic precipitate is probably forming, as is shown by the fact that in this stage cold work produces ferromagnetism, probably by

[5] See E. C. Stoner, *Magnetism and Matter* (Methuen and Company, London, 1934), page 312; and J. W. Shih, Phys. Rev. **38**, 2051 (1931).

altering the lattice structure of the precipitate. The precipitate may possibly be face-centered cubic gamma-iron containing copper, or iron atoms in great concentration on the lattice points of the copper lattice.

This work was made possible by grants from the Joseph Henry Fund of the National Academy of Sciences, and the Penrose Fund of the American Philosophical Society covering some of the costs of the experiments.

NOVEMBER 15, 1939 PHYSICAL REVIEW VOLUME 56

The Rotation-Vibration Energies of Tetrahedrally Symmetric Pentatomic Molecules. II

WAVE H. SHAFFER, HARALD H. NIELSEN AND L. H. THOMAS
Mendenhall Laboratory of Physics, Ohio State University, Columbus, Ohio

(Received September 18, 1939)

A general discussion of a method which may be used to obtain the first-order Coriolis splitting of the harmonic and combination states of ν_3 and ν_4 is presented. The method is applied to obtain these splittings of $2\nu_3$, $2\nu_4$ and $\nu_3+\nu_4$ and to derive the stabilized wave functions for these states. With these functions the selection rules and the elements of the matrix of the second-order Hamiltonian $H^{(2)\prime}$ have been calculated for these states.

I. INTRODUCTION

IN Part I of this paper[1] we have given the quantum-mechanical Hamiltonian for the investigation of the vibration-rotation energies of the XY_4 type molecules, including all terms which may contribute to the energy to second order of approximation. In addition to the harmonic oscillator and rigid spherical top terms of the zeroth order, the Hamiltonian includes cubic and quartic anharmonic terms, centrifugal expansion terms, all possible types of Coriolis and other interactions between rotation and oscillation. The Hamiltonian was transformed by a contact transformation into $H^{(0)}+\lambda H^{(1)\prime}+\lambda^2 H^{(2)\prime}$ so that to second approximation only the Coriolis interaction terms between rotation and the threefold degenerate oscillations ν_3 and ν_4 are contained in $H^{(1)\prime}$. This facilitates the calculation of the energies to second approximation which otherwise would be very difficult because of the high degree of degeneracy of the zeroth-order energies. In Part I we have calculated and set down the elements of the matrix H accurate to second order of approximation for the states $V_1\nu_1$, ν_2, $V_1\nu_1+\nu_3$, $V_1\nu_1+\nu_4$, $\nu_2+\nu_3$ and $\nu_2+\nu_4$.

Part II deals with the energies of the states $2\nu_3$ (or $2\nu_4$) and $\nu_3+\nu_4$, which are, respectively, six- and ninefold degenerate because of the degeneracy of ν_3 and ν_4. The manner in which this degeneracy is removed by the first-order Coriolis terms $H^{(1)\prime}$ is discussed and calculations are made on the selection rules and the second-order energies.

[1] W. H. Shaffer, H. H. Nielsen and L. H. Thomas, Phys. Rev. **56**, 895 (1939).

II. THE FIRST-ORDER CORIOLIS INTERACTION ENERGIES

We shall discuss first a general method of treating the first-order Coriolis interaction terms $H^{(1)\prime}$ which can be written in the form:

$$H^{(1)\prime}=-(\zeta_3/A_0)(\mathbf{J}_3\cdot\mathbf{J})-(\zeta_4/A_0)(\mathbf{J}_4\cdot\mathbf{J}), \quad (1)$$

where $\mathbf{J}_3$ and $\mathbf{J}_4$ are the internal angular momenta associated with ν_3 and ν_4, respectively, and $\mathbf{J}$ is the total angular momentum of the molecule. It is readily shown from a study in spherical polar coordinates of the threefold degenerate modes ν_3 and ν_4 as isotropic three-dimensional oscillators that the quantum number J_3 may assume the values V_3, V_3-2, V_3-4, $\cdots 0$ or 1 (and J_4 the values V_4, V_4-2, etc.) where V_3 and V_4 are the vibrational quantum numbers associated with ν_3 and ν_4, respectively. The total internal angular momentum of the molecule is thus:

$$\mathbf{J}_2=\mathbf{J}_3+\mathbf{J}_4, \quad (2)$$

where $\mathbf{J}_2$ may evidently take the values:

$$J_2=J_3+J_4,\quad J_3+J_4-1,\quad \cdots|J_3-J_4|. \quad (3)$$

Thus the total angular momentum of the molecule, $\mathbf{J}$, becomes

$$\mathbf{J}=\mathbf{J}_1+\mathbf{J}_2, \tag{4}$$

$\mathbf{J}_1$ being the angular momentum of the rotation of the molecular framework. J_1 may take the values:

$$J_1=J+J_2,\quad J+J_2-1,\quad \cdots|J-J_2|. \tag{5}$$

When only one of the vibrational quantum numbers V_k ($k=3$, 4), is different from zero it follows that $\mathbf{J}_k\equiv\mathbf{J}_2$ so that

$$H^{(1)\prime}=(-\zeta_k/A_0)(\mathbf{J}_2\cdot\mathbf{J})=(-\zeta_k/A_0)(\mathbf{J}_k\cdot\mathbf{J}).$$

It is readily shown with the aid of (4) that:

$$H^{(1)\prime}=(-\zeta_k/A_0)\{(\mathbf{J}_2\cdot\mathbf{J}_2)+(\mathbf{J}\cdot\mathbf{J})-(\mathbf{J}_1\cdot\mathbf{J}_1)\}, \tag{6}$$

which when $V_k=1$ leads directly to the eigenvalues of $H^{(1)\prime}$ given in Part I and elsewhere. When V_3 and V_4 both are different from zero, the substitution of (2) and (4) into (1) yields:

$$\begin{aligned}H^{(1)\prime}=&-(1/2A_0)\{(\zeta_3+\zeta_4)(\mathbf{J}_2\cdot\mathbf{J}_2)\\&+2\zeta_3(\mathbf{J}_3\cdot\mathbf{J}_1)+2\zeta_4(\mathbf{J}_4\cdot\mathbf{J}_1)\\&+(\zeta_3-\zeta_4)(\mathbf{J}_3\cdot\mathbf{J}_3)+(\zeta_4-\zeta_3)(\mathbf{J}_4\cdot\mathbf{J}_4)\}.\end{aligned} \tag{7}$$

The only nonvanishing matrix elements of the quantities $(J_i\cdot J_i)$ are diagonal in all the quantum numbers and have the values:

$$J_i(J_i+1)\hbar^2\ (J_i \text{ denoting } J,\ J_3,\ J_4,\ J_1, \text{ or } J_2). \tag{8}$$

A method similar to that of Condon and Shortley[2] yields the following nonvanishing matrix elements of $(\mathbf{J}_3\cdot\mathbf{J}_1)$ and $(\mathbf{J}_4\cdot\mathbf{J}_1)$:

$$\begin{aligned}&\left.\begin{matrix}(J_2|(\mathbf{J}_3\cdot\mathbf{J}_1)|J_2)\\(J_2|(\mathbf{J}_4\cdot\mathbf{J}_1)|J_2)\end{matrix}\right\}\\&=[\pm J_3(J_3+1)\mp J_4(J_4+1)+J_2(J_2+1)]\\&\times[J(J+1)-J_1(J_1+1)-J_2(J_2+1)]\\&\qquad\times\hbar^2/4J_2(J_2+1),\end{aligned} \tag{9}$$

$$\begin{aligned}&\left.\begin{matrix}(J_2|(\mathbf{J}_3\cdot\mathbf{J}_1)|J_2-1)\\-(J_2|(\mathbf{J}_4\cdot\mathbf{J}_1)|J_2-1)\end{matrix}\right\}\\&=[(J_2-J_3+J_4)(J_2+J_3-J_4)(J_2+J_3+J_4+1)\\&\times(J_3+J_4-J_2+1)(J+J_2-J_1)]^{\frac{1}{2}}\\&\times[(J+J_1-J_2+1)(J+J_1+J_2+1)\\&\qquad\times(J_1+J_2-J)/4J_2^2(4J_2^2-1)]^{\frac{1}{2}}(\hbar^2/2).\end{aligned} \tag{10}$$

The matrix elements in (9) and (10) are diagonal in the quantum numbers J, J_1, J_3 and J_4.

III. The Eigenfunctions and Eigenvalues of H for $2\nu_3$, $2\nu_4$ and $\nu_3+\nu_4$

A. The state $2\nu_3$ (and $2\nu_4$)

For the state $2\nu_3$, $V_3=2$ and $V_1=V_2=V_4=0$. The zeroth-order energy for this state is:

$$E^{(0)}=\tfrac{1}{2}h(\nu_1+2\nu_2+7\nu_3+3\nu_4)+J(J+1)(\hbar^2/2A_0). \tag{11}$$

From the foregoing it is evident that $J_2(=J_3)$ may take the values: (a), $J_2=2$ and (b), $J_2=0$. It follows from (5) that the corresponding values of J_1 are: (a) $J_2=J\pm2$, $J\pm1$, J and (b) $J_1=J$. Eq. (6) together with (8) leads at once to the following eigenvalues $E_i^{(1)}=\epsilon_i(\zeta_3\hbar^2/A_0)$:

$$\begin{aligned}&\text{(a)}\quad J_1=J:\ \epsilon_0=0;\\&\text{(b)}\quad J_1=J+2:\ \epsilon_{\mathrm{I}}=2J;\quad J_1=J+1:\ \epsilon_{\mathrm{II}}=J-2;\quad J_1=J:\ \epsilon_{\mathrm{III}}=-3;\\&\qquad\qquad J_1=J-1:\ \epsilon_{\mathrm{IV}}=-(J+3);\quad J_1=J-2:\ \epsilon_{\mathrm{V}}=-2(J+1).\end{aligned} \tag{12}$$

Thus the sixfold vibrational degeneracy of the state $2\nu_3$ is removed by $H^{(1)\prime}$. There remains, however, a $(2J+1)$ degeneracy in the quantum number K which can be removed only by terms of second and higher orders in H, and a $(2J+1)$-fold degeneracy in the magnetic quantum number M.

The wave functions required for our further work are the functions which will diagonalize $H^{(0)}+\lambda H^{(1)\prime}$. Treated in spherical polar coordinates, the wave functions characteristic of the state $2\nu_3$, which to zeroth approximation is sixfold degenerate, are the following:

$$\begin{aligned}&\text{(a)}\quad \chi_0(JK'M)=3^{-\frac{1}{2}}\{\phi(200)+\phi(020)+\phi(002)\}R(JK'M),\\&\text{(b)}\quad \chi_1(JK'M)=2^{-1}\{\phi(200)-\phi(020)+2^{\frac{1}{2}}i\phi(110)\}R(JK'M),\\&\qquad \chi_2(JK'M)=2^{-\frac{1}{2}}\{\phi(101)+i\phi(011)\}R(JK'M),\\&\qquad \chi_3(JK'M)=6^{-\frac{1}{2}}\{2\phi(002)-\phi(200)-\phi(020)\}R(JK'M),\\&\qquad \chi_4(JK'M)=-2^{-\frac{1}{2}}\{\phi(101)-i\phi(011)\}R(JK'M),\\&\qquad \chi_5(JK'M)=2^{-1}\{\phi(200)-\phi(020)-2^{\frac{1}{2}}i\phi(110)\}R(JK'M),\end{aligned} \tag{13}$$

where $R(JK'M)$ denotes a wave function of the spherical top and $\phi(n_1n_2n_3)=\phi(n_1)\phi(n_2)\phi(n_3)$, $\phi(n_i)$ being the wave function of a linear harmonic oscillator associated with the coordinate q_i. As

[2] E. U. Condon and G. H. Shortley, *Introduction to Atomic Spectra* (Cambridge University Press, 1935), Section 12[3].

in Part I, $n_1+n_2+n_3=V_3$. It is readily shown that the wave functions we require are the following linear combinations of the functions (13); for case (a), $\Psi_0(JK'M)=\chi_0(JK'M)$; for case (b), $\Psi_s(JKM)=a_s\chi_1(JK+2M)+b_s\chi_2(JK+1M)+c_s\chi_3(JKM)+d_s\chi_4(JK-1M)+e_s\chi_5(JK-2M)$. In matrix notation we may write:

$$\|\Psi\|=\|A\|\cdot\|\chi\|=\left\|\begin{matrix}\Psi_{\mathrm{I}}\\ \Psi_{\mathrm{II}}\\ \Psi_{\mathrm{III}}\\ \Psi_{\mathrm{IV}}\\ \Psi_{\mathrm{V}}\end{matrix}\right\|=\left\|\begin{matrix}e_1 & d_1 & c_1 & b_1 & a_1\\ e_2 & d_2 & c_2 & b_2 & a_2\\ e_3 & d_3 & c_3 & b_3 & a_3\\ e_4 & d_4 & c_4 & b_4 & a_4\\ e_5 & d_5 & c_5 & b_5 & a_5\end{matrix}\right\|\cdot\left\|\begin{matrix}\chi_5\\ \chi_4\\ \chi_3\\ \chi_2\\ \chi_1\end{matrix}\right\|. \tag{14}$$

The matrix A of (14) is identical, element for element, with the matrix in Table 2[3] of reference 2 where j_1 and m are replaced by J and K, respectively.

The selection rules have been determined by investigating the nonvanishing elements of the electric moment. This has been done by two different methods: first, by use of the quadratic terms in the electric moment together with the eigenfunctions (14); second, by use of the linear terms in the electric moment together with wave functions corrected by taking into account cubic terms in the potential energy. The two methods yield identical results for both selection rules and the quantum-mechanical amplitudes.

The selection rules governing transitions between rotation levels in the normal state and the Coriolis components of the state $2\nu_3$ are the following: (a) Transitions to ϵ_0 from the normal state are forbidden; (b) $\Delta J=0, -1$ to ϵ_{I}; $\Delta J=0, \pm1$ to ϵ_{II}, ϵ_{III}, ϵ_{IV}; $\Delta J=0, +1$ to ϵ_{V}. The selection rules for K and M are the same as in the case of transitions to $V_1\nu_1+\nu_3$, *viz.*, $\Delta K=0$, $\Delta M=0, \pm1$.

The actual relative intensities of the lines are proportional to the quantities $B(J'K', JK)$ which denote the squares of the absolute values of the amplitudes for transitions $(J'K')$ to (JK). The values of $B(J'K', JK)$ for the state $2\nu_3$ are given below:

(a) $J_2=2, J_1=J+2$:

$$B(J-1K, JK)=0,$$
$$B(JK, JK)=J[(J+2)^2-K^2][(J+1)^2-K^2]/(J+1)^2(J+2)(2J+1)(2J+3),$$
$$B(J+1K, JK)=(2J+1)K^2[(J+2)^2-K^2]/(J+1)^2(J+2)(2J+3)^2;$$

(b) $J_2=2, J_1=J-2$:

$$B(J-1K, JK)=(2J+1)K^2[(J-1)^2-K^2]/J^2(J-1)(2J-1)^2,$$
$$B(JK, JK)=(J+1)(J^2-K^2)[(J-1)^2-K^2]/J^2(J-1)(4J^2-1),$$
$$B(J+1K, JK)=0;$$

(c) $J_2=2, J_1=J+1$:

$$B(J-1K, JK)=(J+2)[J^2-K^2][(J+1)^2-K^2]/2J^2(J+1)(4J^2-1), \tag{15}$$
$$B(JK, JK)=(J-2)^2K^2[(J+1)^2-K^2]/2J^2(J+1)^2(J+2)(2J+1),$$
$$B(J+1K, JK)=J[3K^2-(J+1)(J+2)]^2/2(J+1)^2(J+2)(2J+3)(2J+1);$$

(d) $J_2=2, J_1=J-1$:

$$B(J-1K, JK)=(J+1)[3K^2-J(J-1)]^2/2J^2(J-1)(4J^2-1),$$
$$B(JK, JK)=(J+3)^2K^2(J^2-K^2)/2J^2(J+1)^2(J-1)(2J+1),$$
$$B(J+1K, JK)=(J-1)(J^2-K^2)[(J+1)^2-K^2]/2(J+1)^2J(2J+1)(2J+3);$$

(e) $J_2=2, J_1=1$:

$$B(J-1K, JK)=3(2J+3)K^2(J^2-K^2)/2J^2(J+1)(2J-1)^2,$$
$$B(JK, JK)=3[3K^2-J(J+1)]^2/2J^2(J+1)^2(2J-1)(2J+3),$$
$$B(J+1K, JK)=3(2J-1)K^2[(J+1)^2-K^2]/2(J+1)^2J(2J+3)^2.$$

As a further check on the reliability of these amplitudes we have verified that they are consistent with the principle of spectroscopic stability.

The second-order energy corrections are obtained by solving for the roots of the secular determinant $|(K|H^{(2)'}|K')-E^{(2)}\delta_{K',K}|$, the elements of which are obtained after the manner of Part I. These are listed below, the quantities a, b, c, d, and e being the elements of the matrix A given in (15).

$$(K|H^{(2)\prime}|K)=(\hbar^2/2A_0)\{R_0+fR_1+f^2R_2+(b_i^2-c_i^2+d_i^2)R_3+(a_i^2+e_i^2)fR_4+(b_i^2+d_i^2)fR_5$$
$$+[a_i^2(K+2)^2+e_i^2(K-2)^2]R_6+c_i^2K^2R_7+[b_i^2(K+1)^2+d_i^2(K-1)^2]R_8+[a_i^2(6f(K+2)^2$$
$$-5(K+2)^2-7(K+2)^4)+b_i^2(6f(K+1)^2-5(K+1)^2-7(K+1)^4)+c_i^2(6fK^2-5K^2-7K^4)$$
$$+d_i^2(6f(K-1)^2-5(K-1)^2-7(K-1)^4)+e_i^2(6f(K-2)^2-5(K-2)^2-7(K-2)^4)]R_9$$
$$+(a_ib_i(2K+3)[f-(K+1)(K+2)]^{\frac{1}{2}}+b_ic_i(2K+1)[f-K(K+1)]^{\frac{1}{2}}/6^{\frac{1}{2}}+c_id_i(2K-1)$$
$$\times[f-K(K-1)]^{\frac{1}{2}}/6^{\frac{1}{2}}+d_ie_i(2K-3)[f-(K-1)(K-2)]^{\frac{1}{2}})R_{10}+(a_ib_i(2f-6K^2-18K-15)$$
$$\times[f-(K+1)(K+2)]^{\frac{1}{2}}+3b_ic_i(2f-6K^2-6K-3)[f-K(K+1)]^{\frac{1}{2}}/6^{\frac{1}{2}}+3b_ic_i(2f-6K^2+6K-3)$$
$$\times[f-K(K-1)]^{\frac{1}{2}}/6^{\frac{1}{2}}+d_ie_i(2f-6K^2+18K-15)[f-(K-1)(K-2))^{\frac{1}{2}})R_{11}+(2a_i^2[8(K+2)^3$$
$$+(K+2)-4f(K+2)]+b_i^2[8(K+1)^3+(K+1)-4f(K+1)]-d_i^2[8(K-1)^3+(K-1)$$
$$-4f(K-1)]-2e_i^2[8(K-2)^3+(K-2)-4f(K-2)])(R_{11}/2)+(6^{-\frac{1}{2}}a_ic_i[f-K(K+1)]^{\frac{1}{2}}$$
$$\times[f-(K+1)(K+2)]^{\frac{1}{2}}-\tfrac{1}{2}b_id_i[f-K(K-1)]^{\frac{1}{2}}[f-K(K+1)]^{\frac{1}{2}}$$
$$+6^{-\frac{1}{2}}c_ie_i[f-K(K-1)]^{\frac{1}{2}}[f-(K-1)(K-2)]^{\frac{1}{2}})R_{12}\},\quad(16)$$

in which the parameters R_s are the following quantities:

$$R_0(2\nu_3)=(A_0/2)\{39d_1+7d_3+9d_5+12d_6+3d_{10}+14d_{11}+7d_{18}+3d_{20}+7d_{21}+14d_{22}-7d_{23}/2+3d_{27}$$
$$+6d_{28}-3d_{29}/2+3d_{30}+3d_{31}+9d_{33}\}-(9/4)+9\zeta_3^2/2+(7/2)[(\omega_4/\omega_3)+(\omega_3/\omega_4)]\zeta_{34}^2$$
$$+(7/4)[(\omega_2/\omega_3)+(\omega_3/\omega_2)]\zeta_{23}^2+(3/4)[(\omega_2/\omega_4)+(\omega_4/\omega_2)]\zeta_{24}^2-3\zeta_{34}^2-(A_0/4)\{10c_1^2/3\omega_3$$
$$+c_2^2(14\omega_3\omega_4+18\omega_3^2-12\omega_4^2)/\omega_4(4\omega_3^2-\omega_4^2)+c_3^2(14\omega_4-3\omega_3)/(4\omega_4^2-\omega_3^2)+c_4^2/3\omega_4$$
$$+42c_5(c_7+c_{11}+c_{12})/\omega_1+c_5^2(188\omega_3^2-63\omega_1^2+28\omega_1\omega_3)/\omega_1(4\omega_3^2-\omega_1^2)+(c_6^2/(\omega_1^4+\omega_3^4+\omega_4^4$$
$$-2\omega_1^2\omega_3^2-2\omega_1^2\omega_4^2-2\omega_3^2\omega_4^2))[3\omega_3(\omega_3^2-\omega_4^2-\omega_1^2)+7\omega_4(\omega_4^2-\omega_3^2-\omega_1^2)+7\omega_1(\omega_1^2-\omega_3^2-\omega_4^2)$$
$$+6\omega_1\omega_3\omega_4]+3c_7^2(6\omega_4+5\omega_1)/(2\omega_4+\omega_1)+18c_7(c_{11}+c_{12})/\omega_1+c_8^2(44\omega_3^2+28\omega_2\omega_3$$
$$-27\omega_2^2)/\omega_2(4\omega_3^2-\omega_2^2)+(c_9^2/(\omega_2^4+\omega_3^4+\omega_4^4-2\omega_2^2\omega_3^2-2\omega_2^2\omega_4^2-2\omega_3^2\omega_4^2))[6\omega_2\omega_3\omega_4$$
$$+3\omega_3(\omega_3^2-\omega_4^2-\omega_2^2)+7\omega_4(\omega_4^2-\omega_3^2-\omega_2^2)+7(\omega_2^2-\omega_3^2-\omega_4^2)]+6c_{10}^2/(\omega_2+2\omega_4)$$
$$+18c_{11}c_{12}/\omega_1+11c_{11}^2/\omega_1+36c_{12}^2(\omega_1+\omega_2)/\omega_1(\omega_1+2\omega_2)+5c_{13}^2/16\},$$
$$R_1(2\nu_3)=(\hbar/2A_0)\{3\zeta_{23}^2/\omega_3+3\zeta_{24}^2/2\omega_4+1/\omega_2+2/\omega_1+2\zeta_{34}^2[3\omega_3(\omega_3^2+3\omega_4^2)-8\omega_4(\omega_4^2+3\omega_3^2)]$$
$$\times(3\omega_3\omega_4(\omega_3^2-\omega_4^2))^{-1}+\zeta_{23}^2(5\omega_2^3+15\omega_2\omega_3^2-9\omega_2^2\omega_3-3\omega_3^3)/3\omega_2\omega_3(\omega_2^2-\omega_3^2)$$
$$+\zeta_{24}^2(\omega_3-\omega_4)^2/\omega_2\omega_4(\omega_2+\omega_4)\}+(\hbar^2/2A_0^2\omega_2^2)+(\hbar/A_0)(A_0/6\omega_1^3)^{\frac{1}{2}}(7c_5+3c_7+3c_{11}+3c_{12}),$$
$$R_2(2\nu_3)=-(\hbar^2/6A_0^2)\{5/2\omega_2^2+8/\omega_1^2+(3/4)(\zeta_{23}^2/\omega_3^2+\zeta_{24}^2/\omega_4^2)\},$$
$$R_3(2\nu_3)=(A_0/2)(-6d_1+3d_6)+3\zeta_3^2/2+(A_0/4)\{3(2\omega_3^2-\omega_4^2)c_2^2/\omega_4(\omega_4^2-4\omega_3^2)-8\omega_3^2c_5^2/\omega_1(4\omega_3^2-\omega_1^2)$$
$$-(9\omega_2^2-28\omega_3^2)c_8^2/\omega_2(4\omega_3^2-\omega_2^2)\},$$
$$R_4(2\nu_3)=(\hbar/2A_0)\{\zeta_{23}^2/\omega_3+2a_1/\omega_2+(4/3)(3\omega_3^2+\omega_4^2)\zeta_{34}^2/\omega_3(\omega_3^2-\omega_4^2)$$
$$+(4/3)(\omega_2^2+3\omega_3^2)\zeta_{23}^2/\omega_3(\omega_2^2-\omega_3^2)\},$$
$$R_5(2\nu_3)=R_4/4,\quad R_6=-3R_4/2,\quad R_7=3R_4/4,\quad R_8=3R_4/4,\quad R_9=(\hbar^2/4A_0^2)(1/\omega_2^2-\tfrac{1}{2}\zeta_{23}^2/\omega_3^2),$$
$$R_{10}(2\nu_3)=(\hbar/A_0)\{3\zeta_{23}^2/4\omega_3+c_1\zeta_{23}A_0^{\frac{1}{2}}/\omega_3^{\frac{3}{2}}-c_2\zeta_{24}A_0^{\frac{1}{2}}/\omega_4^{\frac{3}{2}}+(\omega_4^2+3\omega_3^2)\zeta_{34}^2/\omega_3(\omega_3^2-\omega_4^2)\},$$
$$R_{11}(2\nu_3)=(\hbar^2\zeta_{23}^2/2A_0^2\omega_3^2),\quad R_{12}(2\nu_3)=-3R_4(2\nu_3)/2-R_{10}(2\nu_3).$$
$$(K|H^{(2)\prime}|K+2)=(K+2|H^{(2)\prime}|K)=(\hbar^2/2A_0)\{-2c_ie_i(+2)6^{-\frac{1}{2}}(f-3K^2)+b_id_i(+2)[f-3(K+1)^2]$$
$$-2a_ic_i(+2)6^{-\frac{1}{2}}[f-3(K+2)^2]-a_ia_i(+2)[f-(K+2)(K+3)]^{\frac{1}{2}}[f-(K+3)(K+4)]^{\frac{1}{2}}$$
$$+b_ib_i(+2)[f-(K+1)(K+2)]^{\frac{1}{2}}[f-(K+2)(K+3)]^{\frac{1}{2}}+c_ic_i(+2)[f-K(K+1)]^{\frac{1}{2}}$$
$$\times[f-(K+1)(K+2)]^{\frac{1}{2}}+d_id_i(+2)[f-K(K-1)]^{\frac{1}{2}}[f-K(K+1)]^{\frac{1}{2}}$$
$$-e_ie_i(+2)[f-(K-1)(K-2)]^{\frac{1}{2}}[f-K(K-1)]^{\frac{1}{2}}\}R_{13},\quad(17)$$

where $R_{13}=(A_0\omega_3/2\hbar)R_{11}$.

$$(K|H^{(2)\prime}|K+4)=(K+4|H^{(2)\prime}|K)=(\hbar^2/2A_0)\{[a_ic_i(+4)6^{-\frac{1}{2}}(f-(K+2)(K+3))^{\frac{1}{2}}(f-(K+3)$$
$$\times(K+4))^{\frac{1}{2}}-\tfrac{1}{2}b_id_i(+4)(f-(K+1)(K+2))^{\frac{1}{2}}(f-(K+2)(K+3))^{\frac{1}{2}}+c_ie_i(+4)6^{-\frac{1}{2}}(f-K(K+1))^{\frac{1}{2}}$$
$$\times(f-(K+1)(K+2))^{\frac{1}{2}}]R_{14}-[a_ia_i(+4)(f-(K+2)(K+3))^{\frac{1}{2}}(f-(K+3)(K+4))^{\frac{1}{2}}$$
$$\times(f-(K+4)(K+5))^{\frac{1}{2}}(f-(K+5)(K+6))^{\frac{1}{2}}+b_ib_i(+4)(f-(K+1)(K+2))^{\frac{1}{2}}(f-(K+2)(K+3))^{\frac{1}{2}}$$
$$\times(f-(K+3)(K+4))^{\frac{1}{2}}(f-(K+4)(K+5))^{\frac{1}{2}}+c_ic_i(+4)(f-K(K+1))^{\frac{1}{2}}(f-(K+1)(K+2))^{\frac{1}{2}}$$
$$\times(f-(K+2)(K+3))^{\frac{1}{2}}(f-(K+3)(K+4))^{\frac{1}{2}}+d_id_i(+4)(f-K(K-1))^{\frac{1}{2}}(f-K(K+1))^{\frac{1}{2}}$$
$$\times(f-(K+1)(K+2))^{\frac{1}{2}}(f-(K+2)(K+3))^{\frac{1}{2}}+e_ie_i(+4)(f-(K-1)(K-2))^{\frac{1}{2}}(f-K(K-1))^{\frac{1}{2}}$$
$$\times(f-K(K+1))^{\frac{1}{2}}(f-(K+1)(K+2))^{\frac{1}{2}}](R_4/2)+[a_ib_i(+4)(f-(K+2)(K+3))^{\frac{1}{2}}(f-(K+3)$$
$$\times(K+4))^{\frac{1}{2}}(f-(K+4)(K+5))^{\frac{1}{2}}+(3b_ic_i(+4)/6^{\frac{1}{2}})(f-(K+1)(K+2))^{\frac{1}{2}}(f-(K-2)(K+3))^{\frac{1}{2}}$$
$$\times(f-(K+3)(K+4))^{\frac{1}{2}}+(3c_id_i(+4)/6^{\frac{1}{2}})(f-K(K+1))^{\frac{1}{2}}(f-(K+1)(K+2))^{\frac{1}{2}}(f-(K+2)(K+3))^{\frac{1}{2}}$$
$$+d_ie_i(+4)(f-K(K-1))^{\frac{1}{2}}(f-K(K+1))^{\frac{1}{2}}(f-(K+1)(K+2))^{\frac{1}{2}}]R_{11}\},\quad(18)$$

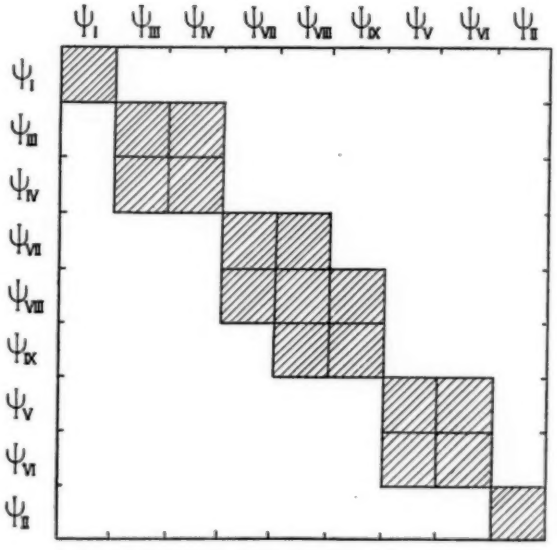

FIG. 1. Matrix of H_1 for the state $\nu_3+\nu_4$.

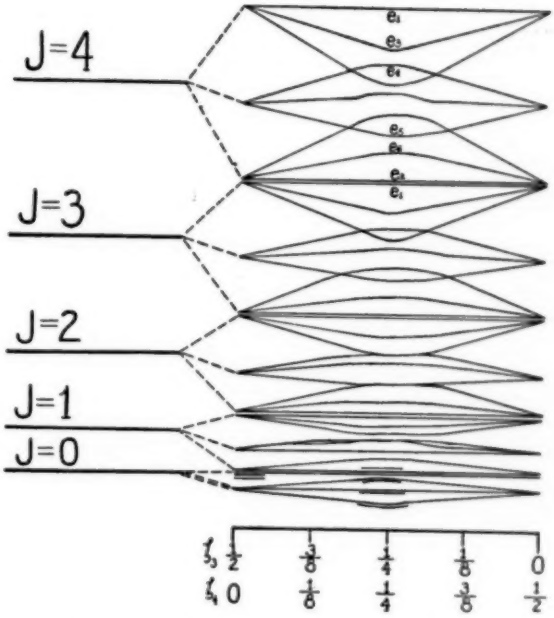

FIG. 2. Coriolis levels for state $\nu_3+\nu_4$ of XY_4.

where $R_{14}(2\nu_3)=-3R_4(2\nu_3)/4+R_{10}(2\nu_3)/2$.

Since the state $2\nu_4$ is entirely similar to the state $2\nu_3$ the above discussion is directly applicable to it. The elements of the matrix $H^{(2)\prime}$ for that state may be obtained from (16), (17) and (18) simply by interchanging ζ_3 and ζ_4 and, as well, those other quantities (discussed in Part I) which there must be interchanged to obtain the matrix elements of $V_1\nu_1+\nu_4$ from those of $V_1\nu_1+\nu_3$.

B. The state $\nu_3+\nu_4$

In the state $\nu_3+\nu_4$ the vibration quantum numbers take the following values: $V_3=V_4=1$, $V_1=V_2=0$ so that the zeroth-order energy becomes:

$$E^{(0)}{}_{\nu_3+\nu_4}=(h/2)(\nu_1+2\nu_2+5\nu_3+5\nu_4)+J(J+1)(\hbar^2/2A_0). \tag{19}$$

From (2), it follows that $J_3=J_4=1$ and from (3) that J_2 may be (a) $J_2=2$, (b) $J_2=1$ and (c) $J_2=0$. The corresponding values of J_1 are (a) $J_1=J\pm2$, $J\pm1$, J (b) $J_1=J\pm1$, J and (c) $J_1=J$. With the aid of (7),(8), (9) and (10) it is possible to set up the matrix of $H^{(1)\prime}$ for the state $\nu_3+\nu_4$. It will be a step matrix and will have the appearance of the Fig. 1. In the figure the symbols I, II, etc., represent the

following combinations of quantum numbers: I: $J_1=J+2$, $J_2=2$; II: $J_1=J-2$, $J_2=2$; III:

$J_1=J+1$, $J_2=2$; IV: $J_1=J+1$, $J_2=1$; V: $J_1=J-1$, $J_2=2$; VI: $J_1=J-1$, $J_2=1$; VII: $J_1=J$, $J_2=2$; VIII: $J_1=$J, $J_2=1$; IX: $J_1=J$, $J_2=0$. Solution of the secular determinant of Fig. 1 yields for the state $\nu_3+\nu_4$ the following nine Coriolis components into which the zeroth-order levels (19) are split by $H^{(1)\prime}$. Denoting these by $E_i^{(1)}$ which is set equal to $(e_i\hbar^2/A_0)$ we have:[3]

$$\begin{aligned}
&J_1=J+2: \quad e_1=J(\zeta_3+\zeta_4); \quad J_1=J-2: e_2=-(J+1)(\zeta_3+\zeta_4);\\
&J_1=J+1: e_{3,4}=\tfrac{1}{2}\{(J-1)(\zeta_3+\zeta_4)\pm[(J+1)^2(\zeta_3-\zeta_4)^2+4\zeta_3\zeta_4]^{\frac{1}{2}}\};\\
&J_1=J-1: e_{5,6}=-\tfrac{1}{2}\{(J+2)(\zeta_3+\zeta_4)\mp[J^2(\zeta_3-\zeta_4)^2+4\zeta_3\zeta_4]^{\frac{1}{2}}\}.
\end{aligned} \tag{20}$$

$J_1=J$: $e_{7,8,9}$ are the roots of the cubic equation:

$$e^3+2(\zeta_3+\zeta_4)e^2+[(3/4)(\zeta_3+\zeta_4)^2-(1/4)(4J^2+4J-1)(\zeta_3-\zeta_4)^2]e-J(J+1)(\zeta_3+\zeta_4)(\zeta_3-\zeta_4)^2=0.$$

[3] An independent method not based on the vector addition of angular momenta has been used to check the above results.

The manner in which the Coriolis levels depend on the values of ζ_3 and ζ_4 ($\zeta_3+\zeta_4=\frac{1}{2}$) is illustrated in Fig. 2 where the parent rotational levels are indicated by $J=0$, 1, 2, etc. In the diagram the Coriolis levels e_1 of J and e_2 of $J+1$ are shown separated in order simply to clarify the illustration. It is interesting to note that the nine Coriolis levels associated with a given value of J become three levels for the case $\zeta_3=0$, $\zeta_4=\frac{1}{2}$, each of which is threefold degenerate. Under these conditions the Coriolis pattern is entirely like that for the state ν_4 where $\zeta_4=\frac{1}{2}$, a result which is quite natural since setting $\zeta_3=0$ corresponds effectively to reducing the internal angular momentum associated with ν_3 to zero. The values ζ_3 and ζ_4 for methane have been determined by Johnston and Dennison[4] to be equal to 0.0345 and 0.4655, respectively. This indicates that the first-order Coriolis levels of $\nu_3+\nu_4$ should in that case fall into three sets of three nearly coincident levels.

The basic wave functions Ψ_{I}, Ψ_{II}, $\cdots$, Ψ_{IX} used in setting up the matrix $H^{(1)\prime}$ in the form of Fig. 1 fall into three sets corresponding to $J_2=2$, $J_2=1$ and $J_2=0$. They are linear combinations of the following preliminary functions

$$\begin{aligned}
&\chi_0=-3^{-\frac{1}{2}}\{F(\nu_3)H(\nu_4)+G(\nu_3)G(\nu_4)+H(\nu_3)H(\nu_4)\}R(JKM);\\
&\chi_1=F(\nu_3)F(\nu_4)R(JK+2M);\quad \chi_2=2^{-\frac{1}{2}}\{F(\nu_3)G(\nu_4)+G(\nu_3)F(\nu_4)\}R(JK+1M);\\
&\chi_3=-6^{-\frac{1}{2}}\{F(\nu_3)H(\nu_4)-2G(\nu_3)G(\nu_4)+H(\nu_3)F(\nu_4)\}R(JKM);\\
&\chi_4=-2^{-\frac{1}{2}}\{H(\nu_3)G(\nu_4)+G(\nu_3)H(\nu_4)\}R(JK-1M);\quad \chi_5=H(\nu_3)H(\nu_4)R(JK-2M);\\
&\chi_6=2^{-\frac{1}{2}}\{F(\nu_3)G(\nu_4)-G(\nu_3)F(\nu_4)\}R(JK+1M);\quad \chi_7=2^{-\frac{1}{2}}\{H(\nu_3)F(\nu_4)-F(\nu_3)H_4)\}R(JKM);\\
&\chi_8=2^{-\frac{1}{2}}\{H(\nu_3)G(\nu_4)-G(\nu_3)H(\nu_4)\}R(JK-1M),
\end{aligned}\tag{21}$$

where $F(\nu_3)$, $G(\nu_3)$ and $H(\nu_3)$ are the basic wave functions for ν_3 defined in Part I and where $F(\nu_4)$, $G(\nu_4)$ and $H(\nu_4)$ are the corresponding functions for the state ν_4. It is not difficult to show that the required combinations are the following ones:

$$\|\Psi\|_{(J_2=2)}=\|A\|\cdot\|\chi\|_{(J_2=2)},\tag{22a}$$

where $\|\Psi\|_{(J_2=2)}=\|\Psi_{\mathrm{I}}\Psi_{\mathrm{II}}\Psi_{\mathrm{III}}\Psi_{\mathrm{IV}}\Psi_{\mathrm{V}}\|$, $\|\chi\|_{(J_2=2)}=\|\chi_5\chi_4\chi_3\chi_2\chi_1\|$ and A is identically the same transformation matrix which occurs in (14);

$$\left\|\begin{matrix}\Psi_{\mathrm{VI}}\\ \Psi_{\mathrm{VII}}\\ \Psi_{\mathrm{VIII}}\end{matrix}\right\|_{(J_2=1)}=\left\|\begin{matrix}\gamma_1 & \beta_1 & \alpha_1\\ \gamma_2 & \beta_2 & \alpha_2\\ \gamma_3 & \beta_3 & \alpha_3\end{matrix}\right\|\cdot\left\|\begin{matrix}\chi_8\\ \chi_7\\ \chi_6\end{matrix}\right\|=\|B\|\cdot\|\chi\|_{(J_2=1)},\tag{22b}$$

in which the matrix B is identical with the one in Table 2[3] of reference 2 when j_1 and m have been replaced, respectively, by J and K; and

$$\Psi_{\mathrm{IX}}=\chi_0.\tag{22c}$$

The actual eigenfunctions of $H^{(1)\prime}$ corresponding to the eigenvalues $E_i^{(1)}$ of (20) will once more be linear combinations of the functions $\Psi(J_2=2)$, $\Psi(J_2=1)$, and $\Psi(J_2=0)$ and may be written:

$$\Psi(E_i^{(1)})=A_i\Psi(J_2=2)+B_i\Psi(J_2=1)+C_i\Psi(J_2=0),\tag{23}$$

where the A_i, B_i and C_i are the normalized first minors of the secular determinant of the matrix in Fig. 1. These may readily be obtained for special values of ζ_3 and ζ_4.

Using the wave functions (23), the selection rules governing the transitions between the normal vibration state and the Coriolis component levels $E_i^{(1)}$ of the state $\nu_3+\nu_4$ have been determined in the same manner as for the state $2\nu_3$ and are found to be the following:

$$\Delta J=0,\ -1 \text{ to } E_1^{(1)};\quad \Delta J=0,\ +1 \text{ to } E_2^{(1)};\quad \Delta J=0,\ \pm1 \text{ to } E_s^{(1)} \quad \text{where } s=3,\ 4,\ \cdots 9.$$

As before the selection rules for K and M are $\Delta K=0$, $\Delta M=0,\ \pm1$. It is found in evaluating the nonvanishing elements of the electric moment, that only that part of the wave function (23) will contribute which depends upon $J_2=2$. These elements are again proportional to the quantities

[4] M. Johnston and D. M. Dennison, Phys. Rev. **48**, 868 (1935).

$B(J'K', JK)$ obtained in connection with $2\nu_3$, the proportionality constants being the squares of the A_i which occur as coefficients of $\Psi(J_2=2)$ in (23). For the limiting cases $\zeta_3=0$, $\zeta_4=\frac{1}{2}$ (and $\zeta_3=\frac{1}{2}$, $\zeta_4=0$) it has again been verified that the principle of spectroscopic stability is obeyed.

The matrix of $H^{(2)'}$ may now be set up using as the stabilized wave functions, the functions $\Psi(E_i^{(1)})$ of (23). There are no matrix elements of $H^{(2)'}$ which involve different values of J_2, i.e., all such integrals as $\int \bar{\Psi}(J_2=2)H^{(2)'}\Psi(J_2=1)dv$, etc., vanish, The $(K|K')$ matrix elements of $H^{(2)'}$ thus take the form

$$(K|H^{(2)'}|K')=A_iA_i'(K|H^{(2)'}|K')_{J_2=2}+B_iB_i'(K|H^{(2)'}|K')_{J_2=1}+C_iC_i'(K|H^{(2)'}|K')_{J_2=0},$$

where $(K|H^{(2)'}|K')_{J_2}=\int\bar{\Psi}(J_2JKM)H^{(2)'}\Psi(J_2JK'M)dv$, J_2 taking the values 2, 1, 0. The elements $(K|H^{(2)'}|K')_{J_2}$ are given below:

$$\begin{aligned}(K|H^{(2)'}|K)_{J_2=2}=(\hbar^2/2A_0)\{&R_0+R_1f+R_2f^2+(b_i^2-c_i^2+d_i^2)R_3+(a_i^2+e_i^2)fR_4+(1/4)(b_i^2+d_i^2)fR_4\\
&-(3/2)[a_i^2(K+2)^2+e_i^2(K-2)^2]R_4+3c_i^2K^2R_4/2+(3/4)[b_i^2(K+1)^2+d_i^2(K-1)^2]R_4\\
&-[6^{-\frac{1}{2}}a_ic_i(f-(K+1)(K+2))^{\frac{1}{2}}(f-K(K+1))^{\frac{1}{2}}+\tfrac{1}{2}b_id_i(f-K(K+1))^{\frac{1}{2}}(f-K(K-1))^{\frac{1}{2}}\\
&+6^{-\frac{1}{2}}c_ie_i(f-K(K-1))^{\frac{1}{2}}(f-(K-1)(K-2))^{\frac{1}{2}}](R_5+3R_4/2)+[a_ib_i(2K+3)(f-(K+1)(K+2))^{\frac{1}{2}}\\
&+6^{-\frac{1}{2}}b_ic_i(2K+1)(f-K(K+1))^{\frac{1}{2}}-6^{-\frac{1}{2}}c_id_i(2K-1)(f-K(K-1))^{\frac{1}{2}}-d_ie_i(2K-3)(f-(K-1)\\
&\times(K-2))^{\frac{1}{2}}]R_5+[a_ib_i(2f-6K^2-18K-15)(f-(K+1)(K+2))^{\frac{1}{2}}+(3b_ic_i/6^{\frac{1}{2}})(2f-6K^2-6K-3)\\
&\times(f-K(K+1))^{\frac{1}{2}}+(3c_id_i/6^{\frac{1}{2}})(2f-6K^2+6K-3)(f-K(K-1))^{\frac{1}{2}}+d_ie_i(2f-6K^2+18K-15)\\
&\times(f-(K-1)(K-2))^{\frac{1}{2}}]R_6+[a_i^2(8(K+2)^3+(K+2)-4f(K+2))+(b_i^2/2)(8(K+1)^3+(K+1)\\
&-4f(K+1))-(d_i^2/2)(8(K-1)^3+(K-1)-4f(K-1))-e_i^2(8(K-2)^3+(K-2)-4f(K-2))]\\
&\times(-R_6/2)+[a_i^2(6f(K+2)^2-5(K+2)^2-7(K+2)^4)+b_i^2(6f(K+1)^2-5(K+1)^2-7(K+1)^4)\\
&+c_i^2(6fK^2-5K^2-7K^4)+d_i^2(6f(K-1)^2-5(K-1)^2-7(K-1)^4)+e_i^2(6f(K-2)^2-5(K-2)^2\\
&-7(K-2)^4]R_7.\end{aligned}\tag{24}$$

where

$$\begin{aligned}R_0(\nu_3+\nu_4)=(A_0/2)\{&21(d_1+d_5)+9d_3+7(d_6+d_{10})+16d_{11}+5(d_{18}+d_{21}+d_{27})+10(d_{22}+d_{28})\\
&+3(d_{30}+d_{31}+3d_{33})-(5/2)(d_{23}+d_{29})\}+2(\zeta_3-\zeta_4)^2+6\zeta_3\zeta_4+4[(\omega_4/\omega_3)+(\omega_3/\omega_4)]\zeta_{34}^2\\
&+(45/16)[(\omega_2/\omega_3)+(\omega_3/\omega_2)]\zeta_{23}^2+(45/16)[(\omega_2/\omega_4)+(\omega_4/\omega_2)]\zeta_{24}^2-(9/4)-2\zeta_{34}^2-(A_0/4)\\
&\times\{(5/3)(c_1^2/\omega_3+c_4^2/\omega_4)+(4\omega_3+7\omega_4)c_2^2/\omega_4(2\omega_3+\omega_4)+(4\omega_4+7\omega_3)c_3^2/\omega_3(2\omega_4+\omega_3)\\
&+6\omega_3c_2^2/(4\omega_3^2-\omega_4^2)+6\omega_4c_3^2/(4\omega_4^2-\omega_3^2)+5(10\omega_3+7\omega_1)c_5^2/\omega_1(2\omega_3+\omega_1)\\
&+5(10\omega_4+7\omega_1)c_7^2/\omega_1(2\omega_4+\omega_1)+50c_5c_7/\omega_1+15(c_5+c_7)(c_{11}/\omega_1+c_{12}/\omega_1)\\
&+(c_6^2/(\omega_1^4+\omega_3^4+\omega_4^4-2\omega_1^2\omega_3^2-2\omega_1^2\omega_4^2-2\omega_3^2\omega_4^2))[6\omega_1\omega_3\omega_4+5\omega_3(\omega_3^2-\omega_4^2-\omega_1^2)\\
&+5\omega_4(\omega_4^2-\omega_3^2-\omega_1^2)+9\omega_1(\omega_1^2-\omega_3^2-\omega_4^2)]+2(4\omega_3+7\omega_2)c_8^2/\omega_2(2\omega_3+\omega_2)+2c_8c_{10}/\omega_2\\
&+2(4\omega_4+7\omega_2)c_{10}^2/\omega_2(2\omega_4+\omega_2)+11c_{11}^2/\omega_1+18c_{11}c_{12}/\omega_1+36(\omega_1+\omega_2)c_{12}^2/\omega_1(2\omega_2+\omega_1)\\
&+5c_{13}^2/16\omega_2+(c_9^2/(\omega_2^4+\omega_3^4+\omega_4^4-2\omega_2^2\omega_3^2-2\omega_2^2\omega_4^2-2\omega_3^2\omega_4^2))[5\omega_3(\omega_3^2-\omega_4^2-\omega_2^2)\\
&+5\omega_4(\omega_4^2-\omega_3^2-\omega_2^2)+9\omega_2(\omega_2^2-\omega_3^2-\omega_4^2)+6\omega_2\omega_3\omega_4]\},\\
R_1(\nu_3+\nu_4)=(\hbar/2A_0)\{&(9/4)(\zeta_{23}^2/\omega_3+\zeta_{24}^2/\omega_4)+1/\omega_2+2/\omega_1-(a_1+a_2)/2\omega_2\\
&+11\zeta_{34}^2(\omega_3-\omega_4)^2/3\omega_3\omega_4(\omega_3+\omega_4)+(\zeta_{23}^2/3\omega_2\omega_3)(4\omega_2^3-9\omega_2^2\omega_3+12\omega_2\omega_3^2-3\omega_3^3)/(\omega_2^2-\omega_3^2)\\
&+(\zeta_{24}^2/3\omega_2\omega_4)(4\omega_2^3+12\omega_2\omega_4^2-9\omega_2^2\omega_4-3\omega_4^3)/(\omega_2^2-\omega_4^2)+(\hbar/A_0\omega_2^2)\\
&+(2A_0/3\omega_1^3)^{\frac{1}{2}}(5c_5+5c_7+3c_{11}+3c_{12})\},\\
R_2(\nu_3+\nu_4)=&-(\hbar^2/6A_0^2)[8/\omega_1^2+5/2\omega_2^2+(3/4)(\zeta_{23}^2/\omega_3^2+\zeta_{24}^2/\omega_4^2)],\\
R_3(\nu_3+\nu_4)=&(A_0/2)(d_8-2d_3+2d_{11})+(A_0/4)[-2c_1c_3/\omega_3-2c_2c_4/\omega_4-4\omega_3c_2^2/(4\omega_3^2-\omega_4^2)\\
&-4\omega_4c_3^2/(4\omega_4^2-\omega_3^2)+4c_6^2\omega_1\omega_3\omega_4/(\omega_1^4+\omega_3^4+\omega_4^4-2\omega_1^2\omega_3^2-2\omega_1^2\omega_4^2-2\omega_3^2\omega_4^2)\\
&+6c_8c_{10}/\omega_2+3\omega_2(\omega_2^2-\omega_3^2-\omega_4^2)c_9^2/(\omega_2^4+\omega_3^4+\omega_4^4-2\omega_2^2\omega_3^2-2\omega_2^2\omega_4^2-2\omega_3^2\omega_4^2)],\\
R_4(\nu_3+\nu_4)=(\hbar/2A_0)\{&\tfrac{1}{2}(\zeta_{23}^2/\omega_3+\zeta_{24}^2/\omega_4)+(a_1+a_2)/\omega_2+2\zeta_{34}^2(\omega_3-\omega_4)^2/3\omega_3\omega_4(\omega_3+\omega_4)\\
&+2\zeta_{23}^2(\omega_2^2+3\omega_3^2)/3\omega_3(\omega_2^2-\omega_3^2)+2\zeta_{24}^2(\omega_2^2+3\omega_4^2)/3\omega_4(\omega_2^2-\omega_4^2)\},\\
R_5(\nu_3+\nu_4)=(\hbar/2A_0)\{&(3/4)(\zeta_{23}^2/\omega_3+\zeta_{24}^2/\omega_4)+(c_1+c_3)(\zeta_{23}/\omega_3)(A_0/\omega_3)^{\frac{1}{2}}-(c_2+c_4)(\zeta_{24}/\omega_4)(A_0/\omega_4)^{\frac{1}{2}}\\
&-\zeta_{34}^2(\omega_3-\omega_4)^2/\omega_3\omega_4(\omega_3+\omega_4)\},\\
R_6(\nu_3+\nu_4)=&(\hbar^2/2A_0)(\zeta_{23}^2/\omega_3^2+\zeta_{24}^2/\omega_4^2),\\
R_7(\nu_3+\nu_4)=&(\hbar^2/4A_0^2)[1/\omega_2^2-\tfrac{1}{2}(\zeta_{23}^2/\omega_3^2+\zeta_{24}^2/\omega_4^2)].\end{aligned}$$

In the above $a_1=-c_8(A_0/3\omega_2)^{\frac{1}{2}}$ and $a_2=-c_{10}(A_0/3\omega_2)^{\frac{1}{2}}$.

$$(K|H^{(2)\prime}|K+2)_{J_2=2}=(K+2|H^{(2)\prime}|K)_{J_2=2}=(\hbar^2/2A_0)\{-a_ia_i(+2)(f-(K+2)(K+3))^{\frac{1}{2}}\times(f-(K+3)(K+4))^{\frac{1}{2}}+\tfrac{1}{2}b_ib_i(+2)(f-(K+1)(K+2))^{\frac{1}{2}}(f-(K+2)(K+3))^{\frac{1}{2}}+c_ic_i(f-K(K+1))^{\frac{1}{2}}(f-(K+1)(K+2))^{\frac{1}{2}}+\tfrac{1}{2}d_id_i(+2)(f-K(K-1))^{\frac{1}{2}}(f-K(K+1))^{\frac{1}{2}}-e_ie_i(+2)(f-(K-1)(K-2))^{\frac{1}{2}}(f-K(K-1))^{\frac{1}{2}}-(2/6^{\frac{1}{2}})a_ic_i(+2)(f-3(K+2)^2)-b_id_i(+2)(f-3(K+1)^2)-(2/6^{\frac{1}{2}})c_ie_i(+2)(f-3(K-2)^2)\}R_8, \quad (25)$$

where: $R_8(\nu_3+\nu_4)=(1/4)R_6$.

$$(K|H^{(2)\prime}|K+4)_{J_2=2}=(K+4|H^{(2)\prime}|K)_{J_2=2}=(\hbar^2/2A_0)\{[6^{-\frac{1}{2}}a_ic_i(+4)(f-(K+2)(K+3))^{\frac{1}{2}}\times(f-(K+3)(K+4))^{\frac{1}{2}}+6^{-\frac{1}{2}}c_ie_i(+4)(f-K(K+1))^{\frac{1}{2}}(f-(K+1)(K+2))^{\frac{1}{2}}+\tfrac{1}{2}b_id_i(+4)\times(f-(K+1)(K+2))^{\frac{1}{2}}(f-(K+2)(K+3))^{\frac{1}{2}}](-3R_4/4+\tfrac{1}{2}R_5)+[a_ia_i(+4)(f-(K+2)(K+3))^{\frac{1}{2}}\times(f-(K+3)(K+4))^{\frac{1}{2}}(f-(K+4)(K+5))^{\frac{1}{2}}+b_ib_i(+4)(f-(K+1)\times(K+2))^{\frac{1}{2}}(f-(K+2)(K+3))^{\frac{1}{2}}(f-(K+3)(K+4))^{\frac{1}{2}}(f-(K+4)(K+5))^{\frac{1}{2}}+c_ic_i(+4)\times(f-K(K+1))^{\frac{1}{2}}(f-(K+1)(K+2))^{\frac{1}{2}}(f-(K+2)(K+3))^{\frac{1}{2}}(f-(K+3)(K+4))^{\frac{1}{2}}+d_id_i(+4)(f-K(K-1))^{\frac{1}{2}}(f-K(K+1))^{\frac{1}{2}}(f-(K+1)(K+2))^{\frac{1}{2}}(f-(K+2)(K+3))^{\frac{1}{2}}+e_ie_i(+4)(f-(K-1)(K-2))^{\frac{1}{2}}(f-K(K-1))^{\frac{1}{2}}(f-K(K+1))^{\frac{1}{2}}(f-(K+1)(K-2))^{\frac{1}{2}}](R_7/2)\times[a_ib_i(+4)(f-(K+2)(K+3))^{\frac{1}{2}}(f-(K+3)(K+4))^{\frac{1}{2}}(f-(K+4)(K+5))^{\frac{1}{2}}+(3/6^{\frac{1}{2}})b_ic_i(+4)(f-(K+1)(K+2))^{\frac{1}{2}}(f-(K+2)(K+3))^{\frac{1}{2}}(f-(K+3)(K+4))^{\frac{1}{2}}+(3/6^{\frac{1}{2}})c_id_i(+4)(f-K(K+1))^{\frac{1}{2}}(f-(K+1)(K+2))^{\frac{1}{2}}(f-(K+2)(K+3))^{\frac{1}{2}}+d_ie_i(+4)(f-K(K-1))^{\frac{1}{2}}(f-K(K+1))^{\frac{1}{2}}(f-(K+1)(K+2))^{\frac{1}{2}}](R_6/2)\}, \quad (26)$$

$$(K|H^{(2)\prime}|K)_{J_2=1}=(\hbar^2/2A_0)\{R_0'+fR_1'+f^2R_2'+[(\alpha_i^2+\gamma_i^2)f-\alpha_i^2(K+1)^2+2\beta_i^2K^2-\gamma_i^2(K-1)^2]R_3'-\alpha_i\gamma_i(f-K(K-1))^{\frac{1}{2}}(f-K(K+1))^{\frac{1}{2}}(R_3'+R_4'/2)+2^{-\frac{1}{2}}\beta_i[\alpha_i(f-K(K+1))^{\frac{1}{2}}\times(2K+1)-\gamma_i(f-K(K-1))^{\frac{1}{2}}(2K-1)]R_4'+[\alpha_i^2(6f(K+1)^2-5(K+1)^2-7(K+1)^4)+\beta_i^2(6fK^2-5K^2-7K^4)+\gamma_i^2(6f(K-1)^2-5(K-1)^2-7(K-1)^4)R_5'+2^{\frac{1}{2}}\beta_i[\alpha_i(2f-6K^2-6K-3)(f-K(K+1))^{\frac{1}{2}}+\gamma_i(2f-6K^2+6K-3)(f-K(K-1))^{\frac{1}{2}}]R_6'+[-\alpha_i^2(8(K+1)^3+(K+1)-4f(K+1))+\gamma_i^2(8(K-1)^3+(K-1)-4f(K-1))]R_6', \quad (27)$$

where

$$R_0'(\nu_3+\nu_4)=(A_0/2)\{21(d_1+d_5)+7(d_3+d_6+d_{10})-d_8+18d_{11}+10(d_{18}+d_{20}+d_{21}+d_{27})+20(d_{22}+d_{28})-(5/2)(d_{23}+d_{29})+3(d_{30}+d_{31}+3d_{33})\}-(9/4)+2(\zeta_3-\zeta_4)^2+5[(\omega_3/\omega_4)+(\omega_4/\omega_3)]\zeta_{34}^2+(5/2)[(\omega_2/\omega_3)+(\omega_3/\omega_2)]\zeta_{23}^2+(5/2)[(\omega_2/\omega_4)+(\omega_4/\omega_2)]\zeta_{24}^2-4\zeta_{34}^2+(A_0/4)\{(-5/3)(c_1^2/\omega_3+c_4^2/\omega_4)+2c_1c_3/\omega_3+2c_2c_4/\omega_4-(4\omega_3+7\omega_4)c_2^2/\omega_4(\omega_4+2\omega_3)-(4\omega_4+7\omega_3)c_3^2/\omega_3(\omega_3+2\omega_4)-6\omega_3c_2^2/(4\omega_3^2-\omega_4^2)-6\omega_4c_3^2/(4\omega_4^2-\omega_3^2)-5(10\omega_3+7\omega_1)c_5^2/\omega_1(\omega_1+2\omega_3)-5(10\omega_4+7\omega_1)c_7^2/\omega_1(2\omega_4+\omega_1)-50c_5c_7/\omega_1-30c_5(c_{11}+c_{12})/\omega_1-30c_7(c_{11}+c_{12})/\omega_1+4c_8c_{10}/\omega_2-18c_{11}c_{12}/\omega_1-2(4\omega_3+7\omega_2)c_8^2/\omega_2(2\omega_3+\omega_2)-5c_6^2[\omega_3(\omega_3^2-\omega_4^2-\omega_1^2)+\omega_4(\omega_4^2-\omega_3^2-\omega_1^2)+\omega_1(\omega_1^2-\omega_3^2-\omega_4^2)+2\omega_1\omega_3\omega_4]/(\omega_1^4+\omega_3^4+\omega_4^4-2\omega_1^2\omega_3^2-2\omega_1^2\omega_4^2-2\omega_3^2\omega_4^2)-c_9^2[5\omega_3(\omega_3^2-\omega_4^2-\omega_2^2)+5\omega_4(\omega_4^2-\omega_3^2-\omega_2^2)+8\omega_2(\omega_2^2-\omega_3^2-\omega_4^2)+\omega_2\omega_3\omega_4]/(\omega_2^4+\omega_3^4+\omega_4^4-2\omega_2^2\omega_3^2-2\omega_2^2\omega_4^2-2\omega_3^2\omega_4^2)-2c_{10}^2(4\omega_4+7\omega_2)/\omega_2(2\omega_4+\omega_2)-11c_{11}^2/\omega_1-36(\omega_1+\omega_2)c_{12}^2/\omega_1(\omega_1+2\omega_2)-(5/16)(c_{13}^2/\omega_2)\},$$

$$R_1'(\nu_3+\nu_4)=(\hbar/2A_0)\{(11/4)(\zeta_{23}^2/\omega_3+\zeta_{24}^2/\omega_4)+1/\omega_2+2/\omega_1+(a_1+a_2)/2\omega_2+(\hbar/A_0\omega_2^2)+3(\omega_3-\omega_4)^2\zeta_{34}^2/\omega_3\omega_4(\omega_3+\omega_4)+[(2\omega_2^3+6\omega_2\omega_3^2-3\omega_2^2\omega_3-\omega_3^3)\zeta_{23}^2/\omega_2\omega_3(\omega_2^2-\omega_3^2)]+(8A_0/3\omega_1^3)^{\frac{1}{2}}(5c_5+5c_7+3c_{11}+3c_{12})+[(2\omega_2^3+6\omega_2\omega_4^2-3\omega_2^2\omega_4-\omega_4^3)\zeta_{24}^2/\omega_2\omega_4(\omega_2^2-\omega_4^2)]\},$$

$$R_2'(\nu_3+\nu_4)=R_2(\nu_3+\nu_4),$$

$$R_3'(\nu_3+\nu_4)=(-\hbar/2A_0)\{(3/8)(\zeta_{23}^2/\omega_3+\zeta_{24}^2/\omega_4)+(3/4\omega_2)(a_1+a_2)-\tfrac{1}{2}(\omega_3-\omega_4)^2\zeta_{34}^2/\omega_3\omega_4(\omega_3+\omega_4)+(\omega_2^2+3\omega_3^2)\zeta_{23}^2/2\omega_3(\omega_2^2-\omega_3^2)+\tfrac{1}{2}(\omega_2^2+3\omega_4^2)\zeta_{24}^2/\omega_4(\omega_2^2-\omega_4^2)\},$$

$$R_4'(\nu_3+\nu_4)=(-\hbar/2A_0)\{(3/4)(\zeta_{23}^2/\omega_3+\zeta_{24}^2/\omega_4)+(c_1+c_3)(\zeta_{23}/\omega_3)(A_0/\omega_3)^{\frac{1}{2}}-(c_2+c_4)(\zeta_{24}/\omega_4)(A_0/\omega_4)^{\frac{1}{2}}-(\omega_3-\omega_4)^2\zeta_{34}^2/\omega_3\omega_4(\omega_3+\omega_4)\},$$

$$R_5'(\nu_3+\nu_4)=(\hbar^2/4A_0^2)[1/\omega_2^2-\tfrac{1}{2}(\zeta_{23}^2/\omega_3^2+\zeta_{24}^2/\omega_4^2)], \quad R_6'(\nu_3+\nu_4)=R_6(\nu_3+\nu_4)/4;$$

$$(K|H^{(2)\prime}|K+2)_{J_2=1}=(K+2|H^{(2)\prime}|K)_{J_2=1}=(\hbar^2/2A_0)\{\alpha_i\gamma_i(+2)(2f-6(K+1)^2)+\alpha_i\alpha_i(+2)\times(f-(K+1)(K+2))^{\frac{1}{2}}(f-(K+2)(K+3))^{\frac{1}{2}}-2\beta_i\beta_i(+2)(f-K(K+1))^{\frac{1}{2}}(f-(K+1)(K+2))^{\frac{1}{2}}+\gamma_i\gamma_i(+2)(f-K(K-1))^{\frac{1}{2}}(f-K(K+1))^{\frac{1}{2}}\}R_7', \quad (28)$$

where $R_7(\nu_3+\nu_4)=(\hbar/16A_0)(\zeta_{23}^2/\omega_3+\zeta_{24}^2/\omega_4)$.

$$(K|H^{(2)'}|K+4)_{J_2=1}=(K+4|H^{(2)'}|K)_{J_2=1}=(\hbar^2/2A_0)\{(f-(K+1)(K+2))^{\frac{1}{2}}(f-(K+2)(K+3))^{\frac{1}{2}}\}$$
$$\times\{\alpha_i\gamma_i(+4)(-\tfrac{1}{2}R_3'+R_4'/4)+2^{\frac{1}{2}}[\alpha_i\beta_i(+4)(f-(K+3)(K+4))^{\frac{1}{2}}+\beta_i\gamma_i(+4)$$
$$\times(f-K(K+1))^{\frac{1}{2}}]R_6'-[\alpha_i\alpha_i(+4)(f-(K+3)(K+4))^{\frac{1}{2}}(f-(K+4)(K+5))^{\frac{1}{2}}+\beta_i\beta_i(+4)$$
$$\times(f-K(K+1))^{\frac{1}{2}}(f-(K+3)(K+4))^{\frac{1}{2}}+\gamma_i\gamma_i(+4)(f-K(K+1))^{\frac{1}{2}}(f-K(K-1))^{\frac{1}{2}}](R_5'/2)\}, \quad (29)$$

$$(K|H^{(2)'}|K)_{J_2=0}=(\hbar^2/2A_0)\{R_0''+fR_1''+f^2R_2''+(6fK^2-5K^2-7K^4)R_3''\}, \quad (30)$$

where:

$$R_0''(\nu_3+\nu_4)=(A_0/2)\{21(d_1+d_5)+7(d_6+d_{10})+11d_3+2d_8+14d_{11}+5(d_{18}+d_{20}+d_{21}+d_{27})$$
$$+10(d_{22}+d_{28})-(5/2)(d_{23}+d_{29})+3(d_{30}+d_{31}+3d_{33})\}-9/4+2(\zeta_3-\zeta_4)^2-\zeta_{34}^2$$
$$+(5/2)[(\omega_3/\omega_4)+(\omega_4/\omega_3)]\zeta_{34}^2(5/4)[(\omega_2/\omega_3)+(\omega_3/\omega_2)]\zeta_{23}^2+(5/4)[(\omega_2/\omega_4)$$
$$+(\omega_4/\omega_2)]\zeta_{24}^2\}-(A_0/4)\{(5/3)(c_1^2/\omega_3+c_4^2/\omega_4)+c_1c_3/3\omega_3+c_2c_4/3\omega_4$$
$$+(4\omega_3+7\omega_4)c_2^2/\omega_4(2\omega_3+\omega_4)+(4\omega_4+7\omega_3)c_3^2/\omega_3(2\omega_4+\omega_3)+5(10\omega_3+7\omega_1)c_5^2/(2\omega_3+\omega_1)\omega_1$$
$$+5(10\omega_4+7\omega_1)c_7^2/\omega_1(2\omega_4+\omega_1)+50c_5c_7/\omega_130(c_{11}+c_{12})(c_5+c_7)/\omega_1+5c_6^2[2\omega_1\omega_3\omega_4$$
$$+\omega_3^3(\omega_3^2-\omega_4^2-\omega_1^2)+\omega_4(\omega_4^2-\omega_3^2-\omega_1^2)+\omega_1(\omega_1^2-\omega_3^2-\omega_4^2)]/(\omega_1^4+\omega_3^4+\omega_4^4$$
$$-2\omega_1^2\omega_3^2-2\omega_1^2\omega_4^2-2\omega_3\omega_4)+c_9^2[5\omega_3(\omega_3^2-\omega_4^2-\omega_2^2)+5\omega_4(\omega_4^2-\omega_3^2-\omega_2^2)$$
$$+9\omega_2(\omega_2^2-\omega_3^2-\omega_4^2)+2\omega_2\omega_3\omega_4]/(\omega_2^4+\omega_3^4+\omega_4^4-2\omega_2^2\omega_3^2-2\omega_2^2\omega_4^2-2\omega_3^2\omega_4^2)$$
$$+2(4\omega_3+7\omega_2)c_8^2/\omega_2(2\omega_3+\omega_2)+2(4\omega_4+7\omega_2)c_{10}^2/\omega_2(2\omega_4+\omega_2)-8\omega_3c_2^2/(\omega_4^2-4\omega_3^2)$$
$$-8\omega_4c_3^2/(\omega_3^2-4\omega_4^2)+8c_8c_{10}/\omega_2+9c_{11}c_{12}/\omega_1+11c_{11}/\omega_1$$
$$+36(\omega_1+\omega_2)c_{12}^2/\omega_1(2\omega_2+\omega_1)+5c_{13}^2/16\omega_2\},$$

$$R_1''(\nu_3+\nu_4)=(\hbar/2A_0)\{(5/2)(\zeta_{23}^2/\omega_3+\zeta_{24}^2/\omega_4)+1/\omega_2+2/\omega_1+(10/3)(\omega_3-\omega_4)^2\zeta_{34}^2/\omega_3\omega_4(\omega_3+\omega_4)$$
$$+(\hbar/A_0\omega_2^2)+[(5\omega_2^3+15\omega_2\omega_3^2-9\omega_2^2\omega_3-3\omega_3^3)\zeta_{23}^2/3\omega_2\omega_3(\omega_2^2-\omega_3^2)]$$
$$+(2A_0/3\omega_1^3)^{\frac{1}{2}}(c_5+c_7+3c_{11}+3c_{12})+[(5\omega_2^3+15\omega_2\omega_4^2-9\omega_2^2\omega_4-3\omega_4^3)\zeta_{24}^2/3\omega_2\omega_4(\omega_2^2-\omega_4^2)]\},$$

$$R_2''(\nu_3+\nu_4)=R_2'(\nu_3+\nu_4); \quad R_3''(\nu_3+\nu_4)=R_5'(\nu_3+\nu_4).$$

$$(K|H^{(2)'}|K+2)_{J_2=0}=(K+2|H^{(2)'}|K)_{J_2=0}=0. \quad (31)$$

$$(K|H^{(2)'}|K+4)_{J_2=0}=(K+4|H^{(2)'}|K)_{J_2=0}=-(\hbar^2/2A_0)(f-K(K+1))^{\frac{1}{2}}$$
$$\times(f-(K+1)(K+2))^{\frac{1}{2}}(f-(K+2)(K+3))^{\frac{1}{2}}(f-(K+3)(K+4))^{\frac{1}{2}}(R_3''/2). \quad (32)$$

IV. Conclusions

The discussion which has here been given in general and applied to the overtones $2\nu_3$ and $2\nu_4$ and the combination frequency $\nu_3+\nu_4$ may readily be applied also to higher overtones and combination bands also. From the formulae in Section II the first-order Coriolis splittings may at once be evaluated. Also the wave functions are obtainable since the elements of the additional transformation matrices required to set up the basic wave functions may be calculated from the formula (5) of Section 14[3] given in reference 2. The calculation of the elements of the matrix $H^{(2)'}$, however, becomes an increasingly laborious and tedious task.

It is interesting to note that the Coriolis resonance interaction becomes of increasing importance as one goes to higher vibration states so that the fine structure of the rotation lines may be expected to become increasingly prominent in the higher harmonics and combination bands.

LETTERS TO THE EDITOR

Prompt publication of brief reports of important discoveries in physics may be secured by addressing them to this department. Closing dates for this department are, for the first issue of the month, the eighteenth of the preceding month, for the second issue, the third of the month. Because of the late closing dates for the section no proof can be shown to authors. The Board of Editors does not hold itself responsible for the opinions expressed by the correspondents.

Communications should not in general exceed 600 words in length.

On the Origin of Cosmic Radiation

In a recent letter[1] to this Journal, E. R. Sabato has criticized the "Cosmic cyclotron" process,[2] which I once suggested might account for the generation of cosmic radiation. The discrepancy between our opinions seems mainly to be due to the fact that Mr. Sabato has not decided—which is necessary—whether to treat the problem in a fixed coordinate system (as I have done) or in a system following the rotation. In the latter case he must take into account the polarization of the stars due to their axial rotation, which I have supposed to be small in a fixed system. If he does this he will no doubt arrive at the same result as I.

I think that when criticizing this old model Mr. Sabato ought to have mentioned that already two years ago I abandoned it in favor of a much more powerful (and simple) one, where the acceleration takes place mainly in the axial direction of the double star.[3] In this case the accelerated particles are hurled out directly into the surrounding space so that the objection (3)—the only correct one of Mr. Sabato's—does not apply to this case.

Since the discovery of cosmic radiation a multitude of hypotheses about its origin has been made. In general the idea is that such an unexpected and remarkable phenomenon must derive its origin from some very extraordinary processes. But before we regard the radiation as an indication of new natural laws, we ought to investigate if it is not possible to explain it in terms of the laws we know already. This is what I have tried to do, and the result is that classical electrodynamics applied to stellar motions and stellar magnetic fields can very well account for the generation of the cosmic rays. In spite of the fact that the theory has need of no assumptions more drastic than that the magnetic moments of some stars surpass that of our sun by some powers of ten, it is able to account for most of the experimental facts and is in conflict with none. It is clearly understood that it is not possible as yet to decide with certainty how the radiation is generated, but as long as there is no evidence against an explanation according to classical laws, there is little need to invent new laws, more or less arbitrary and fantastic.

HANNES ALFVÉN

Forskningsinstitutet för Fysik,
Stockholm 50, Sweden,
August 9, 1939.

[1] E. R. Sabato, Phys. Rev. **55**, 1272 (1939).
[2] E. R. Sabato, Zeits. f. Physik **105**, 319 (1937).
[3] E. R. Sabato, Zeits. f. Physik **107**, 579 (1937).

Evidence for Incorrect Assignment of the Supposed Si^{27} Radioactivity of 6.7-Minute Half-Life

It has been reported[1] that three different radioactive substances are produced by the bombardment of Mg with natural α-particles. One of these, of 2.36-min. half-life, emits negative electrons, and was interpreted as Al^{28}, produced by the reaction Mg^{25} (α, n). This assignment was subsequently proved correct when the same activity was produced from the reactions Al^{27} (d, p); Al^{27} (n, γ); Si^{28} (n, p) and P^{31} (n, α). The second period of 11-min. half-life which was originally assigned to Al^{29} is probably due to an impurity.[2] The third period (6.7 min.) was supposed to be a positron activity and was therefore assigned to Si^{27}, produced by a reaction Mg^{24} (α, n). This assignment meets with several serious difficulties in the light of more recent evidence. (See below.) We have therefore repeated the experiment with the 16-Mev α-particles furnished by the Purdue cyclotron. The result is that there is *no positron activity*, but only negative electrons. This proves that the previous assignment was incorrect and *that the 6.7-min. period is almost certainly* Al^{29}, formed by the reaction Mg^{26} (α, p).

The arguments which led us to suspect the previous assignment as incorrect are the following.

(1) Si^{27} should be produced in the reaction Al^{27} (p, n). Aluminum was bombarded with protons of more than 7 Mev in Rochester, but not a trace of the 6.7-min. activity was obtained although the energy of the protons must have been sufficient to produce the reaction.

(2) The reported positron energy (2.0 Mev) is much too low and the lifetime (6.7 min.) much too long to fall in line with the analogous nuclei which form a very regular sequence in both of these respects.[3] Extrapolating the experimental results obtained with lighter nuclei we should expect about 3.5-Mev positron energy and 4 seconds half-life for Si^{27}. Similar values are obtained from a theoretical estimate of the Coulomb energy.

(3) From the reported positron energy[4] of 2.0 Mev and the known reaction energy[5] of Mg^{24} (α, p) Al^{27}, *viz.* -1.6 Mev, it follows that Si^{27} can only be produced by α-particles of more than 6.2 Mev, whereas Ellis and Henderson report it for 5.4 Mev.

(4) Bothe and Gentner[6] failed to find the activity when irradiating Si with 17-Mev γ-rays. 14.5 Mev should have been sufficient to produce the photoelectric effect, and there is no case known in which a well-established radioactive period could not be obtained by a $\gamma - n$ reaction.

When magnesium of commercial purity is bombarded with 16-Mev α-particles both negative and positive electrons are observed. The latter show a half-life of 4.0 hours and are due to a calcium impurity. The sign of the charge was determined by magnetic resolution using a counter as a detector. With a source of very pure magnesium no positive electrons are observed by this method. The decay curve of the negative emission is similar to that for the total emission and shows the two periods of 2.3 and 6.4 min.

Photographs have been taken in a Wilson cloud chamber beginning 30 minutes after bombardment. At this time the intensity of the 2.3-min. activity is less than 1 percent of the total intensity. A series of 100 photographs taken after this time show that the electrons emitted by the 6.4-min. body are predominantly negative. However, several positive electrons were observed coming from the source. Out of a total of 748 tracks there were 22 positives. The positives were equally numerous at the beginning and end of the run, while the negative emission decreased by a factor of eight. They, therefore, seem to decay with a much longer period than 6.4 min. and may probably be due to a very small calcium impurity in the magnesium. Calculating from the known intensity of a pure calcium target, it turns out that one part in 5000 calcium impurity in the magnesium target would give rise to the observed number of positives.

The new assignment solves all the difficulties mentioned above. The actual Si^{27} has been produced by Kuerti and Van Voorhis[7] since these experiments were begun. Kuerti and Van Voorhis find that Si^{27} is produced by the reaction Al^{27} (p, n) Si^{27} and has a half-life of 3.7 seconds which agrees with the expectation from analogous nuclei (paragraph 2 above).

Measurements of the curvature of 314 tracks of the negative electrons give a rough energy distribution and show that the upper limit of the spectrum is about 2.5 Mev. An absorption curve of the β-rays in aluminum gives an absorption coefficient $\mu/\rho = 5.3$ and a range for the β-rays of 1.10 g/cm². These are consistent with the above value for the upper limit. The γ-rays, if any, associated with the 6.4-min. period are very weak; no ionization could be detected in the electroscope when the aluminum absorber had a thickness corresponding to 1.10 g/cm². With the mass of Si^{29} given in reference 5, the mass of Al^{29} is 28.9893 which fits in well with the masses of the neighboring elements.

We wish to thank Mr. D. R. Elliott of Purdue University for taking the cloud-chamber photographs.

H. A. BETHE

Cornell University,
Ithaca, New York.

W. J. HENDERSON

Purdue University,
Lafayette, Indiana,
October 24, 1939.

[1] C. D. Ellis and W. J. Henderson, Proc. Roy. Soc. **156**, 358 (1936).
[2] W. J. Henderson and R. L. Doran, Phys. Rev. **56**, 123 (1939).
[3] White, Delsasso, Fox and Creutz, Phys. Rev. **56**, 512 (1939).
[4] Alichanow, Alichanian and Dzelepow, Nature **133**, 950 (1934).
[5] M. S. Livingston and H. A. Bethe, Rev. Mod. Phys. **9**, 377 (1937).
[6] W. Bothe and W. Gentner, Zeits. f. Physik **106**, 236 (1937).
[7] G. Kuerti and S. N. Van Voorhis, Phys. Rev. **56**, 614 (1939).

A Study of the Protons from Calcium under Deuteron Bombardment

Targets of CaO have been bombarded by 3.1-Mev deuterons from a cyclotron. Fig. 1 shows an absorption plot of the protons from both a thick and thin target, observation being made at right angles to the incident deuteron beam. Since protons from the reaction $O(dp)$ have a range of only 27 cm the groups at 66 cm and 96 cm corresponding to "Q" values of 4.51 Mev and 6.30 Mev must be attributed to $Ca(dp)$. The 66-cm group is considerably more intense

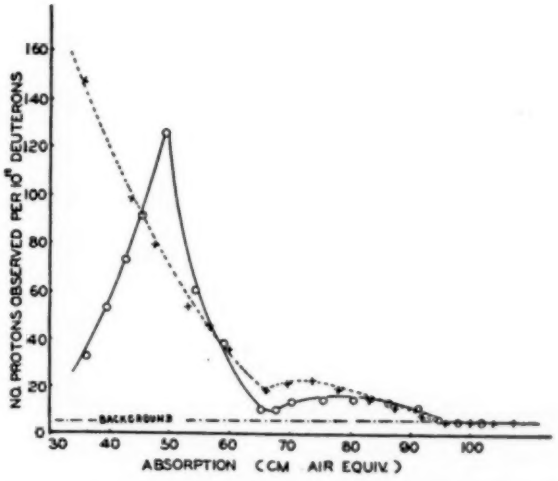

FIG. 1. Absorption plot of the protons from CaO+H². Circles refer to thin target yields; crosses to yields from a thick target. The abundant $O(dp)$ group at 27 cm is not included.

than the corresponding yield from $Sc(dp)$. Sc has only a single stable isotope. Since the element calcium is predominantly Ca^{40} (96.76 percent), one can almost certainly attribute this group to the reaction

$$Ca^{40}+H^2 \rightarrow Ca^{41}+H^1,$$

giving positive evidence for the actual formation of Ca^{41}. Walke[1] has searched unsuccessfully for the radioactivity resulting from such an isotope. Thus one can conclude that Ca^{41} is either stable or else its half-life must be very short or very long. The former view seems untenable both from the result of Nier's[2] work which places an upper limit of $Ca^{41}/Ca^{40} = 1/150{,}000$ and from the fact that adjoining stable isobars are extremely rare. Another possibility is that Ca^{41} may decay to K^{41} via K-electron capture. Such a possibility might explain why its activity was not observed, since the soft x-radiation may have been masked by the electrons from Ca^{45}.

I wish to thank Professor Ernest Pollard for his advice on this work.

WILLIAM L. DAVIDSON, JR.

Sloane Physics Laboratory,
Yale University,
New Haven, Connecticut,
November 1, 1939.

[1] Harold Walke, Phys. Rev. **51**, 439 (1937).
[2] Alfred O. Nier, Phys. Rev. **53**, 282 (1938).

A Study of the Protons from V, Cu, Mn, and Sc under Bombardment by Deuterons

Absorption studies have been carried out on the protons from the following reactions.

1. $V^{51}+H^2 \rightarrow V^{52}+H^1$,
2. Cu^{63}, $Cu^{65}+H^2 \rightarrow Cu^{64}$, $Cu^{66}+H^1$,
3. $Mn^{55}+H^2 \rightarrow Mn^{56}+H^1$,
4. $Sc^{45}+H^2 \rightarrow Sc^{46}+H^1$.

Deuterons of 3.1-Mev energy, accelerated in a cyclotron, were utilized and the average current was 2 microamperes. The protons were detected by a proportional counter operating into a conventional amplifier, the output pulses being fed to a scale-of-10 recording circuit.[1]

Table I gives the ranges of the groups found as well as the resulting "Q" values. Possible groups with ranges less than that of C(dp) protons (34 cm) have been left for further study, since carbon from the oil diffusion pumps is inevitably present on all targets. Assignments of the groups to the reactions responsible are unique except for Cu, since the other targets represent 100 percent isotopes. In the case of Cu assignment is made of the 87.5-cm group to the reaction

$$Cu^{63}+H^2 \rightarrow Cu^{64}+H^1,$$

corresponding to the formation of the ground state of Cu^{64}; and the 99.5-cm group to

$$Cu^{65}+H^2 \rightarrow Cu^{66}+H^1,$$

resulting in the ground state of Cu^{66}. One is led to such an assignment since the former group has double the intensity of the latter group, in keeping with the abundance ratio of the two Cu isotopes. As a check on this the corresponding "Q" values have been used along with Dempster's[2] mean packing fraction for Cu^{63}, Cu^{65} to deduce the masses of Cu^{64} and Cu^{66}. The values obtained are in good agreement with those found from Dempster's[2] packing fractions for Zn^{64} and Zn^{66} together with the maximum β-ray energies from Cu^{64} and Cu^{66} found by Sinma and Yamasaki.[3] However, the magnitude of the probable errors in these latter values is such that the agreement cannot be taken as conclusive proof of the assignment but only as an indication of its correctness. Until the γ-rays given off by Cu under bombardment by deuterons are investigated, it will be impossible properly to assign the 52.5-cm and 66.5-cm groups present.

Table II lists the excitation levels found for the various nuclei; also the masses deduced from the largest energy release found in each reaction. The mass of V^{52} was determined using that of V^{51} as obtained by Davidson and Pollard[4] from the reaction

$$Ti^{48}+He^4 \rightarrow V^{51}+H^1.$$

This in turn involved Dempster's[2] value for the mass of Ti^{48}.

The mass of Mn^{55} was arrived at from Dempster's[2] packing fraction for Fe^{56} and Brown and Mitchell's[5] value for the energy limit of the β-rays from Mn^{56}.

In the case of Sc^{46} the mass was determined with the aid of Pollard's[6] mass value of Sc^{45} which he deduced from the reaction

$$Sc^{45}+He^4 \rightarrow Ti^{48}+H^1,$$

again with the assistance of Dempster's mass for Ti^{48}. The probable error in the (αp) reactions used above was estimated at the relatively large value of ± 0.0005 mass units since natural sources of alpha-particles were employed. It is felt that the much greater yields obtained in the (dp) reactions here reported together with better geometry merit a probable error conservatively placed at ± 0.0003 mass units. The errors in the packing fractions used are those given by the author.

I wish to express my sincere thanks to Professor Ernest Pollard for his assistance and advice in this work.

WILLIAM L. DAVIDSON, JR.

Sloane Physics Laboratory,
Yale University,
New Haven, Connecticut,
October 24, 1939.

TABLE I. *Ranges and "Q" values for the reactions studied.*

Residual Nucleus	Range of Proton Groups (cm air equiv.)			"Q" Values (Mev)		
1. V^{52}	46	80	127.5	+3.10	+5.33	+7.80
2. Cu^{64}	52.5	66.5	87.5	+3.54	+4.35	+5.70
Cu^{66}			99.5			+6.35
3. Mn^{56}	50.5	69	103	+3.40	+4.62	+6.57
4. Sc^{46}	65.5	104.5			+4.48	+6.78

TABLE II. *Excitation levels and calculated masses of several nuclei.*

Nucleus	Excitation Levels (Mev)		Deduced Masses
V^{52}	2.47	4.70	51.9580±.0013
Cu^{64}			63.9572±.0016
Cu^{66}			65.9551±.0016
Mn^{56}	1.95	3.17	
Mn^{55}			54.9643±.0025
Sc^{46}	2.30		45.9682±.0013

[1] D. W. Kerst, Rev. Sci. Inst. **9**, 131 (1938).
[2] A. J. Dempster, Phys. Rev. **53**, 64 (1938).
[3] Keizo Sinma and Fumio Yamasaki, Sci. Papers of the Inst. of Phys. and Chem. Research **35**, 16 (1938).
[4] W. L. Davidson, Jr., and E. Pollard, Phys. Rev. **54**, 408 (1938).
[5] M. V. Brown and Allan C. G. Mitchell, Phys. Rev. **50**, 593 (1936).
[6] Ernest Pollard, Phys. Rev. **54**, 411 (1938).

The Secondary Emission from Evaporated Nickel and Cobalt

In a recent paper[1] the author has derived an equation which connects the shape of the secondary yield (δ) *versus* primary energy (E_p) curve for a metal with certain of the physical constants of the target material. Since the development assumed complete randomness in the orientations of the crystallites of the target, this equation is best tested against the results of measurements on evaporated metals. The purpose of this note is to present δ *vs.* E_p data for evaporated nickel and cobalt, and to compare with the theoretical predictions.

The measurements were made in a simple tube, constructed so that all the elements could be outgassed by electron bombardment. The geometry of the tube had been carefully designed so as to contribute only very small errors to the absolute magnitudes of the quantities meas-

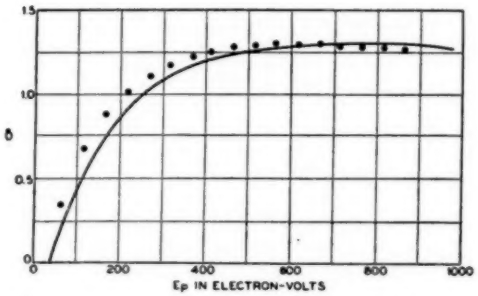

FIG. 1. Secondary yield *vs.* primary energy for nickel.

ured. Various auxiliary measurements fixed the uncertainty in the results at two percent or less. The system was thoroughly outgassed and evacuated before the metal was evaporated. The evaporation was carried out by heating a tungsten filament on which a small loop of nickel or cobalt wire had been hung. The measurements were made immediately after evaporation, during which time the pressure was less than 2×10^{-7} mm Hg, as indicated by an ionization manometer.

The experimental points are shown in Figs. 1 and 2.[2] The theoretically derived curves employed the following constants for the targets:

	Nickel	*Cobalt*
Atomic Volume[3]	11.0×10^{-24} cc/atom	11.0×10^{-24} cc/atom
Max. Fermi Energy[4]	11.6 ev	11.6 ev
Work Function[5]	5.0 ev	4.2 ev

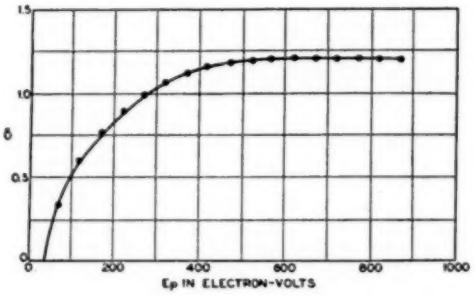

FIG. 2. Secondary yield *vs.* primary energy for cobalt.

The extent of the agreement between theory and experiment is as good as the approximations in the theory allow one to expect in the case of nickel. The extremely close agreement in the case of cobalt is probably fortuitous.

It is a pleasure to acknowledge the work of Mr. C. D. Hartman, who has been of great assistance in making the experimental measurements.

D. E. WOOLDRIDGE

Bell Telephone Laboratories,
New York, New York,
October 2, 1939.

[1] D. E. Wooldridge, Phys. Rev. **56**, 562 (1939).
[2] In these figures E_p is the energy, in electron-volts, of the primary particles just *after* they have penetrated the surface of the target. This exceeds the incident energy by about 16 ev, for nickel and cobalt.
[3] N. F. Mott and H. Jones, *Properties of Metals and Alloys* (Oxford, 1936), p. 318.
[4] Calculated on the assumption of two free electrons per atom. See, for example, reference 3, p. 54.
[5] A. L. Reimann, *Thermionic Emission* (John Wiley and Sons, 1934), p. 99.

Lattice Defects in Silver Halide Crystals

In a previous note[1] in this Journal, the writer pointed out that a value of the activation energy for the formation of lattice defects in ionic crystals could be obtained from a comparison of conductivity measurements at low and high temperatures. The value of the activation energy for silver bromide obtained with the use of this method was then employed in a simple theory to determine the actual number of lattice defects at various temperatures. The computed values were found to be so low even near the melting point as to make it seem unlikely that a comparison of density and lattice constant measurements could be used to decide whether or not the lattice defects consist (a) of pairs of vacancies in the positive and negative ion lattices, as in the alkali halides, or (b) of vacancies in the positive ion lattice and interstitial silver ions as suggested by Jost and Nehlep.[2] The basis for making an estimate of the accuracy of density measurements is provided by the work of Wagner and Beyer.[3]

Briefly, it was found that the ratio r of the number of lattice defect atoms to the number of normal atoms is given by the equation

$$r=\exp(-\epsilon/kT), \tag{1}$$

where ϵ was found to be about 0.36 ev for silver bromide. The principal assumptions made in deriving these results are that (a) the activation energy for ionic conductivity is smaller at low temperatures than at high temperatures because the number of defects becomes constant at low temperatures, and (b) the additional entropy of a crystal containing defects is simply a mixing entropy. If the same method is applied to silver chloride, it is found that the activation energy in (1) is about 0.50 ev.

Since the appearance of the preceding note, Wagner has pointed out to me that experiments carried on by him in cooperation with Koch[4] lead directly to values of the number of lattice defects. These workers have measured the conductivity of silver halide crystals containing small amounts of the corresponding lead halide, which is completely dissolved in the lattice of the silver salt. Since lead is divalent, each lead ion replaces two silver ions, thereby increasing the number of vacancies in the silver ion lattice. They then determine the conductivity associated with the silver ion vacancies from the measured increase of conductivity occurring with increasing lead concentration. This result is then used to determine the number of vacancies, and hence of lattice defects, in the pure crystal. The final expressions for r, the ratio of defect atoms to normal atoms, may be fitted closely with functions of the form

$$\begin{aligned} r(\mathrm{AgBr}) &= 29\exp(-5050/T), \\ r(\mathrm{AgCl}) &= 36\exp(-6250/T). \end{aligned} \tag{2}$$

The activation energies corresponding to the exponents in these expressions are 0.43 ev and 0.54 ev, respectively, which agree with the values 0.36 ev and 0.50 ev, determined above, as closely as may be expected when the difficulty of determining the low temperature activation energy of the conductivity is considered. The fact that the coefficients of the exponents are not unity, as in the simple theory

represented by Eq. (1), presumably indicates that the entropy associated with the lattice defects is not simply a mixing entropy, which is not at all surprising.

In conclusion, it may be said that the directly determined activation energies for the formation of lattice defects in the silver halides are in substantial agreement with those determined by the indirect method discussed in the reference of footnote 1.

FREDERICK SEITZ

Randal Morgan Laboratory of Physics,
University of Pennsylvania,
Philadelphia, Pennsylvania,
October 19, 1939.

[1] F. Seitz, Phys. Rev. **54**, 1111 (1938).
[2] W. Jost and G. Nehlep, Zeits. f. physik. Chemie **B32**, 1 (1936).
[3] C. Wagner and J. Beyer, Zeits. f. physik. Chemie **B32**, 113 (1936).
[4] E. Koch and C. Wagner, Zeits. f. physik. Chemie **B38**, 295 (1938).

The Electric Quadrupole and Magnetic Dipole Moments of Li^6 and N^{14}

The nonspherically symmetric nuclear forces which are invoked in order to account for the existence of the electric quadrupole moment of the deuteron[1] present an opportunity to explain certain discrepancies between the theoretical and observed nuclear magnetic moments.[2] Of particular interest are the cases of Li^6 and N^{14}. On the assumption of intrinsic magnetic moments of the neutron and proton uninfluenced by binding forces one expected the magnetic moments of these nuclei to be equal to that of the deuteron. Such differences as are due to the effects of Coulomb forces and spin-orbit coupling are entirely negligible.[3] However, the observed values give $\mu(H^2)-\mu(Li^6)=0.03$ and $\mu(H^2)-\mu(N^{14})=0.45$ nuclear magnetons.[4]

The expectation of equality of the magnetic moments of H^2, Li^6 and N^{14} was based on the result following from the spherically symmetric force model that the ground state of all three nuclei were the same; *viz.*, $^3S_1$. But with angular dependent forces such as are presented by the meson field theory,[5] this is no longer valid and the ground states of these nuclei will be a mixture of $^3S_1$ and $^3D_1$ with differing amounts of the two. For the two heavier nuclei a greater admixture of the D function might be expected since the D term in Li^6 and N^{14} arises from the lowest configuration, in contrast to H^2, and there should be a smaller energy difference between the S and D levels in the unperturbed state.

It is easy to see that the effect of the D function is to decrease the calculated magnetic moments as experiment requires. In the absence of definite evidence to the contrary we may assume that the differences in magnetic moments are entirely due to the different admixtures of D function. Writing the ground state wave function as

$$\Psi=(1+\beta^2)^{-\frac{1}{2}}[\psi(^3S)+\beta\psi(^3D)] \tag{1}$$

we find

$$\beta=\left(\frac{\mu_H{}^2-\mu}{\mu-\mu'}\right)^{\frac{1}{2}}=\begin{cases}0.25 & \text{for } Li^6\\ 2.4 & \text{for } N^{14},\end{cases} \tag{2}$$

in which μ is the observed magnetic moment and $\mu'=\frac{3}{4}-\frac{1}{2}\mu_{H^2}$ is the magnetic moment associated with the D state. These values of β may be compared with the deuteron case where $\beta=0.07$ (neutral meson theory) and $\beta=0.21$ (symmetrical meson theory).[5] For N^{14} the large deviation from the deuteron moment resulting in the large value of β may be due in part to the fact that in the unperturbed state the spin-orbit splitting[6] brings the $^3D_1$ level closer to the $^3S_1$ level in N^{14} whereas in Li^6 the opposite is true. However, it is not likely that this is the sole factor and it is possible that either or both of the following is operative: (1) As the number of particles in the nucleus increases the angular dependent part of the forces becomes predominant or (2) the deviations from the deuteron moment are not entirely due to different admixtures of states with orbital momentum but other effects (influence of binding?) become more important for greater numbers of particles.

As a consequence of the angular dependence of the forces an electric quadrupole moment should be expected for both Li^6 and N^{14}. While no accurate calculation of the magnitude of these moments may as yet be made, approximate methods should be capable of giving the correct sign of the moments. If the Hartree model is used, and if the small effects due to excitation of the alpha-particle core are neglected so that we have essentially a two-body problem, the quadrupole moments calculated for the three nuclei all have positive sign. Part of the inaccuracies inherent in the model may be eliminated by comparing the ratios of the quadrupole moments. We find

$$Q/Q(H^2)=\begin{cases}27.5\beta^2/1+\beta^2 & \text{(neutral theory)}\\ 8.9\beta^2/1+\beta^2 & \text{(symmetrical theory).}\end{cases}$$

The use of these ratios and the observed value of $Q(H^2)$, together with the values of β determined above, amounts to an empirical determination of the fictitious potential used in the Hartree model. This, of course, depends on the validity of the assumption made above in regard to the source of the anomaly in the magnetic moments. If we use the neutral theory, which would be preferred if the deuteron moment is positive,[5] and with $Q(H^2)=2.5\times10^{-27}$ cm^2,[1] the values of β from (2) give $Q(Li^6)=4\times10^{-27}$ cm^2 and $Q(N^{14})=58\times10^{-27}$ cm^2. These values can at best be regarded as an order of magnitude estimate with considerable uncertainty prevailing in the case of the latter. However, a quadrupole moment increasing rather rapidly with increasing mass is to be expected.

M. E. ROSE

Sloane Physics Laboratory,
Yale University,
New Haven, Connecticut,
October 14, 1939.

[1] J. M. B. Kellogg, I. I. Rabi, N. F. Ramsey and J. R. Zacharias, Phys. Rev. **55**, 318 (1939).
[2] M. E. Rose and H. A. Bethe, Phys. Rev. **51**, 205, 993 (1937). D. R. Inglis, Phys. Rev. **51**, 531 (1937); **53**, 822 (1938).
[3] D. R. Inglis, Phys. Rev. **55**, 329 (1939).
[4] J. M. B. Kellogg, I. I. Rabi, N. F. Ramsey and J. R. Zacharias, Phys. Rev. **55**, 595 (1939). I. I. Rabi, S. Millman, P. Kusch and J. R. Zacharias, Phys. Rev. **55**, 526 (1939). P. Kusch, S. Millman and I. I. Rabi, Phys. Rev. **55**, 1176 (1939).
[5] H. A. Bethe, Phys. Rev. **55**, 1261 (1939).
[6] D. R. Inglis, Phys. Rev. **50**, 783 (1936).

Beta-Decay and Mesotron Lifetime

Yukawa, in his original discussion of mesotrons and nuclear forces,[1] suggested that the mesotron has a finite lifetime, disintegrating into an electron and neutrino, and that β-decay should be described as taking place through a mesotron as intermediary, rather than through direct disintegration of the proton and neutron. For the mesotron of spin zero considered by Yukawa, this point of view led to a β-decay theory fully equivalent to Fermi's, and to a definite prediction of the lifetime of the mesotron in terms of β-lifetimes.

More recently a number of investigators[2] have come to the conclusion that the sign and spin dependence of nuclear forces can best be understood on the supposition that the mesotron has spin one, and obeys the Proca equations. But with this theory serious objections to Yukawa's description of β-decay arise. Treating the heavy particles non-relativistically, the coupling energy between heavy particles and mesotrons takes the form

$$\psi_P^*(g_1 U^0+\kappa^{-1}g_2\boldsymbol{\sigma}\cdot\text{curl }\mathbf{U})\psi_N, \qquad (1)$$

with $U^\lambda=(U^0, \mathbf{U})$ the four-vector mesotron wave function, $\kappa^{-1}=\hbar/\mu c$. The coupling energy between light particles and mesotrons is

$$\psi_\nu^*[g_1'\alpha^\lambda U_\lambda+\kappa^{-1}g_2'\beta\sigma^{\lambda\tau}(\partial U_\lambda/\partial X^\tau-\partial U_\tau/\partial X^\lambda)]\psi_e. \qquad (2)$$

Both terms in (1) are proportional to the momentum of the mesotron; the second term because it involves derivatives of $\mathbf{U}$, the first because of the relation $C^{-1}\dot{U}^0=-\text{div }\mathbf{U}$, which for a mesotron of momentum p and energy E becomes $U^0=\mathbf{U}\cdot pc/E$. Since the mesotron momentum is equal to the sum of the momenta of electron and neutrino, the heavy particle matrix element will thus contribute two powers of the light particle momenta in the expression for the β-lifetime; the lifetime will be connected to the upper limit of the β-spectrum by a seventh power law, rather than the fifth power law required by experimental evidence. The only escape is to deny the mesotron any role in β-decay, and return to direct emission of the light particles by the heavy ones, for example by an interaction

$$f_1(\psi_P^*\psi_N)(\psi_\nu^*\psi_e)+f_2(\psi_P^*\boldsymbol{\sigma}\psi_N)\cdot(\psi_\nu^*\boldsymbol{\sigma}\psi_e). \qquad (3)$$

One is thus forced to give up any theoretical connection between β-decay and mesotron decay; both can take place, but they must be supposed completely independent processes.

This conclusion is not in contradiction with the results of Yukawa and his collaborators[3] for mesotrons obeying the Proca equation, although their calculations seem to give both a satisfactory β-theory and a relation between β-lifetimes and mesotron lifetime. Yukawa does in fact include, in his Lagrangian for the field, terms of type (3). An apparent connection between the lifetimes arises only because he assumes a definite ratio between these terms and terms (1) and (2): $f_1=\kappa^{-2}g_1g_1'$, $f_2=\kappa^{-2}g_2g_2'$. With this choice the β-decay is determined entirely by (3), the contribution of (1) and (2) being smaller by a factor $(E_{max}/\mu c^2)^2$. Since Yukawa's choice seems inadequately motivated, the discrepancy noted by Nordheim[4] between the calculated and observed mesotron lifetimes is purely fictitious.

ROBERT SERBER

Department of Physics,
University of Illinois,
Urbana, Illinois,
October 27, 1939.

[1] H. Yukawa, Proc. Phys.-Math. Soc. Japan **17**, 48 (1935).
[2] Yukawa, Sakata and Taketani, Proc. Phys.-Math. Soc. Japan **20**, 319 (1938); N. Kemmer, Proc. Roy. Soc. **A166**, 127 (1938); Fröhlich, Heitler and Kemmer, *ibid.* **A166**, 154 (1938); H. J. Bhabha, *ibid.* **A166**, 501 (1938).
[3] Yukawa, Sakata, Kobayasi and Taketani, Proc. Phys.-Math. Soc. Japan **20**, 720 (1938).
[4] L. W. Nordheim, Phys. Rev. **55**, 506 (1939).

The Fission of Protactinium

In connection with the recent observation by v. Grosse, Booth and Dunning,[1] that it is possible to produce fission in protactinium by neutrons of less than 2 Mev energy but not by thermal neutrons, we should like to point out that this important discovery would seem to fit very well with the theoretical considerations about the fission mechanism developed by us in a recent paper.[2] This theory rests upon the idea that fission, like other nuclear transmutations initiated by collisions or radiation, takes place in two stages. Of these the first is the formation of a compound nucleus in which the energy is temporarily stored among the different degrees of freedom in a way resembling thermal agitation; the second stage is the transformation of a sufficient portion of this energy into potential energy of deformation of the compound nucleus to lead to its division. The possibility of fission by impact of neutrons of given energy depends, therefore, on the difference between the critical energy E_f of such an unstable deformation and the excitation energy of the compound nucleus, which is determined by the binding energy W_n of the added neutron. The considerations in our paper lead to the estimates for these quantities given in Table I.

According to this table, and in agreement with the observations of v. Grosse, Booth and Dunning, we shall just expect that fission is produced in protactinium more easily than in thorium but less easily than in the isotope U^{235} which, according to the theory, is responsible for the large fission yield of thermal neutrons in uranium. While the accuracy of the estimates of E_f-W_n should be amply sufficient for such qualitative conclusions, it hardly permits

TABLE I. *Estimates of the differences in Mev between the critical energy E_f of unstable deformations and the binding energy W_n of the added neutron.*

COMPOUND NUCLEUS	E_f	W_n	E_f-W_n
$_{92}U^{235}$	5.0	5.4	−0.4
$_{92}U^{238}$	5.3	6.4	−1.1
$_{91}Pa^{232}$	5.5	5.4*	+0.1
$_{92}U^{239}$	5.9	5.2	+0.7
$_{90}Th^{232}$	6.9	5.2	+1.7
$_{90}Io^{231}$	6.5	5.3	+1.2

* By an unfortunate error this quantity was given as 6.4 Mev in Table III of reference 2. It is clear, however, that the case of $_{91}Pa^{232}$ is comparable not to that of $_{92}U^{238}$ but to that of $_{92}U^{235}$, in which the removal of a neutron leads from an isotope of odd neutron number to one of even neutron number.

us to exclude the possibility of fission of protactinium by thermal neutrons; but the yield of such a process should at any rate be very much smaller than in uranium. An accurate determination of the threshold of neutron energy for protactinium fission would of course be very important and might perhaps be most easily obtained by a comparison between the fission yields for fast neutrons of well-defined energy in protactinium, uranium, and thorium, like that provided for the two latter elements by the experiments of Ladenburg, Kanner, Barschall and Van Voorhis,[3] as discussed in Section IV, C (see especially Fig. 6) of our paper.

NIELS BOHR

Institute for Theoretical Physics,
Copenhagen, Denmark.

JOHN A. WHEELER

Palmer Physical Laboratory,
Princeton University,
Princeton, New Jersey,
October 20, 1939.

[1] A. v. Grosse, E. T. Booth and J. R. Dunning, Phys. Rev. **56**, 382 (1939).
[2] N. Bohr and J. A. Wheeler, Phys. Rev. **56**, 426 (1939).
[3] R. Ladenburg, M. H. Kanner, H. H. Barschall and C. C. Van Voorhis, Phys. Rev. **56**, 168 (1939).

On Pair Emission in the Proton Bombardment of Fluorine

The gamma-rays emitted when fluorine is bombarded by protons have been studied by Fowler and Lauritsen, who have shown that these gamma-rays are monochromatic, with an energy of (6.3±0.1) Mev, independent of the proton energy; that they are emitted by an excited oxygen nucleus formed from the compound nucleus Ne^{20} by short range alpha-particle emission; and that they are emitted strongly only at certain well-defined proton energies which correspond to resonance levels in Ne^{20}. To account for the sharpness of these resonances it has been suggested that the parity-angular momentum selection rule prohibits the emission from these states of a long range alpha-particle, with the formation of a normal oxygen nucleus.

Recently Fowler and Lauritsen[1] have shown that under proton bombardment fluorine also emits electron pairs of total energy (5.9±0.5) Mev. The excitation function for the pairs also exhibits resonances, but uncorrelated with those for the gamma-rays—at some energies there are more than 100 times as many gamma-rays as pairs; at others the number of gamma-rays is comparable with, and may be smaller than, the number of pairs. Since, for any multipole order the pair creation internal conversion coefficient for 6-Mev gamma-rays is less than half of one percent, the pair emission must arise from a nuclear transition for which gamma-radiation is strictly forbidden, i.e., either Ne^{20} or O^{16} possesses an excited state with $j=0$ with no lower states of nonvanishing j, from which these pairs must originate. Since Ne^{20} is known from the work of Bonner to have a number of low-lying excited states, we are led to ascribe the pairs to a transition from an excited state of oxygen, with $j=0$ and about 6 Mev excitation energy, to the ground state.

If long range alpha-particle emission from the corresponding Ne^{20} is to be forbidden by the parity-angular momentum selection rule, this state in oxygen must be of odd parity (0^-). A ($0^-\rightarrow 0^+$) transition, however, corresponds to vanishing matrix elements of charge and current density; decay by pair emission can only occur if there is a nonelectromagnetic coupling between nuclear particles and the pair field. Thus, a coupling term of the form suggested by the Gamow-Teller, theory of nuclear forces,

$$(\boldsymbol{\sigma}_{el}\cdot\boldsymbol{\sigma}_{prot}) \quad \text{or} \quad (\boldsymbol{\sigma}_{el}\cdot\boldsymbol{\sigma}_{neut}),$$

would permit this transition to occur with the emission of pairs. A value of the coupling constant much smaller than that suggested by these authors would be sufficient to give a rate of pair emission greater than the rate of the competitive process of two-quantum emission. This latter process takes place by the successive emission of an electric dipole and a magnetic dipole quantum, through the intermediary of states possessing the character 1^+ or 1^-. The lifetime of the 0^- state associated with this method of decay may be roughly estimated at 10^{-6} sec.

The only alternative to this radical suggestion is to assume the excited state in oxygen to be of even parity (0^+). Pair emission, no longer forbidden, proceeds at the rate:

$$\left(\frac{1}{135\pi}\right)\left(\frac{e^2}{\hbar c}\right)^2\left(\frac{\gamma^5}{\hbar^5c^4}\right)\left|\left(\psi_{exc},\ \sum_i r_i^2\psi_{norm}\right)\right|^2,$$

which exceeds the rate of two-quantum emission:

$$\left(\frac{2}{7}\right)\left(\frac{\gamma}{\Delta}\right)^2\left(\frac{1}{135\pi}\right)\left(\frac{e^2}{\hbar c}\right)^2\left(\frac{\gamma^5}{\hbar^5c^4}\right)\left|\left(\psi_{exc},\ \left[\sum_i \mathbf{r}_i\right]^2\psi_{norm}\right)\right|^2$$

since γ, the energy emitted in the transition, is rather less than Δ ($\sim$20 Mev), the mean energy difference between the ground state and the excited states of type 1^- which act as intermediates in the double electric dipole emission process. (The summation in these formulae is to be extended over all nuclear protons.) The quanta would give a weak continuous spectrum extending up to 6 Mev and would not have been observed.

This second alternative involves abandoning the explanation of the long life of the resonance states of Ne^{20} in terms of the parity-angular momentum selection rule. Neither spin nor isotopic spin conservation can appreciably reduce the probability of long range alpha-particle emission. Indeed, if the first excited state of O^{16} is 0^+, it would seem likely on the basis of the alpha-particle model, which could make this intelligible, that this state has the same spin and isotopic spin as the ground state. For this reason we must expect the yield of long range alpha-particles to show resonance at the energies which produce pairs. Some indication that this may be so is afforded by the fact that the maximum pair yield found by Fowler and Lauritsen is under a tenth of the maximum gamma-ray yield, which suggests that the emission of long range alpha-particles competes with the alpha-particle emission leading to the excited state. We should in fact expect that at bombarding energies of the order of 1 Mev, where pair emission becomes appreciable, the Coulomb barrier would not materially reduce the emission probability of even the short range alpha-particles. The value of 10 to 1 suggested by the observed yield of pairs for the ratio of the decay rates of

long and short range alpha-particles is thus a reasonable one. The fact that the gamma-ray yields are larger, and, near the 330-kev resonance, much larger than the yield of long range alpha-particles, makes it necessary to assume that, at least for this γ-ray resonance, the long range alpha-emission is either forbidden or reduced.

If then the excited state is even, we should expect the resonance yield of long range alpha-particles to be comparable with, and probably considerably greater than the yield of pairs. If this is not so, the pair emission itself would seem to provide strong evidence for a nonelectromagnetic coupling between electrons and heavy particles.

J. R. OPPENHEIMER
J. S. SCHWINGER*

University of California,
Berkeley, California,
October 29, 1939.

* National Research Fellow.
[1] W. A. Fowler and C. C. Lauritsen, Phys. Rev. **56**, 840 (1939).

Observation of the Spectrum of Ne V

Previous investigations of the spectra of rare gases[1] have been limited in the extent of ionization which was produced in the gas atom. The development of methods of study of atoms which can be fixed in an electrode in solid form has extended the spectra of such ions to far greater stages of ionization. In an attempt to close some of the gaps in isoelectronic sequence data, experiments have been undertaken to determine whether higher stages of ionization can be studied in the rare gases. This communication is a preliminary report of some observations of the spectra of neon.

A periodic disruptive discharge in neon gas enclosed in Pyrex and quartz capillaries of about 2 mm bore and 15 mm length has been used as a source of light on a 3-meter grazing incidence vacuum spectrograph. On the resulting spectrograms the principal lines of Ne III, Ne IV, and Ne V have been identified.

The wave-lengths of the lines attributed to Ne V are given in Table I. The identification seems certain inasmuch as the lines are well isolated on the plates and their positions can be predicted with good accuracy from isoelectronic sequence data. The wave-lengths given must be regarded as tentative as they may be in error by as much as 0.05A because of the scarcity of standard lines on the plate from which the measurements were taken.

It is expected that refinements of experimental technique will permit fuller development of the spectrum of Ne V and more accurate wave-length measurements. Since the lines due to Ne V are equally as strong as those due to Ne III and Ne IV on the present plates, it is possible that this method will provide for the excitation of still higher stages of ionization. Experiments are being carried out with argon, krypton and xenon.

TABLE I. *Spectrum lines attributed to* Ne V.

λ VAC.	ν CM^{-1}	TRANSITION
572.38	174,708	$2p^2\,{}^3P_2 - 2s2p^3\,{}^3D_{2,1}{}^0$
572.12	174,787	$2p^2\,{}^3P_2 - 2s2p^3\,{}^3D_3{}^0$
569.84	175,487	$2p^2\,{}^3P_1 - 2s2p^3\,{}^3D_{2,1}{}^0$
568.45	175,918	$2p^2\,{}^3P_0 - 2s2p^3\,{}^3D_1{}^0$
483.00	207,039	$2p^2\,{}^3P_2 - 2s2p^3\,{}^3P_3{}^0$
481.30	207,770	$2p^2\,{}^3P_1 - 2s2p^3\,{}^3P_{1,0}{}^0$
480.38	208,168	$2p^2\,{}^3P_0 - 2s2p^3\,{}^3P_1{}^0$

FRED W. PAUL

Mendenhall Laboratory,
Ohio State University,
Columbus, Ohio,
October 31, 1939.
[1] J. C. Boyce, Phys. Rev. **46**, 378 (1934); **47**, 718 (1935); **48**, 396 (1935).

Work Functions of Different Faces of Silver Single Crystals

The work functions of the (100) and (111) faces of silver single crystals have been determined by a photoelectric method after extended outgassing of the crystals in a high vacuum. The crystal faces were prepared by a method described previously.[1] The equilibrium value of the work function for the (100) face is 4.81 ± 0.01 electron volts. This value was obtained after 2283 hours of heating at various temperatures up to visible red heat. 356 hours of additional heating did not change this value. After the crystal had subsequently remained at room temperature for 2130 hours, at a pressure of 1 to 3×10^{-8} mm Hg, the work function decreased to 4.65 ev. After 100 hours of additional heating of the crystal the work function increased to 4.79 ev, and after an additional 118 hours of heating it returned to the equilibrium value of 4.81 ev.

The equilibrium value of 4.75 ± 0.01 ev for the (111) face was obtained after 1227 hours of heating at temperatures similar to those above. This crystal had been outgassed in two previous experiments so that a much shorter time was required to reach the equilibrium value of the work function than for the (100) face. The above equilibrium value was not changed by 407 hours of additional heating. At this time the crystal became slightly contaminated while heating a tantalum plate near it. The effect of the contamination was to cause a failure of the experimental results to fit the Fowler theoretical curve.

Measurements of the contact potential difference, by the Kelvin null method, between the two crystal faces at frequent intervals during outgassing agreed with the differences of the photoelectric work functions to within ± 0.01 volt until the results for the (111) face failed to fit the Fowler theoretical curve.

We believe that these values are the best that can be obtained by heating since silver crystals etch rapidly, thus exposing other faces, when heated at temperatures where appreciable evaporation occurs.[2] The above values may be compared with 4.74 ev, previously obtained by Winch,[3] for polycrystalline silver after heating for 1200 hours which included short intervals at temperatures as high as 850°C where evaporation is rapid.

H. E. FARNSWORTH

Brown University,
Providence, Rhode Island.

RALPH P. WINCH

Williams College,
Williamstown, Massachusetts,
October 24, 1939.
[1] H. E. Farnsworth, Phys. Rev. **40**, 699 (1932).
[2] A larger preliminary value for contact potential difference was previously reported before sufficient outgassing had been carried out. H. E. Farnsworth, Phys. Rev. **51**, 378 (1937).
[3] Ralph P. Winch, Phys. Rev. **37**, 1269 (1931); R. H. Fowler, **38**, 45 (1931).

Erratum: The M_1 and M_2 X-Ray Absorption Edges of Lead

J. W. McGRATH
Michigan State College, Lansing, Michigan
(Phys. Rev. **56**, 765 (1939))

On page 767, two inadvertent errors appear. The O_1 and $O_{2,3}$ notations, wherever they appear, should read Q_1 and $Q_{2,3}$, respectively. In Fig. 1, the labels M_5' and M_4' should be interchanged.

Proceedings of the Metropolitan Section of the American Physical Society

MEETING OF OCTOBER 27, 1939

THE first meeting of the Metropolitan Section of the American Physical Society for the Season 1939–1940 was held at 3 P.M. on Friday, October 27, 1939 in the Pupin Physics Laboratories of Columbia University. The by-laws were amended to provide for holding the two regular meetings of the Section in each year on the fourth Friday in March and the fourth Friday in October unless special circumstances dictate otherwise. The following papers were presented.

Some New Aspects of Neutron Scattering
(a) Experimental. M. D. WHITAKER
(b) Theoretical. O. HALPERN
The Hydrogen Liquefaction Plant at Columbia University. H. A. BOORSE
The Directional Magnetic Properties of Nickel at Liquid Hydrogen Temperature. R. M. BOZORTH AND H. J. WILLIAMS

After the meeting opportunity was afforded for inspection of the hydrogen liquefaction plant.

W. S. GORTON
Secretary-Treasurer

THE AMERICAN INSTITUTE OF PHYSICS

INCORPORATED

ADMINISTRATIVE STAFF

HENRY A. BARTON, *Director*

MADELINE M. MITCHELL, *Publications Manager*

Office: 175 Fifth Avenue, New York, New York

JOURNALS

THE PHYSICAL REVIEW
REVIEWS OF MODERN PHYSICS
JOHN T. TATE, *Editor*
J. W. BUCHTA, *Assistant Editor*

JOURNAL OF APPLIED PHYSICS
ELMER HUTCHISSON, *Editor*

THE JOURNAL OF THE OPTICAL SOCIETY OF AMERICA
THE REVIEW OF SCIENTIFIC INSTRUMENTS
F. K. RICHTMYER, *Editor*

JOURNAL OF THE ACOUSTICAL SOCIETY OF AMERICA
FLOYD A. FIRESTONE, *Editor*

THE JOURNAL OF CHEMICAL PHYSICS
HAROLD C. UREY, *Editor*
JOSEPH E. MAYER, *Assistant Editor*

THE AMERICAN PHYSICS TEACHER
DUANE ROLLER, *Editor*

GOVERNING BOARD

For The American Physical Society:

JOHN T. TATE, *Chairman*
University of Minnesota

GEORGE B. PEGRAM, *Secretary*
Columbia University

KARL T. COMPTON
Massachusetts Institute of Technology

For The Optical Society of America:

E. C. CRITTENDEN
National Bureau of Standards

A. C. HARDY
Massachusetts Institute of Technology

W. B. RAYTON
Bausch & Lomb Optical Company

For The Acoustical Society of America:

FLOYD A. FIRESTONE
University of Michigan

HARVEY FLETCHER
Bell Telephone Laboratories

WALLACE WATERFALL
The Celotex Corporation

For The Society of Rheology:

WHEELER P. DAVEY
Pennsylvania State College

MELVIN MOONEY
United States Rubber Products, Inc.

R. L. PEEK, JR.
Bell Telephone Laboratories

For The American Association of Physics Teachers:

PAUL E. KLOPSTEG
Central Scientific Company

FREDERIC PALMER, JR.
Haverford College

F. K. RICHTMYER
Cornell University

The American Institute of Physics is a membership corporation of which five societies are the founding members. These five societies are the principal national societies devoted to pure and applied physics in America. Their names, and those of their representatives who form the Governing Board of the Institute, are given above. The principal work of the Institute is the publication of journals sponsored by the societies or by itself. The names and the editors of the journals are also listed above.

The broad purpose of the Institute is to represent, in all matters of wide or common interest, the five thousand or more members and subscribers associated with the Founder Societies and the journals. It aims to advance the science and profession of physics, and to promote cooperation between pure research, the applied sciences and the industries. To achieve these aims, it is greatly in need of an endowment and is empowered by law to administer grants and funds of any kind.

CONTENTS

PHYS. REV. 58 (1939) NOVEMBER 15

Rate-Spectra of Iodine . . . . . G. F. TAPE 965

Diffraction of X-Rays by Small Crystalline Particles . . . . . A. L. PATTERSON 972

Scherrer Formula for X-Ray Particle Size Determination . . . . . A. L. PATTERSON 978

Far Infra-Red Absorption Spectrum and the Rotational Structure of the Heavy Water Vapor Molecule . . . . . NELSON FUSON, H. M. RANDALL AND D. M. DENNISON 982

Van der Waals Potential in Helium . . . . . H. MARGENAU 1000

Coefficient of Thermal Diffusion of Methane . . . . . ALFRED O. NIER 1009

Fluctuations, Thermodynamic Equilibrium and Entropy . . . . . EDWIN C. KEMBLE 1013

Precision Determination of the Viscosity of Air . . . . . J. A. BEARDEN 1023

Viscous Force Between Almost-Coaxial Cylinders . . . . . D. R. INGLIS 1041

Magnetic Studies of Solid Solutions. I. Methods of Observations and Preliminary Results on the Precipitation of Iron from Copper . . . . . F. BITTER AND A. R. KAUFMANN 1044

Rotation-Vibration Energies of Tetrahedrally Symmetric Pentatomic Molecules. II. . . . . WAVE H. SHAFFER, HARALD H. NIELSEN AND L. H. THOMAS 1051

Letters to the Editor:

On the Origin of Cosmic Radiation . . . . . HANNES ALFVÉN 1060

Evidence for Incorrect Assignment of the Supposed Sb^{122} Radioactivity of 4.7-Minute Half-Life . . . . . H. A. BETHE AND W. J. HENDERSON 1060

Study of the Protons from Cobalt under Deuteron Bombardment . . WILLIAM L. DAVIDSON, JR. 1061

Study of the Protons from V, Cu, Mn, and Fe under Bombardment by Deuterons . . . . . WILLIAM L. DAVIDSON, JR. 1062

Secondary Emission from Evaporated Nickel and Cobalt . . . . . D. R. WOOLLESTON 1063

Sulfide Defects in Silver Halide Crystals . . . . . FREDERICK SEITZ 1063

Electric Quadrupole and Magnetic Dipole Moments of Li^6 and N^{14} . . . . . M. E. ROSE 1064

Beta-Decay and Mesotron Lifetime . . . . . ROBERT SERBER 1065

Studies of Proteolysis . . . . . NILES BOHR AND JOHN A. WHEELER 1065

On Pair Emission in the Proton Bombardment of Fluorine . . . . . J. R. OPPENHEIMER AND J. S. SCHWINGER 1066

Observation of the Spectrum of $_{92}U$ V . . . . . FRED W. PAUL 1067

Work Functions of Different Faces of Silver Single Crystals . . . . . H. E. FARNSWORTH AND RALPH P. WINCH 1067

Erratum: The M_I and M_{II} X-Ray Absorption Edges of Lead . . . . . J. W. MCGRATH 1068

Proceedings of the Metropolitan Section of the American Physical Society 1068

LANCASTER PRESS, INC., LANCASTER, PA.